The role of Ribose-5-phosphate isomerase A in the regulation of autophagy

Jacob Heintze

A dissertation submitted in partial fulfillment

of the requirements for the degree of

Doctor of Philosophy

of

University College London.

Laboratory of Molecular Cell Biology

University College London

July 22, 2016

I, Jacob Heintze, confirm that the work presented in this thesis is my own. Where information has been derived from other sources, I confirm that this has been indicated in the work.

Abstract

Macroautophagy (hereafter: autophagy), cell signalling and cellular metabolism are tightly linked processes. Multiple examples of metabolites and metabolic enzymes have recently been found to regulate signalling pathways and autophagy. Metabolic reprogramming is one of the hallmarks of cancer and often mediated via aberrant signalling pathways, such as receptor tyrosine kinase (RTK) signalling. Growth factor receptor-bound protein 2 (Grb2) is a key RTK signalling adaptor and is involved in a number of downstream signalling cascades, such as mitogen-activated protein kinase (MAPK) or phosphoinositide 3-kinase (PI3K) pathways, which in turn regulate metabolism through alterations in gene expression or by directly modifying enzymatic activity.

This study investigates the role of ribose-5-phosphate isomerase (RPIA), a key metabolic enzyme in the pentose phosphate pathway (PPP), in the regulation of autophagy and Grb2-mediated signalling. RPIA expression induces Grb2 translocation from an even cytoplasmic distribution to unknown sub-cellular structures, possibly through direct protein-protein interaction. Interestingly, this effect is independent of the catalytic activity of RPIA, suggesting a non-canonical role in signalling. Neither RPIA over-expression, transient knockdown or deletion by CRISPR/Cas9 genome editing resulted in differences in metabolic activity or the MAPK pathway as tested by extracellular signalregulated kinases (ERK) 1/2 phosphorylation and MTT assay.

Furthermore, knockdown of RPIA by shRNA or genomic deletion resulted in an increase of LC3 processing and LC3-positive autophagosomes, suggesting that endogenous RPIA is an inhibitor of basal autophagy. Data from *Saccharomyces cere-*

visiae, mass spectrometry of sugar phosphates and pharmacological treatment assays suggest that RPIA may inhibit autophagy through a non-canonical function. Although the molecular mechanisms by which RPIA acts on Grb2 signalling and how it contributes to the regulation of autophagy are currently not fully understood, this study presents some interesting observations that may have implications in the development of therapeutics that target cancer metabolism or aim to modulate autophagy.

Acknowledgements

I would like to thank all people who have supported me for the past years in my PhD project. First and foremost, I would like to thank Robin Ketteler for supervising, mentoring and supporting me throughout my thesis. He has always been very supportive, with constructive feedback and a positive and engaging mind set. His supervision has helped hugely to guide me through my PhD and also, he supported me in all my extracurricular activities and plans for the future. This has been obvious on multiple occasions, such as the very quick turnaround with helpful comments which - very much - helped me to put everything together that I have worked on for the past few years into this PhD thesis. I will never forget the immense, positive support over the years that I have received from him. Frankly, I do not think I could have wished for a better PhD supervisor.

Next, I would like to thank the Ketteler lab members for continuous support, suggestions, reagents, plasmids, protocols and in tips & tricks in general. Particular thanks go to Joana Costa, Christin Luft, Julia Petschnigg, Alex Agrotis, Niccolo Pengo, Melanie Weber, Janos Kriston-Vizi and Jamie Freemann. All have helped me immensely with one or another aspect of this project. Joana and Melanie have worked on the project once I finished in the lab, and thanks to them part of this thesis could be published. Christin gave fantastic support with general lab techniques and screening equipment. Julia always shared her knowledge on RTK signalling, whereas Alex and Niccolo gave useful advice on autophagy experiments. Janos was my Fiji/image analysis/Opera go-to guru. Jamie always came up with great scientific and general life advice.

Furthermore, the completion of this thesis would not have been possible without the continuous support from my family, friends and my wonderful girlfriend Kate. I am grateful to all of you for patiently listening to my moaning about failed experiments and slow progression with respect to thesis completion.

Also, I would like to thank Eduard Struyss for analysing the sugar phosphates in our HeLa CRISPR cell lines via mass spectroscopy. Furthermore, I would like to thank Chris Stefan and Heike Omnus for reagents, plasmids, yeast strains and general help with the budding yeast experiments.

Additionally, I would like to thank my PhD thesis committee members Buzz Baum, Martin Raff, Dan Cutler and Paul Gissen. Big thanks goes to the LMCB student and postdoc community, in particular to current (and past) Mole, DeBruin, Baum, Cutler, Gissen, Henriques, Mercer, Lloyd, Saiardi, Paluch and Marsh lab members. Also thanks to past (and current) Moss, Futter and Matter lab members at the Institute of Ophthalmology, where I did my first rotation.

Contents

List of Figures

List of Tables

Abbreviations used in this study

αKG ..... α-ketoglutarate

2-PG 2-phosphoglycerate

3-PG 3-phosphoglycerate

6PGDH ..... 6-phosphogluconate dehydrogenase

AA ..... amino acids

Ac-CoA ..... Acetyl-coenzme A

ACACA ..... Ac-CoA carboxylase

ACL ..... ATP-citrate lyase

ADP ..... Adenosine diphosphate

Ambra1 ..... activating molecule in Beclin-1-regulated autophagy

AMP ..... adenosine monophosphate

AMPK ..... AMP-activated protein kinase

ARTD ..... ADP-ribosyltransferase diphtheria toxin-like

ATG ..... Autophagy (protein)

ATP ..... adenosine triphosphate

Bcl-2 ..... B-cell CLL/lymphoma-2

Bif-1 ..... Bax-interacting factor 1

BNIP3 ..... Bcl-2/adenovirus E1B protein-interacting protein

BRCA-1 ..... breast cancer 1

C. elegans ..... Caenorhabditis elegans

CAD ..... Carbamoyl-phosphate synthetase 2, aspartate transcarbamylase, and dihydroorotase

cADPR ..... cyclic ADP-ribose

cAMP ..... cyclic AMP
cGMP ..... cyclic guanosine monophosphate
CMA ..... Chaperone-mediated autophagy
Co-IP ..... co-immunoprecipitation
CRC ..... colorectal cancer
CRISPR ..... clustered regularly-interspaced short palindromic repeats
DAPK ..... death-associated protein kinase
DEPTOR ..... DEP-domain containing mTOR-interacting protein
DHAP ..... Dihydroxyacetone phosphate
DMSO ..... Dimethyl sulfoxide
DNA ..... deoxyribonucleic acid
dR5P 2-deoxy-ribose 5-phosphate
DUSPs ..... dual specificity phosphatases
D. melanogaster ..... drosophila melanogaster
E4P erythrose-4-phosphate
EGF ..... epidermal growth factor
EGFR ..... epidermal growth factor receptor
EM ..... electron microscopy
ESCRT ..... endosomal sorting complexes required for transport
ER ..... endoplasmic reticulum
ERK ..... extracellular signal-regulated kinase
Ets ..... E twenty-six (transcription factor)
F1(2),6P ..... fructose-1(2)-6-bisphosphate
F6P fructose-6-phosphate
FASN ..... fatty acid synthase
FCS ..... fetal calf serum
FGFR2 ..... fibroblast growth factor receptor 2
FLAG ..... amino acid sequence DYKDDDDK
G3P glyceraldehyde-3-phosphate
G6P glucose-6-phosphate

G6PDH . . . . . glucose-6-phosphate dehydrogenase
GABARAP . . . . . Gamma-aminobutyric acid receptor-associated protein
GAPDH . . . . . glyceraldehyde-3-phosphate dehydrogenase
GDP . . . . . guanosine diphosphate
GEF . . . . . GTPase exchange factor
GFP . . . . . green fluorescent protein
Grb2 . . . . . growth factor receptor bound protein 2
GS . . . . . glutamine synthetase
GSK . . . . . glycogen synthase kinase
GTP . . . . . guanosine triphosphate
hsc70 . . . . . heat shock cognate 70 kDa protein
HCC . . . . . human hepatocellular carcinoma
HDR . . . . . homology-directed repair
HGFR . . . . . hepatocyte growth factor receptor
HIF . . . . . hypoxia-inducible factor
HK . . . . . hexokinase
HPLC . . . . . high pressure liquid chromatography
IMP . . . . . inosine monophosphate
JNK1 . . . . . c-jun N-terminal kinase 1
kDa . . . . . kilodalton
LAMP-2A . . . . . lysosome-associated membrane protein type 2A
(MAP)LC3 . . . . . (microtubule-associated protein) light chain 3
LDHA . . . . . lactate dehydrogenase A
LRS . . . . . Leucyl-tRNA Synthetase
MAPK . . . . . mitogen-activated protein kinase
MEFs . . . . . mouse embryonic fibroblasts
MEK . . . . . MAPK/ERK Kinase
MG-132 . . . . . N-(benzyloxycarbonyl)leucinylleucinylleucinal
MKK . . . . . MAPK Kinase 1
MKPs . . . . . MAP kinase phosphatases

mRNA ..... messenger RNA
MS ..... mass spectroscopy
mSin1 ..... mammalian stress activated protein kinase interacting protein 1
mLST8 ..... mammalian lethal with SEC13 protein 8
mTOR ..... mammalian target of rapamycin
mTORC1 ..... mammalian target of rapamycin complex 1
NaAD ..... nicotinic acid adenine dinucleotide
NAC ..... N-acetylcysteine
NAD^+ ..... oxidised nicotinamide adenine dinucleotide
NADH ..... reduced nicotinamide adenine dinucleotide
$NADP(^+)$ ..... oxidised nicotinamide adenine dinucleotide phosphate
NADPH ..... reduced nicotinamide adenine dinucleotide phosphate
NaMN ..... nicotinic acid mononucleotide
NH_4 ..... Ammonia
NHEJ ..... non-homologous-end-joining
P5C pyrroline-5-carboxylate
PAM ..... protospacer adjacent motif
PAS ..... pre-autophagosomal structure
PBS ..... phosphate-buffered saline
PC ..... pyruvate carboxylase
PDGFR ..... platelet derived growth factor receptor
PDH ..... pyruvate dehydrogenase
PDK1 ..... pyruvate dehydrogenase kinase 1
PDK-1 ..... phosphoinositide-dependent kinase-1
PE ..... phosphatidylethanolamine
PEP ..... phosphoenolpyruvate
PFK ..... phosphofructokinase
PGDH ..... phosphoglycerate dehydrogenase
PHD ..... prolyl hydroxylase
PKC ..... protein kinase C

PI (PtdIns) . . . . . phosphatidylinositol
PI3K . . . . . phosphoinositide 3-kinase
POX (PRODH) . . . . . proline dehydrogenase
PP2A . . . . . protein phosphatase 2A
PPP . . . . . pentose phosphate pathway
PRAS40 . . . . . 40kDa Proline-rich Akt substrate
PROTOR . . . . . protein observed with Rictor
PRPP phosphoribosyl-5-pyrophosphate
PPAT . . . . . phosphoribosylpyrophosphate amidotransferase
PRPS . . . . . phosphoribosyl-5-pyrophosphate synthase
PTB . . . . . phosphotyrosine binding
PTEN . . . . . phosphatase and tensin homologue deleted on chromosome 10
PYCR1 . . . . . pyrroline-5-carboxylate reductase
R5P ribose-5-phosphate
Raf . . . . . rapidly accelerated fibrosarcoma
RAPTOR . . . . . regulatory associated protein of mTOR
RB1CC1 (FIP200) . . . . . RB1-inducible coiled-coil protein
Rheb . . . . . Ras homolog enriched in brain
Ri5P ribulose-5-phosphate
RNA . . . . . ribonucleic acid
ROS . . . . . reactive oxygen species
RPIA . . . . . ribose-5-phosphate isomerase A
rpm . . . . . rotations per minute
RT . . . . . room temperature
RTK . . . . . receptor tyrosine kinase
Rubicon . . . . . RUN domain and cysteine-rich domain containing Beclin 1-interacting protein
S. cerevisiae . . . . . Saccharomyces cerevisiae
S6K1 . . . . . ribosomal protein S6 kinase
S7P sedoheptulose-7-phosphate

SAICAR ..... succinylaminoimidazolecarboxamide ribose-5-phosphate
SAPK ..... stress-activated protein kinase
SCD ..... stearoyl-CoA desaturase
SD ..... standard deviation
SDS-PAGE ..... sodiumdodecyl-sulfate polyacrylamide gel-electrophoresis
SGK ..... serum/glucocorticoid-regulated kinase
sgRNA ..... single guide RNA
SH (domains) ..... Src homology
shRNA ..... short hairpin RNA
siRNA ..... small interfering RNA
SIRT ..... sirtuin
SOS ..... son-of-sevenless
STAT3 ..... signal transducer and activator of transcription 3
TALDO ..... Transaldolase
TALEN ..... Transcription activator-like effector nuclease
TCA cycle ..... tricarboxylic acid cycle
TFs ..... transcription factors
TKT ..... transketolase
TKTL1/2 ..... transketolase-like 1/2
TSC1/2 ..... tuberous sclerosis complex 1/2
UBL ..... ubiquitin-like
ULK 1/2 ..... unc-51 like autophagy activating kinase 1
UMP ..... uridine monophosphate
UVRAG ..... Ultra-Violet irradiation Resistance-Associated Gene
VDAC ..... voltage-gated anion-dependent channel
VHL ..... von Hippel-Lindau E3 ligase
VPS ..... vacuolar protein sorting
X5P ..... xylulose- 5-phosphate
YPD ..... yeast extract peptone dextrose
ZFN ..... zinc-finger nucleases

Chapter 1

INTRODUCTION

1.1 Autophagy

1.1.1 Overview

Autophagy is a highly conserved process by which certain cellular components are degraded inside the cell through fusion with lysosomes[1]. The term autophagy is derived from ancient greek and means eating of self. Engulfed material is broken down into basic components and released into the cytosol for metabolic use, including for energy production and biosynthesis pathways. The key role of autophagy in cells is to maintain cellular nutrient and energy homeostasis under various conditions[2]. Approximately 1-1.5% of cellular proteins are degraded by autophagy per hour at basal rates, even under nutrient-rich conditions in the liver[3]. Several human diseases, including cancer, neurodegenerative disorders and increased susceptibility to infectious diseases have been linked to autophagy[4] (see section 1.1.5). Moreover, genetic knockout studies of core autophagy components in mice lead to death after birth, partly due to lack of sufficient energy reserves between placental metabolism and breast feeding[5]. In contrast to the proteasomal degradation system, autophagy is not just restricted to degradation of proteins but can also break down lipids, DNA and RNA[6,7]. Furthermore, the ubiquitin-proteasomal system consumes energy in form of ATP in the process of degradation, whereas autophagy can generate ATP through breakdown of macromolecules[7]. Autophagy is a very dynamic process which occurs at low levels, under basal conditions in all cells[8]. Multiple

signalling inputs regulate autophagy (looked at in detail in section 1.1.5), including many metabolites and a number of metabolic enzymes. The process is tightly regulated - basal levels play an important role in cellular homeostasis and fine tuning allows cells to adapt and survive in response to multiple stress conditions[9].

1.1.2 Types of autophagy

Currently, three defined types of autophagy in mammalian cells have been characterised. All have in common that contents are subject to lysosomal proteolytic degradation[10]. Once the engulfed cargo is exposed to resident proteases and lipases inside a lysosome, macromolecules are broken down to liberate free amino and fatty acids[11] (see section 1.1.4).

1.1.2.1 Macroautophagy

Macroautophagy, the most studied type of autophagy, is the process in which cellular contents are delivered and degraded by lysosomes (mammalian cells) or vacuoles (budding yeast) and recycled[12]. This is achieved by formation of double membrane-bound vesicles, referred to as an autophagosomes. They enclose various types of cellular material, including large structures prior to fusion with lysosomes (see figure 1.1). This process occurs via selective or non-selective mechanisms[13]. Damaged organelles, for example, are removed by organelle-specific macroautophagy processes such as mitophagy (degradation of mitochondria), pexophagy (degradation of peroxisomes) and ribophagy (degradation of ribosomes). This is generally achieved by cargo receptors that recognise cargo targeted for degradation, such as p62. Non-selective (cytoplasmic) macroautophagy (hereafter referred to as autophagy, unless otherwise stated) occurs at a basal level stimulated by different types of starvation (see section 1.1.5).

1.1.2.2 Microautophagy

Microautophagy, by contrast, is characterised by direct engulfment of cytoplasmic cargo into the lysosome (mammalian cells) or vacuole (budding yeast) through invagination of the lysosomal membrane. Microautophagy is important in the maintenance of organellar size, membrane homeostasis and cell survival under nitrogen

restriction[14]. Large structures can also be engulfed through microautophagy, and the process occurs via selective or non-selective mechanisms, such as micropexophagy or micromitophagy[10,13,14]. There is significant overlap in the autophagic core machinery and regulation with the other autophagy types, but this subject has been thoroughly reviewed elsewhere (see[14,15]).

1.1.2.3 Chaperone-mediated autophagy (CMA)

Chaperone-mediated autophagy (CMA) is a specialised form of autophagy that involves the direct translocation of unfolded, cytoplasmic proteins across the lysosomal membrane. This is mediated by a complex of chaperone proteins, including heat shock cognate 70 kDa protein (hsc70)[3]. Since membrane reorganisation is not involved, large structures, such as organelles can not be degraded via CMA[3] and the process is always selective[13]. Protein complexes are recognized by the lysosomal membrane receptor LAMP-2A (lysosomal-associated membrane protein 2A), resulting in their unfolding and degradation[6].

1.1.3 Autophagic core machinery

The core autophagy machinery is highly conserved from yeast to mammalian cells. In fact, key cellular components were first discovered in Saccharomyces cerevisiae (named in order of discovery, e.g. ATG1) and mammalian homologs have been identified. Whereas in budding yeast there is only one isoform for each gene in the pathway (e.g. ATG8), multiple isoforms exist in humans (e.g. LC3 family, see 1.1.4.2). In yeast, phagophore membrane formation is formed at a specialised compartment known as the pre-autophagosomal structure (PAS), a structure not found in mammals[8]. Yeast also don't have lysosomes, but instead one large vacuole[16]. To date, there are at least 36 genes involved in autophagic processes, all playing various roles in the molecular mechanism[12,17]. Out of those, 17 are considered essential to the core machinery for all types of autophagy[4,18]. In the literature, autophagy proteins are often divided into different functional groups, according to their involvement:

(1) ULK1 complex (or known as Atg1-ULK1 complex)

(2) VPS34 kinase complex (or known as PI3K or Beclin-1 complex)

(3) ATG12-ATG5-ATG16L complex

(4) LC3 conjugation system

In the following sections we will review how these complexes contribute to the process of autophagy.

1.1.4 Cellular and molecular mechanism

Autophagy involves the formation of vesicles (autophagosomes) that enclose portions of the cytoplasm. The process consists of a number of stages, (see figure 1.1). Autophagosome formation is controlled by a complex network and interplay of activating and/or inhibitory proteins (also see section 1.1.5). In this section, various stages of mammalian autophagy at looked at in more detail.

1.1.4.1 Induction and phagophore formation

In mammals, autophagy induction (also referred to as nucleation) is characterised by the formation of a flat double membrane (also known as phagophores). Currently, it is not completely clear as to where exactly in the cell the initiation of phagophore formation takes place and this topic is highly controversial in the field[20]. There is evidence that the membrane is likely to be derived primarily from the endoplasmic reticulum (ER) and possibly from the trans-Golgi and/or endosomes[21–23]. Other sources of phagophore membrane have been reported, such as plasma membrane and nuclear envelope[24,25], suggesting that there probably is not a requirement for a unique source of membrane. However, *de novo* membrane formation can not be excluded as a possibility due to a lack of suitable transmembrane proteins markers in autophagosomal membranes[10]. Two major protein complexes are involved in the regulation of phagophore formation:

ULK1 complex

The first complex is composed of the serine/threonine kinase Unc-51-like kinase 1 (ULK1), ATG13, ATG101, and RB1-inducible coiled-coil protein 1 (RB1CC1 also known as FIP200)[26,27]. ULK1 and ULK2 are orthologs of yeast ATG1[28]. The activation of ULK1/2 kinase leads to activation of ATG13 and FIP200[29]. The fully ac-

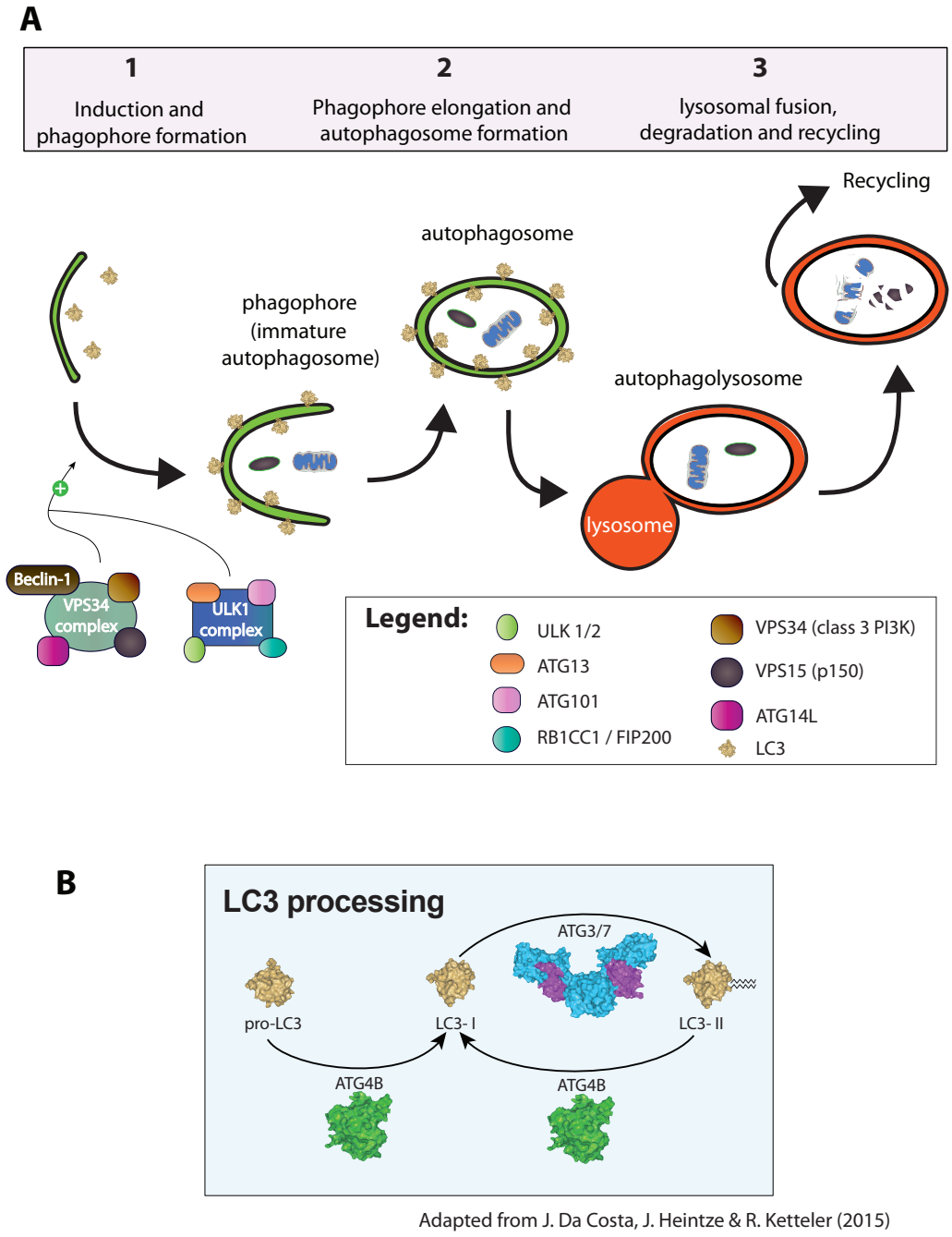

Figure 1.1: A) **Stages of autophagy biogenesis.** In the process of autophagosome formation, the molecular marker LC3 in its lipidated form gets incorporated into the maturing autophagosome. The phagophore induction is regulated by ULK1 and VPS34 kinase complexes. Autophagosomes fuse with lysosomes in order to degrade macromolecules and organelles. These are recycled and used for biosynthesis or energy generation. B) **LC3 processing**. Pro-LC3 gets proteolytically cleaved by ATG4B to LC3-I, which gets lipidated by addition of a PE-anchor via AGT3/7 to LC3-II. ATG4B also delipidates LC3-II to LC3-I. Figures are adapted from J. Da Costa, J. Heintze & R. Ketteler (2015)[19]

tivated complex is required to activate Beclin-1 (mammalian homologue of ATG6) by phosphorylation, which is a core part of the VPS34 kinase complex. Together with ATG2 and ATG18, the ULK1 complex regulates the cycling of ATG9 to and from the site of autophagosome formation.

VPS34 complex

The class III PI3K plays a positive role (compared to class I PI3K, see section 1.4.5.1) in the regulation of autophagy. The activated VPS34 complex generates PI(3)P, essential for phagophore nucleation. VPS34 is the catalytic subunit and aside from autophagy, is also involved in various membrane-sorting activities. Other proteins in the complex are Beclin-1, VPS15 (also known as p150) and Atg14L. Furthermore, a number of additional regulatory subunits that either promote or inhibit phagophore formation associate with the complex. These include the coiled-coil protein Ultra-Violet irradiation Resistance-Associated Gene (UVRAG), B-cell CLL/lymphoma-2 (Bcl-2), Bax-interacting factor 1 (Bif-1), Activating Molecule in Beclin-1-Regulated Autophagy (Ambra1),[30–32]. Rubicon (RUN domain and cysteine-rich domain containing beclin 1-interacting protein) and Bcl-2 negatively regulate autophagy via the VPS34 complex, whereas UVRAG, Bif-1, ATG14L and Ambra1 promote autophagy. These studies indicate that multiple complexes can exist within the cell and that they can tune the level of autophagy as needed[33]. Activated ULK1 and VPS34 complexes localize to the site of phagophore initiation, where they in turn activate downstream autophagy components.

1.1.4.2 Elongation and autophagosome formation

Sequestration and engulfment of cellular material proceeds as the phagophore membrane elongates. The phagophore elongation eventually leads to the formation of an autophagosome, which can be seen by electron microscopy as a double-membraned closed organelle.

ubiquitin-like (UBL) conjugation systems

Two crucial protein complexes involved in this stage of autophagy have been described to be ubiquitin-like (UBL) conjugation systems. Ubiquitin conjugation systems are composed of ubiquitin-activating enzymes (E1), ubiquitin-conjugating en-

zymes (E2), ubiquitin ligases (E3) and UBL proteins. As for canonical ubiquitin conjugation systems, these occur in multi-step processes in autophagosome formation. For both systems, ATG7 is the activating E1[34]. It transfers two UBLs, ATG8 and ATG12, to each cognate E2 enzyme (ATG3 and ATG10, respectively)[3]. ATG12 is then conjugated to ATG5 by formation of a covalent bond. ATG5-ATG12 forms a non-covalent complex with multiple copies of the coiled-coil protein ATG16L. This ATG16L complex localises to the site of the forming autophagosome and is essential for the elongation of the nascent phagophore[33].

LC3 family

The ATG5ATG12-Atg16L complex on the phagophore is the E3 for ATG8[35]. This conjugation system is fairly unique, since the lipid phosphatidylethanolamine (PE) is ligated to ATG8, rather than a protein. In mammalian cells, six ATG8 homologues exist, known as the microtubule-associated protein 1 light chain 3/gamma-aminobutyric acid receptor-associated protein (MAP1LC3/GABARAPs or short LC3s and GABARAPs) that form the LC3 family. Amongst those, there are LC3A, LC3B, LC3B2 and LC3C in the LC3 sub-family; and GABARAP, GABARAPL1 and GABARAPL2 in the GABARAP family[19,36]. The predominant and most characterised form of LC3 for the study of autophagy is LC3B (hereafter abbreviated to LC3). The nascent peptide of LC3 (known as pro-LC3) is proteolytically cleaved by the cysteine protease ATG4 family, of which ATG4B is the most prevalent and catalytically active[37]. This cleavage of pro-LC3 to LC3-I is required for autophagy, but can be bypassed by a recombinant LC3-G120 mutant[38]. LC3-II is found on both the inner and the outer surfaces of the autophagosome[16] (see figure 1.1). During autophagy, the synthesis and processing of LC3 is increased and it is used as a marker to monitor levels of autophagy in cells[12]. Recently, 67 interactions with other cellular proteins were reported in a large-scale proteomic study for the mammalian LC3 family[39].

LC3 family members also play an important role in selective autophagy: A number of ubiquitin-binding proteins, including p62 (also known as sequestosome 1 or SQSTM1)[40], Optineurin (OPTN)[41], NDP52[42] and NBR1[43] were found to be cargo

receptors for autophagy substrates[44]. Some of them play key roles in immunity, such as OPTN and NDP52. They interact with LC3 via a LIR (LC3-interacting region) motif that enables specific targeting to autophagosomes. To insure that proteins targeted for degradation are sequestered, many of the cargo receptors can recognise different ubiquitin chain linkages and thereby confer selectivity[45].

1.1.4.3 Fusion, degradation and recycling

The LC3 family proteins are thought to be involved in membrane tethering, hemifusion and possibly in the fusion of the phagophore membrane ends to form a closed autophagosome[46]. Many of the fundamental questions in the late stages of autophagy still remain unknown[47], but it is thought that the fusion event is mediated by the same machinery that is involved in homotypic vacuole membrane fusion. After the autophagosome has formed and is fully maturated, it fuses with an endosome or a lysosome[48]. This process is achieved via dynein-mediated transport along microtubules[49]. Fusion requires a number of proteins, including the VPS family, RAB7, endosomal sorting complexes required for transport proteins (ESCRTs) and SNAREs[50]. Most of those proteins are also involved in other cellular events, such as ER-golgi trafficking. Vesicular cargo is degraded by a series of lysosomal/vacuolar acid hydrolases[10].

The building blocks from the degradation of the macromolecules, in particular amino acids, are available for ATP-generating pathways and for maintenance of cellular functions like protein, DNA and RNA synthesis[4]. Lysosomal fusion is the final step in autophagy, and complete autophagic flux requires full lysosome function[4]. Therefore, lysosomotrophic agents such as ammonium chloride or vacuolar-type H+-ATPase inhibitors such as bafilomycin A1 are employed to experimentally inhibit autophagy[12]. They alter the pH of the lysosome and thereby impair autophagolysosome formation and flux[33]. Interestingly, the reduction of cytosolic pH (acidification) has recently been been shown to induce mitophagy and autophagy in SHSY5Y neuroblastoma cells[51]. Furthermore, ATG9, ATG2, ATG18 (WIPI-1 in mammals) and ATG21 have also been described to participate in transfer and recycling of components from the autophagosome membrane[4,48,52]. Taken together, the

formation of autophagosomes is a complex cellular process which can be regulated at multiple steps, by multiple mechanisms.

1.1.5 Regulation of autophagy

The regulation of autophagy is finely balanced by integration of multiple signals, including metabolites, ROS (see section 1.2.3), growth factors and other cellular cues. The regulatory network is very complex, since there are basal levels of autophagy in most cell types, and cells need the ability to respond to stimuli and conditions in a variety of scenarios and intensities. Regulation can occur via (fast) post-translational modifications and via (slow) transcriptional/translational reprogramming[2]. This section of the thesis will primarily focus on the regulation within individual cells. However, one should note that autophagy regulation is also crucial on a whole-organism level, manifested by roles in physiological processes such as development, aging and exercise.

1.1.5.1 Autophagy and disease

Misregulation of autophagic pathways have been widely implicated in many pathophysiological processes such as metabolic and neurodegenerative disorders, cardiovascular and pulmonary diseases and cancer[53,54]. For instance, accumulation of toxic or mutant proteins in brain tissue is found in many neurodegenerative conditions and autophagy promotes cell survival by their removal[55]. Disruption of autophagy-specific genes in neuronal cells (such as ATG5 and ATG7) lead to neurodegeneration in mice[56,57]. Deficiencies in autophagy have also been associated with a variety of cardiac pathologies, since the process is essential for general maintenance, repair, and adaptation of the heart tissue[58]. Furthermore, autophagy plays an important role in immune defence against invading bacteria and other pathogens. Upon cellular infection, autophagy is involved in the regulation of inflammation, antigen presentation, engulfment of microorganisms and degradation[59]. For instance, a mutation in the Atg16L gene that causes the inhibition of autophagy has been linked to Crohn's disease, which is a type of inflammatory bowel disease[60].
It is widely accepted that autophagy plays a key role in cancer, as it can both to

promote and inhibit tumorigenesis[53]. As outlined in chapter 1.2, reprogramming of metabolism is highly beneficial to cancer cells. On a cellular level, there need to be mechanisms to cope with the high demand of nutrients in order to support proliferation, growth and to deal with metabolic stress[10]. On a tissue level, there may be a lack of adequate nutrients before angiogenesis inside the tumor has occurred sufficiently[61]. Basal autophagy maintains intracellular organelle homeostasis by eliminating damaged organelles and proteins, thereby reducing genome instability and ROS (e.g. by eliminating damaged mitochondria, (see section 1.2.3))[62]. However, tumour cells may exploit the autophagic mechanism to facilitate tumour growth and to overcome nutrient-limiting conditions. The tumor microenvironment can be modulated via autophagy by supplying nutrients, promoting angiogenesis and by modulating the inflammatory response[63]. For instance, upregulation of autophagy via oncogenic Ras (see section 1.4.3) results in an increase in cell viability and tumorigenic potential by facilitating glycolysis and mitochondrial metabolism[64–66], leading to autophagy addiction for those cells[2]. Deletion of RB1CC1, a promoting factor of the UKL1 complex, inhibits mammary tumorigenesis in mice[67]. Furthermore, deletion of ATG7 in mice leads to Ras-mediated tumor supression in non-small- cell lung cancer (NSCLC)[62].

On the other hand, supressing autophagy or limiting autophagic flux can also promote tumorigenesis. A number of tumor supressor genes are part of the core autophagic machinery. Beclin-1 has been found to be mono-allelically deleted in human breast, ovarian and prostate cancer[53]. However, the role of Beclin-1 as a tumor supressor is still somewhat controversial, since a recent study suggested that the loss of the neighbouring gene breast cancer 1 (BRCA-1) is actually the primary factor for tumorigenesis[68]. Another tumor suppressor is UVRAG, which is mono-allelically deleted in colorectal cancer (CRC),[10]. Other known tumor supressors, such as p53, Bcl-2 and PTEN, have also implications in the regulation of autophagy[69]. As can be seen, the relationship of cancer and autophagy is relatively complex and depends on the mutational background. Hence, one should carefully consider the context-dependent role for the design of autophagy-based cancer thera-

peutics[61]. Taken together, understanding the regulation of autophagic pathways has implications for treatment of diseases, including cancer.

1.1.5.2 The regulation of phagophore initiation

The best studied regulators of starvation-induced autophagy are mTORC1 (see section 1.4.5.3), which forms part of the PI3K/Akt/mTOR axis (see section 1.4.5) and Adenosine monophosphate-activated protein kinase (AMPK). Both play important roles in the dynamic regulation of anabolic and catabolic processes through monitoring cellular nutrient levels and the cellular energy status (see figure 1.2). In consequence, autophagy is likely to be upregulated if metabolic enzymes or metabolite levels are decreased without compensatory mechanisms. High AMP levels, hypoxia and glucose starvation activate AMPK, which then inhibits mTORC1 and thereby induces autophagy. There are also several cellular mechanisms that monitor amino acid availability and influence the regulation of mTORC1 activity[2]. Much of the mechanistic insights of amino acid levels regulating mTORC1 activity originates from the past decade. For many years, it was known that they are essential in mTORC1 activation, but the exact mechanism(s) remained to be elucidated[70]. A key component in the activation is the regulation of its subcellular localisation and of associated proteins. Under nutrient-rich conditions, mTORC1 is diffused throughout the cytoplasm, but under amino acid starvation it localised rapidly to puncta, which were reported to be late endosomes/lysosomes[71]. Initial research efforts focussed on the mTORC1 activator Ras homolog enriched in brain (Rheb) and its negative regulator tuberous sclerosis complex (TSC)1/2 complex, see section 1.4.5.3)[72]. Rheb is located on late endosomal/lysosomal membranes, and multiple signal inputs such as Akt and ERK1/2 (see sections 1.4.4.3, 1.4.5.2 and 1.4.5.3 and figure 1.2) mediate TSC1/2 inhibition. mTORC1 can only be activated by binding to Rheb when the complex is recruited to these compartments. However, the activation through Rheb is not enough, as shown in $TSC2^{-/-}$ double knockout mouse embryonic fibroblasts (MEFs) under amino acid starvation conditions[73].
mTORC1 recruitment to late endosomes/lysosomes is mediated by cytosolic Rag (small) GTPases, which bind to raptor (mTORC1 subunit) in their active state and

thereby promote mTORC1 activity[74]. The family is composed of RagA-D which form heterodimers and bind to GDP or GTP. Rag GTPase activity is controlled by guanine exchange factors (GEFs) and GTPase-activating proteins (GAPs). One of the identified amino acid sensors is Leucyl-tRNA Synthetase (LRS), the enzyme that loads leucine onto its cognate tRNA for protein translation[75]. LRS acts as a GAP for the $RagD^{GTP}$/$RagB^{GDP}$ complex and thereby promotes mTORC signalling[75] in a non-canonical (i.e. not related to protein translation) function of this metabolic enzyme.

Another promoting factor is the pentameric protein complex named ragulator (also referred to as LAMTOR), which has been shown to play an important role in the recruitment of mTORC1 via monitoring amino acid levels[76]. Ragulator is composed of p18, p14, MP1, HBXIP, and C7orf59, which act in concert to bind to and tether Rags to the lysosomal membrane. Very recently, member 9 of the solute carrier 38 family (SLC38A9) was identified as a dynamic component of the Rag-Ragulator complex, depending on amino acid levels and the nucleotide binding state[77,78]. SLC38A9 was shown to transport arginine *in vitro*, over-expression disrupts amino acid sensitivity of mTORC1 signalling, whereas loss of SLC38A9 represses mTORC1 activation, particularly by arginine[78]. Once mTORC1 is activated, it inhibits phagophore initiation by phosphorylation of ULK1 and ATG9. ULK1 and ATG13 have multiple phosphorylation sites and their status depends on multiple signalling inputs[4]. ULK1 is also phosphorylated by AMPK directly under starvation conditions[79].

The regulation of autophagy is also tightly linked to the regulation of apoptosis. As discussed in section 1.1.4, the VPS34 complex is only functional in autophagy when interacting with Beclin-1. Thus, any modifications that disrupt or increase the interaction between Beclin-1 and its inhibitory binding partners can stimulate or inhibit autophagy. Under nutrient-rich conditions, Beclin-1 forms a complex with the apoptotic protein Bcl-2[2]. This interaction can be disrupted by death-associated protein kinase (DAPK)-mediated phosphorylation of Beclin-1 and

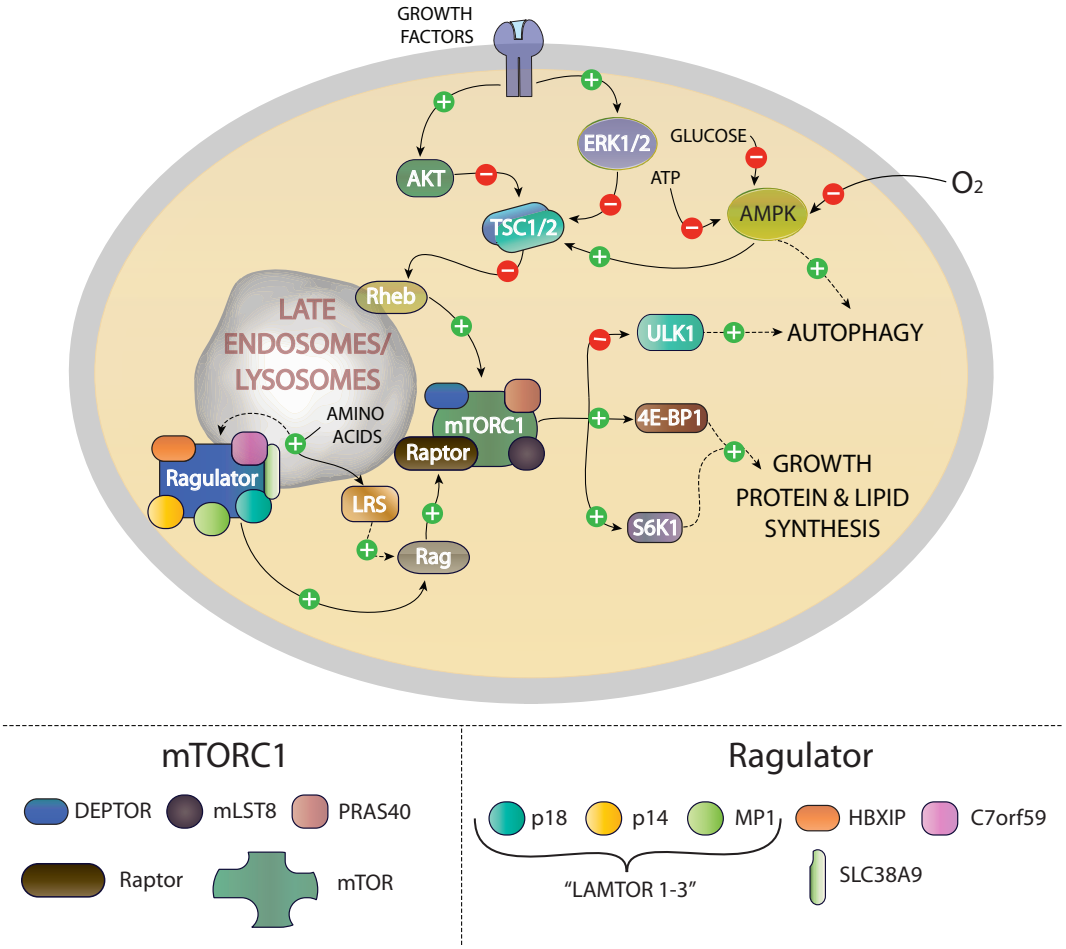

Figure 1.2: Regulation of mTORC1 signalling Growth factors, intracellular ATP concentrations, O_2 availability and endosomal/lysomal amino acid levels regulate autophagy via AMPK and the mTORC1 complex (mTOR, DEPTOR, mLST8, PRAS40 and raptor). Akt, ERK1/2 and AMPK inhibit TSC1/2-mediated inactivation of $Rheb^{GTP}$. Rheb is located on late endosomes/lysosomes and activates mTORC1 if bound to GTP. Rag GTPases, also postive regulators of mTORC1 signalling, are activated by the ragulator complex (composed of p18, p14, MP1, HBXIP, and C7orf59). This complex and associated proteins (LRS, SLC38A9) thether the Rag GTPases to the membrane and thereby contribute to the activation of mTORC1. Once active, mTORC1 phosphorylates downstream targets such as 4E-BP1 and S6K1, thereby increasing growth, lipid and protein biosynthesis. It also phosphorylates and thereby inactivates the ULK1 complex, which decreases phagophore initiation.

JNK1 (also known as MAPK8)-mediated phosphorylation of Bcl-2[80,81]. On the other hand, serine/threonine kinase 4 (STK4) inhibits autophagy by phosphorylation of Beclin-1 to enhance its interaction with BCL2[82]. Akt inhibition (see section 1.4.5.2) can also lead to an increase of autophagy, as the kinase phosphorylates and inhibits Beclin-1[83,84]. Under nutrient rich conditions, AMPK phosphorylation inhibits the non-autophagic function of VPS34; whereas under glucose starvation, ATG14 promotes AMPK-mediated phosphorylation of Beclin-1, thereby stimulating autophagy[48]. Furthermore, the metabolite trehalose was shown to reduce the p62/Beclin-1 ratio and thereby increases autophagy in the mouse brain frontal cortex[85].

1.1.5.3 Other regulatory mechanisms

Interestingly, several metabolites from different pathways have also been reported to regulate autophagosome formation independently from mTORC1. Ammonia (NH_4), the byproduct of glutamine degradation (glutaminolysis), stimulates autophagy via an ATG5-dependent mechanism, but not via mTORC1 or ULK1[86]. This is interesting from a metabolomic perspective, since glutaminolysis replenishes TCA cycle intermediates oxaloacetate or α-ketoglutarate (see 1.2.5), but competes with other nitrogen-dependent biosynthetic pathways, such as nucleotide synthesis[87]. However, recently glutaminolysis was also shown to be required for normoxic accumulation of HIF1α[88] (see section 1.2.8). Furthermore, high NH_4 levels are toxic, so autophagy stimulation may act as a survival mechanism in this instance.

Leucine depletion can also induce autophagy in an mTORC1-independent fashion, at least in mouse C2C12 myotubes[89]. Further studies in skeletal muscle revealed that LC3 and Bcl-2/adenovirus E1B protein-interacting protein (BNIP3) transcription is controlled via FoxO-dependent transcription[90] (see section 1.4.5.4). FoxO signalling is dependent on Akt activity, but not on mTORC1 (see 1.14).

ROS molecules (see section 1.2.3) are essential in low concentration as signalling molecules for autophagy induction[91]. However, they have also been shown to modulate ATG4B activity[92,93]. It remains unclear which ROS, whether it may be H_2O_2,

superoxide or another ROS, is the predominant regulator or whether different ROS play different roles in autophagy[93,94].

Interestingly, Acetyl-coenzyme A (Ac-CoA), the cofactor for multiple metabolic reactions and acetyl group donor for post-translational modifications (such as histones), was found to be involved in the regulation of autophagy in *S. cerevisiae* as well[95]. Fluctuations in Ac-CoA levels that effectively modulate autophagy were also confirmed in human cells (HCT-116) and a mouse model[96]. Inhibition of the Ac-CoA synthesis pathway induces autophagy, whilst high Ac-CoA levels have an inhibitory effect. It is thought that this may in part be achieved by acetylation of ATG3 or ATG7[95]. A number of compounds have been reported to induce autophagy in an mTORC1-independent fashion, although their mode of action remains illusive, suggesting additional mechanisms on a molecular level to regulate autophagy[97]. Taken together, numerous cellular enzymes and metabolites can affect the autophagic pathway. Considering that research efforts in cancer metabolism and autophagy have only taken off in the past few years, it is likely that various regulatory mechanisms still remain unknown.

1.2 Metabolic reprogramming in cancer

Cancer is a cumulative name for a number of devastating human illnesses, contributing to millions of mortalities each year worldwide[98]. $>$1.5 million invasive cancers were reported in 2012 in the US alone[98]. In the UK, $>$350,000 cases were diagnosed in 2013, which on average means 960 cases per day or one every two minutes (source: Cancer Research UK[99]). Amongst the most common types are mammary (breast), prostate, lung and bowel cancer, accounting 53% of all new cases in the UK in 2013. The 10-year survival rate is roughly 50%, since $>$160,000 deaths were caused by tumors in 2012. In the past decades, there has been great progress in diagnostic and therapeutic efforts in order to reduce incidence and mortality rates, especially for some types (e.g. stomach and bladder). Nonetheless, the incidence of diagnosis in Great Britain has increased by 30% compared to the late 1970s. Diagnosis for some tumor types (e.g. thyroid, liver, oral, and kidney) have increased

markedly, others have very poor diagnosis (e.g. pancreas) and high mortality (e.g. lung, bowel, breast and prostate).

The persistence and severity of this global health problem can be partially explained by the vast genetic heterogeneity of aberrant cells within and between tumors[100]. Large-scale DNA analyses of tumours, enabled through recent advantages in genome sequencing, showed an abundant and heterogeneous mutation load in cancer cells[101]. Within the tumor environment, there is a huge selection pressure for survival and proliferative capacity. This is why different tumors can acquire a vast array of mutations that cause malignance, metastasis and/or confer to drug resistance.

Over the past decades of research, several hallmarks of tumorigenesis have been identified. These include the upregulation of proliferative signalling, uncontrolled proliferation, avoidance of immune system responses, induction of angiogenesis, cell death resistance and alterations in metabolism[102]. Despite genetic heterogeneity within and between tumors, it is becoming evident that a number of metabolic alterations are required for malignant cancer cells[103]. Metabolic reprogramming is characterised by alterations in intracellular and extracellular metabolites that have profound effects on gene expression, cellular differentiation, and the tumor microenvironment. A number of metabolites play a crucial role in cancer metabolism - either their cellular levels as metabolic intermediates for biosynthesis, or as regulatory molecules. Glucose and glutamine are regarded as the two main substrates for proliferating cells, providing ATP, carbon and nitrogen sources for macromolecular synthesis[104,105]. Recent studies suggest that cellular metabolic reprogramming is accomplished by altered expression levels, isoform specificity and post-translational modifications, all fine-tuning individual enzymatic activity[11,102,106–108]. In this section, I will present key metabolic pathways in the cell and also specifically review the recent findings regarding metabolic reprogramming of cancer cells.

1.2.1 Oxidative phosphorylation

A universal metabolic requirement for any (physiological or tumor) cell is to generate energy in form of ATP. Under physiological conditions, ATP is produced via

oxidative phosphorylation (see figure 1.3 A) . Glucose is converted to pyruvate via glycolysis (see section 1.2.4), where it enters the TCA cycle (see section 1.2.5). Coenzyme nicotinamide adenine dinucleotide (NADH), which is generated by dehydrogenases in the process, acts as a donor in the electron transport chain (complexes I-IV), with oxygen (O_2) acting as an electron acceptor. This chain of reaction creates a gradient across the mitochondrial inner membrane, enabling movement of protons through ATP synthases. One molecule of glucose generates a net gain of two ATPs via glycolysis, but a net gain of 36 ATPs via oxidative phosphorylation. Therefore, it is more energy-efficient to utilise oxidative phosphorylation in order to generate ATP. However, this pathway requires adequate supply of O_2 (normoxic conditions), highlighting the importance of respiratory and cardiovascular systems across the animal kingdom. When O_2 supply is limited (hypoxic conditions), cells compensate ATP production by increasing the rate of glycolysis via the hypoxia response pathway (see figure 1.3 B and section 1.2.8). The increased consumption of glucose has a metabolic side effect: During glycolysis, NAD^+ is required, which is usually achieved by reduction of NADH via complex I in the electron transport chain. Therefore, pyruvate is reduced to lactate by lactate dehydrogenase (LDH), which is then excreted to the extracellular environment. This reaction also oxidises NADH, regenerating the cellular pool of NAD^+. ATP production via the glucose - lactate route is also known as glucose fermentation.

1.2.2 Warburg Effect

Interestingly, most likely all cancer cells have adopted a different metabolic strategy whereby they seem to depend on glycolysis for ATP production (also referred to as aerobic glycolysis)[109]. Both under normoxic and hypoxic conditions, cancer cells have very high consumption of glucose, high lactate excretion, a lower activity in the TCA cycle and lower rates of mitochondrial oxidative phosphorylation. This is quite remarkable, considering that cancer cells have such a high demand for energy in order to proliferate rapidly. Furthermore, it may seem counter-intuitive, since glycolysis is much less efficient for ATP production, and glucose fermentation increases acidity in the tissue. The abnormal ratio of glucose consumption/aerobic

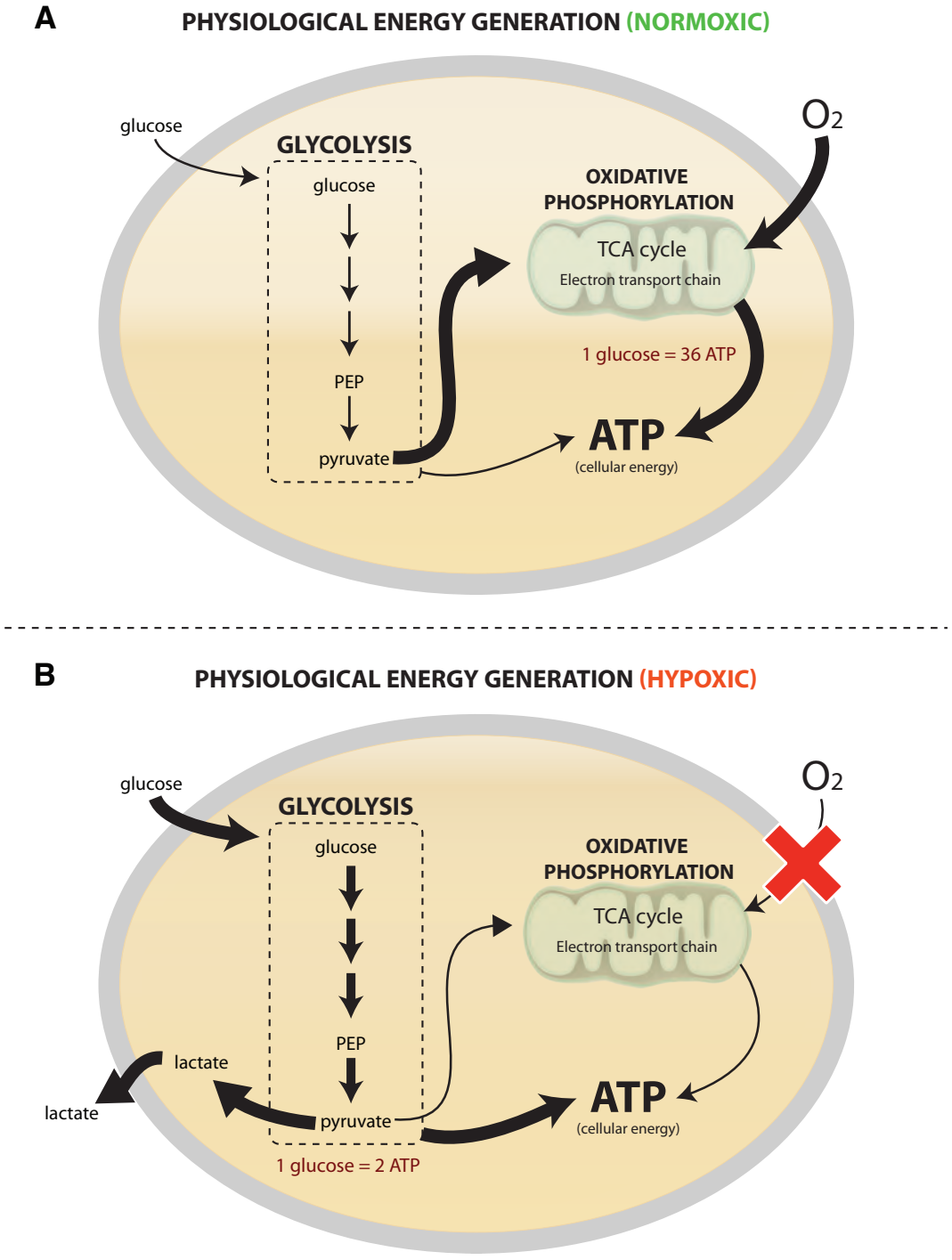

Figure 1.3: A) **ATP production under normoxic conditions**. Most the the ATP in the cell is generated via the electron transport chain in mitochondria, which is utilising reducing power that is generated by the TCA cycle. B) **ATP production under hypoxic conditions**. Under oxygen depletion, glycolysis is the main pathway to generate ATP. Excess pyruvate is converted to lactate and excreted from the cell. PEP - phosphoenolpyruvate.

respiration was first observed almost a century ago by Otto Warburg[110] and is also referred to as the Warburg effect. For decades, the Warburg effect was acknowledged, but almost nothing was known as to how and why cancer cells behave in such a fashion. Some of the cellular and molecular mechanisms have emerged only in the past few years, so we are only beginning to understand the complex network of dynamic metabolic regulation. However, it should be noted that aerobic glycolysis is not an exclusive feature of cancer cells, but also found under normoxic conditions in rapidly dividing physiological cells[111]. Growth factor or cytokine - activated macrophages and T-cells, for example, heavily rely on aerobic glycolysis, which is controlled via PI3K/Akt signalling (see section 1.4.5)[112]. Recent modelling data suggests that aerobic glycolysis is in fact more energy-efficient when cellular glucose uptake is high, due to limited solvent capacity of mitochondria versus glycolytic enzymes[109].However, cancer cells require much more than just ATP for proliferation. It is becoming clear that the heavy glucose uptake is also required for matching the metabolic needs of biosynthesis pathways (see sections 1.2.4, 1.2.5, 1.2.6, 1.2.9 and 1.3).

1.2.3 Reactive oxygen species

Another key requirement for cancer cells is protection against excessive levels of reactive oxygen species (ROS), also referred to as oxidative stress. ROS are a group of temporarily existing oxygen molecules that carry unpaired electrons, making them highly reactive with other molecules. They have been described as a double-edged sword in cancer biology[113], due to their dual role. On one hand, they are important physiological intra- and intercellular signalling molecules, regulating essential processes such as cell cycle progression[114] and autophagy[115] (see section 1.1.5). However, excessive levels block cell cycle progression and trigger apoptosis[11]. Increased ROS levels are usually concomitant with nutrient (glucose, amino acid) starvation and hypoxia[2] (see section 1.2.8). The cell predominantly eliminates ROS by non-enzymatic reactions with reduced glutathione, which is produced by NADPH-dependent reductases[103]. Excessive ROS levels are mainly caused by high metabolic activity, damaged mitochondria (including defective oxidative phospho-

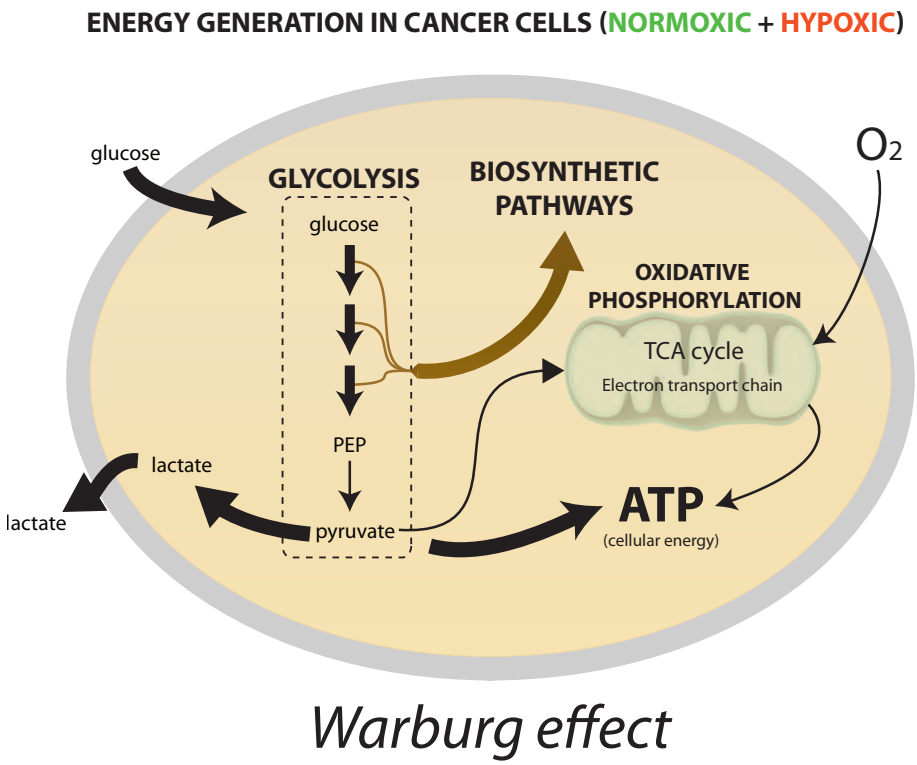

Figure 1.4: Warburg effect. Cancer cells predominantely have low rates of oxidative phosphorylation and higher glucose consumption, irrespective of the presence or absence of oxygen. It has become clear in the recent years that cancer cells supress parts of the TCA cycle and thereby oxidative phosphorylation. Instead, there is an increased demand of glucose due to high metabolic needs for biosynthesis pathways.

rylation) and hypoxic conditions, which are all features commonly found in tumors. NADPH, they key component for maintaining reduced glutathione, is predominantly produced via the oxidative phase of the Pentose Phosphate Pathway (PPP) (see section 1.3). In the following sections I will re-visit the key metabolic cellular pathways and discuss currently known molecular mechanisms by which cancer cells achieve metabolic reprogramming.

1.2.4 Glycolyis

Glycolysis describes 10 cytosolic reactions, mediating the catabolic breakdown of glucose (see figure 1.5). In the process, 1 molecule of glucose gets converted to 2x pyruvate, with a net production of 2x ATP and 2x NADH. Various metabolites of glycolysis are precursors to other metabolic pathways, and those can also feed into

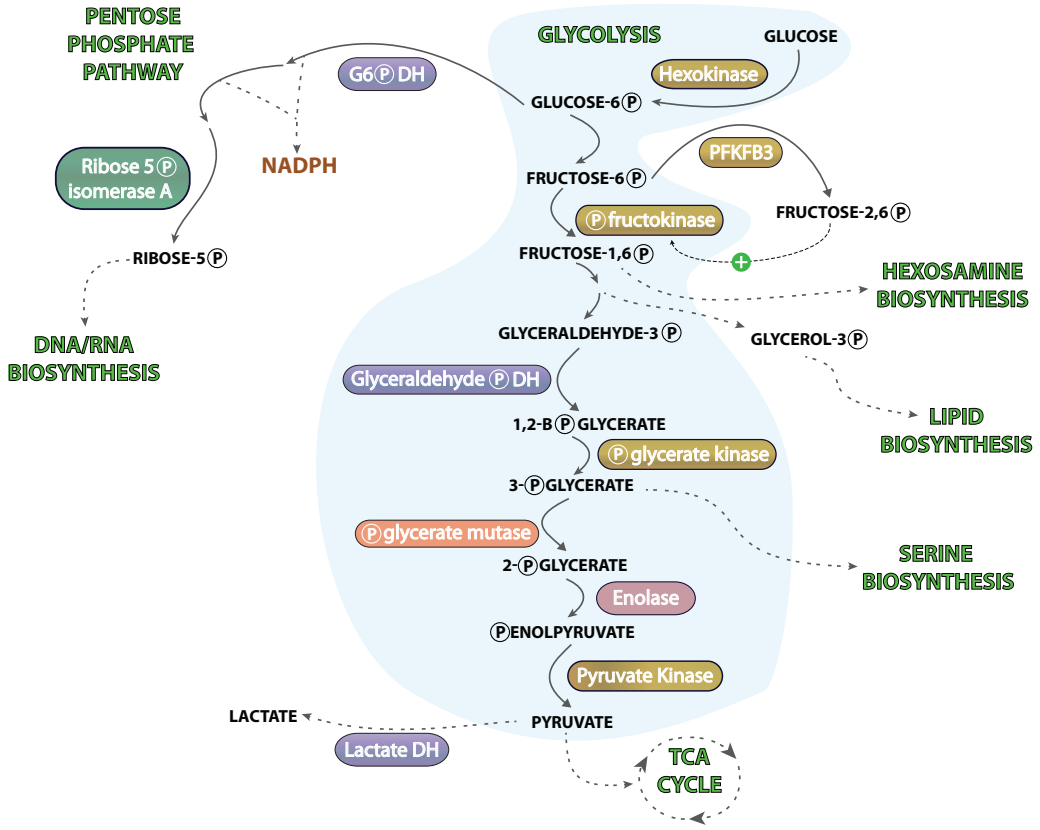

Figure 1.5: Overview of metabolites and enzymes in glycolysis and precursors of diverging pathways. Glucose metabolism generates a number of precursors for other anabolic pathways, such as nucleotide, lipid and amino acid metabolism. DH - Dehydrogenase, encircled Ps indicate ”phosphate”

different stages of glycolysis. Metabolic reprogramming, in order to increase synthesis of anabolic pathways, is achieved by some key enzymes and metabolite levels in this pathway. In particular, three enzymes have been found to play a substantial role: Hexokinase (HK), Phosphofructokinase (PFK) and Pyruvate kinase (PK).

1.2.4.1 Hexokinase

Hexokinases catalyse the first step of glycolysis, by converting glucose to glucose-6-phosphate (G6P). Apart from glycolysis, G6P is also utilised in a variety of other pathways, including, glycogenesis, the PPP, (see section 1.3) and the hexosamine biosynthetic pathway. G6P also directly regulates HK activity by in a negative feedback loop. There are four mammalian isoforms of HK (I-IV), of which HK-I and HK-II have a higher affinity for glucose and an N-terminal mitochondrial binding motif. HK-II has been identified to be involved in tumor development,

manifested by induced gene expression of HK-II and downregulation of HK-IV in tissues that don't normally express HK-II[116]. Furthermore, HK-II can interact with the voltage-gated anion channel (VDAC) in outer membrane of mitochondria[117,118]. This interaction gives HK-II preferential access to ATP (permeates the channel) and prevents binding of the pro-apoptotic factor Bax to the channel that would otherwise cause cytochrome c release and thereby trigger apoptosis[118,119]. The upregulation of HK-II expression is likely to be mediated via the Akt-mTORC1-HIF-1α signalling cascade[120] (see sections 1.2.8 and 1.4.5)

1.2.4.2 Phosphofructokinase

Phosphofructokinases convert fructose-6-phosphate (F6P) to fructose-bisphosphates (F1,6P and F2,6P). The reaction of F6P to F1,6P is the third step of glycolysis, it is essentially an irreversible reaction catalysed by PFK-1 and plays a crucial role in cellular metabolism[121,122]. Prior to this conversion in glycolysis, G6P and F6P may be used as a precursor for the ribonucleoside family via the PPP (see sections 1.2.9 and 1.3). Many different metabolites, enzymes and signalling pathways have been identified to modulate PFK-1 activity[123]. Those factors control its catalytic activity and consequently affect a number of processes, such as carbon flux, oxidative stress and tumor formation. High AMP levels increase its activity, but the most potent activator of PFK-1 is F2,6P. This regulation of PFK-1 activity is mediated by PFK-2. F6P to F2,6P conversion is reversible and most PFK-2 isoforms have both kinase and phosphatase activity. The expression of different PFK-2 isoforms that vary in activity is a powerful mechanism for metabolic reprogramming.

Interestingly, the PFKFB3 isoform of PFK-2 is reported to have almost no phosphatase activity and is expressed in a number of cancer cells. PFKFB3 kinase activity is regulated by a number of factors, including Ras (see section 1.4.4), AMPK (see section 1.4.5.3), the oncogenic transcription factor MYC and certain metabolite levels[122]. In T-cells from rheumatoid arthritis patients, glucose metabolism, redox balance and autophagy (see section 1.1) were reported to be impaired because of insufficient PFKFB3 activity and those phenotypes could be reverted by over-expression[124,125]. Another study in HCT-116 colon adenocarcinoma cells re-

ported that knockdown or pharmacological inhibition of PFKFB3 also leads to an increase of basal autophagy[126]. Furthermore, knockdown of the isoform PFKFB4 was found to increase non-selective and p62-dependent autophagy in a GFP-p62 based shRNA high-content screen, and also reported PFKB3 as a hit[127].

PFK-1 activity is negatively regulated by a number of key cellular metabolites. These include ATP, lactate, downstream glycolysis intermediate phosphoenolpyruvate (PEP, see section 1.2.4.3) and the TCA cycle metabolite citrate (see section 1.2.5), thereby all contributing factors of diverting carbon flux from glycolysis. PFK-1 activity has also been shown to be reduced by O-linked β-N-acetylglucosamine glycosylation.[123,128]. This post-translational modification was found to specifically occur in multiple tumors (lung, breast, prostate, liver, colon and cervical cancers), especially in late stages of malignancy[128].

1.2.4.3 Pyruvate kinase

Pyruvate kinases convert PEP to pyruvate, mediating the last step of glycolysis before the TCA cycle[129]. As outlined in section 1.2.4.2, high PEP levels reduce upstream glycolysis via inhibition of PFK-1. Furthermore, the product pyruvate can be converted to lactate and then excreted. 4 isoforms of PK exist in humans and are expressed in different cell types: PKM1, PKM2, a liver (L) and an erythrocyte isoform (R)[103,130]. In most cells, PKM1 is preferentially expressed and is most active as a tetramer. PKM2, however, is expressed in the majority of cells undergoing proliferation, including essentially all cancer cells[131]. It exists in a tetrameric or a dimeric complex, but is much less catalytically active compared to the other isoforms. Overall, preferential PKM2 expression slows TCA cycle entry and thereby is a key mediator of the Warburg effect and metabolic reprogramming[131].

Furthermore, PKM2 plays many key roles independent of its direct metabolic function[132] it regulates protein phosphorylation, transcription, and cell signal transduction. The isoform is involved in a positive regulatory feedback loop by binding HIF-1α in a complex with prolyl hydroxylase 3 (PHD3)[132,133]. It phosphorylates the TF signal transducer and activator of transcription 3 (STAT3) at Y705 and thereby activates transcription of MAP kinase kinase 5 (MEK5) in the MAP kinase pathway[134].

PKM2 also directly binds to and phosphorylates histone H3 at T11 upon epidermal growth factor receptor (EGFR) activation. PKM2-dependent H3 modifications are key for expression of cyclin D1 and c-Myc, leading to tumor cell proliferation, cell-cycle progression, and brain tumorigenesis[134,135].

Furthermore, PKM2 binds directly and selectively to tyrosine-phosphorylated peptides that result in release of the allosteric activator F1,6P, leading to inhibition of PKM2 enzymatic activity[136]. Recently, it has also been reported that PKM2 binds to transglutaminase type 2 (TG2) and that the interplay has a role in autophagy regulation[137]. This study is in accordance with data suggesting ammonia as a metabolite regulating autophagy[86] (see section 1.1.5). Therefore, enzymes and/or metabolites from major metabolic pathways can control autophagic flux.

Cumulatively, those findings show that PKM2 plays an important role in the growth and metabolic reprogramming of cancer cells.[131]. Furthermore, PKM2 was amongst the first metabolic enzymes to be implicated in exerting non-canonical functions that affect other cellular pathways.

1.2.5 TCA cycle

As outlined in section 1.2.1, the TCA cycle (see figure 1.2.5) plays an important role for oxidative phosphorylation by generating the reducing agents that feed into the electron transport chain. The complete cycle consists of 10 chemical reactions in the mitochondrial lumen, carried out by 7 enzymes. For one molecule of pyruvate is consumed, the net gain for the cycle is 3 NADH + 1 GTP + 2 CO_2 and QH_2. TCA cycle intermediates are also precursors for other biosynthetic pathways (see sections 1.2.6, 1.2.7 and 1.2.9). Therefore, some activity of the TCA cycle is required, even if oxidative phosphorylation is suppressed. Many of the TCA cycle (and affiliated) enzymes and their metabolites play an important role in cancer metabolism. In fact, tumor cells depend on intact mitochondria for some key biosynthetic reactions (see figure 1.6).

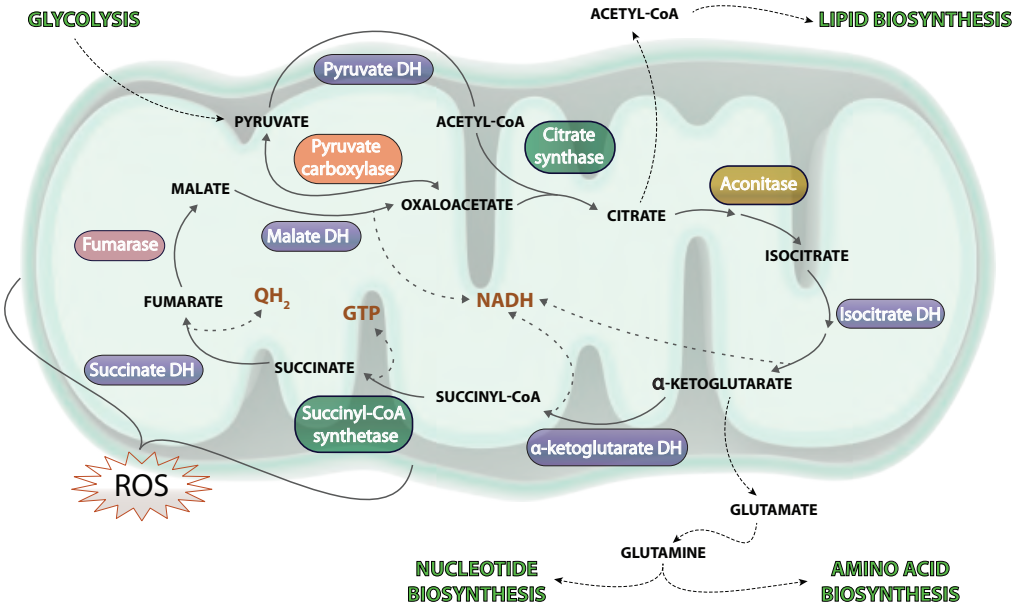

Figure 1.6: Overview of metabolites and enzymes in the TCA cycle. The TCA cycle takes place in the mitochondrial lumen. Apart from generating NADH, it also serves a key role for biosynthetic pathways. High TCA cycle activity contributes to the generation of ROS. DH - Dehydrogenase

1.2.5.1 Pyruvate entry

The carbon source of the TCA cycle is primarily glycolytic pyruvate. As outlined in 1.2.1 and 1.2.4, cancer cells have adopted various strategies to reduce pyruvate entry into the TCA cycle for ATP production, but it is required for biosynthetic pathways. Pyruvate is utilised by two enzymes: Pyruvate dehydrogenase (PDH) and Pyruvate carboxylase (PC).

PDH is a mitochondrial multimeric protein complex that catalyses the formation of Acetyl-Coenzyme A (Ac-CoA) from pyruvate and oxaloacetate. This conversion is the link of glycolysis to the TCA cyle. Acetyl-CoA is an important cellular cofactor that is required for multiple biochemical reactions, but its main function in the TCA cycle is as a carbon source for oxaloacetate (4 carbons) to citrate (6 carbons) conversion by citrate synthase. Interestingly, Ac-CoA was recently reported to be involved in starvation-induced autophagy[96] (see section 1.1.5). One of the key regulators of PDH is pyruvate dehydrogenase kinase 1 (PDK1)[103]. Downregulation of PDH activity via PDK1-mediated phosphorylation uncouples glycolysis from TCA

cycle entry. PDK-1 expression is regulated by a number of oncogenic signalling pathways, for example via the oncogene myc[11]

PC replenishes the pool of TCA cycle intermediates by converting pyruvate to oxaloacetate. This step is important, especially when TCA cycle intermediates are used for other biosynthetic pathways. Recently, PC was found to be over-expressed in human breast cancer tissue and PC activity was essential in highly metastatic cells in culture (MDA-MB-231 cells)[138]. Another study in human non-small-cell lung cancer (NSCLC) reported that PC over-expression enhances growth and knockdown decreases cell proliferation and colony formation[139]. Growth was also reduced in a mouse xenograft model. Furthermore, lipid and nucleotide biosynthesis was inhibited and altered ROS levels were observed.

1.2.5.2 Isocitrate Dehydrogenase

Isocitrate dehydrogenase 1 (IDH1) and IDH2 catalyze the oxidative decarboxylation of isocitrate to α-ketoglutarate (α-KG or known as 2-oxoglutarate). α-KG can also be converted into glutamate (and glutamine) (see section 1.2.6). Furthermore, it is the substrate of several dioxygenase enzymes. (see section 1.2.8). Interestingly, a number of cancer studies have reported a gain-of-function mutations in both IDH1 and IDH2, resulting in production of the oncometabolite 2-hydroxyglutarate (2-HG), which is chemically similar to α-KG[103]. It is thought that elevated levels of 2-HG competitively inhibit several dioxygenase enzymes that use α-KG as a substrate. This includes PHD2, the enzyme that destabilizes and thereby accelerates degradation of HIF-1α (see section 1.2.8).

1.2.6 Amino acid synthesis

There are 20 different L-type amino acids used for protein synthesis in all cells. Out of those, 9 are essential for humans to be taken up by diet as there are no biosynthetic pathways to generate those. As seen in this section cells have the ability to shift metabolic pathways for synthesis of non-essential amino acids according to the biosynthetic requirements.

1.2.6.1 Glutamine

It was first observed in 1950 by Harry Eagle that HeLa cells require 10- to 100-fold molar excess of glutamine compared to other amino acids[140]. The key role of glutamine in cancer cell metabolism has since been confirmed in multiple cell lines and *in vivo* tumors[141]. Besides glucose, glutamine is likely to be the second main contributor to *de novo* biosynthesis many cellular molecules as it is the source of reduced nitrogen. Glutamine is also crucial for purine and pyrimidine biosynthesis (see section 1.2.9). The uptake of glutamine is primarily mediated by the plasma membrane transporter solute carrier family 1 A5 (SLC1A5). Interestingly, loss of SLC1A5 was recently shown to inhibit cellular growth and induce autophagy[142]. Furthermore, glutamine contributes to the uptake of essential and non-essential amino acids: L-type amino acid transporter 1 (LAT1, or also known as SLC7A5) is a neutral amino acid antiporter that can exchange intracellular glutamine for leucine, isoleucine, valine, methionine and aromatic amino acids (phenylalanine, tyrosine and tryptophan)[11,143]. LAT1 is an obligate exchanger and requires an efflux substrate such as glutamine[143,144]. Together, these findings suggest a 2-step process by which glutamine levels effectively control proliferation via mTORC1 activity[142] (see sections 1.1.5 and 1.4.5.3). When glutamine is plentiful, essential amino acids (including leucine) are imported into the cell and activate mTORC1. In the absence of glutamine, intracellular leucine levels are low, mTORC1 is inhibited and autophagy is activated. Glutamine synthetase (GS) can also generate glutamine from α-ketoglutarate (a TCA-cycle intermediate) or vice versa, thereby feeding into the TCA cycle (see section 1.2.5) in a glycolysis-independent fashion. The enzyme has been reported to be over-expressed in Hepatocellular carcinoma (HCC)[145], but its regulation remains poorly understood[11].

1.2.6.2 Arginine

Arginine is a non-essential amino acid and also derived from glutamine. However, under certain metabolic conditions it can become essential. Arginine is composed of four nitrogen atoms, therefore serving as a precursor for many pathways, includ-

ing polyamine, creatine, agmatine, and pyrroline-5-carboxylate (P5C) and proline biosynthesis. Polyamine levels are elevated in proliferating cells and have been shown to promote tumor growth and inhibit apoptosis[146]. *De novo* biosynthesis of arginine forms part of the urea cycle. Two enzymes in the pathway, argininosuccinate lyase (ASL) and argininosuccinate synthase (ASS1) have been reported to be epigenetically silenced in an number of cancers, including HCC and renal cell carcinoma[11,147]. This silencing is associated with resistance to chemotherapy and poor prognosis[11,148]. It is quite striking that cancer cells would metabolically prefer to rely on exogenous arginine, rather than producing it themselves. Possible explanations for this so far have been that by downregulating ASL and ASS1, aspartate and ornithine accumulate and be can used for nucleotide and polyamine synthesis, respectively[11].

1.2.6.3 Proline

Proline biosynthesis is also closely linked to other metabolic pathways such as the TCA cycle (see section 1.2.5) , urea cycle, and the PPP (see section 1.3) via the pentose shunt. The amino acid is produced via P5C, which derives either from glutamate or ornithine. Interestingly, high cellular P5C concentrations stimulate 5-phosphoribosylpyrophosphate (PRPP) levels, which is a precursor for nucleotide synthesis[149] (see section 1.2.9). P5C is a substrate for pyrroline-5-carboxylate reductase (PYCR1), which is upregulated by the oncogenic transcription factor *c-myc*[150]. Furthermore, it was recently identified as one of the genes most commonly over-expressed in tumors[151]. There is some evidence that PYCR1 plays a role in replenishing the cellular pool of $NADP^+$ and thereby contributes to the oxidative phase of the PPP (see section 1.3), resulting in an increase in pyrimidine synthesis[152] (see section 1.2.9). The antagonist for PYCR1, the enzyme proline oxidase (POX) (also referred to as proline dehydrogenase (PRODH)), mediates proline degradation in the mitochondria[153]. In the process, electrons are fed via $FADH_2$ generation into the electron transport chain (see section 1.2.1), thereby increasing production of ATP[150]. This pathway is glycolysis-independent and therefore provides an alternative mechanism to generate ATP and promote survival when glucose

levels are low. However, the process also increases cellular ROS levels[154] (see section 1.2.3). Overexpression of POX was reported to induce apoptosis, trigger cell cycle arrest *in vitro* and to suppress tumor formation in a mouse xenograft model[150]. These events are likely to be mediated via ROS signalling[153] and suggest that POX is a tumor supressor. POX expression is upregulated via the energy level sensor AMPK and downregulated by the oncogenic transcription factor *c-myc*. Interestingly, recent findings suggest a more complex role for POX than previously anticipated, depending on conditions of the microtumor environment: Under low glucose conditions, POX main function is to generate ATP, but under hypoxic conditions, the key role is to induce basal autophagy via ROS[150] (see sections 1.1.5 and 1.2.3). Therefore, POX can act as a pro-survival or pro-apoptotic factor, depending on the context. Overall, the role of altered proline synthesis and degradation pathways in cancer cells is still not very well understood[11].

1.2.6.4 Diversion of glycolysis intermediates

For a number of non-essential amino acids, glucose is usually the supplier of the carbon source. Synthesis of aromatic amino acids for instance, require PEP and E4P (see sections 1.2.4.3 and 1.3) as precursors. Serine, glycine and cysteine biosynthesis originates from 3-phosphoglycerate (3-PG), a metabolite of glycolysis (see section 1.2.4). The enzyme that mediates the first step of this pathway is phosphoglycerate dehydrogenase (PGDH). Interestingly, the gene for the enzyme was either found to be amplified or upregulated in melanoma and breast cancer[155]. Metabolic isotope labelling showed that diversion of glycolytic flux to anabolic pathways can be beneficial to tumor development. Interestingly, the glycolytic enzyme phosphoglycerate mutase 1 (PGAM1), which converts 3-PG, to 2-phosphoglycerate (2-PG), was found to play a key role in metabolic reprogramming. 3-PG directly inhibits 6-phosphogluconate dehydrogenase (6PGDH) in the oxidative phase of the PPP (see section 1.3), whilst 2-PG activates PGDH to converge 3-PG into the first step of serine biosynthesis pathway[156,157]. Therefore, nucleotide and amino acid biosynthesis are directly affected by modulating the catalytic activity of this glycolytic enzyme.

1.2.7 Fatty acid metabolism

Fatty acid metabolism is associated with various cellular events, including energy generation, lipid synthesis, and post-translational modifications. Whilst the *de novo* synthesis is low in most cells, tumorigenic tissues have a dramatically increased demand for lipids in order to facilitate growth and to alter membrane composition for protection against oxidative stress[158,159]. A number of lipogenic enzymes, including ATP-citrate lyase (ACL)[160], Ac-CoA carboxylase (ACACA)[161], fatty acid synthase (FASN)[162] and stearoyl-CoA desaturase (SCD)[163] have been reported to be over-expressed in many types of cancers.

The biosynthesis and modification of fatty acid chains is tightly linked to the coenzyme and substrate Ac-CoA. One of the main sources of Ac-CoA in the cell is via the TCA cycle (see section 1.2.5), which is generated in the mitochondria. Ac-CoA can not be transported directly to the cytoplasm, but citrate can be exported and cleaved to oxaloacetate and Ac-CoA by ACL[160]. Oxaloacetate is reimported into the mitochondria via malate conversion, in order to maintain the pool of TCA cycle intermediates[11]. Cytosolic Ac-CoA is the substrate for various pathways, including fatty acid and cholesterol synthesis, as well as protein acetylation and prenylation[160]. The rewiring of Ac-CoA for biosynthesis, rather than for TCA cycle use, is controlled via the PI3K/Akt signalling pathway[164] (see section 1.4.5). Akt phosphorylates ACL, and thereby expands the cytosolic pool of Ac-CoA. The fatty acid synthesis pathway commences with the carboxylation of Ac-CoA to malonyl-CoA, which is synthesised by ACACA. The next steps are sequential synthesis reactions to form the 16-carbon fatty acid chain palmitate. These condensation reactions are catalysed by FASN, which is a large (250 kDa) multifunctional, homodimeric complex. Interestingly, a recent study in ovarian cancer cells showed that pharmacological inhibition or shRNA mediated knockdown of FASN induces basal autophagy and lysosomal degradation of PI3K signaling proteins[165]. In summary, fatty acid synthesis is tightly linked to other biosynthetic pathways and controlled by cellular signalling pathways.

1.2.8 Hypoxia response

Low O_2 concentrations (hypoxia) are a common feature in a tumor microenvironment. When O_2 is limited, ATP production predominantely via the TCA cycle in the mitochondria will lead to oxidative stress (see section 1.2.3). The consequences of low O_2 availability are counteracted by tumor cells via regulation of TFs such as hypoxia-inducible factor (HIF) complexes. The HIF-1 (hypoxia inducible factor 1) signaling pathway plays a key role in the regulation of cellular metabolism. Under normoxic conditions, the HIF-1α subunits are hydroxylated by the prolyl hydroxylase 2 (PHD2) enzyme, resulting in their recognition by the E3 ubiquitin ligase von Hippel-Lindau tumor suppressor (VHL) and subsequent degradation[166]. This hydroxylation reaction is O_2-dependent and also requires the TCA cycle intermediate α-KG (see section 1.2.5). Under hypoxic conditions, prolyl hydroxylation is suppressed due to lack of O_2, allowing HIF-1α to escape VHL-mediated degradation. HIF-1 then accumulates and leads to an increased expression of many HIF-1 target genes. These include glucose transporters and several key enzymes of glycolysis, such as HK-II, PFK-1 and PKM2[129,167]. This transcriptional regulation increases ATP generation in the cytosol by conversion of glucose to pyruvate[168]. HIF-1 also promotes lactic acid production by upregulating lactate dehydrogenase A (LDHA). This facilitates a sufficiently high cytoplasmic NAD^+:NADH, crucial for glycolytic flux through the NADH-dependent enzyme glyceraldehyde-3-phosphate dehydrogenase (GAPDH). Furthermore, it promotes expression of PDK1[169], reducing TCA cycle activity (see section 1.2.5). It also limits glucose flow into certain biosynthetic pathways that are dependent on TCA cycle intermediates. This includes citrate[167], an inhibitor of PFK-1 (see section 1.2.4.2), thereby shifting glucose metabolism to the PPP (see section 1.3). Certain metabolites, including succinate, fumarate and ROS are inhibitors of PHD2 activity, therefore stabilising HIF-1α and mediating the hypoxia response[105]. HIF-1α mRNA levels are also increased via the Akt/mTORC1 signalling cascade[70] (see section 1.4.5). Overall, HIF-1α stabilisation impacts the flux of multiple metabolic pathways[103].

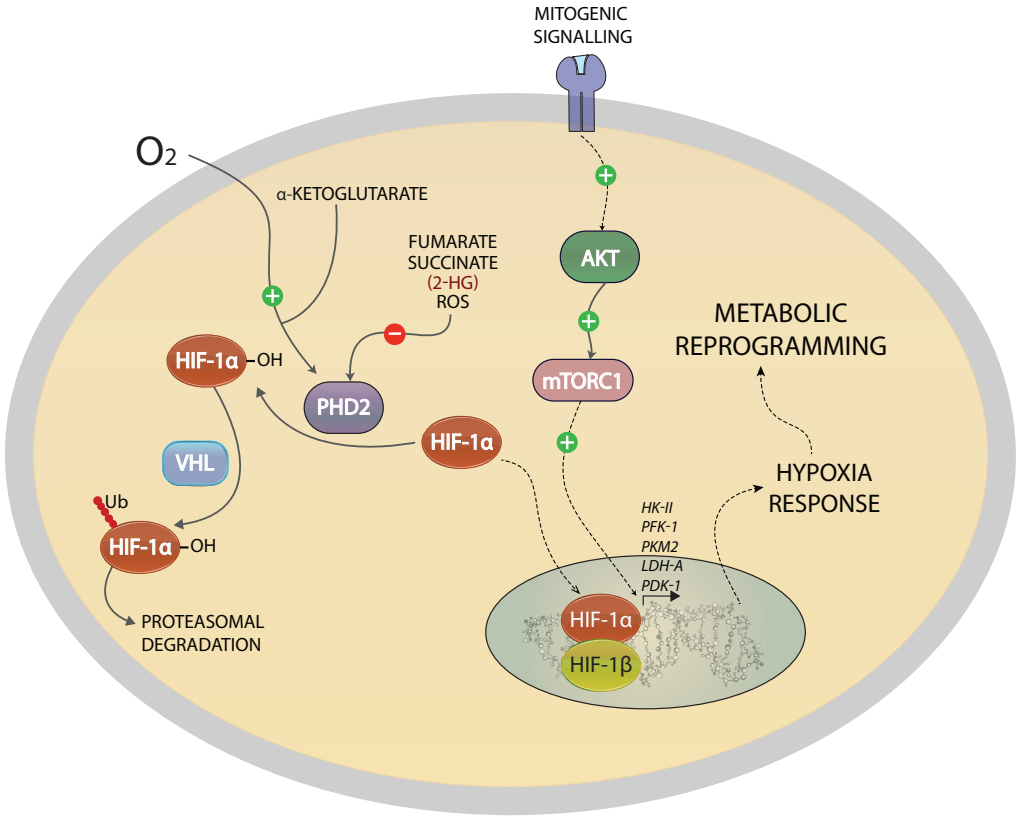

Figure 1.7: Hypoxia response. The hypoxia response is mediated via the HIF-1α subunit and regulates a number of metabolic enzymes. Under normoxic conditions, the HIF-1α subunits are hydroxylated PHD2, which targets them for degradation. However, the hydroxylation reaction can be modulated by various inputs. Under hypoxic conditions, the hydroxylation reaction is suppressed and HIF-1α to escapes VHL-mediated degradation.

1.2.9 Nucleotide synthesis

A universal feature of almost all cells is the generation of nucleotides (see figure 1.8). These are utilised for multiple cellular purposes, including:

(1) as precursors for DNA, RNA and $NAD(P)^+$ synthesis

(2) as energy carriers (ATP, GTP)

(2) as secondary messengers (cAMP, cGMP, di-cAMP-cGMP)

(4) as cofactors for anabolic synthesis pathways (ATP, GTP)

(5) as regulators in metabolic and signalling pathways (AMP)

All nucleotides are composed of a base (guanine, adenine, thymine, cytidine or uracil) and a 5-carbon pentose, either ribose 5-phosphate (R5P) or 2-deoxyribose

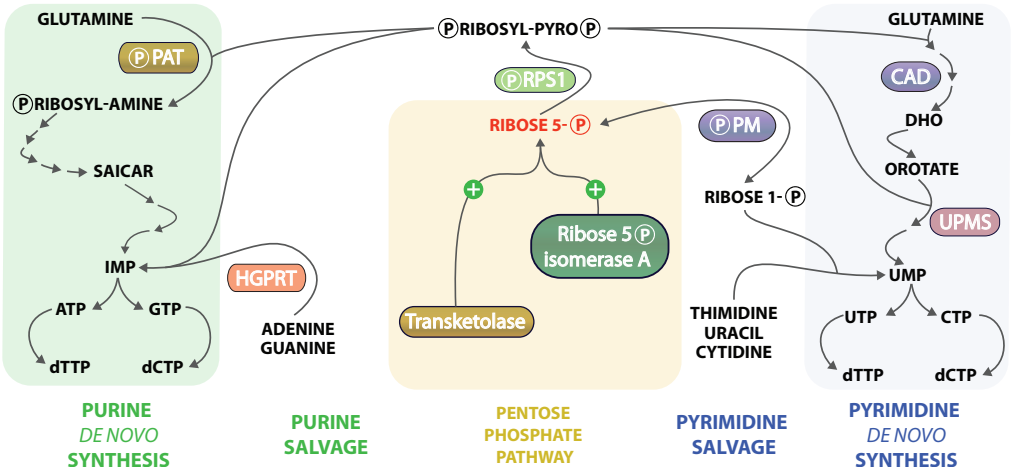

Figure 1.8: Nucleotide synthesis pathways: Four pathways (purine and pyrimidine *de novo* and salvage) contribute to the generation of nucleotides in the cell. All require phosphoribosylpyrophosphate (PRPP), which is generated from ribose-5-phosphate via the pentose phosphate pathway, either through ribose-5-phosphate A isomerase or transketolase (see figure 1.9). PRPP is produced by enzymes in the PRPS family.

5-phosphate (dR5P). Bases are either produced through *de novo* synthesis or acquired by nutrient uptake (if available to the cell). *De novo* nucleotide synthesis takes place via pyrimidine (thymine, cytidine and uridine) and purine (guanine and adenine) biosynthesis. Importantly, 5-phosphoribosyl-1-pyrophosphate (PRPP) is required as a precursor for all four pathways that contribute to nucleotide synthesis (purine/pyrimidine *de novo*/salvage pathways) (see figure 1.8). So far, three different enzymes that have PRPP synthetase activity were identified: PRPS1, PRPS2, and PRPS1L1 (PRPS1-like 1)[170]. PRPS1L1 is expressed only in a few tissues. Interestingly, shRNA-mediated PRPS1L1 knockdown increased autophagic flux in a GFP-p62 based high content screen in prostate cancer (Beclin1$^{+/-}$ stable EGFP-p62 iBMK) cells[127] (see section 1.1.4.2).

1.2.9.1 Purines

The nucleotides (d)ATP and (d)GTP are generated via a common precursor inosine monophosphate (IMP) in the purine synthesis pathway. This pathway is composed of 10 enzymatic steps, mediated by 6 enzymes. The first and rate-limiting step is catalysed by phosphoribosylpyrophosphate amidotransferase (PPAT), which

requires glutamine and PRPP to generate 5-phosphoribosyl-1-amine. Interestingly, the downstream intermediate succinylaminoimidazolecarboxamide ribose-5-phosphate (SAICAR) was recently reported to specifically bind to PKM2 (but not PKM1), thereby stimulating enzymatic activity and promoting tumor survival[106] (see section 1.2.4.3). The authors found that increased SAICAR concentrations in human lung cancer (A549) cells consequently increased cellular energy levels, glucose uptake, and lactate production.[106].

1.2.9.2 Pyrimidines

On the other hand, uridine monophosphate (UMP) is the common precursor for dTTP, UTP and (d)CTP in the pyrimidine synthesis pathway. This pathway consists of 6 intermediates and all reactions are catalysed by 3 enzymes. The purine and pyrimidine salvage pathways are an important part of nucleotide metabolism, as the *de novo* synthesis pathways are very energy consuming: 5 ATP are required for 1 molecule of IMP. Interestingly, one of the major enzymes of the pathway, Carbamoyl-phosphate synthetase 2, aspartate transcarbamylase, and dihydroorotase (CAD), was recently shown to form distinct puncta upon stimulation of amino acids in an mTORC1-dependent manner[171,172]. These findings support the notion of localised sub-cytoplasmic structures/complexes that are involved in biosynthesis.

1.2.9.3 NAD biosynthesis

The *de novo* biosynthesis of molecules in the NAD family is closely linked to nucleotide synthesis. The common precursor nicotinic acid adenine dinucleotide (NaAD) contains two phosphoribosyl nucleotide moieties, one of which is ATP and one which is a nicotinic acid mononucleotide (NaMN). The latter is produced via tryptophan in a *de novo* synthesis pathway,[173], but other precursors include nicotinic acid, nicotinamide or nicotinamide riboside in salvage pathways[174]. The NAD family of molecules is, like nucleotides, used for multiple cellular processes[174]. As outlined in sections 1.2.1 and 1.2.3, NAD(P)H is an important electron donor for the electron transport chain, gluthathione reduction and a co-factor for enzymatic reactions. More recently, the NAD family has also been found to be involved in non-redox reactions: these molecules can be substrates of ADP-ribosyl cyclases in

order to generate cyclic ADP-ribose (cADPR), a second messenger which plays a role in Ca^{2+} signalling[175]. Furthermore, NAD is used by ADP-ribosyltransferases for post-translational modification purposes of various proteins. As with ubiquitination, there are multiple types of ADP-ribosylation (e.g. poly- or mono-) and so far they have been linked to processes like DNA repair, transcription control, signal transduction, and ER stress pathways[176]. Interestingly, several members of the ADP-ribosyltransferase diphtheria toxin-like (ARTDs or also referred to as PARPs) or the sirtuin (SIRT) family have been associated with the regulation of metabolism and autophagy[176]. ARTD10 for instance, was found to colocalise with p62 in HeLa cells[177]. The NAD-dependent deacetylase SIRT1 was reported to be a positive regulator for H_2O_2-induced autophagy[178]. On the other hand, pharmacological inhibition of SIRT1 in MCF-7 human breast cancer cells was found to increase autophagic cell death[179]. Furthermore, SIRT1-mediated deacetylation has been described to fine-tune FoxO signalling (see section 1.4.5.4) by directing the TF to selective targets. SIRT3 has been associated with the regulation of mitochondrial complexes (see section 1.2.1), it increases IDH activity (see section 1.2.5), it also increases fatty acid catabolism and it may play a role in amino acid metabolism[180].
Conclusively, the current evidence suggests that NAD levels, the NAD^+:NADH ratio and NADPH availability all have a profound effect on cellular metabolism and autophagy.

1.3 Pentose Phosphate pathway

Most metabolic cancer studies to this point have focused on glucose and glutamine alterations, but cancer cells utilize a great variety of other nutrients[11]. Their contribution to tumorigenesis remains largely understudied. One of those is Ribose-5-phosphate (R5P) a, precursor of *de novo* synthesis of all molecules in the ribonucleoside family (including DNA, RNA and NAD(P)H)[181] (see figure 1.8). Due to high proliferation rates and strong metabolic requirements, nucleotide synthesis is essential to cancer cells[182]. In fact, aberrant signalling, for instance when mediated by oncogenic Ras (see section 1.4.3), can divert glycolytic flux to biosyn-

thetic pathways such as the Pentose Phosphate Pathway (PPP)[108,183]. The PPP is an essential pathway for a number of cellular processes. Depending on the tissue and conditions, between 5-30% of glucose is diverted into the PPP[181]. *De novo* R5P synthesis is a key outcome of the PPP. The second key metabolite generated by the PPP is NADPH from $NADP^+$. In its reduced form, it is a key component for protection against excessive intracellular ROS (see section 1.2.3)[184–187].

1.3.1 Overview

The PPP is composed of an oxidative and a non-oxidative phase (see figure 1.9 for an overview). The oxidative phase of the PPP produces two molecules of NADPH per molecule of G6P, in three irreversible enzymatic reactions. First, Glucose-6-phosphate dehydrogenase (G6PDH) converts G6P to 6-phospho-gluconolactone and generates one molecule of NAPDH. Second, phosphogluconolactonase converts 6-phosphogluconolactone to 6-phosphogluconate. Third, 6-phosphogluconate dehydrogenase (6PGDH) converts 6-phosphogluconate to ribulose-5-phosphate (Ri5P) and NAPDH.

Ri5P then is the starting point of the non-oxidative phase of the PPP. All enzymatic reactions in the non-oxidative phase of the PPP are reversible, allowing cells to adapt to the dynamic metabolic demands. Ri5P is converted to R5P and xylulose-5-phosphate (X5P) by ribose-5-phosphate isomerase (RPIA, see chapter 1.3.3) and pentose epimerase, respectively. The enzymes in the TKT family transfer two carbon groups from X5P to R5P to generate sedoheptulose-7-phosphate (S7P) and glyceraldehyde-3-phosphate (G3P). Transaldolase (TALDO) transfers three-carbon groups from S7P to G3P to generate erythrose-4-phosphate (E4P) and fructose-6-phosphate (F6P). Finally, TKT transfers two-carbon groups from X5P to E4P to generate G3P and F6P. A number of the metabolites in the non-oxidative phase can re-enter glycolysis, showing a tight link between both pathways.

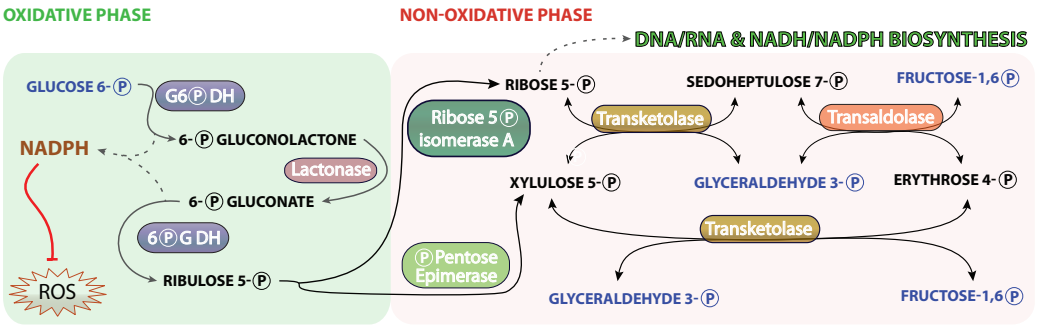

Figure 1.9: Pentose phosphate pathway overview. When glucose is channeled through the oxidative phase (essentially irreversible), NADPH is generated in the process. RPIA forms part of the non-oxidative arm of pentose phosphate pathway and generates R5P, which is a precursor for all ribonucleoside molecules (see figure 1.8). Molecules in blue are also part of the glycolytic pathway. Via joint action of TKT and TALDO, R5P can be also be generated from glycolysis intermediates.

1.3.2 Glucose-6-phosphate dehydrogenase

A number of enzymes from the PPP have been found to play a role in cancer metabolism. Glucose-6-phosphate dehydrogenase (G6PDH) and enzymes in the TKT family (transketolase-like 1 (TKTL1) and TKTL2), for instance, were reported to be significanlty up-regulated in cervical, lung, gastric, colorectal, and endometrial cancers[181,188,189]. G6PDH is the rate-limiting enzyme in the PPP and plays key roles in cell survival and cellular redox homeostasis. Interestingly, G6PDH dimerisation is required for enzymatic activity, and then enzyme has been reported to be present in higher-order complexes as well. G6PDH activity and expression levels are regulated by several signaling pathways through post-translational modifications and changes in gene expression. For instance, epidermal growth factor (EGF) stimulation triggers the release of bound G6PDH (from currently unknown structures) to the soluble fraction, which increases the activity[190]. Furthermore, the $NADP^+$/NADPH ratio is another known modulator for G6PDH activity. Whilst $NADP^+$ is essential for function, the product NADPH is a negative regulator of G6PDH. However, G6PDH activity is continuously kept higher in cancer cells compared to normal tissue, since they have a very high rate of NADPH consumption[191]. Furthermore, the tumor supressor p53 inhibits glucose entry intro the oxidative phase of the PPP through direct binding to G6PDH[192].

1.3.3 Ribose-5-phosphate isomerase A

Ribose-5-phosphate isomerase A (RPIA, alternatively: Phosphoriboisomerase; ribose 5-phosphate epimerase; ribose 5-phosphate isomerase A) is a 30kDa (311 residues) enzyme that catalyses the isomerase reaction of Ri5P to R5P[193], thereby playing a key role in the PPP. R5P can be converted to other phosphorylated sugars (see figure 1.8) via the enzyme Phosphoribosylpyrophosphate (PRPP) synthase, a conversion that is the first step in purine, pyrimidine, histidine and NAD family biosynthesis. Ribose-5 phosphate isomerases are conserved from bacteria to mammals, due to the key role in metabolism (see figure 1.10). Interestingly, there is an additional N-terminal stretch of 74 amino acids that is only found in mammals, but not in insects(e.g. *D. melanogaster*), budding yeast (e.g. *S. cerevisiae*) or bacteria (e.g. *E.coli*). The aspartate (D) residue at position 160 is crucial for the catalytic function in humans[194–196]. Furthermore, scansite analysis revealed a potential Grb2 - SH3 binding motif (P19) (see section 1.4.3) in this amino acid stretch, as well as predicted Akt (see section 1.4.5.2), AMPK kinase and ERK (see section 1.4.4.3) binding motifs[197].

There is a human *RPIB* gene, but it is thought to be a pseudo-gene and expression or function has yet to be determined[194]. Comparatively little knowledge of RPIA has been accumulated over the years, and most of the work done on the enzyme has been in bacteria or lower eukaryotes.

The results that have been published, however, are very interesting indeed. In a *D. melanogaster* study (Wang et al[198]) in 2012, the authors generated and studied a strain with low RPI levels in neuronal cells (RPIA homolog, see figure 1.10). They reported enhanced lifespan, increased resistance to oxidative stress and higher levels of NADPH. Interestingly, this effect was due to specific neuronal promoters, but was not observed when RPI was depleted in the entire organism. There were also no significant phenotypes regarding life span when RPI was over-expressed. The paper did not describe a molecular mechanism for the observed increase in life span, but they speculated TOR signalling (see 1.4.5.3) may be involved. Another group of scientists discovered a single patient with RPIA deficiency[199]. The phenotype

was characterised as leukoencephalopathy and peripheral neuropathy in humans, due to a point mutation and a truncation in the other allele. Intriguingly, one of the reported mutations in the patient (deletion of a G nucleotide a position 540) does not match the RPIA sequence deposited on publicly available nucleic acid database repositories (such as the International Nucleotide Sequence Database Collaboration), however, the residue in question is likely to be in position 762. The authors probably assumed that the expression of RPIA starts at a putative second start codon (see figure 1.10), but they do not show any western blot or proteomic data confirming this assumption. Other findings in metabolic diseases, such as transaldolase (TALDO) deficiency[200] indicate that defects in pentose and polyol metabolism may form a new area of inborn metabolic disorders[201].

The "aging" group that studied RPI in fruit flies[198] published another paper in 2014, on this occasion studying RPIA in human hepatocellular carcinoma (HCC) patients and transformed liver cancer cell lines (Ciou et al[202]). They identified RPIA as an oncogene, with increased proliferation upon over-expression, mediated via MAPK (ERK) signalling. Their cellular findings on increased proliferation upon RPIA over-expression were backed up with a mouse xenograft model. Recently, Xu et al[185] also confirmed that RPIA expression is upregulated almost two-fold in HCC tumors. Another study in human colorectal cancer (CRC) cells showed that down-regulation of microRNA 124, which occurs frequently in CRC patients, increased transcription of RPIA and PRPS1 mRNAs, thereby re-wiring glucose metabolism to nucleotide synthesis[191]. However, another study in breast cancer found that the locus of RPIA is hypermethylated (i.e. inactivated) via STAT1-mediated signalling. Cumulatively, this indicates that the role of RPIA in cancer may depend on tissue type. In conclusion from the current literature, there are some interesting findings that link RPIA to signalling, cancer and neurodegeneration. Therefore, studying RPIA further was of particular interest given the dependence of cancer cells on metabolic signalling and autophagy[107,131,203] (see sections 1.2 and 1.1).

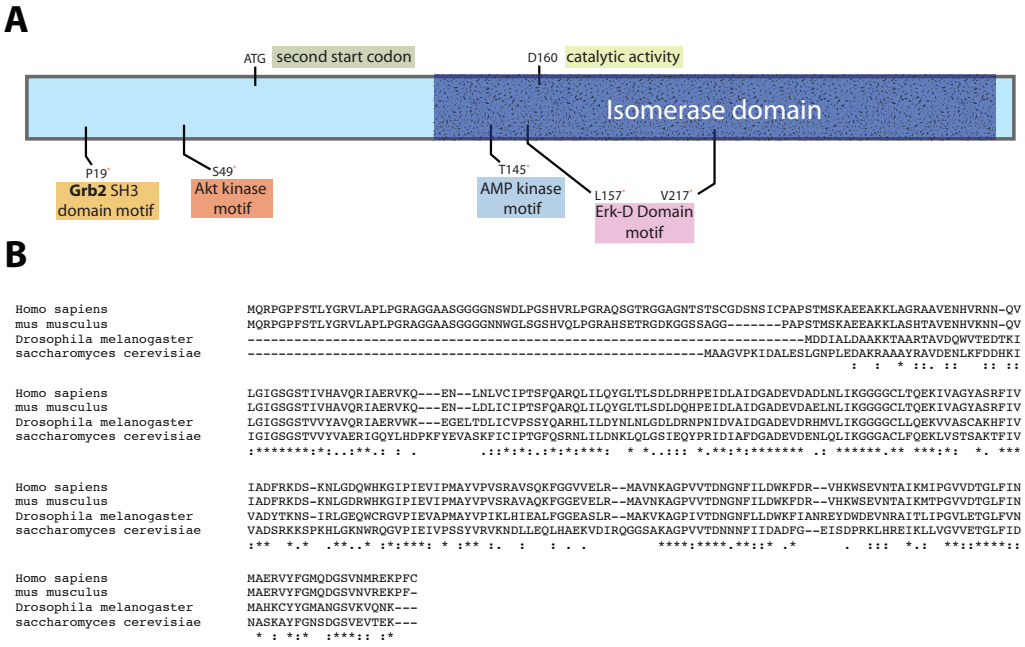

Figure 1.10: RPIA DNA and protein sequence A) RPIA has a putative second start codon and its catalytic activity depends on residue D160. A number of potential residues in RPIA could be modulated by signalling factors. Prediction from protein sequence was performed wirth Scansite 3. B) Protein sequence comparison of RPIA in human (*Homo sapiens*), mouse (*Mus musculus*), fruit fly (*Drosophila melanogaster*) and budding yeast (*S. cerevisiae*) reveals that the mammalian peptide has an additional 74 residues at its N-terminal compared to other homologs. Sequences were obtained from the International Nucleotide Sequence Database Collaboration (GenBank) and sequence alignment was performed using ClustalW.

1.3.4 Transketolase

Transketolase (TKT) is part of the non-oxidative arm of the PPP and catalyses the reaction of G3P and F6P to X5P and E4P, and vice versa (see figure 1.9). The compound oxythiamine was identified as a potent inhibitor of TKT, since the enzymatic function is thiamine pyrophosphate-dependent[204]. Since the enzymatic reactions are reversible, the direction of metabolic flux in the PPP can be regulated depending on different conditions (such as oxidative stress) in the cell. If NADPH demands exceed those of R5P, it can be produced through the oxidative arm via conversion of R5P back to G6P (mediated by TKT, TALDO and phosphoglucoisomerase)[205]. On the other hand, if R5P is in high demand for biosynthesis, TKT and TALDO reverse the reactions and channel glycolysis intermediates G3P and

F6P into the non-oxidative phase[103,205]. Interestingly, the non-oxidative arm of the PPP for nucleotide synthesis is used up to 80% by some cancer cells, as radiolabelled ^{13}C-glucose experiments indicate[204]. Mechanistically, it has been shown that TKT binds to and is regulated by Akt (see section 1.4.5.2)[206]. Phosphorylation enhances TKT enzymatic activity and thereby increases carbon flow through the non-oxidative phase of the PPP. Upstream regulation of Akt was shown to be mTORC2 (see section 1.4.5.3) and lysine dependent.

Therefore, elevated expression of non-oxidative PPP enzymes are often upregulated in cancers[184–187], and some cancer cells even induce the expression of TKT-like genes[207]. However, whether they have TKT enzymatic activity, is still currently controversial in the field[208]. The role of TALDO in cancer is currently still unclear. Although TALDO expression has been shown to be increased in cancerous liver cells[205], genomic deletion of TALDO in mice increases the prevalence to develop HCC[209]. This may have to do with disturbing the redox balance permanently and therefore generating excessive ROS, ultimately causing mutations and cancer.

Another study recently linked the PPP to autophagy in *Dictyostelium discoideum*: the serine/threonine kinase Atg1 (see section 1.1.3) was identified to interact with TKT[210]. The authors report that the activity of endogenous TKT is affected by changes in expression levels of ATG1. In HEK293T cells, they found that ULK1 positively regulates TKT, and this regulation is ULK1 kinase activity dependent. Taken together, the data suggest crosstalk between the PI3K/Akt/mTOR pathway, the PPP and autophagy.

1.4 Grb2-mediated signalling

1.4.1 Receptor tyrosine kinases

Regulation of autophagy and metabolism (see sections 1.1 and 1.2) is mediated by a number of signalling pathways. In this section, receptor tyrosine kinases (RTKs) and some of their downstream signalling cascades will be introduced. RTKs are a major class of molecules mediating the transmission of information from extracellular signalling factors to the inner of the cell. They are key regulators of many

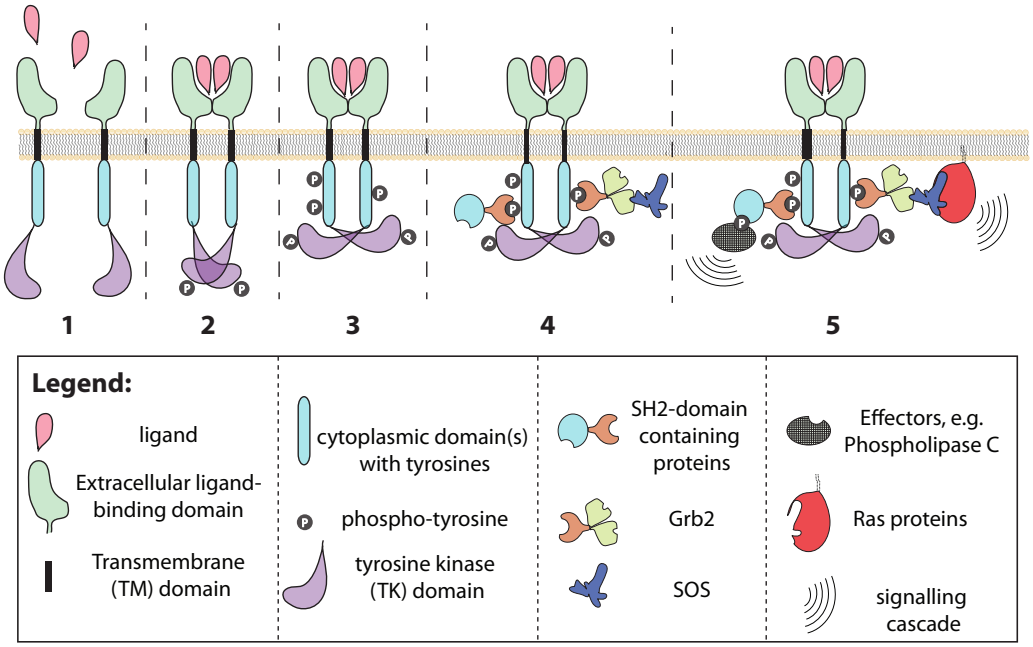

Figure 1.11: Receptor tyrosine kinase signalling cascade 1) Dimerisation and ligand binding 2) first phase transphosphorylation, increasing catalytic activity by 50-200 fold. 3) second phase transphosphorylation. 4) recruitment of docking and adapter proteins (e.g. Grb2) that bind phosphorylated tyrosine residues on the receptor. 5) Phosphorylation of recruited adapter proteins and recruitment of downstream signalling molecules (e.g. PLC or Ras) leading to recruitment of other proteins (e.g. kinases) that amplify and diversify the signalling network.

cellular processes, including proliferation, migration and differentiation[211]. The mechanism of activation, the overall structure and key components of signalling pathways are largely conserved from *C.elegans* to humans[212]. Aberrant signalling has been shown to cause a variety of diseases, including inflammation, diabetes, various cancers, severe bone disorders, arteriosclerosis and angiogenesis[211,213]. Those result from genetic changes that affect the abundance, activity, sub-cellular localization or the regulation of RTKs. So far, 58 RTKs have been identified in humans, and they are classified into 20 subfamilies[211,212]. In cancer cells, two important subfamilies are class I (EGFR family) and class II (insulin receptor family)[213].

All RTKs have three characteristic structural domains in common:

(1) extracellular ligand-binding domain (N-terminal)

(2) a transmembrane domain (single transmembrane-spanning helix)

(3) cytoplasmic tyrosine kinase domain(s) (C-terminal)

The general view for the mechanism of action for RTKs is that upon ligand binding on the extracellular side, the receptors undergo conformational changes that lead to dimerisation and transautophosphorylation of tyrosine residues on the C-terminal intracellular domain, creating a docking site for adaptor proteins that mediate downstream signalling[211]. Ligand binding is usually associated with receptor homo- or heterodimerisation, although some RTKs, such as the insulin receptor, are composed of constitutive, disulphide bond-linked dimers. The C-terminal domain is composed of a protein tyrosine kinase domain and can contain juxtamembrane regulatory regions. Prior to ligand activation, each receptor is autoinhibited and inactive[214]. The exact mechanism of autoinhibition is variable across RTK subfamilies. Whereas the insulin receptor family is activated via trans-phosphorylation, the EGFR family monomers dimerise such that an activator lobe of one monomer binds to a receiver lobe on the other, leading to the required conformational change for activation. Once active, it proceeds to sequential tyrosine trans-phosphorylation events.

1.4.2 Grb2

At that point, the signalling pathways are amplified and diversified. Further receptor phosphorylation may be aided by binding of adaptor proteins, which can also be phosphorylated themselves by the receptor. Adaptors often contain Src homology 2 (SH2) and phosphotyrosine binding (PTB) domains, which allow association with activated receptors, as well as domains that enable interactions with downstream signalling effectors. One of the key adaptors is growth factor receptor bound protein 2 (Grb2), which binds to phosphorylated tyrosine motifs via the SH2 domain. Grb2 plays an important role as a crucial regulator of mitogenic signalling[100,215].

A number of RTKs are able to recruit Grb2 via the SH2 domain. Amongst those are epidermal growth factor receptor (EGFR),platelet derived growth factor receptor(PDGFR) and hepatocyte growth factor receptor (HGFR)[100,216].

Grb2 is ubiquitously expressed in all tissues during development[217] and knockout causes embryonic lethality in mice[218]. The protein is mainly known to promote

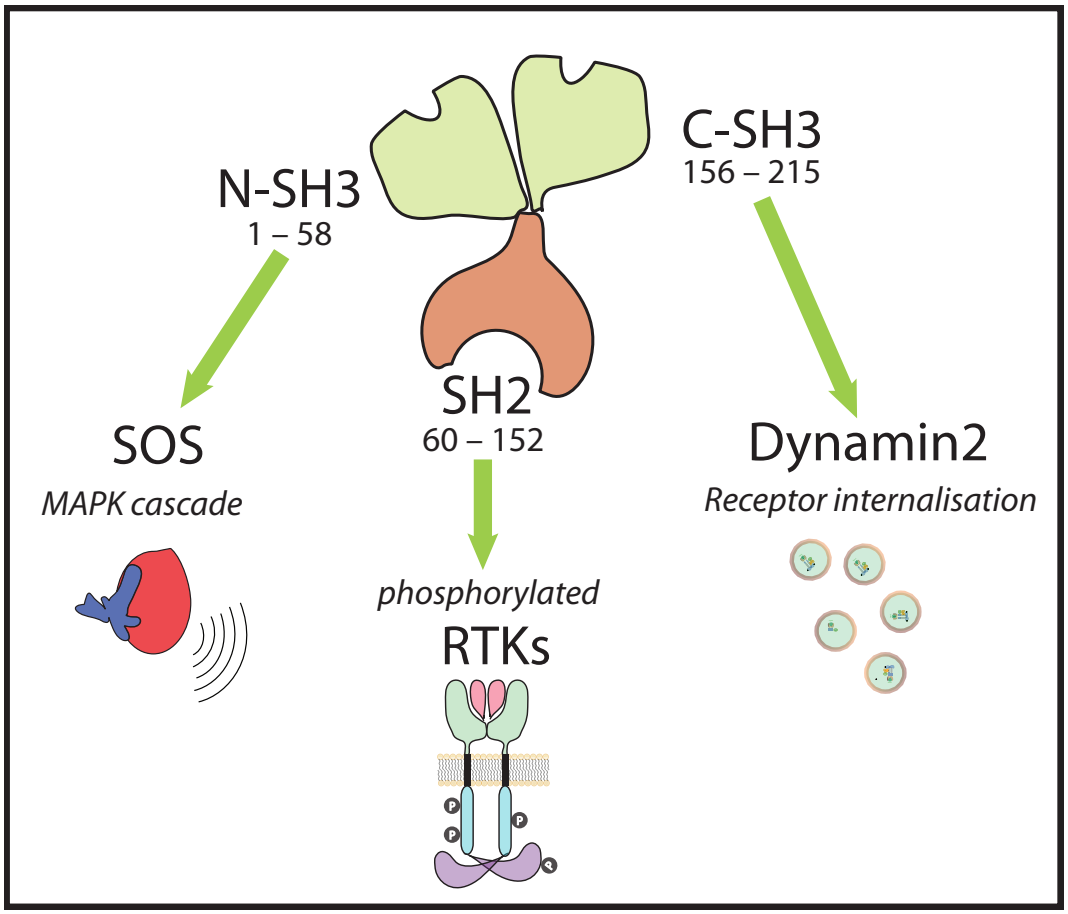

Figure 1.12: Grb2 domain structure. Grb2 is a key adaptor protein in linking receptors to many signalling cascades. Names of domains and residues are indicated. N-SH3: N-terminal src homology 3 domain, SH2: Src homology 2 domain, C-SH3: C-terminal SH3 domain

RTK signalling, however, an inhibitory role in basal (non-ligand) phosphorylation of fibroblast growth factor receptor 2 (FGFR2) has been reported[219,220]. Apart from its SH2 domain, it contains two flanking src homology 3 (SH3) domains[221] and has no enzymatic activity itself (see modular organisation of Grb2 in figure 1.12). The C-terminal SH3 domain of Grb2 can bind to dynamin2, which is important for clathrin-mediated endocytosis after receptor activation[222].

1.4.3 Grb2-Ras signalling pathway

Grb2 also binds strongly to the proline-rich motifs in Son-Of-Sevenless (SOS)[223–225] via the SH3 domains. SOS is a GEF that activates family members of Ras, which are a class of small GTPases. These are proteins that are activated

when bound to GTP, and inactive when bound to GDP. In humans, there are four highly homologous Ras proteins of approximately 21 kDa size: H-Ras, N-Ras, K-Ras4A and K-Ras4B, whereby the latter two are different splice variants[226]. Binding of prenylated (membrane bound) Ras proteins to EGFR via adaptors leads to increased clustering at certain membrane locations, where Ras is tethered and activated[227]. Ras activation can subsequently lead toMAPK and PI3K signalling cascade activation (see section 1.4.4), thereby serving as key players to couple cell surface receptors to intracellular signalling pathways[226,228]. Ras itself and associated proteins are frequently mutated in cancers[53,183,229,230]. The most common mutations in Ras are disturbing the binding of GTPase-activating proteins (GAPs), hence constitutively rendering Ras in its active form[226,230]. Interestingly, an oncogenic, constitutively active variant of Ras (K-Ras^{G12D}) was recently shown to divert glucose flux into the PPP in order to increase precursors for various biosynthesis pathways[108,183].

1.4.4 MAPK pathway

Ras activation initiates a number of signalling cascades in different compartments of the cell, leading to amplification and diversification of signals[231]. For most of the downstream effectors, alternatively spliced isoforms have been identified[231]. However, their abundance and activity are usually specific for a cell type or condition, giving certain isoforms unique signalling properties that divert from the main MAPK pathway and hence won't be further discussed here.

1.4.4.1 Raf

In the MAPK pathway, Ras activates Raf family members (A-Raf, B-Raf and C-Raf in humans), which are cytoplasmic serine/threonine kinase proteins[232] ranging from 70 - 100 kDa in size[233] and are also referred to as MAP3K- or MAPKKK-acting kinases in the literature. Whereas C-Raf (or referred to as Raf-1) is ubiquitously expressed, A-Raf has been detected in multiple tissues, such as heart, intestine, spleen, cartilage, thymus and cerebellum[234]. B-Raf is present in multiple isoforms and is strongly expressed in the fetal brain and adult cerebrum[235]. The current

understanding from mouse knockout studies is, that C-Raf is essential and the other two main isoforms play more specialised roles[232,233]. Raf activity is regulated by a number of kinases and phosphatases, including Akt isoforms (or known as protein kinase B, PKB)[236] (see section 1.4.5.2), Protein Phosphatases 1 and 2a (PP1 and PP2A)[237] and the Raf downstream effector extracellular signal-regulated kinase 1 (ERK1)[238] (see section 1.4.4.3) in a negative feedback loop.

1.4.4.2 MEK

Rafs activate other (MAP2K) serine/threonine kinases, namely MAPK/ERK Kinase 1 (MEK1) and MEK2, also sometimes referred to as MAPK Kinase 1 (MKK1) and MKK2[239]. Both MEKs are conserved in eukaryotes, ubiquitously expressed, share aproximately 80% sequence identity and have a molecular weight of 45 kDa[240]. They are composed of a large, regulatory N-terminal domain, followed by a catalytic domain and a shorter C- terminal region[231] and have been reported as dual-specificity kinases, due to their ability to phosphorylate tyrosine and serine/threonine residues[241]. While Raf isoforms are expressed at relatively low levels, high MEK expression levels ensure amplification of the signaling cascade[240,242]. For activation, MEKs are phosphorylated on two serine residues (S218 and S222 in MEK1, S222 and S226 in MEK2)[231,241,242]. Both MEKs have been found to be important for cell survival *in vitro*[243]. MEK1 has been shown to inhibit MEK2-dependent ERK signaling[244] and ERK can also inhibit MEKs in a negative feedback loop[241]. Interestingly, in a constitutively active K-Ras^{G12D} mouse model, expression levels of several glycolytic genes and RPIA, are significantly decreased by pharmacological inhibition of MEK[183].

1.4.4.3 ERK

MEKs in turn phosphorylate MAPK proteins. This group includes the ERK family (ERK1/2 and ERK5), the p38 kinase family and the c-Jun N-terminal kinase (JNK) family (also referred to as stress-activated protein kinase (SAPK))[245,246]. ERK1/ERK2, also known as p44/p42 MAP kinases, phosphorylate a large variety of nuclear and cytoplasmic substrates involved in many cellular responses, such as cell proliferation, differentiation, survival and motility[243,247]. These various cell

fate decisions are achieved by differences in the duration and magnitude of ERK activity, and by subcellular compartmentalisation[248,249]. The latter is accomplished by scaffolding proteins with varying compositions that restrict ERK signaling cascades to different subcellular compartments[228]. ERK1 and ERK2 are 44- and 42-kDa serine/threonine hydrophilic non-receptor kinases, respectively, with 90% sequence identity in mammalian cells[246,247]. Although there are some indications regarding specific roles[250,251], data from knock-out mice show that they functionally largely compensate each other[246]. Both ERK1 and ERK2 are expressed in most tissues in mammals, with ERK2 expression levels generally higher than those of ERK1[231]. MEKs activate ERK1 and ERK2 on threonine and tyrosine residues (T202/Y204 in ERK1)[239,240]. ERK activity is highly regulated by MAP kinase phosphatases (MKPs), including serine/threonine, tyrosine, and dual-specificity phosphatases (DUSPs), all playing a key role in fine-tuning the magnitude and duration of kinase activation[231,246]. In humans, at least 10 MKPs have been identified[231,249], for some of those, their expression is induced and regulated by MAPK signalling[252]. ERK activity is also regulated by scaffolding proteins that co-localize signalling components and direct the pathways to specific targets[253,254].

1.4.4.4 ERK targets

Once activated, ERKs directly (or indirectly) phosphorylate serine/threonine residues on hundreds of target proteins, predominantly in the nucleus, but also in the cytoplasm, mitochondria, Golgi and ER[245]. Amongst those are cytosolic, growth factor responsive proteins including upstream MAPK components such as EGFR[255], SOS[256] and several MKPs[246,252] that function as negative feedback loops. Nuclear targets generally involve TFs that regulate gene expression, transcriptional repression and chromatin remodeling[245,254]. These include c-Fos and the E twenty-six (Ets) family, amongst which the most studied are Elk-1 and Ets-1[245,246].

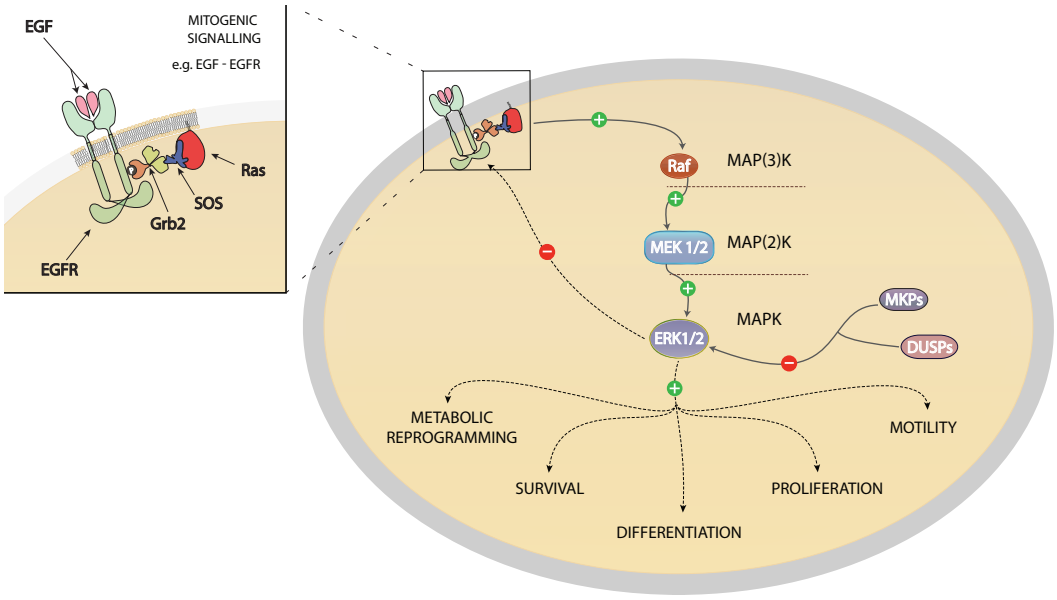

Figure 1.13: MAPK signalling cascade. Upon stimulation with mitogens, Ras activate MAP3Ks (e.g. Raf), which in turn activate MAP2Ks (such as MEK1/2). These in turn activate MAPKs (e.g. ERK 1/2) which promote processes such as metabolic reprogramming, survival, differentiation, proliferation and motility. ERK 1/2 inhibits upstream signalling and is regulated by dual specificity phosphatases (DUSPs) and MAPK phosphatases (MKPs).

1.4.5 PI3K/Akt/mTOR pathway

The phosphoinositide 3-kinase (PI3K)/Akt/mTOR pathway (see figure 1.14) is activated by a number of RTKs and Ras signalling. In general, this pathway and its components play a key role in promoting cellular growth, proliferation, metabolism, transcription, translation, apoptosis, cell cycle progression and survival[229,257,258]. Disturbed activation of the pathway has been associated with a number of human malignancies[259].

1.4.5.1 PI3Ks

There are four classes of PI3K (class I-IV) in humans[258]. Differences in classes are manifested in substrate specificity, though a common function is to phosphorylate the inositol ring 3'-OH group of a phosphatidylinositol molecule (commonly abbreviated to PtdIns or PI)[229]. PI molecules are amphiphilic, membrane-bound phospholipids that play versatile cellular signalling roles, depending on the phosphorylation states of the inositol ring moiety[260]. They can interact directly with

intracellular proteins and influence their subcellular location and/or activity and serve as substrates for phospholipases to generate second messengers[260]. In humans, three -OH groups (3', 4', 5'-OH) can be independently (de-)phosphorylated, creating a large variety of cellular compounds ranging from 0-3 phosphates attached (commonly labelled PI to PI(3,4,5)P_3)[260].

Class I PI3Ks are heterodimers composed of a catalytic subunit and an adaptor/regulatory subunit (p110 and p85, respectively)[259]. PI3K class I proteins that are recruited by activated RTKs are PI3Kα, PI3Kβ and PI3Kδ, via receptor/adaptor/SH2 domain interactions of p85 proteins[229,258]. The p110 subunits can also be activated by Ras[258]. PI3K class I can transiently convert PI(4)P to PI(3,4)P_2 and PI(4,5)P_2 to PI(3,4,5)P_3 on the inner leaflet of the plasma membrane[229].

1.4.5.2 Akt

Phosphorylated PIs recruit PH (pleckstrin homology) domain-containing effectors to the membrane. The most studied effector is the 56kDa serine/threonine kinase Akt (alternatively known as PKB)[261,262]. Other PH-domain proteins recruited by PI(3,4,5)P_3 to the plasma membrane are serum/glucocorticoid-regulated kinase (SGK), and phosphoinositide-dependent kinase-1 (PDK-1, not to be confused with the metabolic regulator pyruvate dehydrogenase kinase 1 (PDK1)), whereby the latter is required for Akt activation on the threonine 308 residue[261]. A second, final activation step of Akt occurs upon phosphorylation of serine 473 by the mTORrictor complex mTORC2 (see section 1.4.5.3). In humans, there are three isoforms of Akt[261]. Akt1(PKBα) has been found to be widely expressed in different tissues, whereas Akt2 (PKBβ) and Akt3 (PKBγ) are tissue-specific. However, mouse knockout studies suggest there is functional redundancy amongst the isoforms[263]. Akt itself regulates multiple biological processes including cell survival, proliferation, growth, and glycogen metabolism[262]. Similarly to ERK1/2, Akt has hundreds of cellular downstream targets, some of which have been thoroughly tested and confirmed[261]. Its role in metabolism is manifested by phosphorylation of targets such as glycogen synthase kinase 3β (GSK3β). Akt regulation is achieved by a variety of mechanisms, including inhibition of membrane recruitment. For instance,

the phosphatases "phosphatase and tensin homologue deleted on chromosome 10" (PTEN) and SH2 domain-containing inositol 5-phosphatase type 2 (SHIP2) can convert PI(3,4,5)P_3 to PI(4,5)P_2[264], thereby abolishing Akt recruitment. PTEN has been established to be a tumour suppressor[257].

1.4.5.3 mTOR

The mechanistic (originally: mammalian) target of rapamycin (mTOR) is one of the best studied regulators to multiple cellular responses, including growth, proliferation and autophagy. The mTOR serine/threonine kinase phosphorylates a broad range of cellular targets, has multiple regulators and effectors, is conserved from *S. cerevisiae* to mammals and is related to the PI3K family.[70,265]. A thorough review of mTOR signalling can be found here: Lapante et al[266]. It was originally identified due to its sensitivity to rapamycin[267], however, mTOR signalling is comprised of two different complexes (mTORC1 and mTORC2) with very different targets and functions[265,266]. mTORC2 is not inhibited by rapamycin. Subunit composition can vary depending on function and subcellular localisation, but both complexes contain mTOR, DEP-domain containing mTOR-interacting protein (DEPTOR) and mammalian lethal with SEC13 protein 8 (mLST8, or alternatively called GβL)[265,268–271]. mTORC2 is additionally composed of Rictor, protein observed with Rictor (PROTOR) 1/2, and mammalian stress activated protein kinase interacting protein 1 (mSin1)[266,269,272]. The mTORC1 complex specifically contains regulatory associated protein of mTOR (Raptor) and 40kDa Proline-rich Akt substrate (PRAS40, or called AKT1S1)[273].

mTOR targets

Major cellular processes, such as protein and lipid synthesis and autophagy, are controlled by mTORC1 (see section 1.1.5). In particular, mTORC1 promotes ribosome biosynthesis and mRNA translation through its well-characterised substrates S6 kinase 1 (S6K1) and eukaryotic translation initiation factor 4E (eIF4E)-binding protein 1 (4E-BP1)[70,274,275] (see figure 1.2). Targets of mTORC2 include SGK and PKC (protein kinase C). mTORC2 also activates Akt[276], whilst Akt can indirectly activate mTORC1 via TSC2 and Rheb[266]. Activated Akt phosphorylates

TSC2[70,277], which is a GAP for Rheb when in complex with TSC1. $Rheb^{GTP}$ enhances mTORC1 activity. Therefore, Akt-mediated phosphorylation of TSC2 inhibits TSC1-TSC2 complex formation, leading to prolonged activivities of Rheb and mTORC1[278]. ERK1/2 (see section 1.4.4.3) also inhibits TSC2 via phosphorylation, highlighting one of many links between different signalling cascades.

mTOR regulation

Upstream regulation of mTORC2 is not fully understood, possibly it is activated via growth factors/Ras[266]. Much more is known about mTORC1 than mTORC2. Following intracellular and extracellular inputs signal via mTORC1:

(1) growth factors

(2) amino acids

(3) energy status

(4) oxygen

Growth factors, through the RTK-PI3KAkt pathway, positively regulate mTORC1. Amino acids (particularly leucine and arginine) also strongly regulate mTORC1 activity (see section 1.1.5). Cellular energy levels (e.g. glucose concentration) are regulated via AMPK[112], which affects mTORC1 activity directly or indirectly. In response to hypoxia (see section 1.2.8) or a low energy state in form of a high AMP/ATP ratio, AMPK phosphorylates TSC2 (like mTORC2) and increases its GAP activity toward Rheb[279]. AMPK also communicates directly with mTORC1 via phosphorylation of raptor, leading to inhibition of mTORC1. Aberrant PI3K/Akt signalling leads to excessive mTOR signalling as is the case in various cancers[280]. In general, regulation of mTOR activity itself is achieved by dissociation of inhibitory subunits (e.g. PRAS40, DEPTOR) and/or scaffolding proteins (e.g. raptor, rictor, mSin1) by changes in sub-cellular localisation[266]. For instance, PRAS40 is a negative regulator of mTOR, but it is itself inhibited by Akt-mediated phosphorylation[261,281]

1.4.5.4 FoxO

Forkhead box (FoxO) transcription factors form part of a superfamily consisting of 19 subclasses of genes (FoxA - FoxS) that share a highly conserved DNA-binding

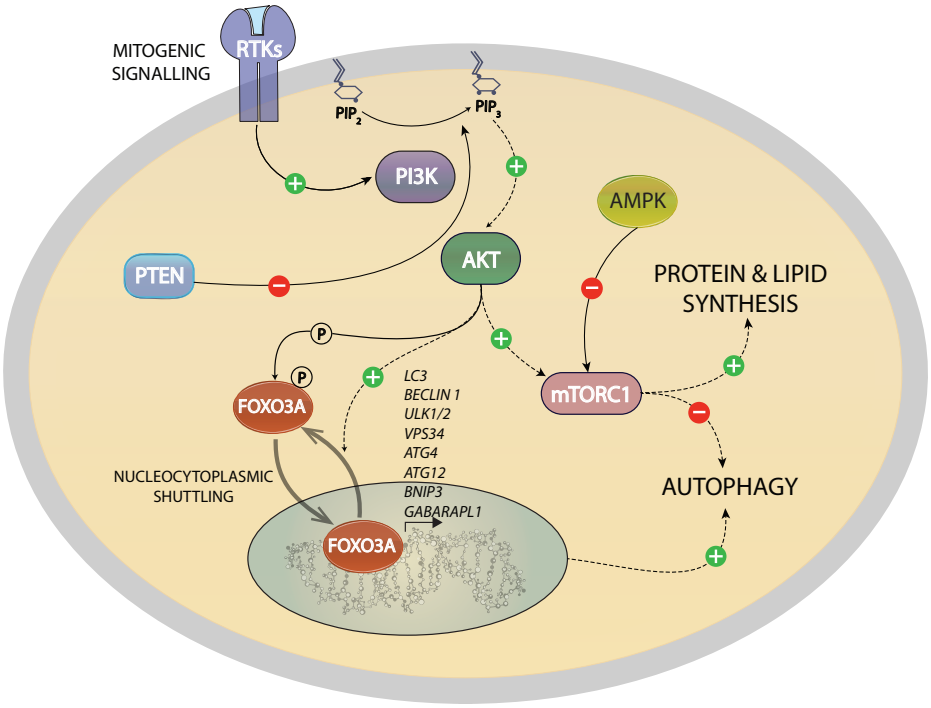

Figure 1.14: Autophagy regulation via FoxO3A. Phosphorylation renders FoxO3A cytoplasmic and therefore not transcriptionally active. In the nucleus, FoxO3A promotes the expression of various genes involved in autophagy. Growth factor signalling increases PI(4,5)P_2 to PI(3,4,5)P_3 conversion, thereby activating Akt. PTEN inhibits Akt signalling by counteracting PI3K. Akt also regulates autophagy via mTORC1. The complex promotes protein and lipid biosynthesis and inhibits autophagy.

Fox domain[282]. Many members of the superfamily are expressed under specific spatial and temporal circumstances and some are ubiquitously expressed[283]. There are four members in mammals (FoxO1, 3a (or FoxO3), 4, 6)[284]. FoxO1, FoxO3a and FoxO4 are ubiquitously expressed in mammalian cells and their loss of activity has been observed in multiple tumors[283]. The FoxO transcription factors are involved in the regulation of metabolism, stress, growth, survival, tumor suppression, differentiation and cell cycle pathways[285]. FoxOs, in particular FOXO3a, have been shown to regulate transcription of a number of autophagyrelated genes including LC3, Beclin 1, ULK1/2, VPS34, ATG4, ATG12, BNIP3 and GABARAPL1[48,90,286,287] (see sections 1.1.3 and 1.1.5). Furthermore, FoxO3a localises to the nucleus under nutrient-starvation conditions[48] and also upregulates FoxO1-mediated transcription, whose targets include ATG7 and other autophagy-related genes[285,286]. FoxO activ-

ity is highly regulated through post-translational modifications that influence their nucleocytoplasmic shuttling[285]. Target genes are activated or repressed through the FoxO domain in the nucleus[288]. One of the key regulators of the FoxO family is Akt (see section 1.4.5.2), promoting nuclear export of FOXO by phosphorylation, which results in inhibition of FOXO-dependent transcription[276,289].

1.5 Rationale for experiments

When first discovered, metabolic enzymes were thought to catalyse reactions in metabolism. However, there is a growing amount of evidence for metabolic enzymes and metabolites to play additional roles in a variety of cellular activities, including signalling, transcription and autophagy. Furthermore, it is becoming clear that those enzymes and metabolites can act on "distant" pathways. However, most of these findings were published only in the last decade, so there is good reason to believe that other metabolic enzymes have additional roles, but they have yet to be characterised.

1.5.1 RPIA - Grb2 experiments

Before I joined the lab, RPIA was identified as a hit in a GFP-tagged Grb2 translocation screen (J. Petschnigg, R. Ketteler, et al, submitted). This screen is described in more detail in chapter 3. Interestingly, out of the 20,000 cDNAs that were screened, RPIA was the only metabolic enzyme that caused a change in localisation (out of 154 hits). Due to its key role in the PPP and its possible involvement in Grb2-mediated signalling, RPIA appeared to be a very interesting enzyme to study. As outlined in chapter 1.2, many metabolic pathways are altered in cancer cells, including glycolysis (section 1.2.4), TCA cycle (section 1.2.5), amino acid synthesis (section 1.2.6) and nucleotide synthesis (section 1.2.9). The growing evidence of enzymes involved in signalling raises questions to what extend PPP enzymes play a role as well (section 1.3).

1.5.2 RPIA in Autophagy

A review of the current literature shows a tight link and many overlaps between metabolism and autophagy (see section 1.1.4). In fact, a number of metabolic en-

zymes, have been associated with the regulation of autophagy. As with biosynthetic regulatory feedback loops, there is good reason to assume some crosstalk of metabolic enzymes and the autophagy machinery. Furthermore, RPIA was identified as an inhibitor of FoxO3A in a cDNA over-expression screen (Ketteler, Na and Seed, unpublished). FoxO signalling has been associated with autophagy, as many genes in the autophagy pathway (such as ATG4B) are regulated via FoxO through transcriptional control (see section 1.4.5.4). Additionally, the Ketteler lab has many tools and expertise to study autophagy in detail, which are readily available in the lab.

Chapter 2

MATERIALS AND METHODS

2.1 Cell lines

HeLa and human embryonic kidney (HEK293T) cells originated from the American Type Culture Collection (ATCC). HepG2 cells were obtained as a kind gift from the Saiardi lab (UCL, LMCB, UK). Other cells lines (stably transduced cell lines, CRISPR cells) were generated from plain cells and described in more detail below. All cell lines were frequently mycoplasma-tested.

2.2 Cell culture

All cell lines were cultured in Dulbecco's modified Eagle's medium (DMEM), +high glucose (25mM), +GlutaMAX™(ThermoFisher Scientific®, 61965-026) and supplemented with 1mM sodium pyruvate (ThermoFisher Scientific®, 11360-070), 100 U/ml Penicillin-Streptomycin (ThermoFisher Scientific®,15140-122) and 10% Fetal Calf Serum (Sigma, 12133C), unless otherwise stated. In this study, this standard culture medium is referred to as full medium/media. All live cells were incubated at 37°C and 5% CO_2. For the stable cell lines, indicated amounts of puromycin was added to full medium. For part of the growth assays performed in figure 4.20, I used DMEM +low glucose (5.6mM), +GlutaMAX™(ThermoFisher Scientific®, 10567-014), supplemented with 100 U/ml Penicillin-Streptomycin and 10% Fetal Calf Serum.

2.3 Molecular biology

2.3.1 Peak/pMOWS vectors

The peak and pMOWS backbone/control vectors originated from Ketteler et al[290]. The shRNA sequence in pLKO.1 shRPIA #4 was cloned into pMOWS 5.2 vectors (containing puromycin N-acetyl-transferase or GFP) immediately upstream of the H1 promoter using *EcoRI* and *BamHI* restriction site cloning. RPIA was sub-cloned using the *EcoRI* and *NotI* restriction sites in peak 14. The catalytic inactive D160A mutant was generated using overlap extension PCR, with 5'-CCTTGCCATCGCTGGTGCTGATG-3' and 5'-CATCAGCACCAGCGATGGCAAGG-3' primers and RPIA WT as template. The resulting mutagenized PCR fragment was subcloned into peak 14 using *EcoRI* and *NotI* restriction sites.

2.3.2 Gateway vectors

Gateway® pDONR™221 vectors (entry clones) were obtained from Thermo Scientific, namely RPIA and Firefly luciferase. pDONR vectors were used to clone relevant sequences into a mammalian destination vector containing a 3x Flag sequence upstream, modified originally from a pLenti6.3/TO/V5-DEST (#A11144, ThermoFisher Scientific®, in table 2.1 annotated as pDEST vector). The cloning reactions were performed by using LR2 clonase according to the manufacturer's instructions. pDEST RPIA D160A was obtained by creating a pDONR construct using AttB PCR arms and peak 14 D160A as a template, followed by subsequent cloning into a pDEST donor template.

2.3.3 Over-expression and knockdown plasmids

A summary of all plasmids used in over-expression and knockdown experiments in this study can be found in tables 2.1 and 2.2. Furthermore, Table 2.3 shows the oligo sequences of the pLKO.1 vectors mentioned in table 2.2. The plasmids pMOWS 5.2 shRPIA puro and pMOWS 5.2 shRPIA contain the same target sequence as pLKO.1 shRPIA #4.

Name of plasmid	gene(s)	tags, mutations, comments	in figures:
pMOWS 4.0	N/A	N/A	3.2, 3.3, 3.4, 3.5, 3.11
pMOS GFP	GFP	N/A	3.2, 3.3, 3.4, 3.6, A.2
peak 14	N/A	N/A - also called ”vector”	3.2, 3.3, 3.4
peak 14 RPIA	RPIA	Flag	3.2, 3.3, 3.5, 3.6, 3.11, A.2, A.1
peak 14 D160A	RPIA	Flag + D160A mutation	3.2, 3.4, 3.11
pMOS GFP-Grb2 (WT)	Grb2	GFP	3.1, 3.2, 3.4, 3.5, 3.6, A.1
GFP-Grb2 (SH2)	Grb2	GFP + R86K mutation	3.6
GFP-Grb2 (NSH3)	Grb2	GFP + L49P mutation	3.6
GFP-Grb2 (CSH3)	Grb2	GFP + G203R mutation	3.6
GFP-Grb2 (NCSH3)	Grb2	GFP + L49P + G203R mutation	3.6
peak 12 GFP-RPIA	RPIA	GFP	3.7, 3.8
pDEST Luc	Firefly Luciferase	3x Flag	3.9, 3.10
pDEST RPIA	RPIA	3x Flag	3.9, 3.10
pDEST D160A	RPIA	3x Flag + D160A mutation	3.9, 3.10
peak 14 ATG4B	ATG4B	Flag	A.2
pMOS GFP-FoxO3A	FoxO3A	GFP	A.1
peak 14 AKT	Akt	Flag	A.1
peak 14 AKT KD	Akt	Flag + T308A mutation	A.1
peak 14 PTEN	PTEN	Flag	A.1

Table 2.1: Over-expression plasmids over-expression plasmids used in experiments as indicated. They were either purchased (pDONR from ThermoFisher Scientific®) or generated by cloning sequences into peak or pMO(W)s vectors

Name of plasmid	target gene(s)	tags, markers, comments	in figures:
pLKO.1	N/A	N/A	4.1
pLKO.1 shRPIA #1	RPIA	N/A	4.1
pLKO.1 shRPIA #2	RPIA	N/A	4.1
pLKO.1 shRPIA #3	RPIA	N/A	4.1
pLKO.1 shRPIA #4	RPIA	N/A	4.1
pMOWS 5.2 puro	N/A	puromycin N-acetyl-transferase	4.2, A.2, A.1
pMOWS 5.2 shRPIA puro	RPIA	puromycin N-acetyl-transferase	4.2, A.2, A.1
pMOWS 5.2 GFP	N/A	GFP	4.3
pMOWS 5.2 shRPIA	RPIA	GFP	4.3
pMOWS 5.2 Grb2	Grb2	puromycin N-acetyl-transferase	A.1
pMOWS 5.2 shRPIA RPIA^{res}	RPIA	shRPIA resistance	3.11
pMOWS 5.2 shRPIA D160A^{res}	RPIA	shRPIA resistance + D160A mutation	3.11

Table 2.2: knockdown plasmids plasmids used in all short hairpin-mediated knockdown experiments. These were either purchased (pLKO.1 from Sigma) or generated by cloning appropriate oligo sequences into pMOWS vectors. This list does not include the sgRNA vectors used for the generation of CRISPR cell lines, please see 2.4

designation	forward oligo shRNA sequence	Clone ID
shRPIA #1	CCGGCGGGTACACAAATGGAGTGAACTCGAGTTCACTCCATTTGTGTACCCGTTTTTG	TRCN0000049408
shRPIA #2	CCGGGCTGATGAAGTAGATGCTGATCTCGAGATCAGCATCTACTTCATCAGCTTTTTG	TRCN0000049409
shRPIA #3	CCGGGAATTGGAAGTGGTTCTACAACTCGAGTTGTAGAACCACTTCCAATTCTTTTTG	TRCN0000049410
shRPIA #4	CCGGGAAGTGAATACAGCTATCAAACTCGAGTTTGATAGCTGTATTCACTTCTTTTTG	TRCN0000049411

Table 2.3: shRNA sequences used in pLKO.1 vectors and pMOWS 5.2 targetting RPIA shRNA vectors were purchased from Sigma. The sequence of shRPIA #4 was cloned into pMOWS 5.2 as described in 2.3.1.

2.4 Transfection methods

Various transfection protocols were used and optimised, depending on cell line, downstream technique and cell seeding format. In general, for experiments in 6-well and 12-well plates (western blotting, virus packaging cell lines, confocal microscopy), 2-5*10^5 cells were seeded one day prior to transfection when $CaCl_2$ precipitation and XtremeGene 9 (Sigma, 06365779001) were used as a transfection method. DMEM was supplemented with chloroquine (25μM) and drops of 1-2.5μg of plasmid DNA mixed with a 5mM final concentration of $CaCl_2$ in HEPES buffer (10mM HEPES, 150mM NaCl, 3mM EDTA, 0.005% Tween-20) were added after 30 minute incubation at room temperature (RT) for $CaCl_2$-mediated transfection. Cells were washed 2x with PBS and incubated with full medium after 6 hours of incubation of the DNA/ $CaCl_2$ complexes on the cells. For XtremeGene 9-mediated transfection, 3μl were mixed with 1-2.5μg of plasmid DNA in serum-reduced optiMEM (ThermoFisher Scientific®, 31985-088) for 30 minutes at RT and cells were then incubated for 16 hours.

For experiments in 96-well or 384-well plates (high throughput imaging, luciferase assays), 0.5-1*10^5 cells were seeded and transfected with lipofectamine® 2000 (ThermoFisher Scientific®, 12566-014). In this transfection method, 0.1-0.2μg of plasmid DNA was mixed with 0.2-0.3μl lipofectamine in optiMEM , incubated for 30 minutes at RT and applied to cells for 16 hours.

2.5 Lentiviral stable cell lines

HEK293T cells were used as a packaging cell line for producing viral particles for stable induction. 5*10^5 cells were seeded in 6 well plates and co-transfected the next day with 100ng pMD2.G (contains VSV-G Env), 900ng psPAX2 (contains

Gag, Pol, Rev, and Tat) (#12259, #12260, both Addgene) and 1μg of lentiviral over-expression or shRNA construct as indicated, using XtremeGene 9 (as described above). In brief, 100 μl Opti-MEM® (ThermoFisher Scientific®, 31985-070) were mixed with 6 μl XtremeGene 9 and left for 5 minutes at RT. DNA, as indicated above, was added and left at RT for another 30 minutes. Mixture was added drop-wise to cells and left for incubation 16-20 hours at 37°C and 5% CO_2. Cell culture medium was replaced with 2ml filtered full medium + 1.1% BSA (Bovine Serum Albumin). Virus particles were harvested after 24 hours and again after 48 hours. The virus-containing media from both harvest rounds were mixed, filtered through a 0.22 μm PDVF filter (GVWP04700, Millipore™) and then either used directly or stored at -80°C by snap-freezing in liquid nitrogen.

Next, target cells were seeded at 3-6*10^4 cells in 12 or 24 well plates and transduced with virus-containing medium + full medium without antibiotics the next day. For cell lines that proved difficult to transduce (e.g. HepG2 cells), 0.5 μl of 8mg/μl hexadimethrine bromide (107689, Sigma) was added to the media. On the following day, selection and expansion of transduced cells with full medium containing 1μg/ml puromycin was performed for a total of 7 days, with selection medium being replaced every 2-3 days. Various dilutions of virus-containing medium (ranging from 10 μl - 300 μl) were tested and compared to each other under puromycin selection, and cells with good survival (compared to non-infected control) but most diluted (wells infected with least virus-containing particles) were chosen for further experiments.

2.6 CRISPR/Cas9 genome editing

For genomic modification at the RPIA locus on chromosome 2p11.2 in HeLa cells, the CRISPR/Cas9 double nicking strategy as described in detail in Ran et al[291] was used. In brief, RPIA specific sgRNAs vectors targeting exon 1 were designed and generated according to the protocol. Oligo sequences for sgRNA generation (see table 2.4) were used to clone into pX335 (containing nCas9). 6.5*10^4 cells were seeded in 24 well plates and co-transfected the next day with 200ng of each sgRNA

vector (and 400ng pX335 with no sgRNA sequence for control, labelled CR-WT) + 100ng pBabe mCherry-puro (empty pMOWS for selection control) using lipofectamine (also, for overall strategy and vectors see figure 4.8). After 48 hours, cells were selected with culture medium containing puromycin (Sigma, P8833) at 1.0 μg/ml. Fresh selection medium was provided every 2-3 days. Cells were selected and expanded for a total of 18 days, with selection control cells completely dead after 7 days. After 10 days, individual clonal colonies were picked using 3mm trypsin-soaked clonal discs and further expanded in 24 well, 6 well and ultimately in 10 cm petri dishes. Genomic DNA was obtained using QuickExtract™DNA Extraction Solution (Cambio, QE09050) and genomic PCR was performed using primers indicated in table 2.5 with Phusion polymerase (NEB). Genomic PCR products were purified using the PCR cleanup kit (Quiagen®) and run on a 2% Agarose gel, or directly sequenced (Source BioScience's Sanger sequencing service), or first cloned into pGEM-T easy (Promega®) vectors prior to sequencing in order to identify the allelic variations on both chromosomes.

2.6.1 sgRNAs design

Primer ID	designation	forward oligo sgRNA sequence	nicking at nucleotide
reverse-strand guide #1292175	g9	CACCGTTGTGTTGCCAGCACCGCCA	155
reverse-strand guide #1292177	g24	CACCGGTCCCAGACTGTGCACGCCC	132
reverse-strand guide #1292179	g6	CACCGACGCCCCGGCAGCCGCACGT	118
reverse-strand guide #1292182	**g14**	CACCGGCCGCACGTGGGAACCCGGG	107
forward-strand guide #1292160	g33	CACCGCAACACAAGCACCAGCTGCG	187
forward-strand guide #1292157	g18	CACCGTCTGGGACCCGTGGCGGTGC	164
forward-strand guide #1292154	**g4**	CACCGTGCCGGGGCGTGCACAGTCT	147
forward-strand guide #1292152	g19	CACCGGTTCCCACGTGCGGCTGCCG	132

Table 2.4: Overview of sgRNA oligos that were used for cloning into pX335 for modification of RPIA. Sequences that were used for the generation of the stable CRISPR cell lines in this study are highlighted in bold.

2.6.2 genomic primers for sgRNA validation

designation	primer sequence	amplifies with regard to start codon
E1-forward	5-GCGAATCCAGATAGGGGTTCCTCGAAGC-3	-122
E1-reverse	5-GCAAGCTTAGCAGGGAAGAGGGGTCTAA-3	+432

Table 2.5: genomic primers primers were purchased from Eurofins.

2.7 Antibodies

All antibodies used in this study, including their dilution factor, are listed in table 2.6.

antibody/stain	Company + Product ID	Dilution used	in Figures:
Hoechst	TFS #33342	1:10 000	3.2, 3.3, 3.4, 3.5, 3.7, 3.8, 4.15
Flag	SA F9291	1:500 (IF&WB)	3.5, 3.9, 3.10, 4.20
CAD	BL IHC-00280	1:500	3.8
Actin	SA A2228	1:2000	3.9, 3.10, 4.4, 4.14, 4.16, 4.20
GFP	CST #2555	1:1000	3.11
pERK	CST #4370	1:1000	3.11, 4.21
ERK	CST #9272	1:1000	3.11, 4.21
LC3	SA L7543	1:1000 (WB) 1:400 (IF)	4.1, 4.3, 4.4, 4.14, 4.15, 4.16
Vinculin	Abcam ab129002	1:10000	4.1
COX IV	CST #4850	1:1000	4.21
RPIA-A1	Abcam ab67080	various dilutions tested	N/A
RPIA-A2	AO - ABIN406525	various dilutions tested	N/A
RPIA-A3	AO - ABIN1537971	various dilutions tested	N/A
RPIA-A4	”home-made”	various dilutions tested	N/A

Table 2.6: All Antibodies used in this study for Western Blotting and Immunofluorescence Antibodies were purchased from companies and diluted as indicated in this table. AO - Antibodies online, BL - Bethyl Laboratories®, CST - Cell Signalling Technologies®, SA - Sigma-Aldrich®, TFS - ThermoFisher Scientific®

2.8 Protein analysis by Western Blotting

2.8.1 Sample preparation

The existing media on the cells was aspirated and they were washed with 1x PBS. Cells were harvested by either trypsinisation/vigorous resuspension or direct lysis. For the former, trypsinised/resuspended cells were collected via centrifugation at 1000 rpm for 3 minutes and then lysed. For the latter, cells were directly lysed with lysis buffer on a shaker at low speed and 4°C for 10 min. In either scenarios, successful detachment of cells from cell culture plates was confirmed using bright-field microscopy. Nonidet P-40 (NP-40) lysis buffer (50 mM Tris-HCl pH 7.4, 200 mM NaCl, 0.1 mM EDTA, 10% Glycerol, 0.5% NP-40) including inhibitors was used to lyse cells. We prepared the lysis buffer with cOmplete (EDTA-free) protease inhibitors (11873580001, Roche®) and PhosSTOP™easypack (4906837001, Roche®) phosphatase inhibitors, according to the manufacturer's instructions. Lysates were transferred to an eppendorf and samples were centrifuged at 13800

rpm for 15 min. The pellet was discarded and the supernatant was transferred to a new tube and stored at -80°C or used immediately. Protein concentration was determined in technical triplicates using the BCA assay kit (Thermo Scientific, #23228) with BSA being used to obtain a standard curve. One μl of lysate was incubated with 100 μl of the reagent for 20-60 minutes at 37°C. The kit functions as a colorimetric 96 well plate-based assay and results were obtained using a VersaMax™ELISA Microplate Reader (Molecular Devices®, USA)

2.8.2 SDS-PAGE

In this study, western blotting was used as a technique to investigate protein expression levels. In brief, proteins from whole cell lysates were separated using SDS- PAGE (sodium dodecyl sulphate-polyacrylamide gel electrophoresis) and then transferred to PVDF membranes for immunoblotting.

SDS-PAGE gels consist of a lower resolving gel and upper stacking gel. In this study I used 7.5% and 4-20% resolving gels (BIO RAD Mini-PROTEAN® TGX™Precast Protein Gels), with the latter being particularly important for separation of LC3 isoforms. To prepare the samples, 15-25 μg of whole cell extract was mixed with an equal volume of 2x SDS loading buffer (125 mM Tris-HCl, pH 6.8, 4% SDS, 5% 2-Mercaptoethanol, 20% glycerol, 0.01% bromophenol blue), and then incubated at 95°C for 5 minutes. Samples were loaded into the wells of the stacking gel after centrifugation for 10s at 10 000 rpm. The BIO RAD Mini-PROTEAN® tetra system was used (BIO RAD, Hemel Hempstead, UK). SDS-PAGE gels were run using standard SDS-PAGE running buffer (25 mM Tris base, 250 mM glycine, 0.1 % SDS) at 20 V for 20 minutes for penetration of the stacking gel and then at 100V until the bromophenol blue dye front had run off.

The gels were removed from the tank and assembled for transfer to a PVDF membrane (Immobilion® - FL #IPFL00010) using the BIO RAD Mini Trans-Blot® Electrophoretic Transfer Cell system, following the manufacturer's instructions. Tanks were filled with transfer buffer (25 mM Tris, 250 mM glycine and 20 % methanol) plus an ice block to prevent over-heating, and were run at 100 V for 60 min at RT or at 4°C overnight.

2.8.3 Immunoblotting

After removal of membranes from the transfer tank, ponceau S (Sigma, P3504) was used to confirm transfer of proteins and gave a good indication whether equal loading between samples had been achieved. Membranes were then blocked in blocking solution (5% skimmed milk powder (Oxoid, LP0031)) dissolved in PBS-T (20 mM Tris pH 7.6, 136 mM NaCl, 0.05 % Tween)) for 1 hour at RT. Primary and secondary antibodies were also diluted in blocking solution and stored at -20 °C and 4°C between uses, respectively.

After blocking, membranes were incubated with primary antibody (see table 2.6 for antibody dilutions and sources) for 16-20 hours at 4°C. Membranes were then washed four times with PBS-T for 5 min on a shaker at low speed. In most cases, secondary fluorescently-labelled antibodies (IR-Dye® 800CW goat anti-rabbit, 926-32211 and IR-Dye® 680RD goat anti-mouse, 926-68070) were used for visualisation and quantification of protein bands.
Secondary antibodies were diluted to 1:10 000 in blocking solution. For the goat anti-mouse antibody, SDS was added to a final concentration of 0.02%. Membranes were incubated in secondary antibody for one hour at RT on a low speed shaker and washed four times in PBS-T for 5 min each. Protein bands were visualised using an LI-COR Odyssey® infrared imaging system. Fluorescent detection is more accurate for quantification than enzyme-based visualisation techniques, because the relationship of signal and the amount of target protein is linear, not exponential.

In a few occasions (stated in figure captions), secondary horseradish peroxidase-conjugated antibodies were used and equally diluted in blocking solution. Membranes were incubated in secondary antibody for one hour at RT. Protein bands were visualised using enhanced chemiluminescence (ECL) solutions (Perkin Elmer, Seer Green, UK), with Amersham Hyperfilm ECL (GE Healthcare).
Quantification of blots was performed using the densitometry tool from ImageJ (NIH, Bethesda, MD, USA).

2.9 Immunofluorescence

2.9.1 Sample preparation

Cells were seeded, depending on downstream imaging conditions. For low-throughput, cells were seeded at concentration of 1-1.5*10^5 cells per well in 12 well plates on glass coverslips. For high-throughput, cells were seeded at concentration of 5-15*10^3 cells per well in 96 well plates. On the following day, cells were transiently transfected with over-expression and knockdown constructs (for plain cells) or not transfected, if cells were modified already (CRISPR cells, stably transduced cells), as stated in the figure legends. The following day (or after appropriate knockdown, as indicated), after treatment whereever indicated, cells were washed 1x with PBS, fixed and with 4%PFA for 15 minutes at RT. For LC3 immunofluorescence, cells were fixed from 15 minutes in 100% cold methanol at -20°C and washed 3x with PBS. If no antibody staining was necessary, cells were stained for nuclei with Hoechst 33342 (ThermoFisher Scientific®,H1399) for 5-15 minutes at a 1:10 000 dilution directly after fixation, followed by 1x wash with PBS. Whenever antibody staining was performed, nuclear staining was performed at the end of staining.

The following steps were all performed at RT. After washing 1x with PBS, cells were quenched with 50mM NH_4Cl for 20 minutes and washed 1x with PBS, followed by permeabilisation with 0.1% TX-100 (Roche, 10743119103) for 10 minutes and washed 1x. Blocking was performed by using 3% goat serum in PBS (blocking solution) for 30 minutes and incubated with primary antibodies in blocking solution as indicated in the figures. Antibody dilutions are summarised in 2.6 and staining duration varied between 1-3 hours, as recommended by the supplier. After washing 3x with PBS, cells were incubated with Alexa Fluor® series of secondary antibodies at 1:400 dilution, including goat mouse/rabbit Alexa® 488/568/647, (all ThermoFisher Scientific®, A-11001, A-11034, A-11004, A-21090, A-21443, A-21235) using the appropriate antibody for 1 hour. For low-throughput, cells were then washed 2x with PBS and mounted on microscope slides using prolong gold (ThermoFisher Scientific®, P36934). For reporter cell lines, such as GFP-LC3 (figure 4.2), permeabilisation and antibody staining was omitted.

2.9.2 Image acquisition

Images in this study were acquired on two microscopes: An Opera LX® (Perkin Elmer, Waltham, MA, USA) High Content Screening confocal microscope or an inverted confocal microscope (Leica TCS SPE, Leica®, Newcastle Upon Tyne, UK) using various objectives (20x, 40x, 63x) and digital zoom (1.0 to 3.0) as stated in the figure legends. Scale bars were added and contrast was enhanced by 0.05% using Fiji on images acquired on the SPE, unless otherwise stated.

2.9.3 Image analysis

2.9.3.1 Columbus

One big advantage of the Opera is that it can acquire a large number of images easily, which is very useful for high throughput screening. Additionally, I found that many image-based experiments can also be performed on this microscope, hence the number of biological replicates and images per well is usually large in this study. Images acquired using the Opera were analysed using Columbus™ software. Figure 2.1 gives an overview of the image analysis protocol to identify puncta that was used for most imaging experiments.

(1) Nuclei in images were identified using the nuclear (405nm emission) channel and method C, with a common (intensity) threshold of >0.4 and an area of $>50\ \mu m^2$. Other optimisation parameters, such as split factor, individual threshold and contrast were optimised based on experimental conditions.

(2) Cells in images were identified using the 488nm or 562nm (when 488nm signal was not available) emission channels and method A of ”find cytoplasm”, with an individual (intensity) threshold of >0.25. Other optimisation parameters, such as split factor, individual threshold and contrast were optimised based on experimental conditions.

(3 + 4) Cell selection was refined by measuring intensity and morphology properties. Based on these parameters, cells could be selected based on relative differences to background intensities, therefore too large or small background features could be excluded from the analysis. Chosen parameters

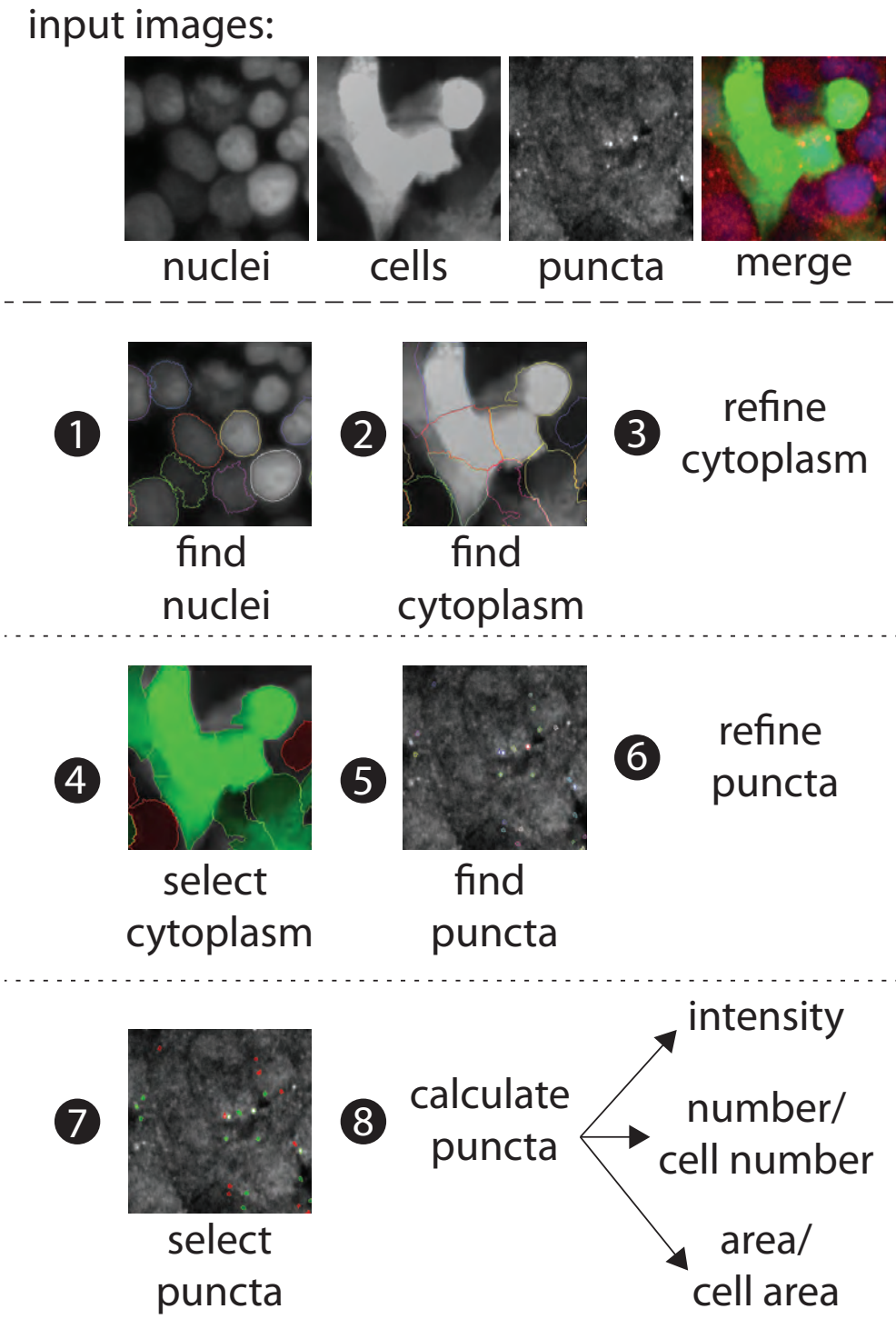

Figure 2.1: Workflow of puncta analysis. Most images in this study were analysed using Columbus™ software.

were verified for each experiment by cross-comparing images from different wells&conditions.

(5) Puncta in images were identified using the 488nm or 562nm emission channel and spot detection method A, which is based on relative spot intensity compared to the immediately surrounding pixels. The exact settings for relative spot intensity were optimised for different experiments and kept constant for repeats and almost identical experiments. The chosen value was verified for each experiment by cross-comparing images from different wells&conditions. Splitting coefficient optimisation parameter was set to <0.865.

(6 + 7) Puncta selection was refined by measuring intensity and morphology properties. Based on parameters such as spot roundness, spot area and spot intensity, puncta selection could be further refined by could be excluding oddly shaped or sized false positives from the analysis. Wherever possible, puncta selection was restricted to previously selected cytoplasm. Chosen parameters were verified for each experiment by cross-comparing images from different wells&conditions.

(8) Calculations of selected puncta were performed based on multiple parameters to ensure accurate findings. Usually, I measured puncta number and divided that by cell number and cell area. We also compared puncta area to cell area and looked at puncta intensity wherever appropriate.

2.9.3.2 Fiji

Whenever images were acquired with the Leica® TCS SPE, images were analysed in Fiji, rather than Columbus. Cells numbers were obtained by identifying and counting nuclei in the 405nm channel, using a median filter to create a homogeneous nuclear intensity and the ”find maxima” function. For puncta analysis (488nm channel), we also used ”find maxima” function with noise settings =50, followed by output=point selection.

2.10 Statistical analysis

Puncta measurements and western blot densitometric data were obtained as described above. The mean of data points were analysed for statistic significance on the *null*-hypothesis, as commonly assessed by a parametric, two-tailed (unpaired, independent) student's t-test. The p-values <0.05 (indicated in this study as "*") have a confidence interval of 95%, in other words there is a 95% likelihood that the data points are not randomly obtained. Equally, "**"=$p<0.01$, "***"= $p<0.001$ and "****" $p<0.0001$. Furthermore, unpaired analysis assures that treatments, knockdown & overexpression effects may be different to the control in both directions. In other words, there is no statistical bias as to whether there may be an increase or decrease compared to the control.

2.11 Metabolic activity assays

In general, I used the protocol as described in[202] and followed the manufacturers instructions from the 3-(4,5-dimethylthiazol-2-yl)22,5-diphenyltetra-zolium bromide (MTT) assay (Millipore™, CT02). The MTT assay measures NAD(P)H-dependent cellular oxidoreductase activity. In this study it was used as a proxy to examine cell proliferation. For RPIA over-expression, stable cell lines expressing either Flag-RPIA, Flag-D160A or Flag-Firefly-Luciferase were used (see sections 2.1 and 2.1). The cells were seeded at a density of 2-3* 10^3 cells per well in a 96-well plate and incubated in a 37°C and 5% CO_2 incubator. After 1, 3 and 5 days (24, 72 and 120 hours +/- 30 minutes), the medium was removed and replaced with 100 μl of 10% MTT-containing medium onto the cells followed by 4 hours of incubation at 37°C and 5% CO_2. The MTT-containing medium was discarded and 100 μl of DMSO was added into each well, followed by thorough resuspension using a multi-channel pipette. Then the resultant colour density of each well was detected by a VersaMax™ELISA Microplate Reader at OD_{565} as output and OD_{630} as a reference.

2.12 Mass spectroscopy

Indicated cell lines were seeded and grown in 10cm petri dishes until confluent. Cells were trypsinised, pelleted and sent off for measurements of phosphorylated sugars. Liquid chromatography and mass spectroscopy (MS) were carried out by Eduard Struys at the Metabolic Unit in the Clinical Chemistry department, Medical Center, De Boelelaan 1117, 1081 HV Amsterdam, The Netherlands. The experimental procedure and analysis were performed as described in Huck et al[292]. Briefly, cells were lysed and sugar phosphates were separated by high pressure liquid chromatography (HPLC). Detection was performed using an API-3000 tandem MS (PE-Sciex) containing an electrospray source that operates in the negative-ion mode (Turbo Ion Spray). The settings were individually optimised for each sugar-P measured. The procedure can identify sugar phosphate profiles with clearly distinctive signals for Dihydroxyacetone phosphate (DHAP), R5P and S7P, as well as Ri5P/X5P and F6P/G6P, although the latter two pairs have the same mass and cannot be distinguished.

2.13 *Saccharomyces cerevisiae* experiments

2.13.1 Transformation

The GFP-ATG8 plasmid was generated by Sac1/Xho1 double restriction enzyme digestion cloning. The sequence was cloned from a pRS306 vector into a pRS315 vector. This vector is compatible with the *S. cerevisiae* strain R1158 (originated from BY4741 strain), lacking a gene for methionine synthesis and containing the doxycycline-inducible system that enables targeted knockout. Plasmids and yeast strains were a kind gift from the Stefan lab (LMCB, UCL, UK). WT (R1158) and tetRKI strains were transformed with pRS315 (empty) or pRS315 (GFP-ATG8) as follows: 5ml of yeast extract peptone dextrose (YPD) medium was inoculated with frozen yeast strains. After 48 hours, 1ml of culture was spun down in a bench-top microcentrifuge at 12,000 rotations per minute for 2 minutes at RT. The pellet was resuspended and washed in 1ml of 0.1M lithium acetate in Tris-EDTA (LiAc/TE) solution. After spinning down again, the cell pellet was resuspended in 300μl of

40% Polyethylene glycol in LiAc/TE solution. Approximately 1μg DNA (indicated plasmids) were added with 10μl of salmon sperm DNA (Sigma, pre-boiled) and vortexed. After 6-8 hours, the DNA/cell mixture was heat-shocked for 10 minutes at 42°C, plated and incubated for 3 days in YPD medium lacking methionine at 26°C. Next, different clones were isolated and grown up on another YPD (-methionine) plate.

2.13.2 GFP-ATG8 western blotting

Different transformed yeast strains were cultured in YPD medium lacking methionine for 8 hours. Cells were incubated for 16 hours with or without 20μg/ml doxycycline, followed by incubation with or without 1μg/ml rapamycin for 4 hours. All live cell incubation steps were performed at 26°C. Next, cell numbers were normalised by measuring the OD_{600}. Volumes representing equivalents of 2.5 ODs were pooled and prepared for western blotting as described in Omnus et al[293]. Briefly, cells were precipitated with 100% Trichloroacetic acid and lysed by sonication. Lysates were loaded and analysed by western blotting as described in section 2.8.

Chapter 3

The role of RPIA in Grb2-mediated signalling

3.1 RPIA induces translocation of GFP-Grb2

3.1.1 Grb2 screen

Growth factor receptor-mediated signal transduction is essential for proliferation and differentiation of cells. These pathways control a number of cellular fates, which include the regulation of metabolism and autophagy. As seen by frequently occurring mutations in multiple cancers, signalling complexes require a tight level of control[213]. A great amount of research in the past decades has helped to understand the underlying principles for most major signaling pathways. However, receptors are often mutated in cancer and have been shown to be able to interact with altered signalling complexes and thereby promote tumorigenesis[294]. This is likely to occur via altered affinities for downstream signalling components. Currently, traditional *in vitro* approaches of discovering anti-cancer therapeutics that target RTK signalling pathways have had only limited success[294]. Therefore the identification of cellular proteins involved in growth factor receptor-mediated signalling is still highly relevant.

In order to identify further proteins involved in signal transduction, a high-troughput, microscopy-based GFP-tagged Grb2 translocation assay was developed in the lab prior to this PhD project. This screening approach was based on the

development of biosensors, which are used for better identification of novel drug targets compared to traditional *in vitro* screening methods[295]. A library of 21.000 unique single cDNA expression vectors were screened for the ability to translocate cytoplasmic GFP-Grb2 to the membrane and other sub-cellular compartments (see figure 3.1). This change in localisation can be mediated either by direct binding to Grb2 or through indirect induction of translocation. Under basal conditions, Grb2 localises to the cytoplasm[69] (see 3.1 A middle panel). When stimulated with EGF, the protein localises to the membrane following RTK phosphorylation (see 3.1 A left panel). The screen identified a number of proteins known to interact with Grb2, e.g. EGFR[221], ERBB2[225], GAB1[100] and dynamin2[296], thus partially validating the approach taken to identify Grb2 regulators. A wide variety of phenotypes for GFP-Grb2 localisation could be observed. Through the screen, a large number of novel proteins that either directly influence the sub-cellular localisation of Grb2 or result from cellular morphological changes were identified. Among the list of hits were a number of proteins with yet unassigned functions and others that had not been associated with signalling before. One of those was the metabolic enzyme RPIA, which became the focus of this study. Metabolic enzymes involved in signalling pathways have sparked a lot of interest recently, since the discovery of signalling factors binding directly and selectively to PKM2[136] and thereby achieving metabolic reprogramming.

3.1.2 Expression of RPIA results in GFP-Grb2 translocation

Seeing as RPIA expression caused translocation of Grb2, a key adaptor in the EGFR-MAPK signalling cascade, it is possible that RPIA either binds to Grb2/EGFR or indirectly has an effect on the EGFR signaling pathway. In order to test this, I first wanted to replicate the findings of the screen in HeLa cells by co-expressing GFP-Grb2 and RPIA. There is an even distribution of GFP-Grb2 in the cytoplasm, as observed in the HEK293T cells that were used in the screen, (see figure 3.2 top panel) under basal conditions (cells were incubated with DMEM + 10% FCS, i.e. full medium). However, when co-expressed with RPIA, bright GFP-Grb2 positive puncta can be observed, varying in size and numbers within the

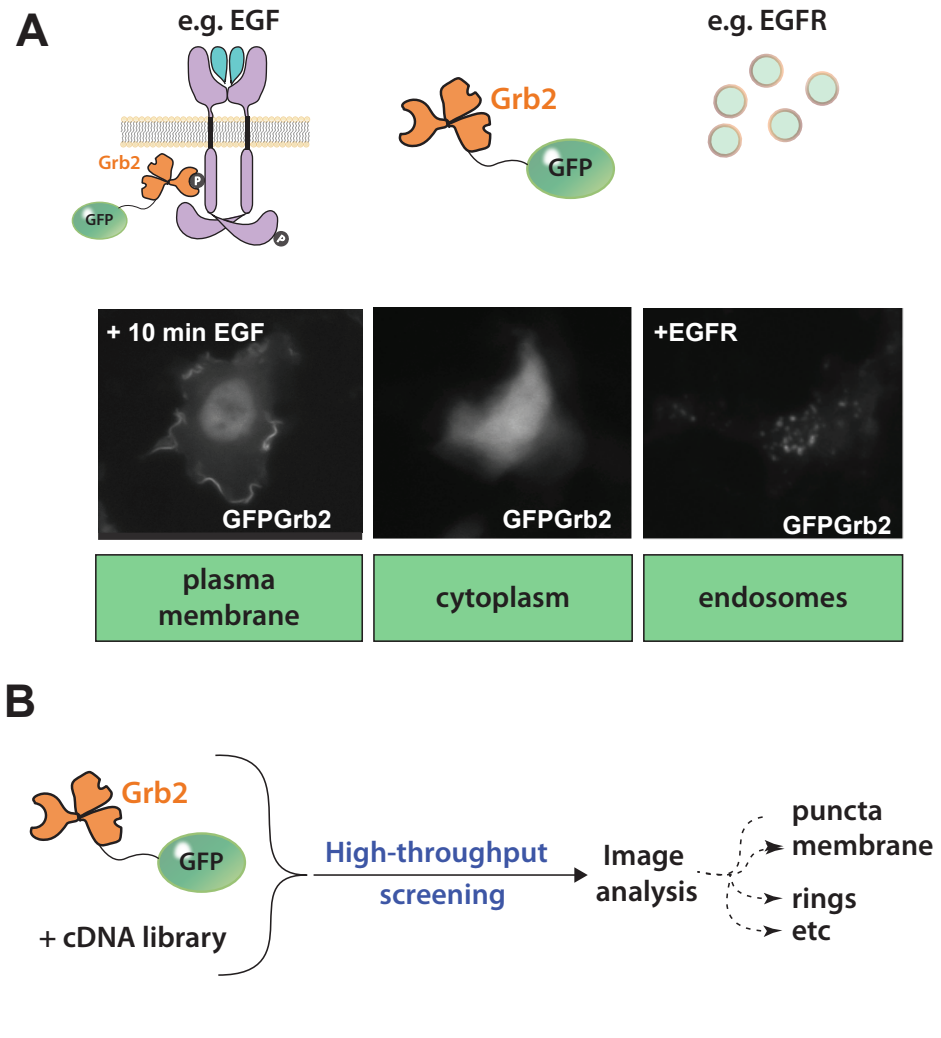

Figure 3.1: Grb2 reporter and high-throughput screen workflow A) The GFP-Grb2 reporter can be localised to different sub-cellular domains. When cells are stimulated with a mitogen such as EGF, GFP-Grb2 localises to the membrane by binding to RTKs such as EGFR (left panel). If cells are unstimulated (middle panel), GFP-Grb2 is located to the cytoplasm. If EGFR is over-expressed (right panel), GFP-Grb2 localises to endosomes. All images are representative images of the screen performed in COS cells (Ketteler & Seed, unpublished). B) Overview of approach taken for the cDNA screen.

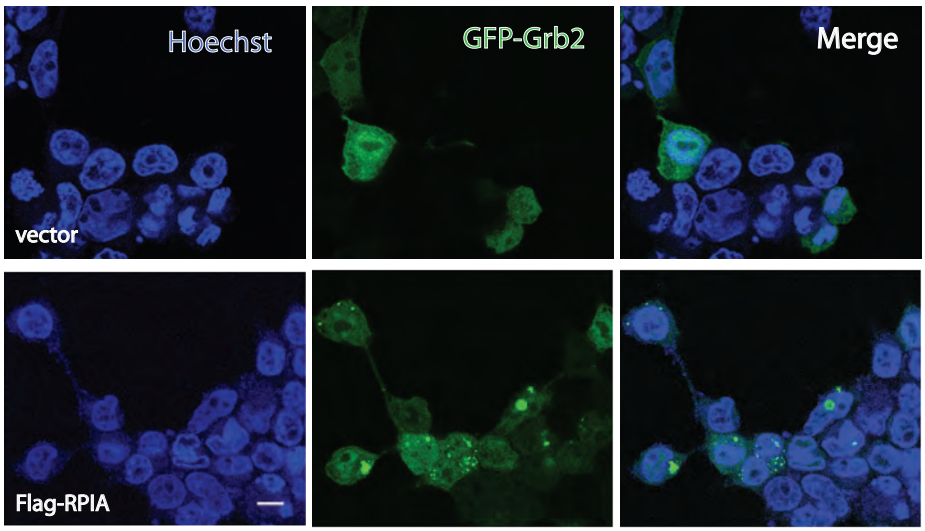

Figure 3.2: RPIA-WT induces translocation of GFP-Grb2 HeLa cells in 6-well plates were co-transfected with a total of 1μg plasmids: pMOS GFP-Grb2 and pMOWS 4.0 or peak14 Flag-RPIA (see table 2.1). After 24hrs, cells were fixed, stained with Hoechst and images were acquired using a Leica SPE3 confocal microscope with a 63x objective. Scale bar: 10μm

cells (see figure 3.2 bottom panel).

3.1.3 RPIA expression does not cause GFP translocation

Next, I investigated whether the translocation phenotype was specific for Grb2, or whether RPIA actually was affecting the localisation of GFP (e.g. forming cytoplasmic aggregates). To address this systematically, I tested co-expression of GFP and GFP-Grb2 with or without RPIA and analysed between 300 and 2000 cells per condition using the Opera LX high-content screening microscope for image acquisition. As previously, RPIA expression resulted in GFP-positive puncta in the Grb2 construct, but it did not significantly increase the number of puncta in GFP expressing cells (see figure 3.3). Furthermore, image analysis showed that the GFP-Grb2 positive puncta are significantly brighter in comparison to the cytoplasmic signal (see figure 3.3 C). The size, intensity or number of GFP-positive puncta that were picked up by the segmentation algorithm were RPIA-independent. Taken together, GFP-Grb2 translocation mediated by RPIA does not depend on the GFP moiety.

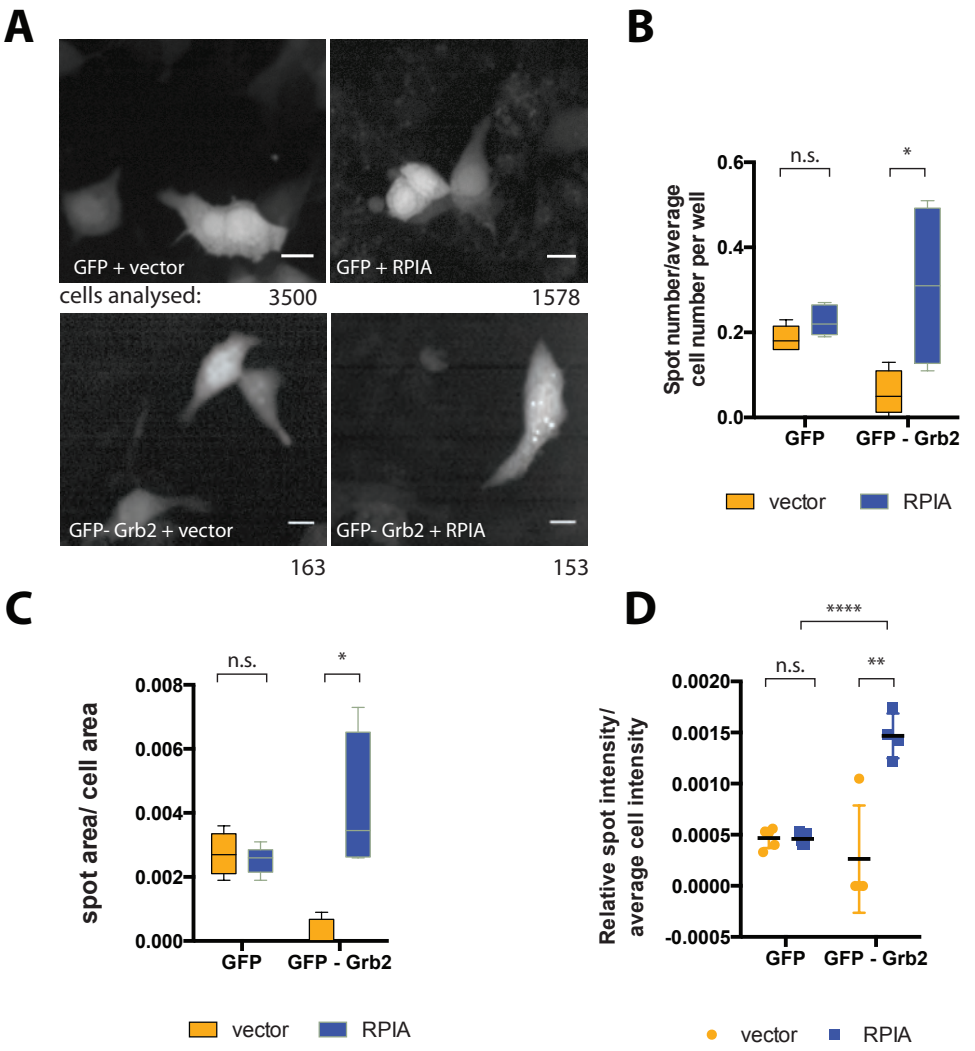

Figure 3.3: Overexpression of RPIA does not affect GFP localisation HeLa cells were transfected with plasmids pMOS GFP, pMOS GFP-Grb2, pMOWS 4.0 and peak14 RPIA (see table 2.1) in 5 replicates on a 96 well plate. After 24hrs, 30 images per well were acquired on an Opera LX microscope and spot image analysis (averaged on all 30 images per well) was performed using Columbus as described in section 2.9.3. A) representative images, scale bar = 10μm B) Box-and-whisker plot indicating B) spot number per average cell number and C) spot area per cell area. D) Scatter plot of relative spot intensity per average cytoplasmic intensity. Data represent median (B,C) and mean (D) SD from two independent experiments. Brackets indicate t-test p-values, n.s.=non significant, *=p<0.05, **=p<0.01, ****=p<0.0001

3.1.4 Catalytically inactive RPIA (D160A) can also translocate GFP-Grb2

Since RPIA is a protein with enzymatic function, the change in localisation of GFP-Grb2 could be mediated either by metabolic effects (R5P levels) or by protein-protein interaction in a non-canonical fashion (unrelated to metabolic activity). In order to investigate this further, I generated a construct in which the catalytic residue of RPIA (aspartic acid) is mutated to alanine (referred to as RPIA-D160A). This residue was previously reported to be essential for the catalytic activity of RPIA[194]. The validity of this construct was independently confirmed in the lab in an *in-vitro* RPIA activity assay (see appendix figure A.1 D). Next, I tested whether RPIA-D160A may also induce the translocation of GFP-Grb2. Indeed, expression of the catalytically inactive mutant also resulted accumulated GFP-Grb2 puncta (see figure 3.4). Therefore, Grb2 translocation mediated by RPIA does not require RPIA isomerase activity.

3.1.5 Flag-RPIA and GFP-Grb2 co-localise

The observed translocation phenotype could somehow be caused by binding of RPIA to Grb2-related signalling complexes. This raised the question of whether RPIA itself may also localise to the GFP-Grb2 positive puncta. In order to address this, I stained the cells with Flag-antibody following co-expression of GFP-Grb2 and Flag-tagged RPIA. Indeed, I found that Flag-RPIA localises to GFP-Grb2 enriched puncta and there was only minimal background staining in cells that were not expressing a Flag-RPIA (see 3.5).

3.1.6 Various GFP-Grb2 mutants also translocate upon RPIA co-expression

In order to better understand potential protein-protein interactions of Grb2 and RPIA, I next tested whether RPIA has the ability to translocate a number of Grb2 constructs that contain point mutations. Grb2 is a modular protein that is composed of three major domains (see figure 1.12). It could be that through mutations in those domains, the translocation phenotype may be abrogated. The mutations in the con-

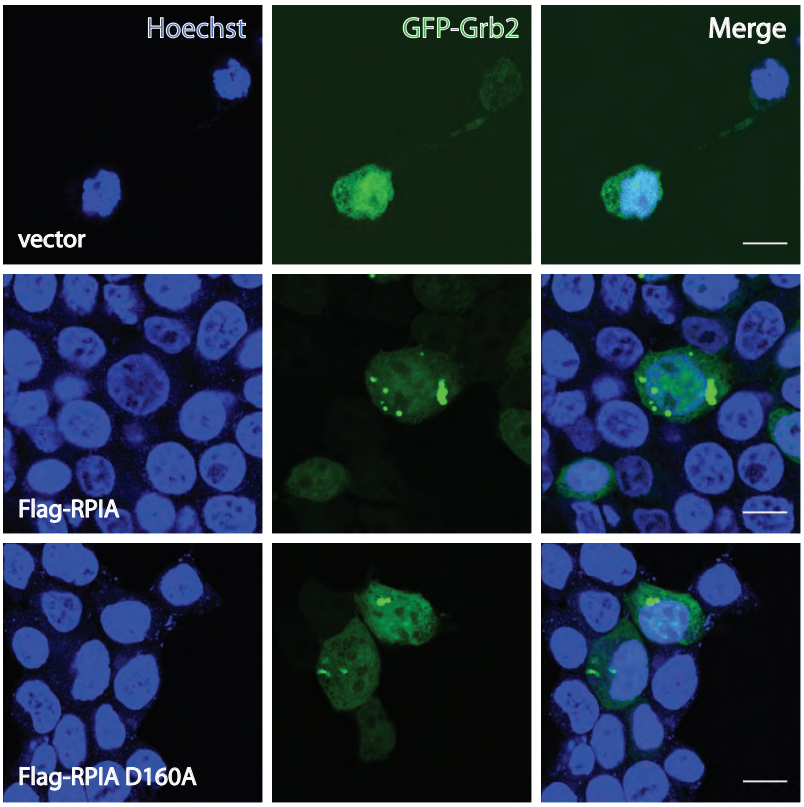

Figure 3.4: RPIA D160A also causes Grb2 translocation. HeLa cells were seeded on coverslips and co-transfected on the following day in a 6 well plate with 2.5μg of plasmids: pMOS GFP-Grb2 and pMOWS 4.0, peak 14 Flag-RPIA or peak 14 Flag-D160A. After 24 hours, cells were fixed and images were acquired using a Leica SPE3 confocal microscope with a 63x objective. scale bar: 10μm

structs used in this experiment were in the N-terminal and C-terminal SH3 domains (L49P, G203R) and the central SH2 domain (R86K). Surprisingly, all GFP-Grb2 mutants, even a double SH3 domain point mutant construct, could be enriched in puncta upon RPIA co-expression (see figure 3.6). This was quite unexpected, since the hypothesis at the time was that the phenotype may be caused by direct interaction of Grb2 via one of the modular domains. How this could be studied further is discussed in chapter 5.1.

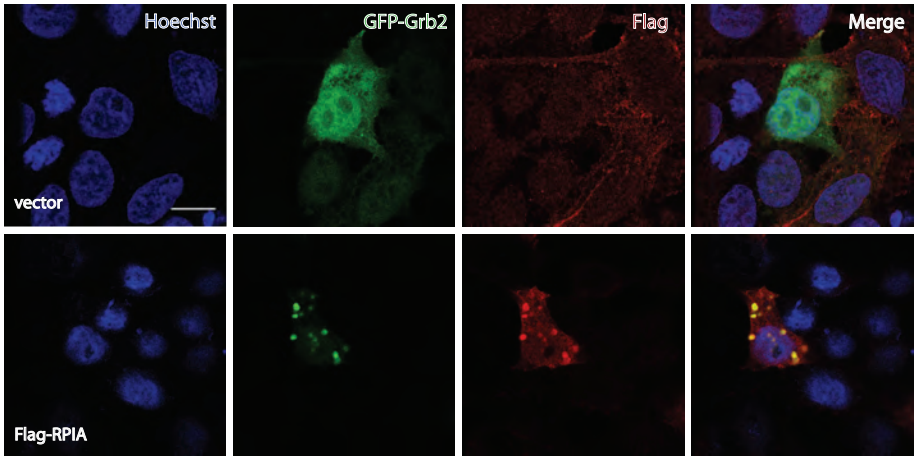

Figure 3.5: RPIA and Grb2 localise to the same spots HeLa cells were co-transfected with a total of 1μg plasmids: pMOS GFP-Grb2 and pMOWS 4.0 (top panel) or p14 Flag-RPIA (bottom panel). Cells were fixed 24 hours after transfection. After fixation, cells were permeabilised and stained with Flag antibody and Hoechst as described in methods. Images were acquired using a Leica SPE3 confocal microscope with a 63x objective. scale bar: 10μm

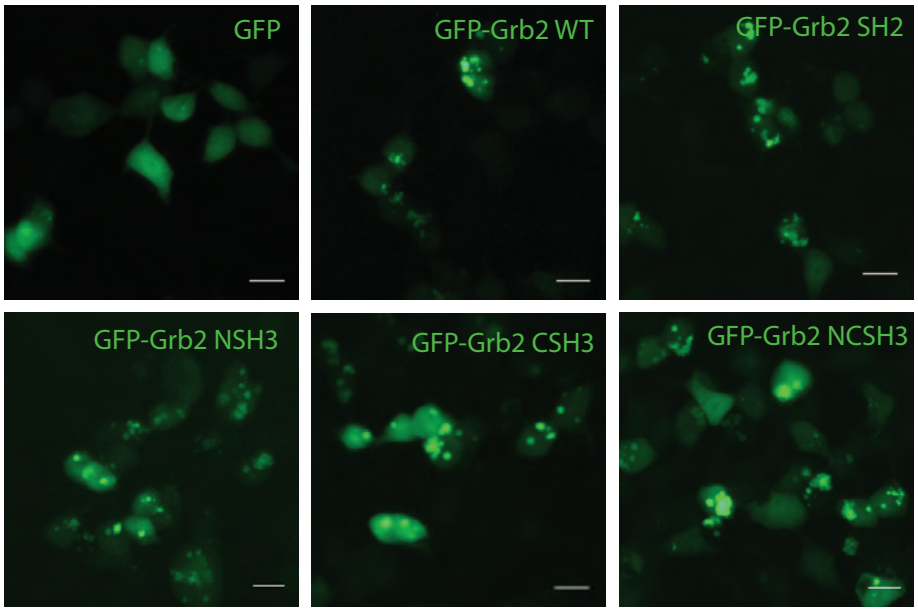

Figure 3.6: Overexpression of RPIA causes various GFP-Grb2 mutants to translocate. HEK293T cells were co-transfected in a 12 well plate with 0.5μg of plasmids: p14 Flag-RPIA + pMOS GFP or indicated GFP-Grb2 plasmids (see table 2.2). After 24hrs, live cell images were acquired with a Leica 2 microscope with a 20x objective. scale bar: 20μm

3.2 Sub-cellular localisation of RPIA

Other metabolic enzymes (such as G6PDH, HK or CAD) had previously been shown to localise to sub-cellular structures or compartments under certain conditions (e.g. mTORC1-dependent). The sub-cellular localisation of proteins can play an important role for their function within the cell, so I wanted to investigate RPIA in this context further. Interestingly, core metabolic reactions such as PPP activity or nucleotide synthesis take place in the cytoplasm[297], but some enzymes have been shown to form clusters within the cytoplasm[171]. To date, PPP enzymes that localise to distinct compartments such as peroxisomes have only been reported in plants and parasitic protozoa (e.g. *Trypanosoma brucei*)[298]. Therefore, RPIA was expected to be localising to the cytoplasm, but sub-cellular localisation studies of RPIA in mammalian systems have not been reported in the literature.

3.2.1 RPIA localises to distinct puncta

Two approaches were taken to determine the subcellular localisation of RPIA. First, I investigated endogenous RPIA localisation by staining HeLa cells with a number of RPIA antibodies that are commercially available (see table 2.6). Under the experimental conditions I tested, no endogenous RPIA could be detected and only background fluorescent signal was observed. It is possible that RPIA is expressed at low levels[299] and/or that the antibodies may not be suitable for immunofluorescence[300]. Using an alternative approach, I transiently over-expressed RPIA with an N-terminal GFP fusion peptide in both HeLa and HEK cells (see figure 3.7). Interestingly, GFP-RPIA localisation is not evenly distributed within the cytoplasm. Instead, distinct puncta that are varying in size and intensity can be observed. Amongst highly transfected GFP-RPIA positive cells there are large, overlapping structures in strongly expressing cells but distinct, smaller puncta are seen in transfected cells with lower expression levels (figure 3.7 upper panel).

3.2.2 RPIA does not localise to CAD puncta

Since other enzymes in the nucleotide biosynthesis pathway have been reported to be in protein complexes that are distinguishable as discrete puncta in cells[171], I

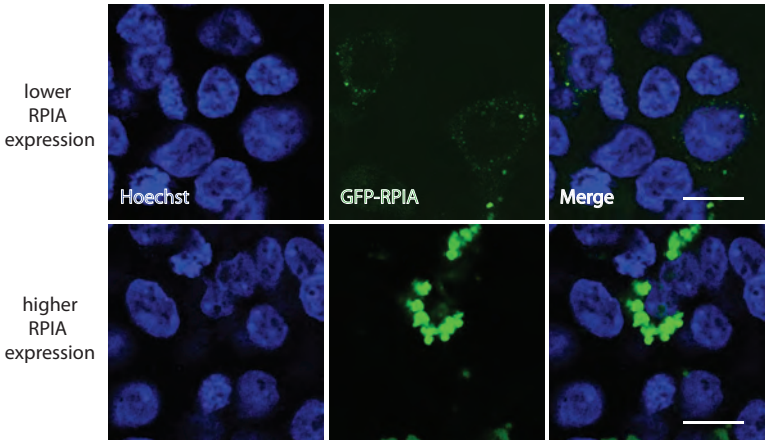

Figure 3.7: RPIA localises to distinct puncta. HeLa cells were transfected with 1μg of p12 GFP-RPIA in 6 well plates. After 24hrs, cells were fixed and stained for hoechst. Images were acquired using a Leica SPE3 confocal microscope with a 63x objective. scale bar: 10μm

tested whether RPIA may also localise to CAD-positive puncta. CAD is a multi-protein complex that synthesises the first step of pyrimidine synthesis (see chapter 1.2.9). Interestingly, the formation of CAD oligomers were recently shown to be controlled via amino acid-mTORC1-S6K signalling and sensitive to rapamycin[172]. This raised the question of whether the observed GFP-RPIA puncta (see figure 3.7) are also controlled via mTORC1. To test this, I starved GFP-RPIA expressing cells by incubation with medium that did not contain amino acids (+/- the mTORC1 inhibitor rapamycin) and performed immunostaining for CAD (see figure 3.8). Interestingly, RPIA did not co-localise with CAD puncta. Furthermore, the distinct RPIA puncta did not appear to be sensitive to starvation or rapamycin as had been reported for CAD[171].

3.3 Metabolic activity and MAPK signalling

Given that Grb2 and MAPK signalling pathways are known to promote cellular growth, it raised the question of whether RPIA expression may have an effect on proliferation, and whether this effect was due to its catalytic activity. The MTT assay is often used as a proxy for proliferation, for instance in Ciou et al[202]. In order to test this hypothesis, I stably transduced HepG2 cells with 3x Flag-tagged

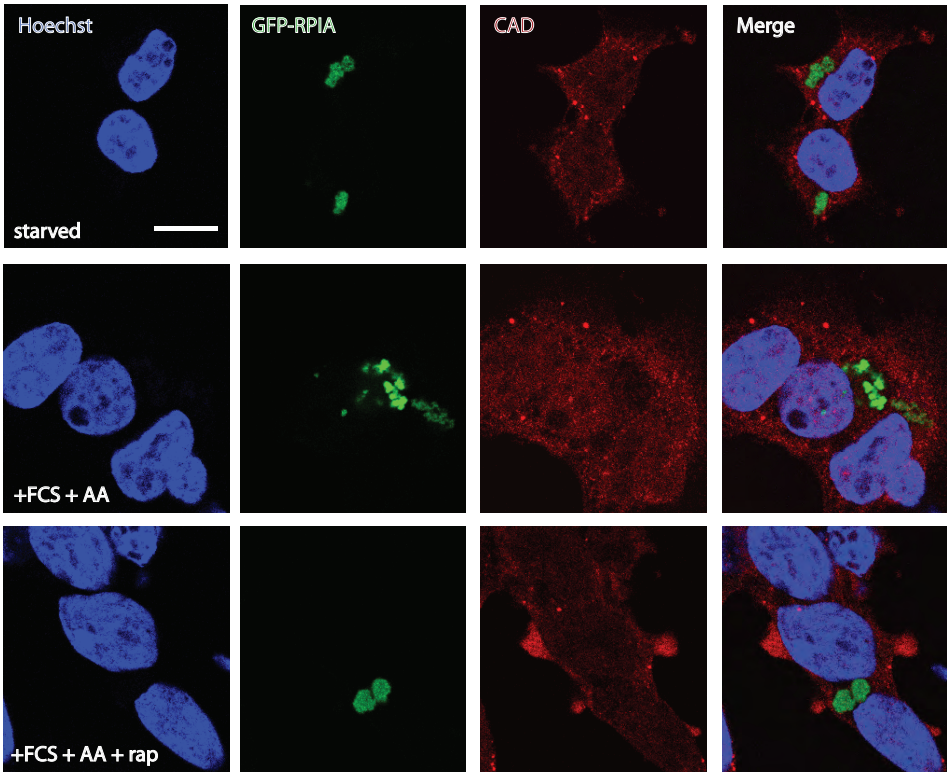

Figure 3.8: RPIA and CAD do not colocalise HeLa cells in 12 well plates were transfected with 500ng p12 GFP-RPIA (see table 2.1) on glass slides. After 24hrs, cells were incubated with DMEM lacking FCS (starved) for 16 hrs, then incubated for 15 min in 1x PBS. Next, cells were then stimulated with full medium (containing 10% FCS and 2 AA) for 1 hr with or without 100nM rapamycin as indicated. Afterwards, cells were fixed, permeabilised and stained for Hoechst and endogenous CAD (see table 2.6). Images were acquired using a Leica SPE3 confocal microscope with a 63x objective. scale bar: 10μm.

WT-RPIA and the catalytic inactive mutant D160A. A firefly luciferase (Luc) construct and non-infected HepG2 cells (control) with identical passage numbers were used as controls. Recombinant cells were selected using puromycin treatment for 96 hours - 100% cell death of a non-infected control population was observed, so I could be confident that the cells were transduced successfully. The expression of the recombinant proteins were confirmed by western blot (see figure 3.9 A). Recombinant Luciferase could be detected at approximately 70kDa and the RPIA constructs at 40kDa, equivalent to the estimated molecular weight of Flag-RPIA.

Interestingly, when metabolic activity of oxidoreductases was assessed using an MTT assay, no differences between the cell lines were observed (see figure 3.9 B).

Although I could detect recombinant protein expression in HepG2 cells, expression levels appeared relatively low, potentially due to the fact that those cells are more challenging to transduct and select at high efficiency. However, there could be a dosis-dependent effect of gene expression that affects the metabolic activity and proliferation rates. To address this better, I stably transduced HEK293T cells using the same experimental procedure and observed very strong over-expression of the recombinant proteins (figure 3.10 A). When proliferation was assessed again, there were no apparent differences in growth between the cells either (figure 3.10 B).

3.4 Altered expression levels of RPIA do not affect ERK 1/2 signalling

Next, I wanted to test whether RPIA expression levels have any effect on MAPK signalling pathway, because it is one of the best studied downstream signalling cascades of Grb2-mediated signalling (see chapter 1.4.3). It could be that RPIA-induced translocation of Grb2 has consequences on the signalling output of the MAP kinase pathway. To test this, I investigated whether a change in RPIA expression levels may affect the phosphorylation status of ERK1/2 . After transient transfection with RPIA knockdown and over-expression constructs (see tables 2.1 and 2.2) cells were starved of growth factors (DMEM + 0.1% FCS) for 16 hours, the MAPK signalling cascade was stimulated with EGF. Next, cell lysates were tested for p-ERK levels and compared to total ERK levels. Interestingly, there were no significant changes in p-ERK1/2 levels (see figure 3.11) upon shRNA-mediated knockdown, over-expression of WT-RPIA ($RPIA^{res}$) or the catalytically inactive mutant ($D160A^{res}$). Comparison between non-treated and EGF-treated cells showed a functional MAP kinase signalling cascade, as indicated by pERK 1/2 levels. Furthermore, the transfection was successful, since the construct with the shRNA or control sequence also contain GFP, which can be detected by western blotting (fig. 3.11 A - GFP antibody). A similar experiment that confirmed those findings was performed with the genomically altered CRISPR/Cas9 RPIA knock-out cells (see chapter 4.6 and figure 4.21). In conclusion, when RPIA levels are

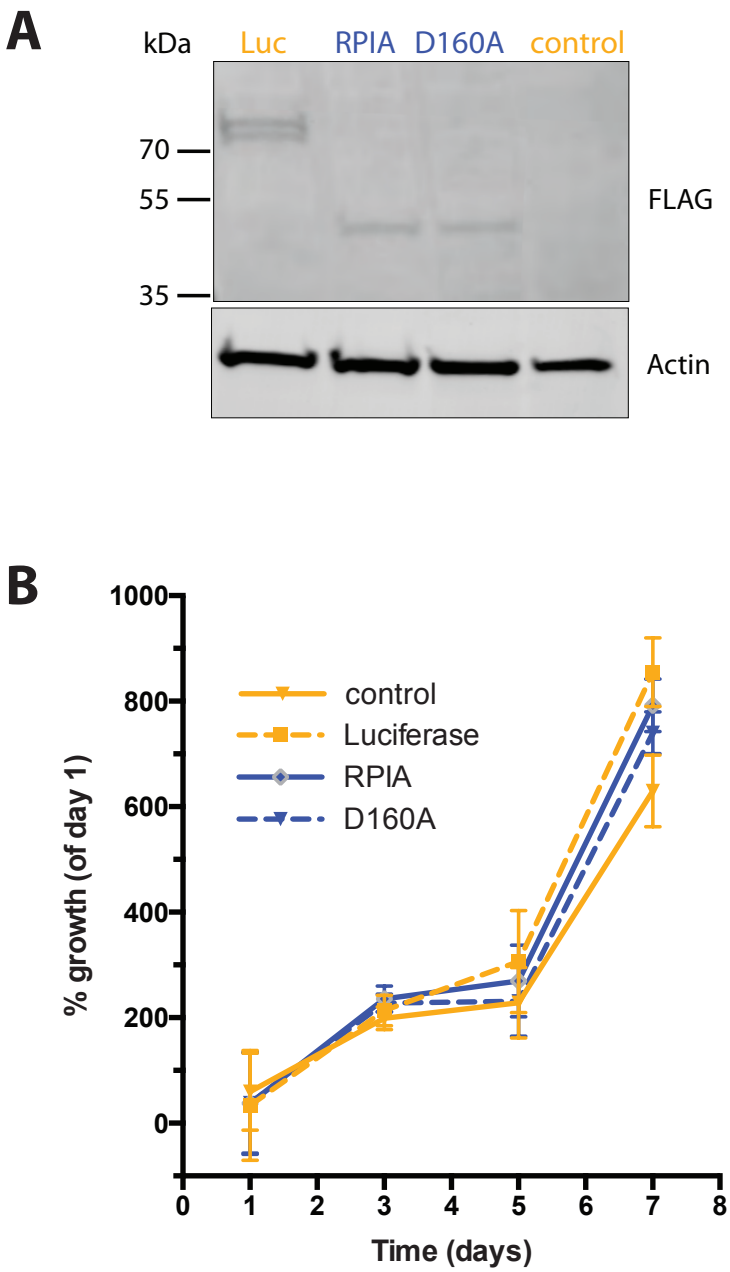

Figure 3.9: Overexpression of RPIA in HepG2 cells does not increase metabolic activity (A) HepG2 cells were stably infected with over-expression constructs (see table 2.1) and presence of recombinant proteins was confirmed by western blot (see table 2.6). (B) MTT assay was used to investigate the effect of over-expression on metabolic activity. HepG2 cells were seeded in six replicates in a 96 well plate at 1000 cells/well. Results are expressed as mean and SD of two independent experiments compared to respective values at 24 hrs.

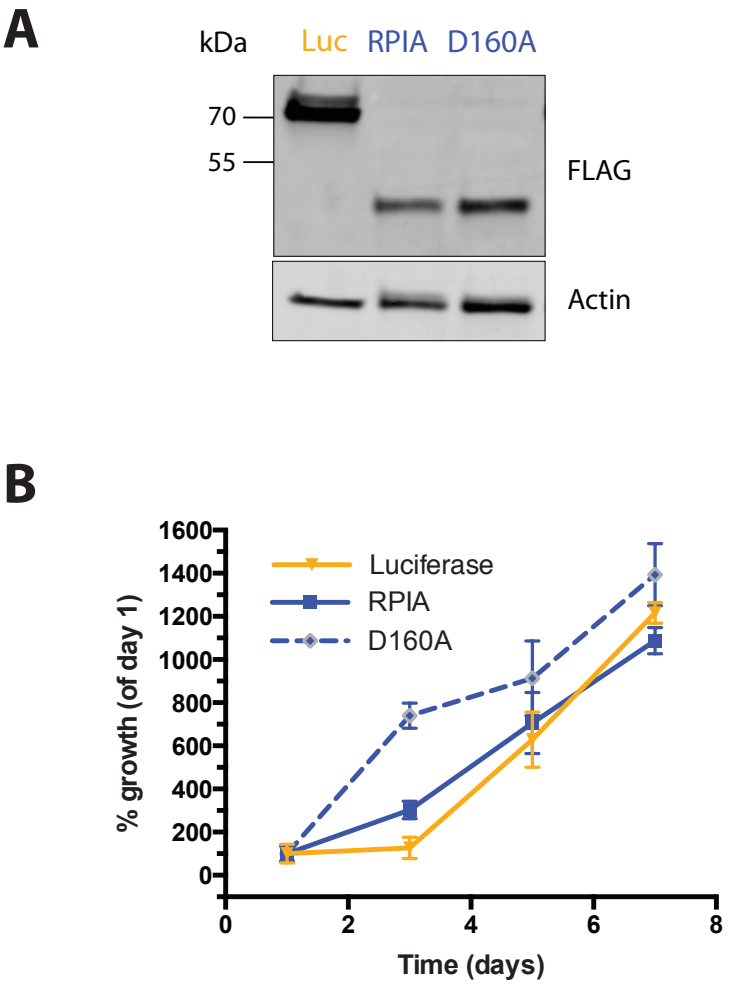

Figure 3.10: Overexpression of RPIA in HEK293T cells does not increase metabolic activity (A) HEK293T cells were stably infected with over-expression constructs (see table 2.1). After 72hrs of puromycin selection, cells were harvested and the presence of recombinant proteins was tested by western blot (see table 2.6). (B) MTT assay was used to investigate the effect of over-expression on metabolic activity. HepG2 cells were seeded in six replicates in a 96 well plate at 1000 cells/well. Results are expressed as mean and SD compared to respective values at 24 hrs.

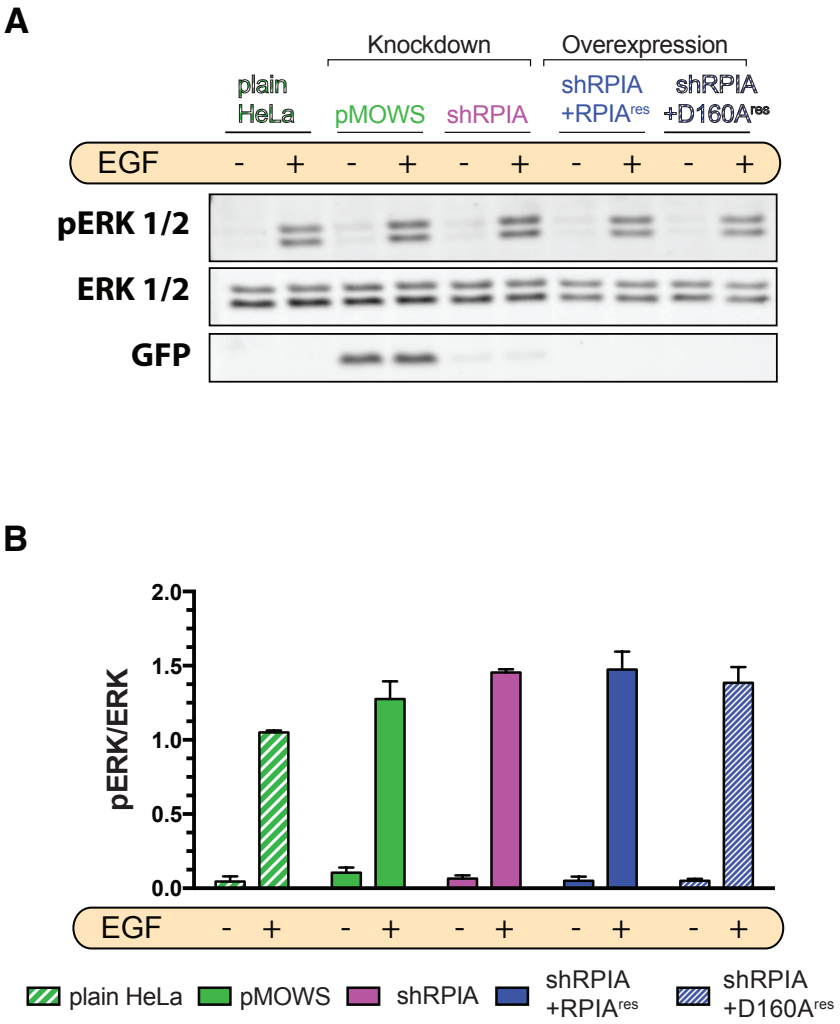

Figure 3.11: RPIA expression does not alter phospho-ERK levels. HeLa cells were mock-transfected or transfected with pMOS GFP, pMOS shRPIA (#4 + GFP). After 48 hrs, cells were washed 2x with PBS and incubated with medium containing low serum (DMEM + 0.1% FCS instead of 10% FCS) for 16 hours. Cells were then stimulated for 5 minutes with starvation medium +/- 100ng EGF as indicated. Cell lysates were separated on 7.5% SDS-PAGE gels and tested with p-ERK, ERK and GFP antibodies for immunoblot analysis. B) Quantification of A) using the densiometric analysis tool from Fiji. Pooled data from analysis from 2 independent experiments.

reduced or elevated in HeLa cells, the p-ERK/ERK ratio is not affected. How these results fit in with what is currently known in the field and how it could be studied further is discussed in chapter 5.2.

Chapter 4

The role of RPIA in the regulation of autophagy

4.1 shRNA-mediated knockdown of RPIA

The recent evidence in metabolic enzymes and metabolites associated with the regulation of autophagy raised an interesting question of whether RPIA may be involved as well. For instance, pharmacological inhibition and shRNA-mediated knockdown of the glycolysis regulator PFKFB3 increased LC3 processing[126]. Considering the importance of R5P synthesis and the ability of metabolites to alter autophagy in the cell, we hypothesised that perturbing RPIA levels may have an effect on autophagy. Parts of this chapter of the PhD thesis have been submitted for publication. At the time of submission for examination, the manuscript **"Ribose 5-phosphate Isomerase A inhibits LC3 processing and basal autophagy"** (J. Heintze, J.R. Costa, M. Weber and R. Ketteler, 2016) was at the stage of addressing the comments of the reviewers. Since then, the manuscript has been accepted in Cellular Signalling (see Heintze et al[312]) and can be accessed via DOI: 10.1016/j.cellsig.2016.06.015. In this section, results are presented regarding the effect of shRNA-mediated knockdown of RPIA on autophagy in HeLa cells.

As outlined in chapter 1.1.4.2, LC3 is a well-established marker protein for investigating the regulation of autophagy[12,301] that can be measured by western blotting and fluorescence. Cellular LC3 localisation changes from an even cytoplasmic

distribution to distinct puncta formation upon activation of autophagy, localising to various stages of autophagy-related organelles (see figure 1.1). This enables measurement of autophagosome formation via microscopy, by measuring either GFP-LC3 puncta or endogenous LC3 puncta (figures 4.2 and 4.3). Furthermore, LC3-I is modified post-translationally by lipidation during the autophagy process to LC3-II (see section 1.1.4.2). The two cellular LC3 isoforms LC3-I and LC3-II can be separated and quantified by western blot due to differential migration patterns on gradient (4-20%) SDS-polyacrylamide gels (figure 4.1). Interestingly, the isoform with the increased molecular weight (LC3-II) migrates faster, possibly as a consequence of increased hydrophobicity[12]. Increased LC3-II levels have been reported to be correlated with induction of autophagy, when normalised to a non-autophagy related control like actin or vinculin[12].

4.1.1 Depletion of RPIA by shRNA increases LC3-processing

In order to study the functional relation of RPIA to autophagy, four different shRNAs sequences targeting human RPIA (pLKO.1 vectors, see table 2.2) were transfected into HeLa cells and western blot analysis of LC3 isoforms from cell lysates was performed after a 72-hour knockdown period. The results show a significant 2.5-3.6 fold increase in LC3-II over LC3-I, thus suggesting an increase in basal autophagy (Figure 4.1 A), with all four sequences being equally effective to cause an increase in LC3-II/LC3-I and loading control (vinculin) ratios. I could also observe a 1.5-2.1 fold increase of LC3-II/Vinculin and a 1.2 fold increase in LC3-II/total LC3 (figure 4.1 B - C).

4.1.1.1 RT-PCR

Similar to the immunofluorescence experiments in chapter 3.2.1, the antibodies against endogenous RPIA used in this study (see 2.6) did not detect RPIA sufficiently to verify successful knockdown (data not shown). Therefore, knockdown efficiency of all shRNAs targeting RPIA was measured by RT-PCR (Figure 4.1 D). Indeed, there was a reduction of expression levels of RPIA by 10-50% compared

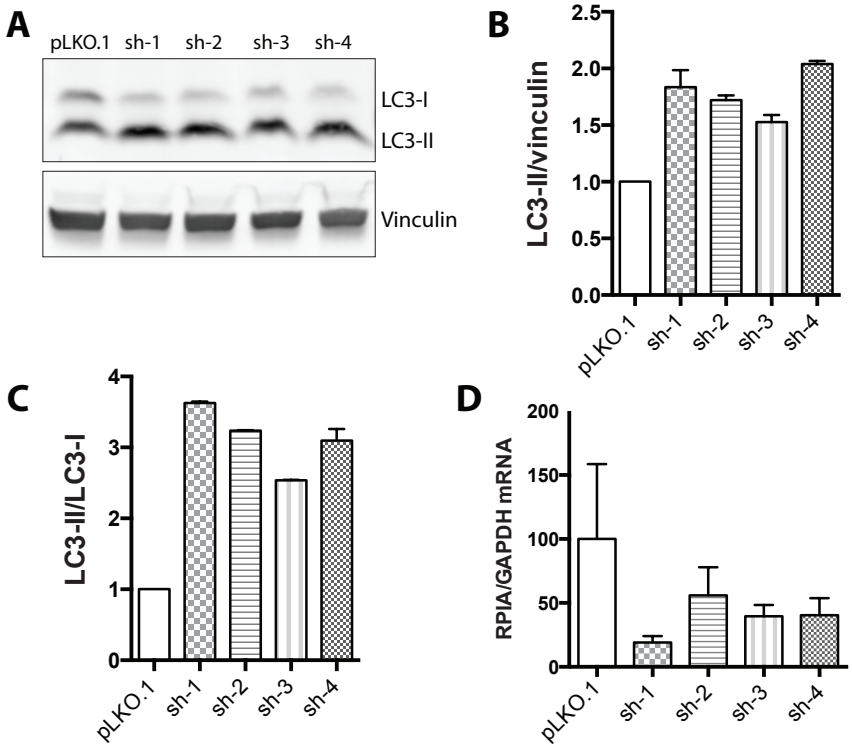

Figure 4.1: LC3 - processing is increased upon shRNA-mediated knockdown of RPIA. A) Immunoblot of LC3-processing in HeLa cells at 72 hour post-transfection with control (pLKO.1) vector or shRNA vectors against RPIA (sh1-4), imaged on the LI-COR Odyssey. B, C) Densitometry analysis of LC-II/Vinculin and LC3-II/LC3-I levels using Fiji. Data represent mean SD, n=2. D) Expression levels of RPIA at 72 hour post-transfection in HeLa cells using qPCR, normalized to GAPDH. Data represent mean SD, n=3

to the control. Next, the #4 shRPIA sequence was cloned into retroviral pMOWS-H1 expression vectors (see chapter 2.3.1), previously found to express transcripts at very high levels in a wide variety of cell types[290]. This enabled experiments using GFP as a transfection marker and a puromycin resistance casette for cellular selection (see table 2.2).

4.1.2 Depletion of RPIA increases puncta in stably expressing GFP-LC3 cell line

In order to establish a potential role of RPIA in the regulation of autophagy, autophagosome formation was tested in HeLa cells that stably express GFP-LC3. Under basal conditions, GFP-LC3 distributes evenly across the cytoplasm, only form-

ing a few LC3-enriched puncta per cell (figure 4.2 A, left panel). Upon induction of autophagy by amino acid starvation and blockage of autophagosomal-lysosomal fusion, enrichment of GFP-LC3 in cells can be observed (figure 4.2 A, right panel). There was a small increase in GFP-LC3 puncta when RPIA levels was depleted under basal conditions, which was very apparent when lysosomal fusion was blocked (figure 4.2 B): compared to control cells, there was a 1.6-fold increase in GFP-LC3 positive puncta in shRPIA cells.

4.1.3 Depletion of RPIA increases endogenous LC3 puncta

In order to further test the findings of increased GFP-LC3 puncta (figure 4.2) and an increase in LC3 processing (figure 4.1), I measured endogenous LC3 puncta under RPIA knockdown conditions. The shRNA pMOWS construct that also expresses GFP (see table 2.2) was used in order to enable better identification of transfected cells. There was an approximately 2-fold increase of LC3-positive puncta compared to control cells under basal conditions (figure 4.3 A), further indicating that RPIA suppresses basal autophagy. This was more evident upon quantification of puncta per cell, puncta per cell area and puncta area per cell area (figure 4.3 B-D) in over 10 000 cells, indicating that this is a robust and quantifiable phenotype.

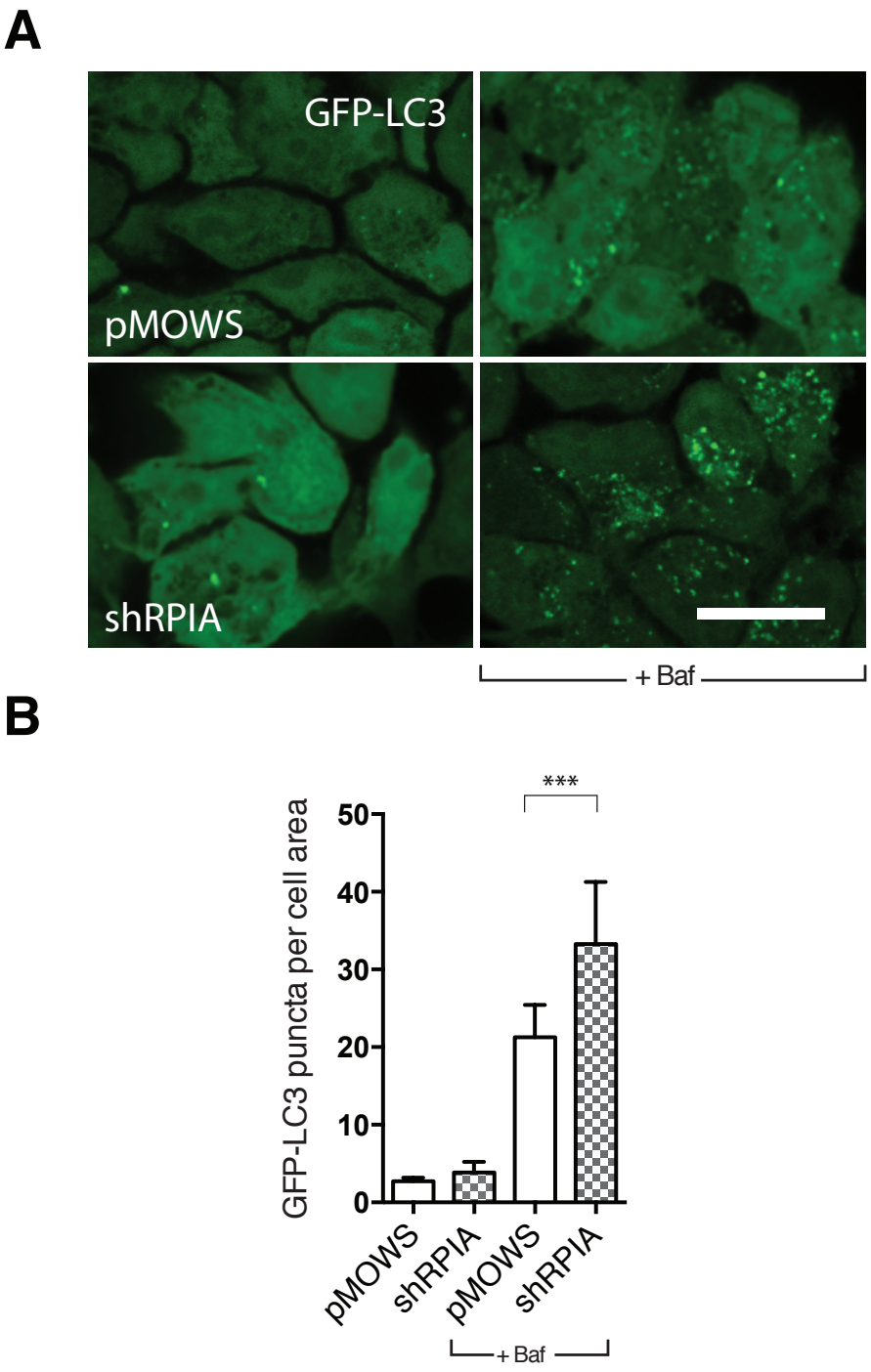

Figure 4.2: Knockdown of RPIA in stably exprssing GFP-LC3 cells increases LC3 puncta A) Stable GFP-LC3 expressing HeLa cells transiently transfected with shRPIA and control vector were incubated with EBSS and with or without 10 nM Bafilomycin for two hours at 37°C and 5% CO_2. Cells were fixed and imaged using an inverted Leica® TCS SPE microscope with a 63x objective, scale bar = 10μm B) Quantification of A) using Fiji for image analysis. Pooled data from analysis of over 500 cells per condition from 2 independent experiments. Bracket indicates t-test p-value; ***=p$<$0.001

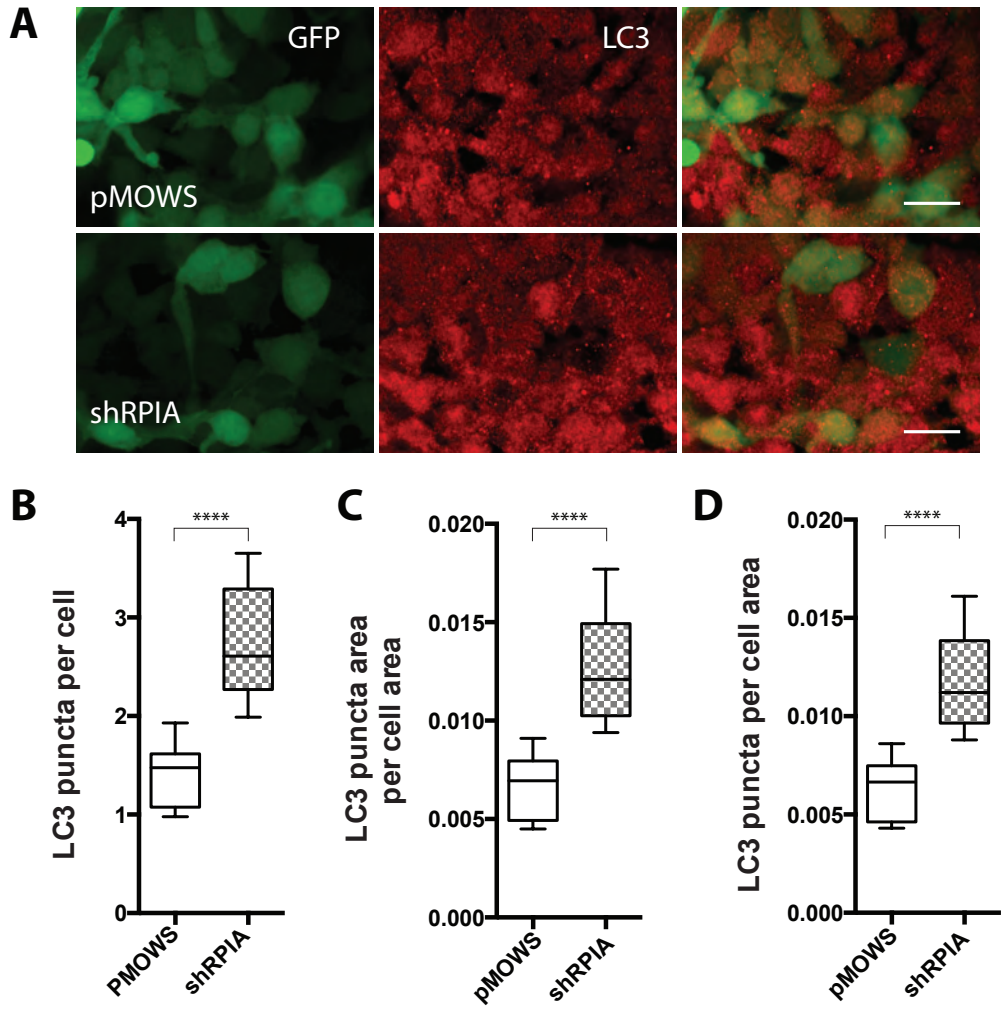

Figure 4.3: Increased endogenous LC3 puncta in RPIA knockdown cells. HeLa cells in 96 well plates were transiently transfected with pMOWS 5.2 GFP shRPIA and control vector (5.2 GFP, see table 2.2) and then incubated for 72 hours at 37°C and 5% CO_2. Cells were fixed and stained with LC3 (Sigma) and imaged using an Opera LX microscope. A) Endogenous LC3 puncta in transfected cells after 72 hours knockdown. Images were acquired on an Opera LX microscope, scale bar = 20 μm. B-D) Image analysis using columbus. Data represent mean SD of 5 000-10 000 cells from 2 independent experiments. Brackets indicate t-test p-values, ****=p<0.0001.

4.2 Pharmacological inhibition of RPIA

4.2.1 LC3-processing is not altered upon treatment with R5P or E4P

Next, I wanted to test whether pharmacological inhibition of RPIA or addition of the product R5P also causes a modulation of LC3 processing. The related sugar E4P has been reported to inhibit RPIA activity[195,302] in some experimental systems. Cells were incubated with 10μM of the compounds for 16 hours. Negative control cells were treated with 1% DMSO for 16 hours, whereas bafilomycin treatment (two hours) was used as a positive control for LC3-II accumulation. The data in figure 4.4 indicate that there was no difference in LC3 processing upon treatment of cells with 10 μM concentrations of E4P and R5P, although cells were indeed capable of LC3 processing as they were responding to bafilomycin treatment (lane 7&8, positive control).

4.2.2 ATG4B luciferase reporter is not altered upon treatment with R5P or E4P

Another autophagy reporter assay has been developed in the lab that measures the cellular activity of ATG4B-mediated proteolytic cleavage of pro-LC3 to LC3-I[12,303,304]. The reporter is based on gaussia luciferase (GLuc) release to the extracellular medium, which can be quantified, for instance by using the chemiluminescent substrate coelenterazine (see figure 4.5 A). GLuc is a reporter enzyme which originates from the marine copepod *Gaussia princeps* that is normally secreted from cells by conventional secretion through an N-terminal signal peptide. Interestingly, GLuc lacking the N-terminus (dN-GLuc) is also rapidly secreted by a non-conventional secretion pathway[303]. In the context of this study, it is important to note that secretion of dN-GLuc is not stress-induced and does not require autophagy[305]. When dN-GLuc is linked to a cytoplasmic protein such as actin, it remains in the cytoplasm. By inserting a protease-susceptible peptide between actin and dN-GLuc, luciferase secretion depends on the protease activity. Therefore, by

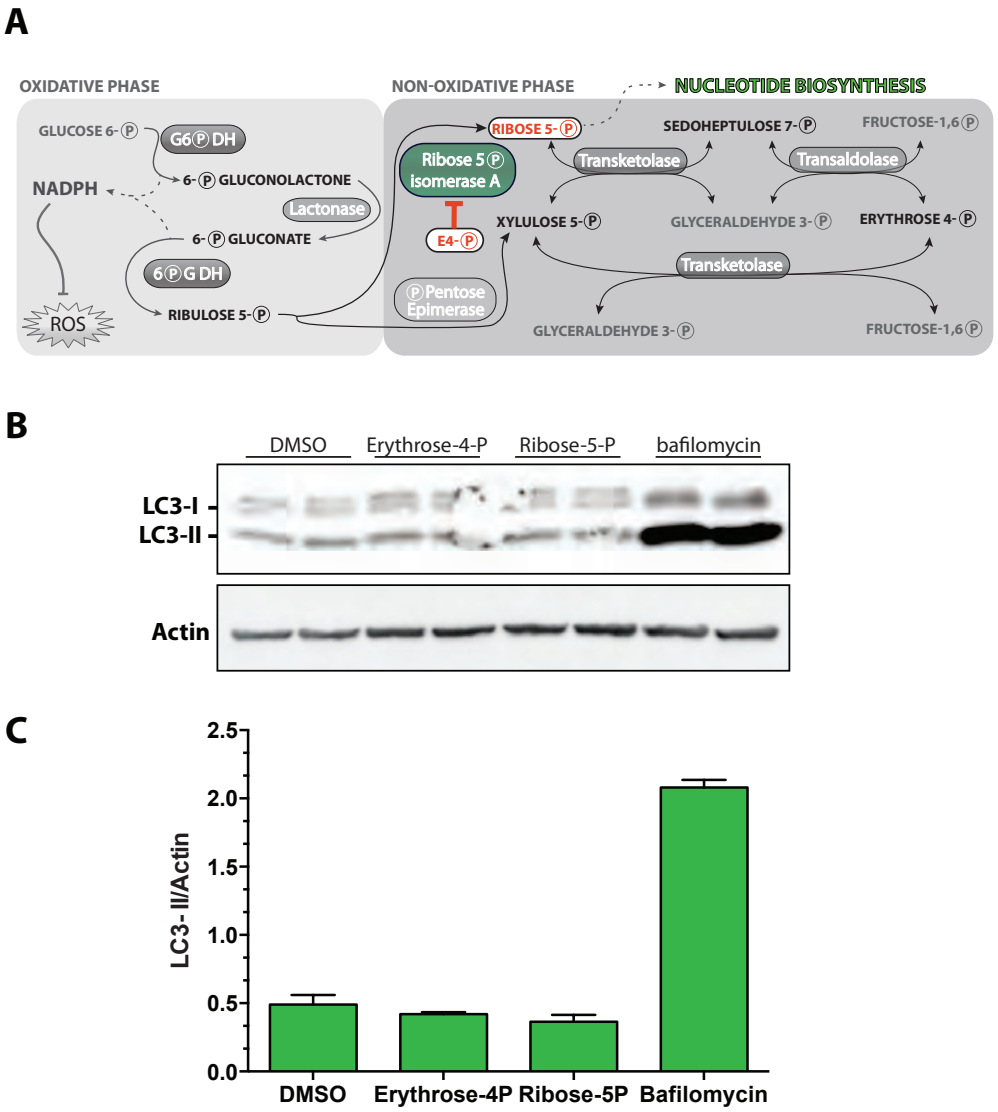

Figure 4.4: Treatment with R5P or E4P does not affect LC3 processing. A) Overview of PPP with indicated position of Riboe-5P and Erythrose-4P (E4P) target RPIA. B) Immunoblot of LC3 processing in HeLa cells (12 well plates) treated with DMSO (1%), E4P, R5P (10μM each) for 16hrs or bafilomycin (10nM) for 2hrs at 37°C (in duplicates). C) Quantification of B), densiometric analysis of LC3-II/actin ratio.

inserting the full-length sequence of pro-LC3, LC3 cleavage via ATG4B can be measured in the supernatant of live cells. This assay is much more compatible for high-content screening approaches than other techniques for measuring autophagy (such as electron microscopy or western blotting). In fact, this approach has been successfully used for high-throughput over-expression and knockdown screens in order to identify novel regulators of ATG4B (Pengo et al, submitted). Some experiments using this reporter were performed prior to the start of this PhD project (see appendix figure A.2) and the results in the context of this study will be discussed in chapter 5.3. Interestingly, shRNA-mediated knockdown of RPIA increased ATG4B reporter activity (Act-LC3-dN-GLuc), but did not affect a control reporter (Act-dN-GLuc).

Next, I wanted to test whether the compounds that did not show any differences in LC3 processing have an effect on ATG4B activity. Recently, it was shown that ROS levels regulate ATG4B[115], so it raised an interesting question of whether the PPP metabolites may affect ATG4B activity. I tested various concentrations of E4P and R5P at a micromolar range in stably expressing Act-LC3-dN-GLuc cells (see figure 4.5), the same reporter cell line used in appendix figure A.2. As a positive control I used a compound (A3) that had previously been shown to strongly induce autophagy (Ketteler lab, unpublished). Doubling the concentration of A3 from 3μM to 6μM caused a 42-fold induction of the reporter (see figure A.2 B), however, no differences in luciferase activity were observed at concentrations up to 100μM for E4P and R5P compared to the negative control DMSO. In summary, the addition of sugar pentoses R5P and E4P to the culture medium does not affect LC3 processing or ATG4B reporter activity.

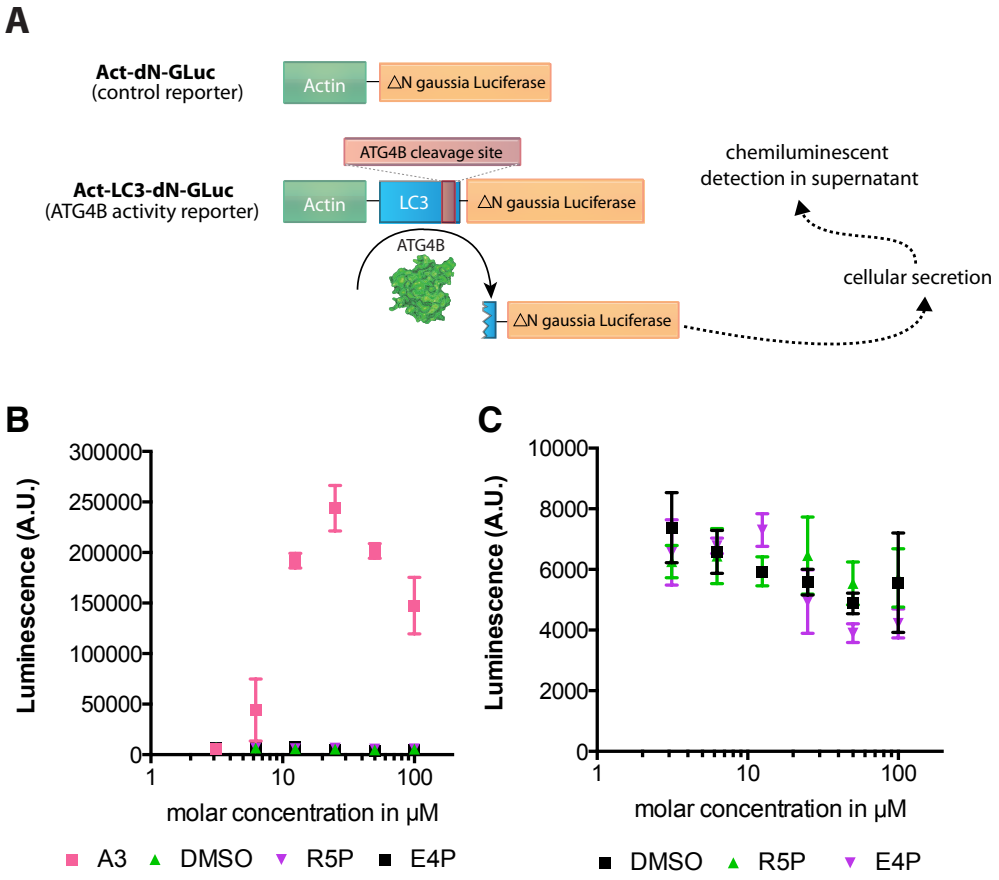

Figure 4.5: Pharmacological inhibition of RPIA or addition of R5P do not modulate ATG4B activity A) Schematic overview of the ATG4B-mediated luciferase release assay. Luciferase is secreted from the cells, depending on the catalytic activity of endogenous ATG4B. The chemiluminescent signal in the supernatant can be measured and correlates to cellular ATG4B activity. B) chemiluminescent signal in supernatant of stably expressing Act-LC3-dN-GLuc cells that were treated with DMSO, E4P, R5P for 16 hours at 37°C in 6 replicates with concentrations as indicated. 10μl of supernatant were used in the Gaussia luciferase release assay and chemiluminescence was measured immediatedly after addition of coelenterazine as described in Luft et al[305]. C) Same data and methodology as in B), excluding positive control A3. Data points are displayed in two graphs, due to the differences in luminescence signal detected. A.U. - arbitrary units.

4.3 The role of RKI in the regulation of autophagy in *saccharomyces cerevisiae*

The data up to this point suggested that RPIA may have a another function apart from the enzymatic reaction, i.e. a non-canonical role in the regulation of autophagy. In order to test this further, I investigated the potential involvement of RPIA in *S. cerevisiae*. Mammalian versions of the RPIA gene have an additional N-terminal stretch of 74 amino acids compared to *E. coli*, *S. cerevisiae* and *D. melanogaster* (see figure 1.10). RPIA depletion may not have an effect on autophagy if this N-terminus is not present. To test this, I used a *S. cerevisiae* strain with a doxycycline-inducible tetOFF system for RKI (tetRKI), the ortholog of RPIA in *S. cerevisiae* (see chapter 1.3.3 and figure 4.6 A). Upon addition of doxycycline, transcription of the mRNA is inhibited and protein levels consequently decrease. The strain was then transformed with GFP-ATG8 (equivalent of GFP-LC3 in mammals, see chapter 1.1.4.2). First, I confirmed that the GFP-ATG8 construct in this strain behaves in response to rapamycin as reported previously[16] (see figure 4.6 B). Indeed, free GFP accumulates in the vacuole and is indicative of increased autophagic flux, validating the use of the GFP-ATG8 reporter in this strain. Next, I compared free GFP and GFP-ATG8 from wild-type and tetRKI strains in the presence or absence of rapamycin and doxycycline (see figure 4.6 C). There was no notable difference in free GFP between the strains, indicating that autophagic flux was not affected. Taken together, the data suggest that RKI levels in *S. cerevisiae* may not play a role in regulating basal or TOR-dependent autophagy, unlike in mammalian cells (see chapter 4.1).

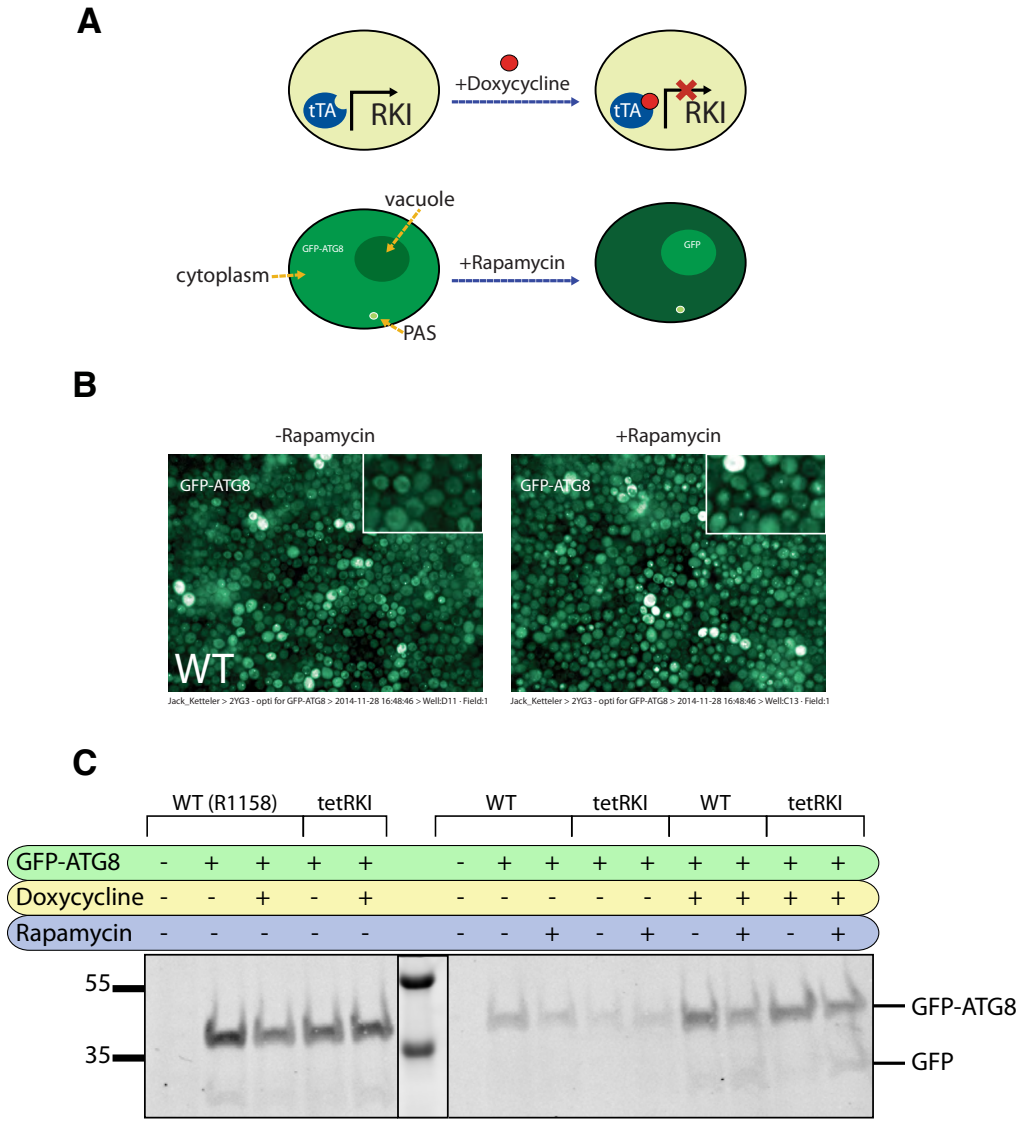

Figure 4.6: RKI depletion in *S. cerevisiae* does not upregulate autophagy. A) Schematic overview of tetOFF system (top panel): the tetracycline transactivator (tTA) protein does not activate transcription in the presence of doxycycline, a stable analog of tetracycline. Schematic overview of GFP-ATG8 in budding yeast (bottom panel): GFP-ATG8 is predominantly cytoplasmic under basal autophagy conditions. When autophagy is induced with rapamycin by inhibition of TOR, the GFP moiety accumulates in the vacuole. PAS - pre-autophagosomal initiation site. B) R1158 WT (wild-type) cells are accumulating GFP in the vacuole upon treatment of 1μg/ml rapamycin for 4 hours. C) analysis of GFP and GFP-ATG8 by western blotting upon treatment of absence or presence of 20μg/ml doxy for 20 hours and 1μg/ml rapamycin for 4 hours as indicated. Lane 6 is the protein molecular weight marker lane

4.4 Generation of CRISPR/Cas9 knockout HeLa cells

Upon prolonged culturing of RPIA-deficient cells with the aid of shRNA mediated knockdown, I observed a weaker phenotype over time, which is an effect that has been observed for other enzymes as well[188]. In order to further validate the shRNA-mediated findings that indicate a role of human RPIA in the regulation of autophagy, I modified the RPIA locus in HeLa cells using CRISPR/Cas9 genome editing technology. How the CRISPR cells were generated, validated and subsequently tested in some of the previously described autophagy assays is presented in this and the next section of the study.

4.4.1 Choice of CRISPR method

CRISPR/Cas9 technology has made modifications to a specific genomic sequence much easier and faster than any other technology available. TALENs and ZFNs that target DNA at a specific locus take a long time to be generated. CRISPR offers a much simpler way of modifying specific regions in the DNA (see figure 4.7). The Streptococcus pyogenes Cas9 (Cas9) nuclease can be targeted to any 20 nucleotide DNA sequence followed by a 5-NGG or 5-NAG protospacer adjacent motif (PAM) in the genome. The system is based on three components: The Cas9 protein is a nuclease that cleaves both strands of DNA. The crRNA binds to a specific region of interest in the genome that contains a 5-NGG or 5-NAG PAM sequence. Finally, the tracrRNA element links the nuclease to the site-specific RNA component. The crRNA and tracrRNA component also exist as a single guide (sgRNA). The Cas9 component has been engineered to achieve alternative functions. In this study, I used the mutant D10A (nCas9), a modification that leads to cleavage of one strand only, instead of a double stranded break (DSB). Previously, it had been shown that more specificity, i.e. less off-target cleavage, can be achieved by using an sgRNA pair in combination with nCas9[291].

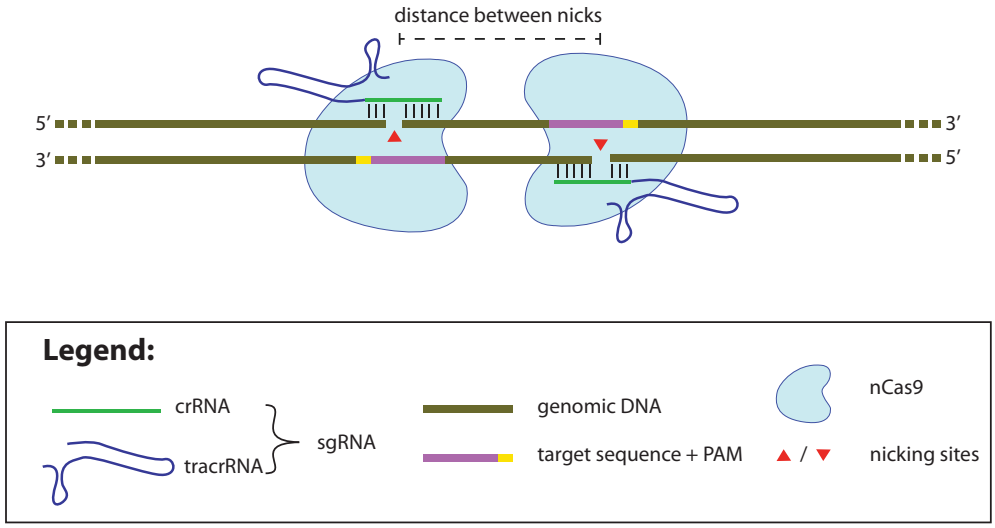

Figure 4.7: CRISPR/nCas9 technique. Two plasmids that contain a sgRNA construct each and $Cas9^{D10A}$, a modified version of wild-type Cas9 that cleaves one DNA strand. By using two sgRNAs with a suitable distance between nicks, localised instability can be generated that leads to the generation of a double-stranded break (DSB) in any region of interest in the genome, without compromising specificity and reducing off-target effects. DSBs are repaired by Non-homologous-end-joining (NHEJ), but this generates insertions/deletions (Indels) that can disrupt gene function.

4.4.2 Optimisation of CRISPR-mediated genome modification

4.4.2.1 Design of sgRNAs

I used the tool http://crispr.mit.edu/ to identify sgRNA target sites of RPIA in humans. It identifies all Cas9 target sites within a 23-500bp DNA sequence of interest, based on a specificity analysis algorithm[306]. For our sgRNA design, I chose to generate sgRNAs to a number of suitable sites on exon 1 (figure 4.9). In total, I generated four "+" and "-" strand sgRNA oligos each, based on top hits from the tool over the first 1000 bp of RPIA exon 1. The list of sgRNA oligos that were then cloned into plasmids can be found in table 2.4.

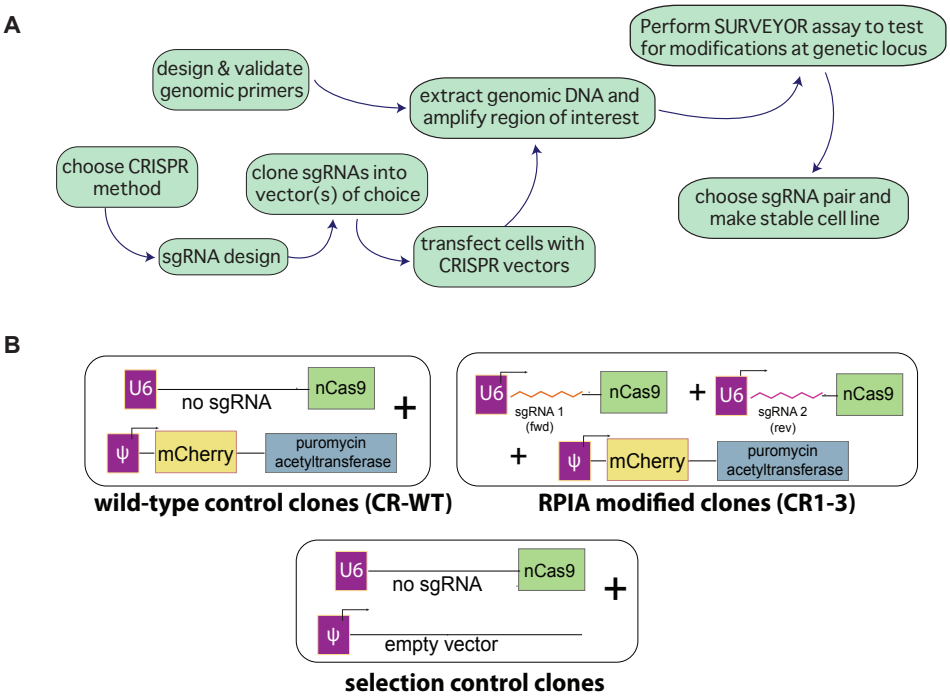

Figure 4.8: CRISPR optimisation pipeline A) Overview of optimisation/setup steps performed in order to generate the stable CRISPR cell line B) plasmid combinations used in the generation of RPIA CRISPR cell lines. Control clones were generated by transfection of empty pX335 vector and a mCherry/puromycin vector. Puromycin was used as a selection marker and mCherry for monitoring successful transfection. An additional control was the selection control group, which also had the pX335 plasmid, but no selection marker. Instead, empty pMOWS 5.2 was used. RPIA modified clones were generated with pX335 vectors that contained sgRNA sequences as indicated in table 2.4. purple boxes indicate promoters in plasmids.

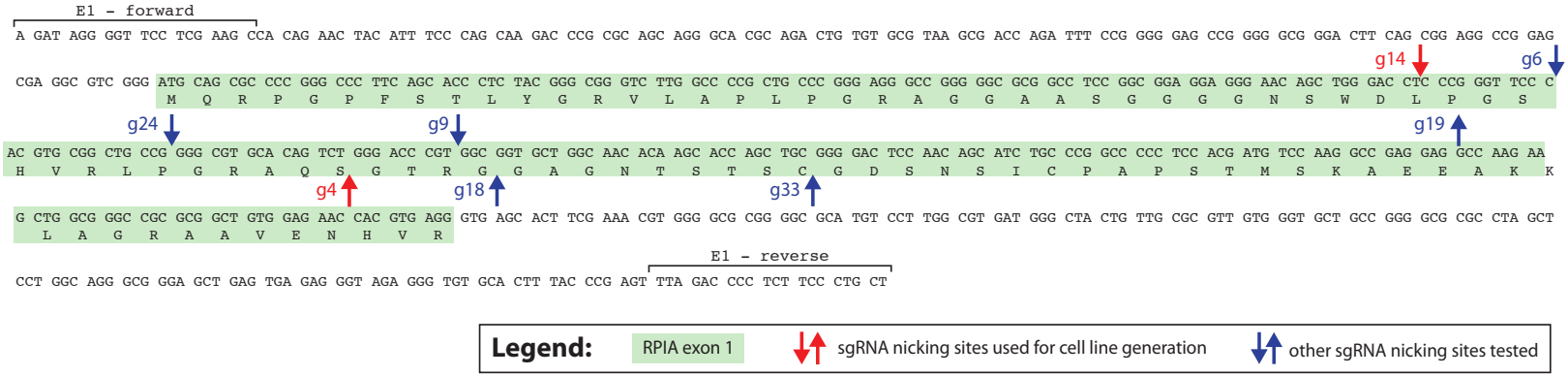

Figure 4.9: Genomic region of RPIA Exon 1 RPIA locus on chromosome 2p11.2, exon 1 is highlighted in a green box. All sgRNA nicking sites used in this study are indicated, as well as genomic primers for validation of modification at the desired locus. Oligo sequences for sgRNAs can be found in table 2.4. Red arrows indicate the nicking sites of sgRNAs that were eventually used for CR1-3 cell line generation.

4.4.2.2 Cloning of sgRNAs into Cas9 vector

Oligos were assembled and cloned into pX335 as described in Ran et al (2013)[291]. In summary, oligos were cloned via *Bbs1* digestion followed by ligation into px335. The restriction site is lost upon ligation into the vector, ensuring the correct insertion upstream of the tracrRNA, the element of the sgRNA that binds to Cas9 and consequently links sequence specificity to nuclease activity. All sequence insertions were verified using Sanger Sequencing and compared to plasmid & genomic sequence using Serial Cloner 2.5.

4.4.2.3 Validation of genomic primers

Next, specific genomic primers that only generate one band from genomic PCR were required to confirm successful modification of RPIA exon 1. These were designed to bind upstream and downstream of Exon 1 and to yield a band of 594bp (as indicated in figure 4.9).

4.4.2.4 SURVEYOR assay to screen for mutations

All cloned sgRNA-containing vectors were used in all logical combinations (only pairs that will generate 5' overhangs, as described in Ran et al[291]) in order to achieve highest modification rates within a cell population. Initially, I intended to use the SURVEYOR assay to quantify the cleavage rates of all possible sgRNA pairs. The SURVEYOR assay is based on nuclease-mediated cleavage of DNA mismatches. In brief, DNA fragments are denatured at 95°C and re-annealed slowly, then incubated with the nuclease, followed by detection of bands after agarose gel electrophoresis. Assuming that at least one locus is modified through non-homologous-end-joining (NHEJ) upon double nicking, one would expect different DNA populations within a single cell and at a cell population level at the modified locus. In the experimental setup, I could qualitatively detect cleavage products when DNA fragments had mismatches, but it was not possible to quantitatively measure different cleavage rates of sgRNA pairs due to strong background bands (figure 4.10). The nuclease activity was confirmed by observing cleavage of amplified, mixed control plasmids (figure 4.10 A lane 3), but not in pure plasmid populations (figure 4.10 A lane 4-

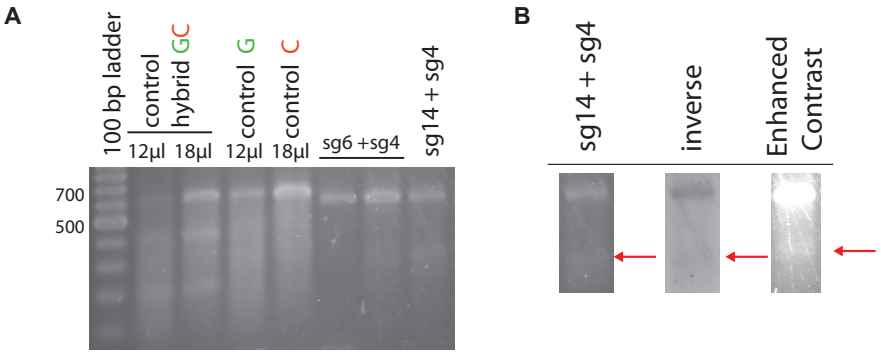

Figure 4.10: Genomic sequence of RPIA in HeLa cells can successfully be modified A) SURVEYOR nuclease assay on amplified PCR products, separated on a 2% agarose gel. Lane 1: 100bp DNA ladder. Lane 2-4: amplified control plasmids that contain a single nucleotide change as described in the manufacturers instructions. Lane 5-7: examples of sgRNA pairs. B) sgRNA pair sg4 + sg14 (from subfigure A) showed a cleavage product. Due to background noise, this is highlighted by colour inversion of the image and enhancing the contrast using Fiji.

5).There was a cleavage product in amplified genomic PCR using sgRNAs sg4 and sg14 (figure 4.10 A lane 7 and B). The distance between the nicks in this pair is 40 nucleotides and their exact location nicking is indicated with red arrows in figure 4.9. Having confirmed that this sgRNA pair is suitable for genome editing of the RPIA locus, I then used those constructs in order to generate a RPIA-modified cell line.

4.4.3 Generation & selection of CRISPR-modified cell clones

4.4.3.1 Transfection of cells

HeLa cells were chosen as target cells, because large-scale mapping of the HeLa cell genome has recently shown that most strains have 2 copy numbers or less for the majority of chromosome 2[307]. Furthermore, HeLa cells were used in previous experiments and they are easy to transfect, select and to isolate individual clones from. RPIA-modified cell lines (in this study referred to as CR1-3) were generated by co-transfection with 2x pX335 (containing sgRNA + nCas9) and a pBABE-mCherry/puromycin containing vector. To control for background nCas9 nuclease activity, I transfected a set of cells with nCas9 and no sgRNA vectors (referred to

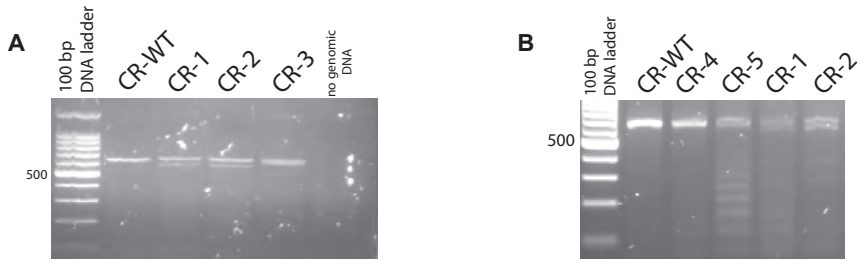

Figure 4.11: Modification of E1 at the RPIA loci in HeLa CRISPR cells. Deletions in CRISPR-RPIA clones can be observed by genomic amplification A) DNA from modified CRISPR HeLa cells was purified and amplified with genomic primers (for sequences see table 2.5 by PCR. Amplification products of CRISPR-RPIA clones (CR1-3) and control (CR-WT) were separated on a 2% agarose gels and labelled with ethidium bromide for visualisation. B) SURVEYOR nuclease assay on amplified PCR products from indicated clones, separated on a 2% agarose gel.

as CR-WT). To control for negative selection, we also transfected a set of cells with empty pX335 and empty pMOWS 5.2 (figure 4.8).

4.4.3.2 Selection of clones

Cells were transfected as described in chapter 2 in more detail. Successful transfection could be observed after 24 hours since a large proportion (40%) of cells was mCherry positive. 48 hours after transfection, cells were selected with puromycin and fresh medium was provided every 2-3 days. The selection and expansion period lasted for a total of 18 days post-transfection, with selection control cells (transfected with empty pX335 and empty pMOWS 5.2) completely dead after 7 days. After 10 days of selection, individual clonal colonies were detached, isolated and expanded. This was done by removing the media, soaking clonal discs in trypsin and transferring them to an empty well in a new place. After clonal expansion, I screened eight clones for modification and tested two control clones (no sgRNA sequence) in the transfected vectors. Out of the RPIA-modified clones, three clones resulted in a differential migration pattern in the amplified genomic PCR products on 2% agarose gels compared to CR-WT (see figure 4.11).

4.4.3.3 Confirmation of modifications

In order to further confirm and validate successful modification at the desired locus, I purified the PCR products of the three clones that showed a differential migration pattern and then sent off the samples for Sanger sequencing. In all three clones (CR1-3), only mixed sequence traces were observed at the expected location but not in the control (CR-WT), indicating modification of the genomic sequence (figure 4.12). However, it could also be the case that only one allele was modified. As this particular CRISPR technology randomly adds or deletes a few base pairs and HeLa cells are diploid for the RPIA locus, if indeed both alleles are mutated, I would expect to recover two different mutations compared to the WT sequence within the genome edited region. In order to identify the exact genomic modifications on both chromosomes at this locus, I sub-cloned the genomic PCR products and re-sequenced individual bacterial clones (figure 4.13 B). Indeed, for all three RPIA-modified clones, I obtained 2 modified genome sequences and did not recover any wild-type sequence. For clone CR-1, all sequenced clones showed out-of-frame mutations, whereas both clones CR-2 and CR-3 showed one in-frame mutation in addition to one out-of-frame mutation each. For clone CR-2, one sequence with a 6 bp insertion was recovered, whereas for CR-3, a 12 bp deletion was identified. For all three clones, only 2 different sequences were recovered, whereas for CR-WT, only the predicted WT sequence was found. Therefore, 2 differentially modified alleles were found in all three clones. Overall, any RPIA mRNA transcripts from both chromosomes in CR-1 are expected to produce missense products that are deficient in translating full-length WT RPIA.

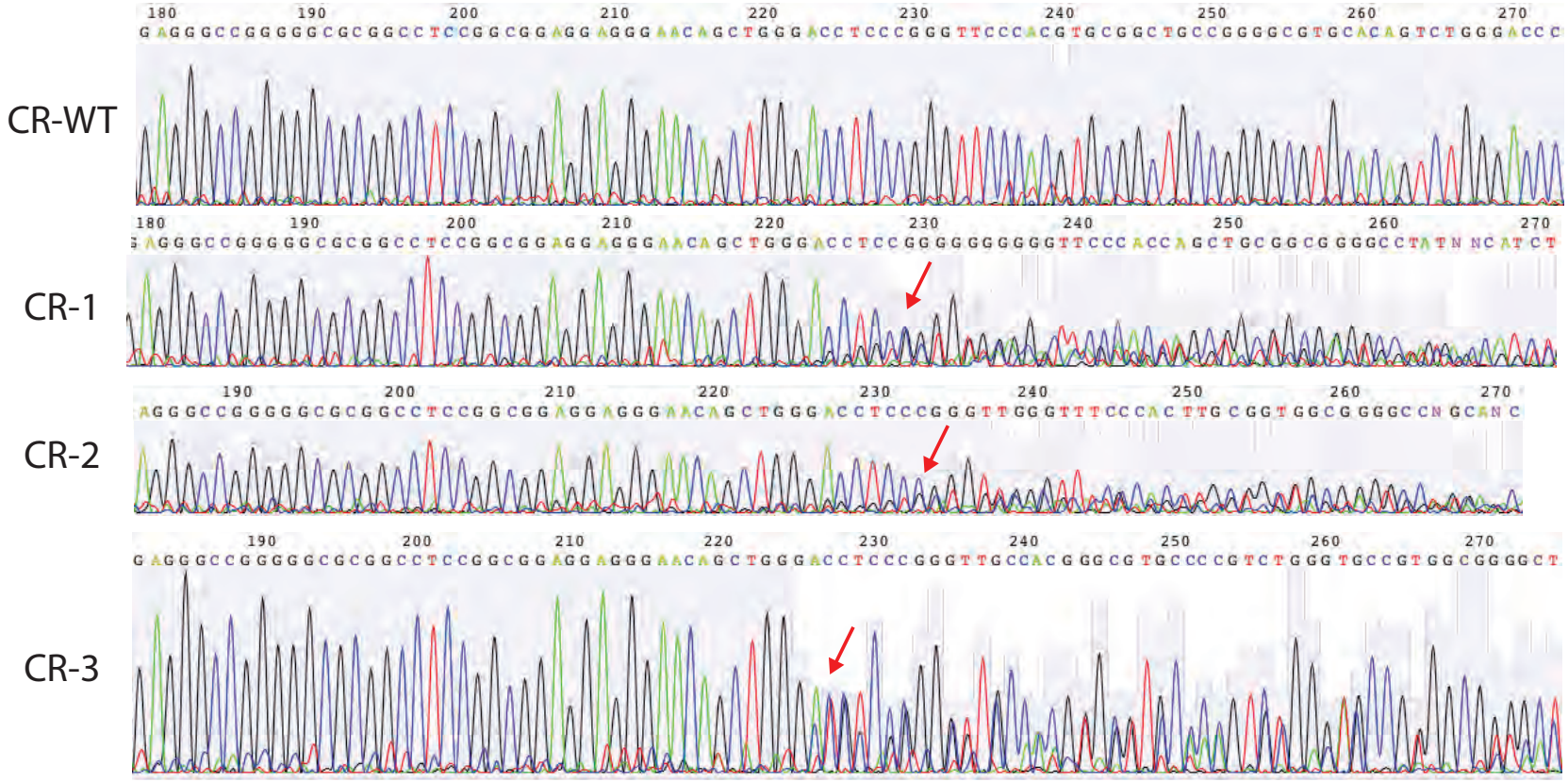

Figure 4.12: Wild-type sequence is altered in CR1-3 clones. Genomic DNA from CRISPR-RPIA clones was purified and DNA region of Exon 1 was amplified by PCR (for primer sequences see table 2.5). Sanger sequencing reaction results of CR-WT and CR1-3 clones for the locus of interest were obtained as indicated. Red arrows show start of mixed base pair reads, indicating a modified sequence on at least one allele.

```
CR-WT  AGGCGTCGGGATGCAGCGCCCCGGGCCCTTCAGCACCCTCTACGGGCGGGTCTTGGCCCCGCTGCCCGGGAGGGCCGGGGGCGCGGCCTCCGGCGGAGGAGGGAACAGCTGGGACCTCCCG------GGTTCCCACGTGCGGCTGCCGGGGCGTGCA
CR-1.1 AGGCGTCGGGATGCAGCGCCCCGGGCCCTTCAGCACCCTCTACGGGCGGGTCTTGGCCCCGCTGCCCGGGAGGGCCGGGGGCGCGGCCTCCGGCGGAGGAGGGAACAGCTGGGACCTCCCGGG-TGGGGTTCCCACGTGCGGCTGCCGGGGCGTGCA
CR-1.2 AGGCGTCGGGATGCAGCGCCCCGGGCCCTTCAGCACCCACTACGGGCGGGTCTTGGCCCCGCTGCCCGGGAGGGCCGGGGGCGCGGCCTCCGGCGGAGGAGGGAACAG----------------------------------------------------
CR-2.1 AGGCGTCGGGATGCAGCGCCCCGGGCCCTTCAGCACCCTCTACGGGCGGGTCTTGGCCCCGCTGCCCGGGAGGGCCGGGGGCGCGGCCTCCGGCGGAGGAGGGAACAGCTGGGACCTCCCGGGTTCGGGTTCCCACGTGCGGCTGCCGGGGCGTGCA
CR-2.2 AGGCGTCGGGATGCAGCGCCCCGGGCCCTTCAGCACCCTCTACGGGCGGGTCTTGGCCCCGCTGCCCGGGAGGGCCGGGGGCGCGGCCTCCGGCGGAGGAGGGAACAG----------------------------------------------------
       ************************************ ********************************************************************************

CR-WT  CAGTCTGGGACCCGTGGCGGTGCTGGCAACACAAGCACCAGCTGCGGGGACTCCAACAGCATCTGCCCGGCCCCCTCCACGATGTCCAAGGCCGAGGAGGCCAAGAAGCTGGCGGGCCGCGCGGCTGTGGAGAACCACGTGAGGGTGAGCACTT
CR-1.1 CAGTCTGGGACCCGTGGCGGTGCTGGCAACACAAGCACCAGCTGCGGGGACTCCAACAGCATCTGCCCGGCCCCCTCCACGATGTCCAAGGCCGAGGAGGCCAAGAAGCTGGCGGGCCGCGCGGCTGTGGAGAATCACGTGAGGGTGAGCACTT
CR-1.2 ----------CTGGGAGCGGTGCTGGCAACACAAGCACCAGCTGCGGGGACTCCAGCAGCATCTGCCCGGCCCCCTCCACGATGTCCAAGGCCGAGGAGGCCAAGAAGCTGGCGGGCCGCGCGGCGGTGGAGAACCACGTGGGGGTGAGCACTT
CR-2.1 CAGTCTGGGACCCGTGGCGGTGCTGGCAACACAAGCACCAGCTGCGGGGACTCCAACAGCATCTGCCCGGCCCCCTCCACGATGTCCAAGGCCGAGGAGGCCAAGAAGCTGGCGGGCCGCGCGGCTGTGGAGAACCACATGAGGGTGAGCACTT
CR-2.2 ----------CTGGGAGCGGTGCTGGCAGCACAAGCACCAGCTGCGGGGACTCCAACAGCATCTGCCCGGCCCCCTCCACGATGTCCAAGGCCGAGGAGGCCAAGAAGCTGGCGGGCCGCGCGGCTGTGGAGAACCACGTGAGGGTGAGCACTT
                 *  *  ************ ************************ ********************************************************************************* ******** *** ** ************
```

Figure 4.13: Allelic variants of RPIA exon 1 in CR-1 and CR-2 clones. Identification of the genomic sequence from both alleles of CR-1 and CR-2. Purified PCR products were sub-cloned into sequencing vectors and isolated from individual bacterial clones. Sequences of CR-WT and CR clones were aligned using ClustalW. Green box indicates nucleotides within exon 1. The red arrow shows the start codon of full-length RPIA

4.5 Testing CRISPR cells in autophagy assays

After the cell model was validated to contain genomic modifications at the RPIA locus (figure 4.13), I wanted to perform experiments that confirm the findings of the knockdown data (see section 4.1). To do this, I assessed the effect of genomic perturbations on LC3 processing and LC3-positive puncta formation in the clones CR-1 and CR-2 compared to them to CR-WT.

4.5.1 LC3 processing is increased in RPIA-depleted cells

Indeed, there is an increase in the ratio of LC3-II over the loading control (actin) under basal conditions as detected by western-blotting (figure 4.14 A, lanes 1-3). When autophagosome fusion with lysosomes was blocked using Bafilomycin A (an inhibitor of lysosome acidification), there is also an expected increase of LC3-II levels compared to mock-treated, but the difference compared to CR-WT cells (figure 4.14 A, lanes 4-6) in not as apparent. Conclusively, the CRISPR-modified RPIA cells have increased LC3-II levels compared to CR-WT control under basal conditions, which was found in five independent experiments (figure 4.14 B).

4.5.2 RPIA-depleted cells display an increase in LC3 puncta

Next, I tested whether the increase in autophagosome formation under RPIA knockdown conditions could also be observed in the RPIA depleted CRISPR clones, as measured by LC3-positive puncta. I expected to observe an increase in LC3 punta when cells were incubated in full medium. Indeed, both clones CR-1 and CR-2 showed a remarkable increase in LC3-positive puncta when compared to CR-WT cells (figure 4.15). Upon treatment with bafilomycin, a further increase in LC3-positive puncta was observed for all three cell lines, but the differences of CR-1 and CR-2 compared to CR-WT were not as apparent (figure 4.15), which is consistent with the findings of LC3-II levels in figure 4.14.

These results were observed in three independent experiments, in the process analysing 10,000-28,000 cells per condition. From this, it can be concluded that LC3-positive puncta are increased in CR-1 and CR-2 clones compared to control cells under basal conditions. However, after keeping cells in culture for a prolonged

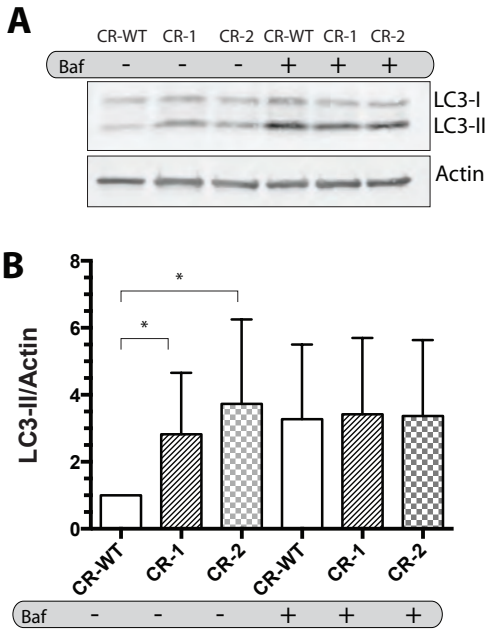

Figure 4.14: LC3 processing is upregulated in RPIA depleted CRISPR cells. Immunoblot showing LC3-processing in CR-1, CR-2 and control cells (CR-WT). Indicated lanes were treated with 10nM bafilomycin for two hours prior to cell lysis. B) Densitometry analysis of relative LC-II/Actin levels using Fiji. Data represent mean SD, n=5. Brackets indicate t-test p-values; *=p$<$0.05

time (above passage number 7), the differences in increased LC3 puncta compared to control were less apparent. This could be due to an established phenomenon that metabolically altered cells adapt to gene deficiencies over time[188].

4.5.3 Pharmacological inhibition of TKT does not alter autophagy

Cumulatively, the data so far suggests that the RPIA protein itself, but not R5P levels, may play role in the regulation of autophagy. In order to address this further and separate potential effects of R5P levels and a non-canonical function of RPIA, I measured LC3 processing as previously, but in the presence of a pharmacological inhibitor of TKT[204]. TKT is the other enzyme in the PPP that can generate R5P (see chapter 1.3) and can be inhibited with the compound oxythiamine. It would be interesting to see whether further reduction of R5P levels in RPIA-depleted cells

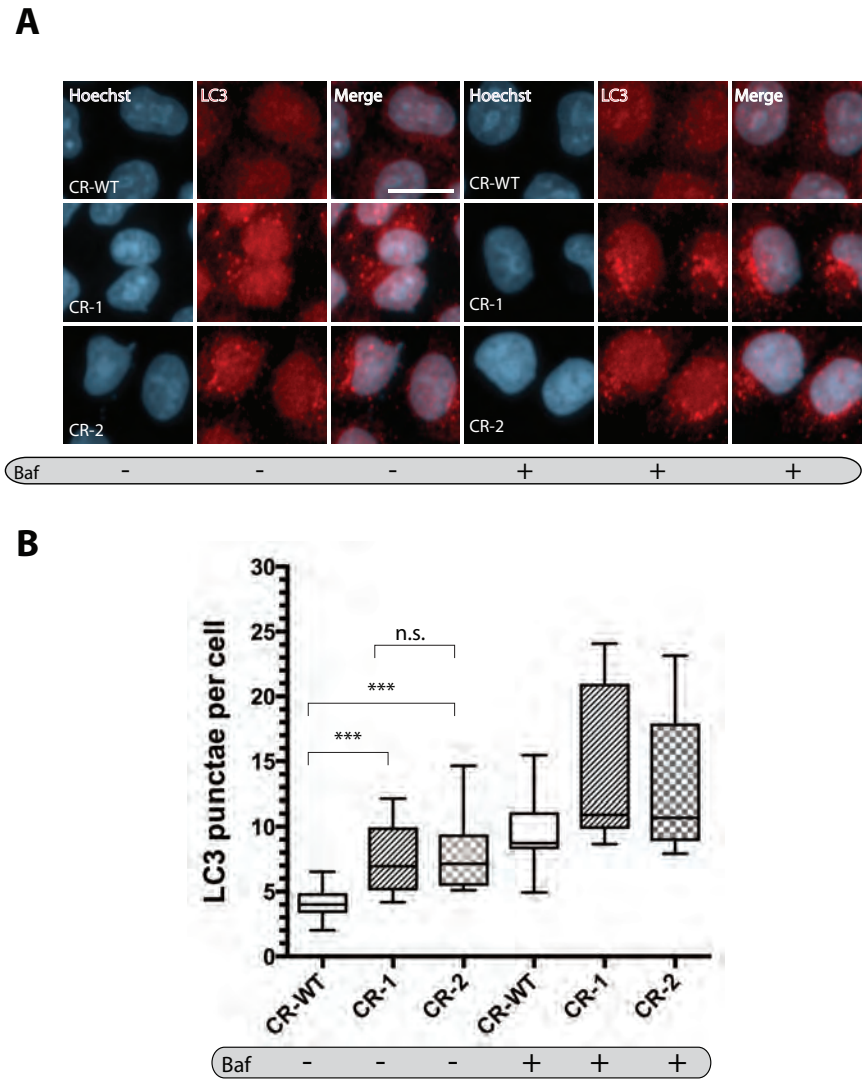

Figure 4.15: LC3 puncta are increased under basal conditions in RPIA-depleted cells. A) Endogenous LC3 punctae in fixed CR-WT, CR-1 and CR-2 that were treated with 10nM bafilomycin for two hours. Images were acquired on an Opera LX microscope, scale bar = 20m. B) Quantification of A) using Columbus image analysis software. 10 000-28 000 cells per condition were analysed in 3 independent experiments. Brackets indicate t-test p-values; ***=$p<0.001$; n.s.= non significant

have a synergistic effect on the regulation of autophagy. On the other hand, if the supression of autophagy via RPIA were non-canonical, there should be no increase in LC3 processing compared to mock-treated cells. Indeed, between oxythiamine-treated and mock-treated cells there was no increase in LC3 processing (see figure 4.16), but an increase in RPIA-depleted cells compared to CR-WT as observed previously (see figure 4.14).

4.5.4 Mass spectrometry

Next, I wondered if RPIA depletion in the CRISPR cells results in metabolite changes in the PPP. In order to investigate this further, I started a collaboration with the group who first identified and reported the patient with RPIA deficiency[199,201]. The group specialises in measuring cellular metabolites of the PPP using metabolomic mass spectrometry (MS). I prepared equal cell numbers of RPIA depleted and CR-WT cells and sent the samples off for measurements. There, the cells were lysed, phosphate sugars were extracted and enriched in the samples as described previously[199,292]. Samples were then analysed using high performance liquid chromatography (HPLC) coupled with tandem mass spectrometry (electrospray ionisation on an API-3000 MS/MS). One should note that distinguishing between alterations of cellular sugar levels that have very similar molecular masses is quite challenging. In addition to that, the PPP metabolites R5P, Ri5P and X5P actually have exactly the same molecular weight (see molecular composition in figure 4.17). However, due to the chromatography conditions, retention times in the column are improved, which effectively increases the signal intensities to above the lower detection limit. This also allows to distinguish between Ri5P/X5P and R5P (see two elution peaks in figure 4.17). However, this technique cannot distinguish between Ri5P/X5P or between G6P/F6P[199]. Furthermore, E4P has a very high threshold of detection, so cellular levels cannot be quantified easily with this technique (see 4.18). The assay also includes an internal reference which allows to compare quantities between samples, in this case ”heavy” glucose 6-P (C^{13}-G6P).

Indeed, various phosphorylated sugar metabolites could be measured simultaneously in HeLa cells (see figures 4.17, 4.18 and 4.19). For technical reasons, this

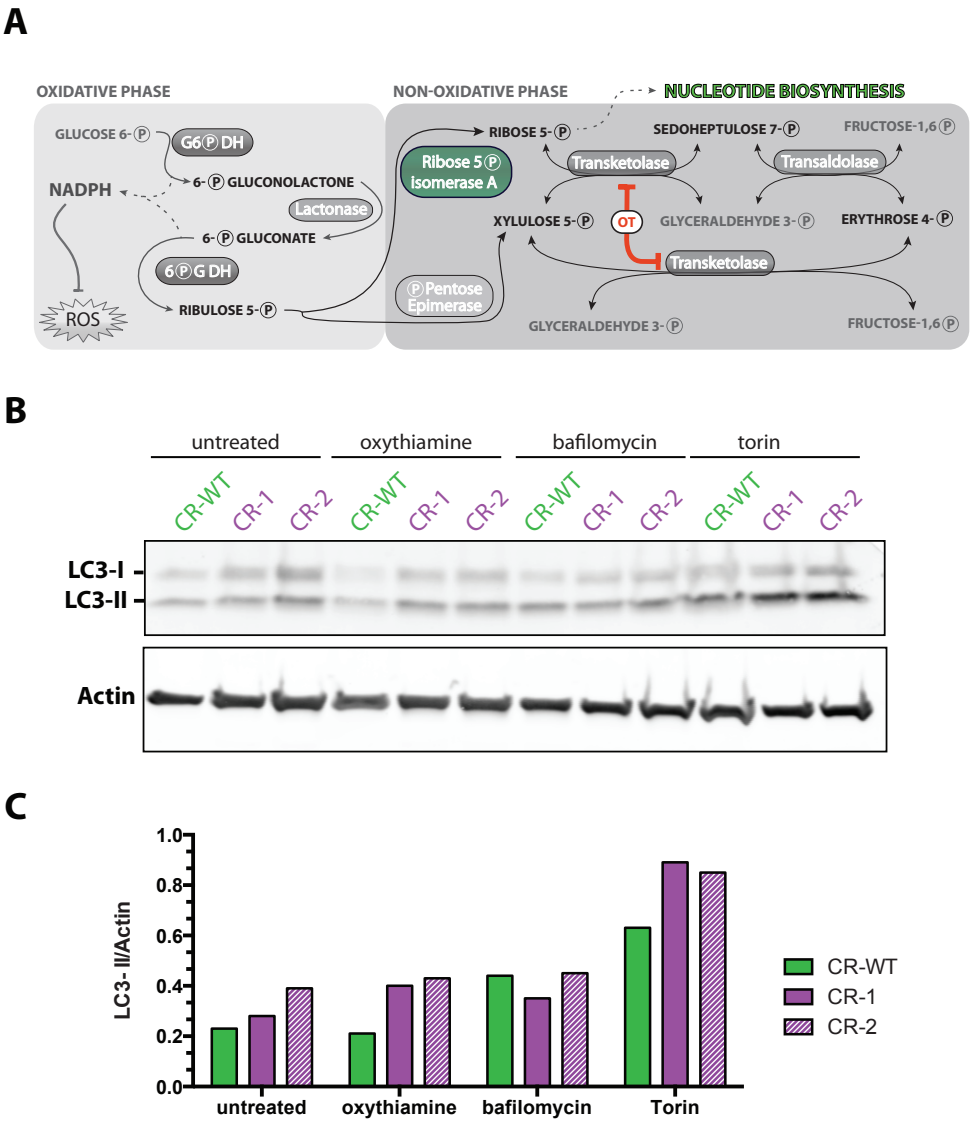

Figure 4.16: Pharmacological inhibition of TKT does not increase LC3 processing. A) Transketolase enzymatic activity is inhibited by oxythiamine (OT) B) HeLa CRISPR control (CR-WT) and clones (CR1, CR2) were treated with OT (10M), bafilomycin (10nM) or torin (250nM) for 2hrs at 37*C. Protein levels were tested by western blotting with the indicated antibodies (for dilutions and origin see table 2.6). C) quantification of B) showing relative LC-II/Actin levels. Densiometric analysis was performed using Fiji, n=1.

assay was only performed on one round of samples so far, but the results were promising. The preliminary data show that in CR-1, the clone that has two frame-shift mutations, there appears to be a reduction in the R5P over X5P/Ri5P ratio (see figure 4.17). There was also a reduction in S7P levels, one of the substrates of the other R5P-generating enzyme TKT. The was no or little differences in R5P levels between CR-2 (clone with only one allele that had a frame-shift mutation) and CR-WT.

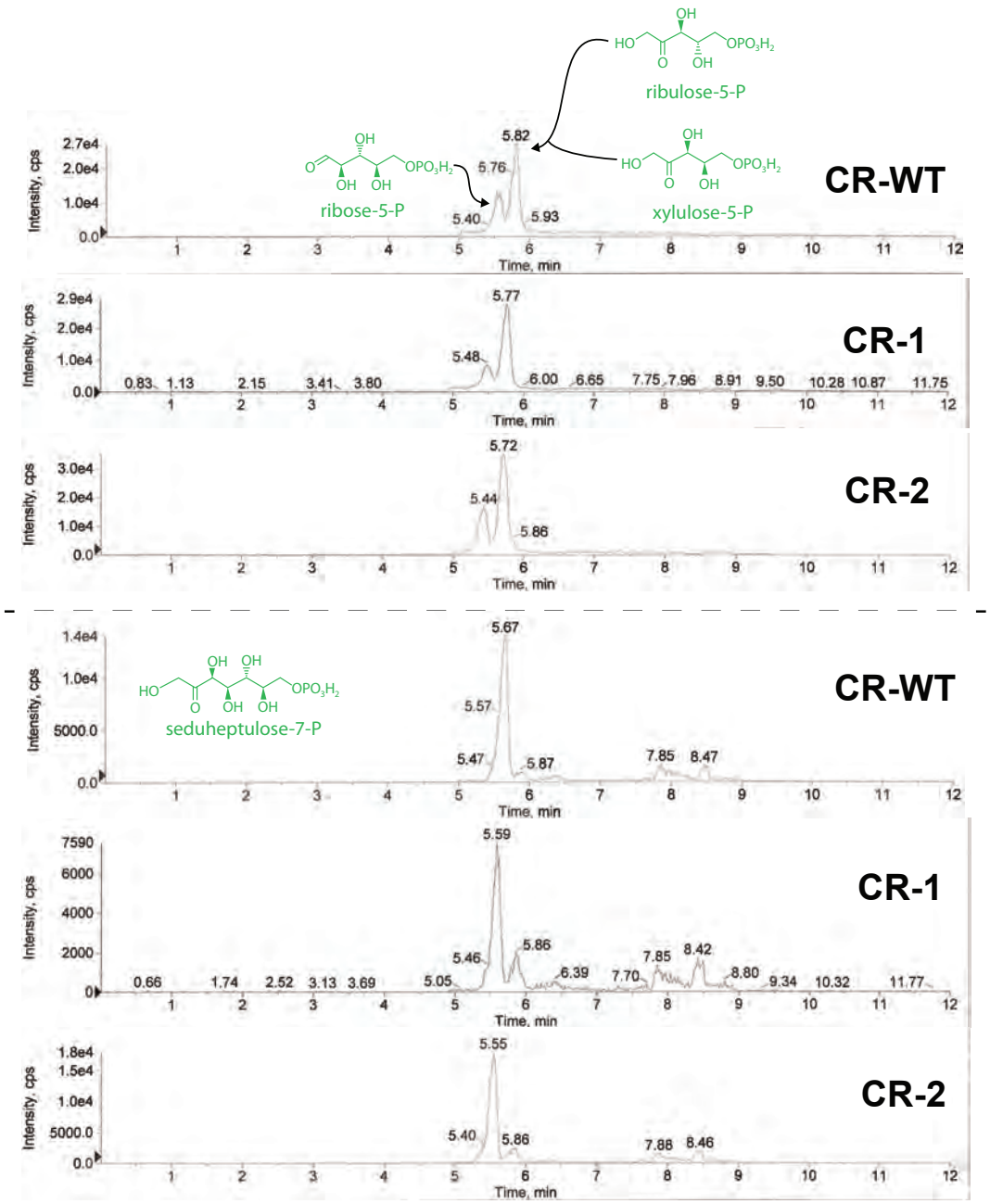

Figure 4.17: R5P and S7P levels in CRISPR cells. CR-WT, CR-1 and CR-2 cells from a 90% confluent 10 cm cell culture dish were sent off for metabolomic mass spectrometry analysis. Phosphate sugars from samples were extracted and enriched using HPLC, followed by electrospray ionisation on an API-3000 MS/MS as described in Huck et al[292]. Plots show intensity (counts per second) and elution time (minutes) of Xylulose-5P (X5P)/ Ribulose-5P (Ri5P) (one peak), Ribose-5P (R5P) and seduheptulose-7P (S7P).

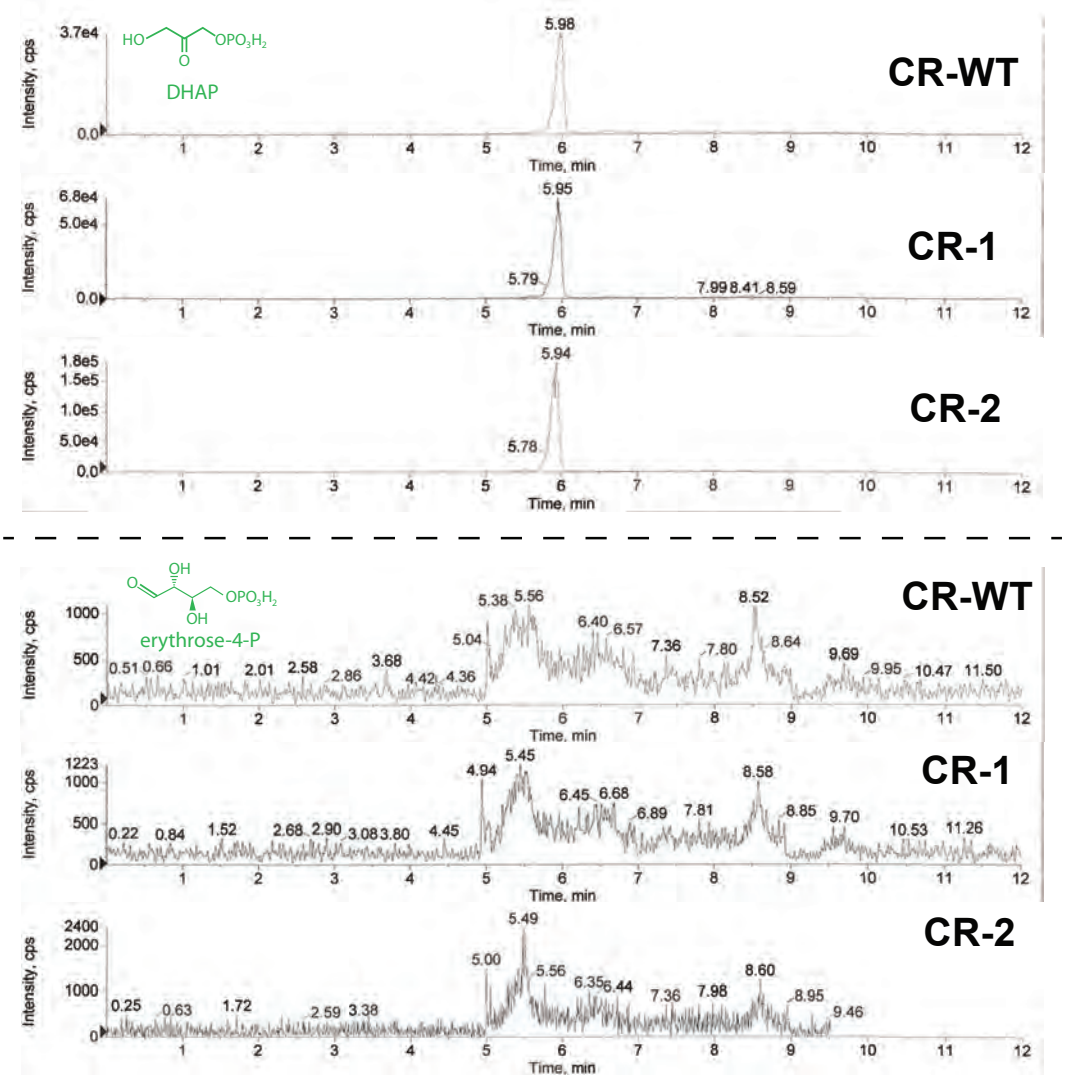

Figure 4.18: DHAP and E4P levels in CRISPR cells. CR-WT, CR-1 and CR-2 cells from a 90% confluent 10 cm cell culture dish were sent off for metabolomic mass spectrometry analysis. Phosphate sugars from samples were extracted and enriched using HPLC, followed by electrospray ionisation on an API-3000 MS/MS as described in Huck et al[292]. Plots show intensity (counts per second) and elution time (minutes) of di-hydroxyacetone-P (DHAP) and Erythrose-4P (E4P), although the latter could not be quantified due to a high lower detection limit.

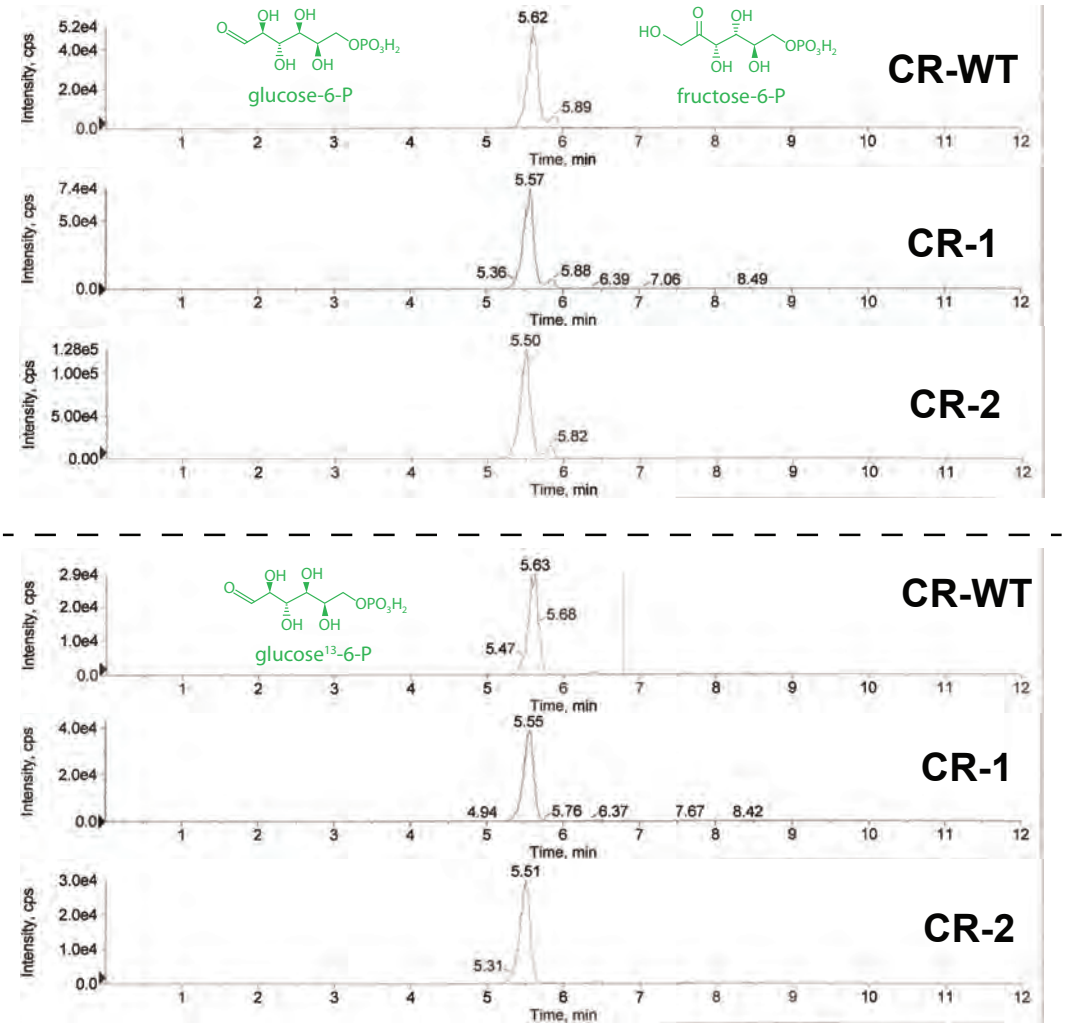

Figure 4.19: G6P/F6P levels in CRISPR cells. CR-WT, CR-1 and CR-2 cells from a 90% confluent 10 cm cell culture dish were sent off for metabolomic mass spectrometry analysis. Phosphate sugars from samples were extracted and enriched using HPLC, followed by electrospray ionisation on an API-3000 MS/MS as described in Huck et al[292]. Plots show intensity (counts per second) and elution time (minutes) of glucose-6P (G6P) and the internal reference "heavy" C^{13} glucose-6P.

4.6 Metabolic activity and MAPK signalling in CRISPR cells

Apart from studying the regulation of autophagy in the CRISPR cells, I also wanted to test whether genomic depletion of RPIA has an effect on metabolic activity and MAPK signalling (see experiments in chapters 3.3 and 3.4). For this, I measured oxidoreductase activity in CR-WT, CR-1 and CR-2 cells using an MTT assay, as performed with in the stably transduced HEK293T and HepG2 cells (see figures 3.9 and 3.10). Interestingly, there is also no apparent difference in proliferation between RPIA-depleted and control cells.

In another study that used an inducible murine K-RAS^{G12D} model to study proliferation, it was reported that the difference in proliferation under RPIA knockdown conditions is more apparent under lower glucose concentration. In order to test whether the effect on growth difference is masked by the high glucose concentration (25mM) in standard DMEM medium, the experiment was repeated with low (5.6mM) glucose medium. Interestingly, no difference in proliferation rates between the clones and the control could be observed (see figure 4.20).

Next, I investigated whether there are any changes in the MAPK signalling cascade in the RPIA-depleted cells, as tested in the shRNA-mediated knockdown experiment (see figure 3.11). In agreement with the previous data, there was no difference in p-ERK/ERK or pERK/COX IV ratio (see figure 4.21).

Concluding from the growth assays and the ERK activation experiments, RPIA does not seem to promote growth or affect the MAPK signalling cascade, at least in HeLa cells.

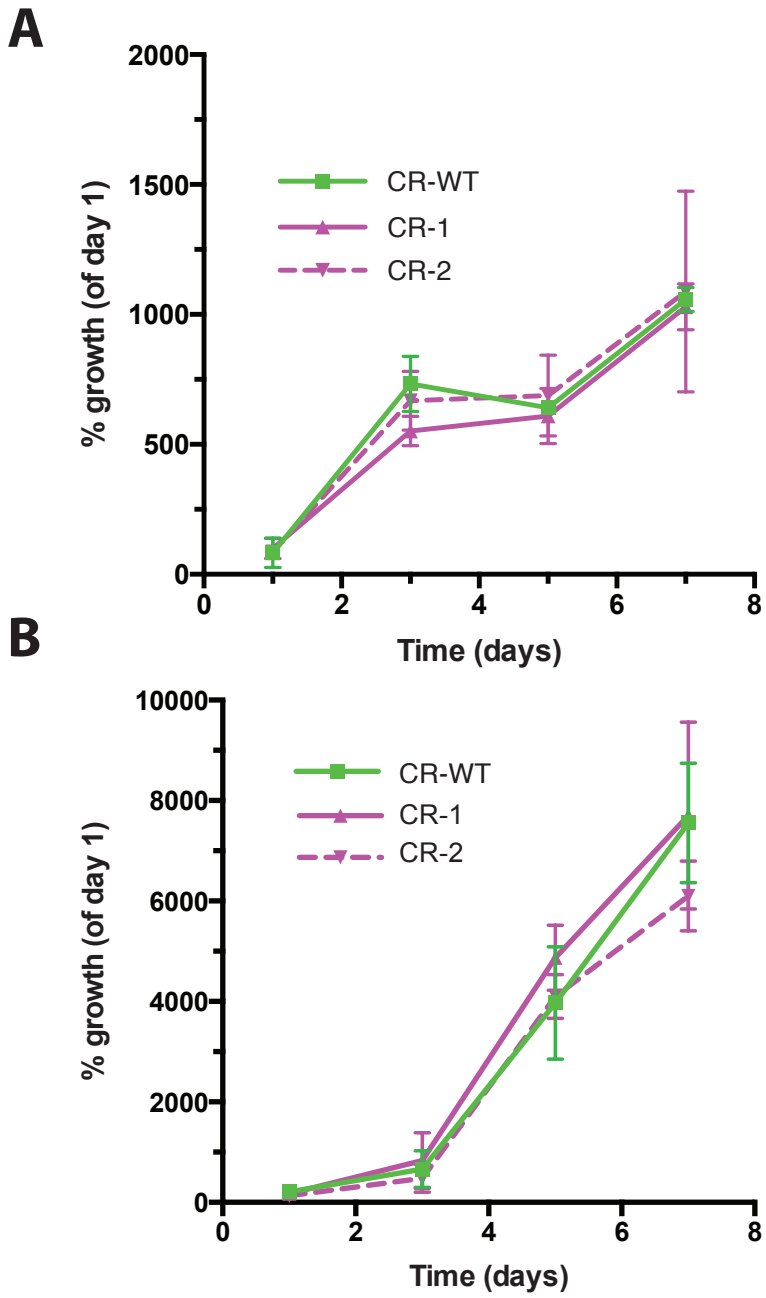

Figure 4.20: Metabolic activity in HeLa CRISPR cell lines is not altered A) HeLa CRISPR control (CR-WT) and clones (CR-1, CR-2) were seeded in six replicates in a 96 well plate at 1000 cells/well. MTT assay was used to investigate differences in metabolic activity rates in full medium containing (A) 25mM glucose or (B) 5.6mM glucose. Results from two independent experiments are expressed as mean and SD compared to respective values at 24 hours.

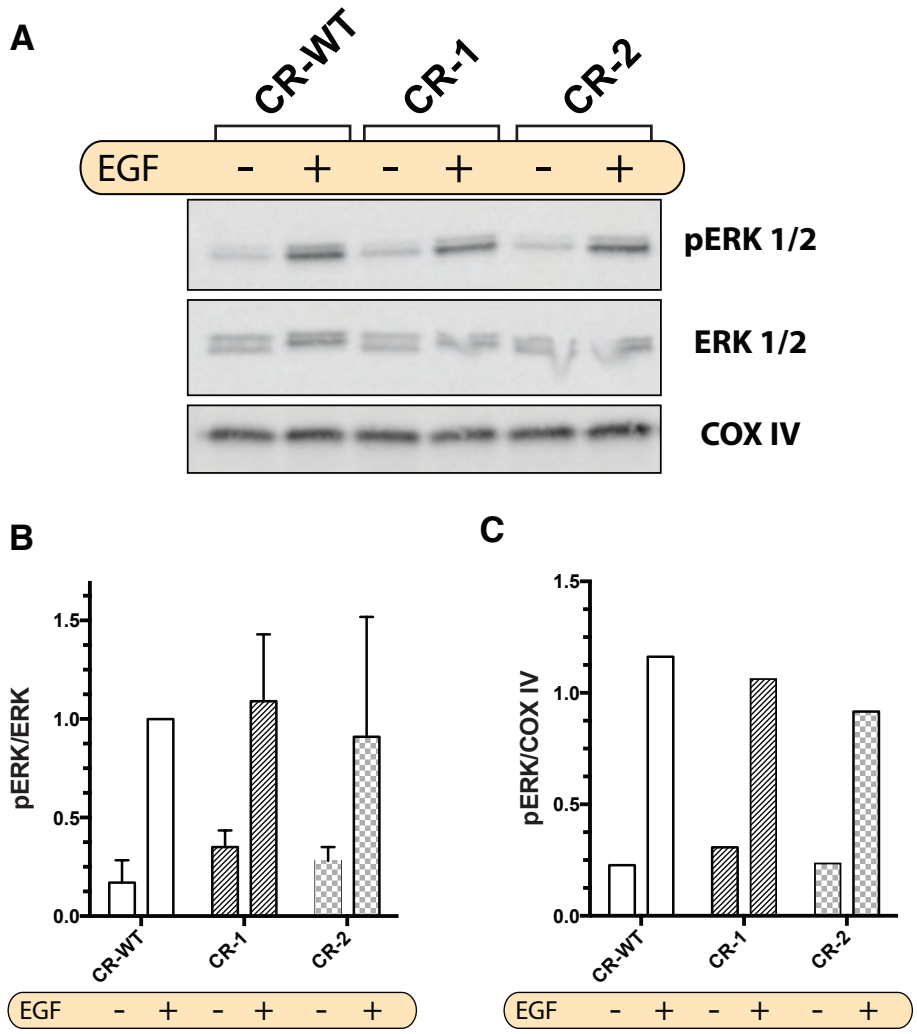

Figure 4.21: RPIA-depletion in HeLa CRISPR cells does not modulate p-ERK signalling. A) CR-WT, CR-1 and CR-2 HeLa cells were washed 2x with PBS and incubated with medium containing low serum (same as full medium but with 0.1% FCS instead of 10% FCS) for 16 hours. Cells were then stimulated for 5 minutes with low serum medium +/- 100ng EGF as indicated. Cell lysates were separated on 7.5% SDS-PAGE gels and tested with p-ERK, ERK and COXIV antibodies for immunoblot analysis. B) Quantification of p-ERK and total ERK levels using the densiometric analysis tool from Fiji from 2 independent experiments (normalised to CR-WT +EGF =1). C) Quantification of p-ERK and COXIV levels from one experiment (normalised to CR-WT +EGF =1)

Chapter 5

DISCUSSION

5.1 RPIA induces Grb2 recruitment

Further findings of interest in this study are the localisation patterns of GFP-Grb2 upon RPIA overexpression and the GFP-RPIA puncta in HeLa cells (see figures 3.2, 3.3, 3.4, 3.5, 3.6). The data indicate that the Grb2 translocation mediated by RPIA does not seem to depend on enzymatic activity or on the classical SH2 and SH3 domains of Grb2. Additionally, RPIA and Grb2 co-localise in a distinct part of the cell, at least partially. Exogenous RPIA expression on its own also results in distinct puncta rather than even cytoplasmic distribution. Intriguingly, the biochemical reactions in the pentose phosphate pathway have been reported to take place in the cytoplasm[181], but the enzymes G6PD, 6GPD and transaldolase in the pathway were shown to aggregate in complexes near glucose transporters in human neutrophils[308]. Interestingly, Scansite 3 analysis of RPIA reveals a number of residues in putative binding motifs, including for an SH3 domain, ERK-D-domain, as well as Akt and AMPK phosphorylation sites (see figure 1.10). It is too soon to draw definite conclusions, but it raises a number of interesting questions that remain to be addressed. Does RPIA bind to MAPK or PI3K signalling components? Is RPIA binding somehow regulating those signalling complexes or vice versa? Is RPIA a phosphorylation target of Akt or AMPK? With high-affinity antibodies against endogenous proteins, one could perform Co-Immunoprecipitation (Co-IP) western blot experiments or pull-down coupled with mass spectrometry to

further study the interactions of RPIA with Grb2 and other proteins. Furthermore, truncation and other point mutant constructs of both RPIA and Grb2 could be of aid to probe which amino acids in the peptide chains are important for this interaction. Perhaps surprisingly, point mutations in the Grb2 constructs did not disrupt RPIA-induced translocation (see figure 3.6). It remains to be studied further whether point mutations on any of the predicted RPIA sites or truncation constructs would abrogate the translocation phenotype. It is possible that those structures are cytoplasmic complexes or that RPIA is (directly or indirectly) tethered to a sub-cellular compartment. Does RPIA localise to trafficking related membrane-bound organelles, such as endosomes, lysosomes and/or autophagosomes? Does it localise to biosynthetic oligomers, such as PPP enzymatic aggregates? One could further investigate the sub-cellular localisation by immunostaining for common organelle markers, such as LC3, EEA-1 or LAMP-1, as well as testing for co-localisation with other enzymes, such as G6PD or 6GPD. Ideally, this would be done without the need of over-expression, for instance with a good antibody against endogenous RPIA or in a fluorescently tagged knock-in RPIA cell line in co-localisation experiments. One could carefully measure and analyse endogenous RPIA sub-cellular localisation under different conditions. The localisation of RPIA may change according to the cell cycle phase, binding to other proteins, post-translational modifications or based on enzymatic activity. There have been rapid advances of CRISPR/Cas9 technology in the past year which could be of great aid to study RPIA further for its role in protein-protein interactions and enzymatic function. Similar strategies which have been notoriously difficult and time-consuming (such as using ZFNs) are now largely being replaced by highly effective CRISPR/Cas9 mediated approaches. For instance, the use of customised donor templates in homology directed repair (HDR), as opposed to NHEJ, enables much quicker generation of endogenous (optionally inducible or tagged) knock-outs and knock-ins cell lines which would be of aid to address some of the raised questions.

5.2 RPIA does not affect metabolic activity or MAPK signalling in HeLa cells

Interestingly, a role for RPIA in oncogenic signalling via PP2A/ERK has been described recently. Ciou et al[202] reported in 2014 that RPIA mRNA expression levels are elevated in HCC patients, especially in late-stage, highly malignant tumors. Further investigation showed that there was reduced metabolic activity (MTT assay, interpreted as cell proliferation rates) in Hep3B and PLC5 liver cancer cell lines upon siRNA-mediated knockdown of RPIA. Metabolic activity measurements from MTT assays are often used as a proxy to measure proliferation rates of cells. However, it may be inadequate to use this assay due to RPIA potentially playing a role in PPP flux and direction, thereby modulating redox signalling. On the other hand, the paper also showed that cells over-expressing RPIA displayed an increase in metabolic activity and enhanced colony formation, with those results being backed up by a tumor growth xenograft mouse model. The liver, one of the most metabolically active tissues, is a key organ for metabolic homoeostasis. Hence, sufficient PPP activity is likely a key determinant for cell and tissue function, and its regulation of high importance. Interestingly, it was reported that metabolic flux is diverted from glycolysis to the PPP in order to increase precursors for biosynthesis in an inducible murine pancreatic ductal adenocarcinoma K-Ras^{G12D} (constitutively active Ras signalling) model[108,183]. However, RPIA may also have an inhibitory role in some cancers, seeing as there is an increase in hyper-methylation at the RPIA locus in breast cancer[309]. The data in this PhD thesis suggest that metabolic activity (see figures 3.9, 3.10 and 4.20), as well as MAPK signalling via ERK1/2 (see figures 3.11 and 4.21), is not altered, at least not in the experiments with HeLa cells (lung cancer cell line). However, it is possible that RPIA expression levels, which lead to altered proliferation rates, may depend on certain mutations in other oncogenes or tumor suppressors, as well as being cell type dependent. Further experiments that alter RPIA expression levels in different (transformed and non-transformed) cells may help to further differentiate the role of RPIA in proliferation. Additionally, it could be tested whether RPIA affects other downstream effectors of Ras, such as

PI3K, p38 and JNK. It would also be interesting to measure other metabolic parameters, such as O_2 and glucose consumption, as well as acidification of the medium, which is indicative of lactate production. These experiments would further investigate whether RPIA plays a role in metabolic reprogramming. Many crosstalks between signalling and metabolic pathways exist, including glycolysis, TCA cycle and the pentose phosphate pathway, and their regulation is especially important for proliferating cells[310]. Therefore, promising drug targets are amongst the enzymes in those central metabolic pathways, especially if they are common between cancer types and are expressed/regulated differentially compared to physiological cells. In the prospect of developing therapeutic strategies to combat cancer metabolism, the role of RPIA in cancer is an interesting topic for further investigation.

5.3 The role of RPIA in the regulation of autophagy

This study identified the metabolic enzyme RPIA, a key component of the PPP to regulate basal autophagy. Upon transient knockdown or genetic perturbation in HeLa cells, autophagosome formation and LC3 processing is upregulated. How exactly this metabolic perturbation is linked to the regulation of autophagy is currently unknown. One hypothesis is that the cell somehow senses and responds to altered R5P levels, and in consequence regulates autophagy as a compensatory mechanism. Another hypothesis is that the protein RPIA itself has a non-canonical role in the regulation of autophagy. There are several examples of enzymes and metabolites acting in a fashion that would support either hypothesis. In the context of what has been reported elsewhere about RPIA and the regulation of autophagy via enzymes and their metabolites, the results of this study will be further discussed here.

RPIA has been described to play a role in several diseases, including a metabolic disorder and as an oncogene in cancer (see section 5.2). The rare metabolic condition was named ribose-5-phosphate isomerase deficiency and there are mutations in both alleles, with one being a truncation that may result in some residual activity[199]. Currently, one patient has been reported with severe neurological symptoms, including seizures, mental retardation, leukoencephalopathy and peripheral neuropathy.

The molecular cause for this is currently not very well understood, especially in the context of which metabolite is causing which effect. It is thought that that the neurological symptoms may have to do with reduced NADPH levels and polyol (e.g. ribitol and D-arabitol) accumulation[201], thereby increasing oxidative stress. However, the effect of polyols on oxidative stress is still controversial. There is *in vitro* data from rat prefrontal cortex lysates showing that polyols actually have an anti-oxidant effect[311]. Also, knockdown of RPI in *D. melanogaster* neurons actually increased NADPH levels[198]. The authors suggested that modulating RPIA levels may serve as therapeutic strategy for neurodegenerative disorders and aging. Both of those fields, as well as autophagy, have been heavily linked to mTOR regulation, so it would be interesting to further investigate any potential role of RPIA in mTOR signalling pathways. Taken together, the role of RPIA is neurodegeneration, aging and autophagy require further investigation.

5.3.1 Molecular mechanisms of autophagy regulation

The metabolic state of cells in the context of regulating autophagy is an emerging field of research (see chapter 1). Absence of growth factors and energy-rich metabolites (glucose, amino acids, Ac-CoA, NAD) as well as certain cellular conditions (hypoxia, high AMP:ATP ratio) have been shown to be strong inducers of autophagy. Although much progress has been made in the past decade with regards to decipher the molecular mechanisms, the interplay between autophagy, metabolism and signalling is still not very well understood. Mechanistic insights of intracellular amino acid sensing[75,77,78], for instance, were only discovered in the past few years.

Several of the contributing factors act through low mTORC1 activity and high AMPK activity (see figure 1.2) in order to induce autophagy. However, other mechanisms exist that are mTORC1 and AMPK independent, such as ROS-mediated regulation of ATG4B activity[92,93] and PI3K/Akt/FoxO signalling[90] (see chapter 1.1.5). There is some preliminary evidence (see appendices) from the lab that RPIA may act via FoxO3A signalling. FoxO3A is a key regulatory transcription factor

in promoting autophagy and its nucleocytoplasmic shuttling status is a key regulatory mechanism of FoxO-dependent transcription (see chapters 1.1.5 and 1.4.5.4). Akt is an inhibitor for FoxoO3A (see 1.4.5.2), whilst the PIP_3 phosphatase PTEN negatively regulates Akt. GFP-FoxO3A localisation is predominantly cytoplasmic when co-expressed with Akt (see figure A.1 A). Similarly, when PTEN is co-overexpressed, GFP-FoxO3A predominantly localises to the nucleus. When RPIA is depleted, GFP-FoxO3A also localises mainly to the nucleus. RPIA overexpression, on the other hand, results in an Akt-like phenotype. When the transcriptional activity of FoxO3A signalling is measured using a luciferase reporter, knockdown of RPIA led to a 2.5-fold increase in activity (figure A.1 B), whilst overexpression of RPIA completely reduced reporter activity to similar values of Akt (figure A.1 C). Furthermore, catalytically inactive Akt did not show a decrease in signalling, but catalytically inactive RPIA also repressed FoxO3A signalling (figure A.1 C). The RPIA overexpression constructs used in figure A.1 C were validated for presence or lack of catalytic activity as described in Apel et al[194] (figure A.1 D).

There are several experiments that would further elucidate the mechanism of RPIA in the regulation of autophagy. Do RPIA levels, or the enzymatic activity, affect the function of known signalling complexes such as AMPK and mTORC1? Does RPIA downregulation result in an increase in ROS levels, which in turn upregulates autophagy? One could investigate mTORC1 and AMPK activity by performing western blot analysis of their phosphorylation status. The experiments could also be performed in the context of pharmacological treatments (e.g. with PI3K inhibitor wortmannin and mTORC1 inhibitor torin) or knockout of regulators (such as $TSC2^{-/-}$ double knockout MEFs) to explore if and where RPIA acts on the PI3K signalling cascade.

Furthermore, there is some other preliminary evidence (see appendix figure A.2) from the lab that links RPIA to the regulation of the core autophagy machinery. It has been shown elsewhere[92,93,115] that ROS can regulate autophagy via ATG4B. Data from the ATG4B-mediated luciferase release assay (Act-LC3-dN-GLuc), the same that was used to measure the effect of PPP metabolites on autophagy regu-

lation (see figure 4.4), currently support both hypotheses of metabolite levels or a non-canonical role for RPIA in the regulation of autophagy. In HEK293T cells stably expressing the ATG4B activity reporter, there was a 4-fold increase in luciferase activity upon shRNA-mediated knockdown of RPIA compared to control cells (figure A.2 B, C). The increase in luciferase release was not observed in cells expressing a control Act-dN-GLuc construct that does not contain the LC3 cleavage motif (figure A.2 C), indicating that shRPIA specifically enhances cleavage of LC3. These results were confirmed in MCF7 cells (figure A.2 D) and fetal liver cells (FLC), which express high levels of RPIA (figure A.2 E)

Therefore, it is possible that knockdown of RPIA alters ROS levels, which regulate ATG4B activity. In order to further establish this, ROS levels could be measured in the CR-1 and CR-2 cells, as well as under transient knockdown conditions. Furthermore, it would be interesting to see whether the increase LC3 processing and autophagosome formation upon RPIA depletion can be reverted using the soluble antioxidant N-acetylcysteine (NAC). In fact, data from the lab indicate that ROS levels are indeed important, as treatment with NAC reversed the increase in LC3 processing and ATG4B reporter activity (see Heintze et al)[312]. In addition, it would also be interesting to study if RPIA plays any particular role in selective autophagy pathways, such as mitophagy.

5.3.2 Metabolites and metabolic enzymes regulate autophagy

In the past decade, multiple enzymes from various metabolic pathways have been associated with the regulation of autophagy. Those regulators (enzymes and metabolites) with a non-canonical role promoting or supressing autophagy were identified from numerous pathways, including protein synthesis (see 1.1.5), glycolysis (see 1.2.4), TCA cycle (see 1.2.5), nucleotide and NAD synthesis (see 1.2.9), fatty acid metabolism (see 1.2.7) and the pentose phosphate pathway (see 1.3). Amongst the enzymes are fatty acid synthase (FASN)[165], phosphofructokinase (PFKFB3)[125,126], transketolase (TKT)[210] and acetyl-Coenzyme A synthase[96].

Interestingly, the molecular mechanisms of regulating autophagy for these enzymes

(or associated metabolites) is quite variable and some mechanistic aspects remain to be elucidated. For instance, pharmacological inhibition of PFKFB3 in HCT116 cells was reported to decrease ATP levels and S6K phosphorylation, as well as cause an accumulation of ROS[126]. All those cellular events can independently stimulate autophagy, so currently it is unclear whether any one of those in particular, or all of them acting synergistically, are crucial for PFKPFB3-mediated inhibition of autophagy.

FASN was shown to inhibit autophagolysosomal degradation of the PI3K signalling components Akt, mTOR, S6K and 4EBP1[165], but does not affect pERK1/2 dependent-MAPK signalling. However, the molecular mechanisms of this specific degradation in the absence of FASN remain unclear. It is unknown whether FASN binds to any of the PI3K signalling proteins or whether there is an indirect regulatory mechanism.

Ac-CoA levels are known to regulate autophagy, but the exact mechanism(s) are not fully elucidated either. It is possible that the acetyltransferase EP300, which has been shown to interfere with ATG5, ATG7 and ATG12 protein activity through acetylation[313], acts as a key sensor of Ac-CoA levels. However, it is also possible that Ac-CoA indirectly regulates mTORC1 activity[96], since Ac-CoA levels negatively correlated with S6K phosphorylation.

The involvement of the PPP enzyme TKT in autophagy is still relatively unclear. It has been suggested that ULK1/2 regulates TKT activity, thereby regulating PPP activity[210]. TKT is the most upregulated enzyme from the PPP in HCC cells and its expression tightly regulated by the Nuclear Factor, Erythroid 2-Like 2 (NRF2)/Kelch-Like ECH-Associated Protein 1 (KEAP1)/BTB and CNC Homolog 1 (BACH1) pathway[185]. This is a key pathway to counteract oxidative stress in cancer cells and TKT expression was shown to be important for the generation of NADPH. Interestingly, that study also confirmed a 2-fold upregulation of RPIA in HCC patients compared to healthy individuals. The study highlighted the importance of PPP activity for cancer proliferation and survival, but did not investigate whether the modulation of ROS levels affected autophagy as well. In contrast,

pharmacological inhibition of TKT with oxythiamine in a proteomic study in MIA PaCa-2 cells changed the expression of multiple proteins, but did not mediate changes in expression levels of any proteins in the autophagic machinery[314]. In this thesis, I also did not observe any differences in basal autophagy upon treatment of oxythiamine (see figure 4.16). Knockdown or knock-out experiments in mammalian systems that prove TKT involvement in autophagy have not been performed by any group as of yet. Considering the major role of autophagy in cellular nutrient homoeostasis, it may not be a surprise to continuously discover additional metabolic enzymes involved in fine-tuning autophagy. As seen in certain cancer cells addicted to autophagy, a certain level of autophagy-mediated degradation is essential for survival and can promote tumorigenesis. Altogether, these findings suggest that additional metabolic pathways and enzymes operate to fine-tune autophagy.

5.3.3 R5P levels or non-canonical function of RPIA?

In this study, we postulate that RPIA levels, or its enzymatic function, can modulate the regulation of basal autophagy. Cells can generate *de novo* R5P by two mechanisms: Either by conversion of Ri5P to R5P (mediated by RPIA), or by conversion of S7P and G3P to R5P and X5P (see figure 1.9). R5P is a crucial precursor for a number of molecules (see chapters 1.2.9 and 1.3): It is also part of histidine, pyrimidine, NAD and cADPR synthesis pathways and is a structural component in all nucleotides. Other related metabolites have been shown to be involved in complex cross-talk networks, so it is plausible that R5P has a signalling role in metabolism and/or autophagy. X5P, for instance, upregulates glycolytic flux in hepatocytes via activation of protein phosphatase 2A (PP2A), which inhibits PFK-2 phosphatase activity[315]. PP2A activity also increases the transcription of lipogenesis genes. Therefore, X5P levels indirectly influence glucose and lipid metabolism. Interestingly, PP2A was also found to be a key regulator of autophagy and ATG4B in the previously mentioned Act-LC3-dN-GLuc screen (Pengo et al. submitted). SAICAR, a purine synthesis intermediate, was also shown to regulate glycolysis

via PKM2. Interestingly, a protective microRNA (miRNA-124) that reduces nucleotide synthesis by targeting RPIA and PRPS1, was found to be downregulated in human colorectal cancer cells[191]. PRPS1 generates PRPP from R5P, which is is the first step for most of the biosynthetic pathways. Indeed, many diseases have been linked to PRPS1/2, including cancer.

5.3.4 Is RPIA essential?

Undoubtely, R5P *de novo* synthesis is essential, but whether RPIA activity is absolutely essential in all cells and organisms is not quite clear. Metabolically, R5P can be generated via transketolase, so there may be compensatory mechanisms In *S. cerevisiae*, the gene RKI (homolog of RPIA) has been reported to be the only metabolic enzyme in the PPP to be essential[316]. I generated a GFP-ATG8 expressing, tet-inducible knock out strain of RKI (see figure 4.6) and observed slower growth, but not a lack of viability. For other eukaryotes, it is still unclear whether RPIA is essential or not on an organism level. Interestingly, reduced expression of RPI in neurons of in *D. melanogaster* actually increased the lifespan[198]. Knockdown of the enzyme in the whole organism did not seem to have any effect. On the other hand, data from the international mouse phenotyping consortium (www.mousephenotype.org) indicate that homozygous RPIA knockout strains have a complete pre-weaning lethality phenotype (see appendix figure A.3). Heterozygous strains, on the other hand, are viable indeed. They appear to have defects in Ca^{2+} levels in the blood stream and a decrease in regulatory T-cell numbers. The Ca^{2+} defects may be due to impaired synthesis of the calcium signalling molecule cADPR[175], but this remains to be investigated.

Interestingly, RPIA has a putative second start codon that would generate a shorter, 237 residue peptide (see figure 1.10). It raises the question whether the data I observe can partially be explained due to expression of a short RPIA that resembles the isomerase protein homologs in all eukaryotes (except mammals) and bacteria. It seems unlikely in the autophagy experiments using transient knockdown conditions (see figure 4.1), since all different shRNAs that were used would target both full-length and the putative truncated mRNA. In the CRISPR cell lines (see section 4.4),

I specifically targeted exon 1 of the full-length peptide, since at the time it was common practice and wisdom to generate mutations in exon 1. Thorough sequencing showed that in both clones, the wild-type sequence in exon 1 was successfully altered in both alleles (see figure 4.13). However, it currently can not be excluded that this putative short peptide is expressed in those cells. It may be possible though that transcription still occurs, and that translation occurs from the second start codon. If the short peptide were expressed, the catalytic role of Ri5P to R5P conversion could still be fulfilled, but full length wild-type RPIA (containing the N-terminal 74 amino acid stretch) is likely not to be present in those cells. If full-length RPIA had any additional, non-enzymatic interactions that affected autophagy, those would be disrupted in the CRISPR cells. This can be further investigated, for instance by performing qPCR with primers specific for full length and for both peptides. Towards the end of the PhD, our lab also intended to order RPIA knock out Hap1 cell lines from Horizon™targeting the catalytic domain in exon 5, so some of the data could be validated in a haploid cell line. In the end, the company reported back to us that their knockout strain is not viable. Altogether, RPIA may be essential in mammals on a whole-organism level and in some isolated cell types.

5.3.5 Does RPIA have a non-canonical role?

There is some preliminary evidence that points to a non-canonical function of RPIA in this study. Upon addition of R5P to the medium, no increase in LC3 processing or ATG4B activity could be observed. Nor was there an increase of LC3 processing upon addition of the RPIA inhibitor E4P (see figures 4.4 and 4.16). Furthermore, although the R5P levels (compared to X5P/Ri5P) are decreased in at least one of the CRISPR clones, there is still an increase in basal autophagy (see figures 4.14, 4.15 and 4.17). Also, preliminary results from the *S. cerevisiae* experiments (see figure 4.6) indicate that the RPIA protein may have acquired additional functionality in mammals. Further experiments are needed to address some outstanding questions and help to test these hypotheses. It would be interesting to see if any of the phenotypes in the autophagy assays can be reverted by rescue experiments, and also, if the catalytically inactive mutant D160A would rescue autophagy inhibition as well.

It would be further evidence for the notion of a non-canonical function, if it does rescue indeed.

A current limitation is given by the time scale of experiments: Efficient shRNA-mediated knockdown takes multiple days, and the generation and isolation of the CRISPR cell clones took weeks. However, metabolic reprogramming through transcriptional changes can occur within hours and post-translational modifications within seconds. Therefore, those studies in mammalian cells would ideally be performed in an inducible knockout model. This would enable measurements of autophagosome formation (for instance, using GFP-LC3) in live cells at multiple time points. By using radiolabelled (heavy) glucose, one could also measure the impact of shRNA-mediated transient knockdown of RPIA and/or in the generated CRISPR cell lines. Also, systematic knockdown or CRISPR knockout of each PPP gene, coupled with measurements of autophagosome formation and PPP flux would help to test the two hypotheses.

Although the lack of effect on LC3 processing and ATG4B activity by pharmacological inhibition of RPIA (figures 4.4 and A.2) indicate a non-canonical role, this hypothesis can be tested in more detail. It is unclear whether the cell has transport mechanisms for internalising phosphorylated sugars (such as E4P, R5P) from the extracellular space. Glucose, for instance, is phosphorylated as soon as it enters in order to keep it in the cytosol. However, large or other charged molecules are taken up by cells, sometimes via unknown mechanisms[317–319]. One option of ruling out those concerns would be to use liposomes as a delivery method, which could also contain a fluorescent marker in order to visualise uptake of E4P and R5P. Additionally, *in-vitro* enzymatic activity of RPIA could be measured with those compounds.

The HPLC-MS/MS analysis of sugar phosphate levels in the CRISPR cells show that this methodology allows at least some differentiation of PPP intermediate levels (see figures 4.17, 4.18 and 4.19). The data agree with the predicted outcomes of the genomically altered cells. The sequences of the alleles in CR-1 (see figure 4.13) should not allow translation of full-length RPIA, which would explain reduced R5P levels. S7P levels may also be reduced because R5P is predominantly synthesised

by TKT, which utilises S7P and G3P for this conversion. The locus of RPIA in one of the CR-2 alleles may allow for translation of a peptide that has two additional residues inserted and it currently can not be ruled out that this peptide has RPIA enzymatic activity. Further experiments using the CRISPR cell lines would help to test this hypothesis, for instance measurements of sugar phosphates after pharmacological treatments. It would be interesting to see if R5P levels in the cells are altered upon TKT inhibition. Equally, one could investigate the effect on PPP intermediates upon induction or inhibition of autophagy. Hopefully, techniques will be developed that allow simultaneous quantification of related metabolites, such as X5P/Ri5P and G6P/F6P.

When those and other novel research tools become available, some interesting experiments could be performed from a systems biology perspective. Currently, we cannot perturb metabolic pathways and directly measure enzymatic activity of multiple enzymes within a cell. Many metabolic enzymes (e.g. G6PDH, HK, PFK1, PKM2) are regulated through numerous inputs from different metabolic and signalling pathways, hence it is difficult to decipher direct and indirect effects of perturbation in a spacial and temporal manner. For instance, addition of the TKT inhibitor oxythiamine had profound proteomic changes that changed considerably over time of treatment[314]. This suggests that there are short-term and long-term changes through metabolic perturbation, which can have opposite effects. Equally, the pyrimidine biosynthesis enzyme CAD forms oligomers (puncta) upon amino acid stimulation via mTORC1 signalling, but does not localise to activated mTORC1[171]. However, elucidation of the molecular mechanisms of complex formation often rely on purified, overexpressed proteins *in vitro*. It is an interesting notion that cytoplasmic enzymes, which are still often considered ”diffused” in the cytoplasm, actually form clusters of localised biosynthesis which are regulated by signalling cascades. Similarly, cytoplasmic enzymes can localise to specific sub-cellular localisations for non-canonical functions, such as HK-II binding to VDAC to inhibit apoptosis[320]. Therefore, it would be interesting to further study the sub-cellular localisation of RPIA in living cells under conditions that disturb metabolic and signalling

pathways. CAD activity was also shown to be important for cell cycle progression, which is consistent with its key role in *de novo* pyrimidine synthesis. It would be interesting to study the potential involvement of RPIA in cell cycle progression, considering that it also plays a major role in the *de novo* synthesis of the precursor PRPP.

Taken together, RPIA plays a key role for cellular metabolism and may exert specific functions in under certain cellular conditions, such as the regulation of metabolism, signalling and autophagy, in a tissue-specific context. In this study, I propose a role for RPIA in the regulation of autophagy, which is of importance for the development of anti-cancer therapeutics that may target this novel mode of regulation.

Chapter 6

GENERAL CONCLUSIONS

6.1 RPIA in Grb2 signalling

Metabolism and signalling are highly linked, there is a complex regulatory network and many examples of crosstalk between distant pathways. This study investigated a potential role of ribose-5-phosphate isomerase A (RPIA), a metabolic enzyme in the pentose phosphate pathway (PPP), in growth factor receptor bound protein 2 (Grb2)-mediated signalling. RPIA plays a key role in the synthesis of ribose-5-phosphate (R5P), which is a precursor to all nucleotides and related metabolites. Grb2 is an adaptor protein that binds to a number of activated Receptor tyrosine kinases (RTK) upon stimulation with growth factors. Here, I report that RPIA induced Grb2 translocation to a currently unknown subcellular compartment in HeLa cells. Interestingly, Grb2 translocation mediated by RPIA did not depend on enzymatic activity and was not mediated via the classical Src homology 2 (SH2) and SH3 domains of Grb2. These findings suggest a non-canonical role for RPIA in signalling. RPIA localisation was enriched in the distinct Grb2 puncta. Expression of RPIA on its own also resulted in distinct puncta which were insensitive to amino acid starvation or mechanistic target of rapamycin complex 1 (mTORC1) inhibition, unlike other metabolic enzymes such as CAD. Furthermore, alterations in RPIA expression levels did not affect the activation status of RTK downstream effectors extracellular signalregulated kinases (ERK) 1/2. Additionally, there was no effect on proliferation upon knockdown or overexpression of RPIA. Taken together,

these findings are interesting in the context of cancer and the regulation of the PPP.

6.2 RPIA in autophagy regulation

Autophagy plays a key role in cells buy maintaining cellular nutrient and energy homeostasis in response to various conditions, including metabolic stress. Data presented in this study suggest that human RPIA plays a role in the regulation of autophagy, potentially in a non-canonical fashion. RPIA depletion, either transiently by shRNA or in CRISPR RPIA knockout cells, results in an upregulation of autophagosome formation (as shown by a number of assays) through a currently unknown mechanism. Pharmacological inhibition of transketolase, the other enzyme that synthesises R5P, did not affect the regulation of autophagy. Addition of an RPIA inhibitor or the product R5P also did not affect the regulation of autophagy. Mass spectrometry analysis of a clone (CR-1) with two out-of-frame mutations in the RPIA gene had reduced R5P levels, but still displayed an increase in LC3 processing. Furthermore, RKI (RPIA homolog) depletion in *S. cerevisiae* does not upregulate autophagy, which indicates a potentially unique level of regulation in mammals. Overall, this study suggests a role for RPIA in the regulation of autophagy, which is important in the context of cancer, neurodegeneration and aging and is of relevance for development of therapeutics.

Appendix A

Supporting data

A.1 FoxO3A experiments

A.2 ATG4B reporter: Act-LC3-dN-GLuc

A.3 Homozygous knockout of RPIA in mice is lethal

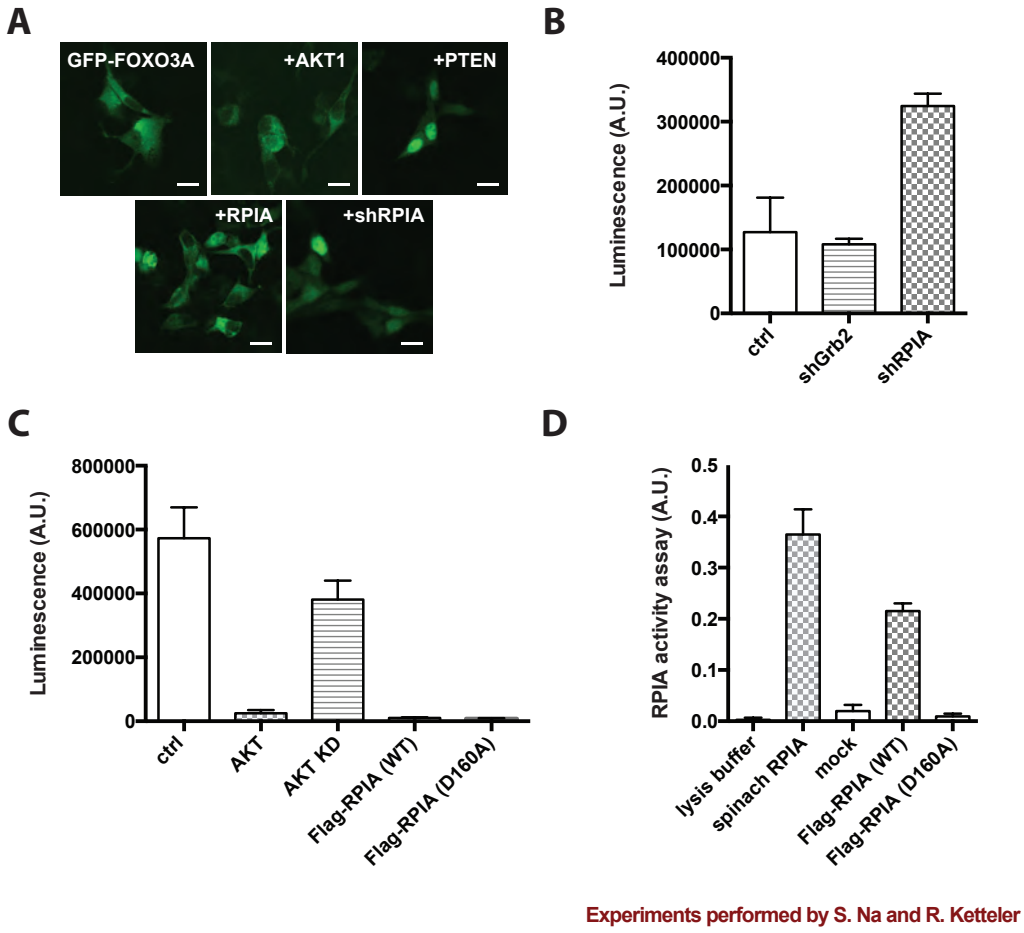

Figure A.1: RPIA inhibits Foxo3A signalling A) HEK293ET cells were co-transfected with GFP-FOXO3A and the indicated cDNA or shRNA expression vectors. Images were acquired using a Zeiss Axiovert 100 microscope. Scale bar = 10m. B) 293ET cells were co-transfected with a FOXO3A-luciferase reporter construct and the indicated shRNA vectors targeting RPIA or Grb2 as control. Empty pMOWS vector was used as an additional control. Cells were cultured for 48 hours and cell lysates were analyzed for luciferase expression. C) 293ET cells were transfected as in B) in the presence of FOXO3A and luciferase expression was monitored. D) Catalytic activity of purified Flag-RPIA and Flag-RPIA D160A were measured using a colorimetric assay as described in[194]. A.U. arbitrary units.

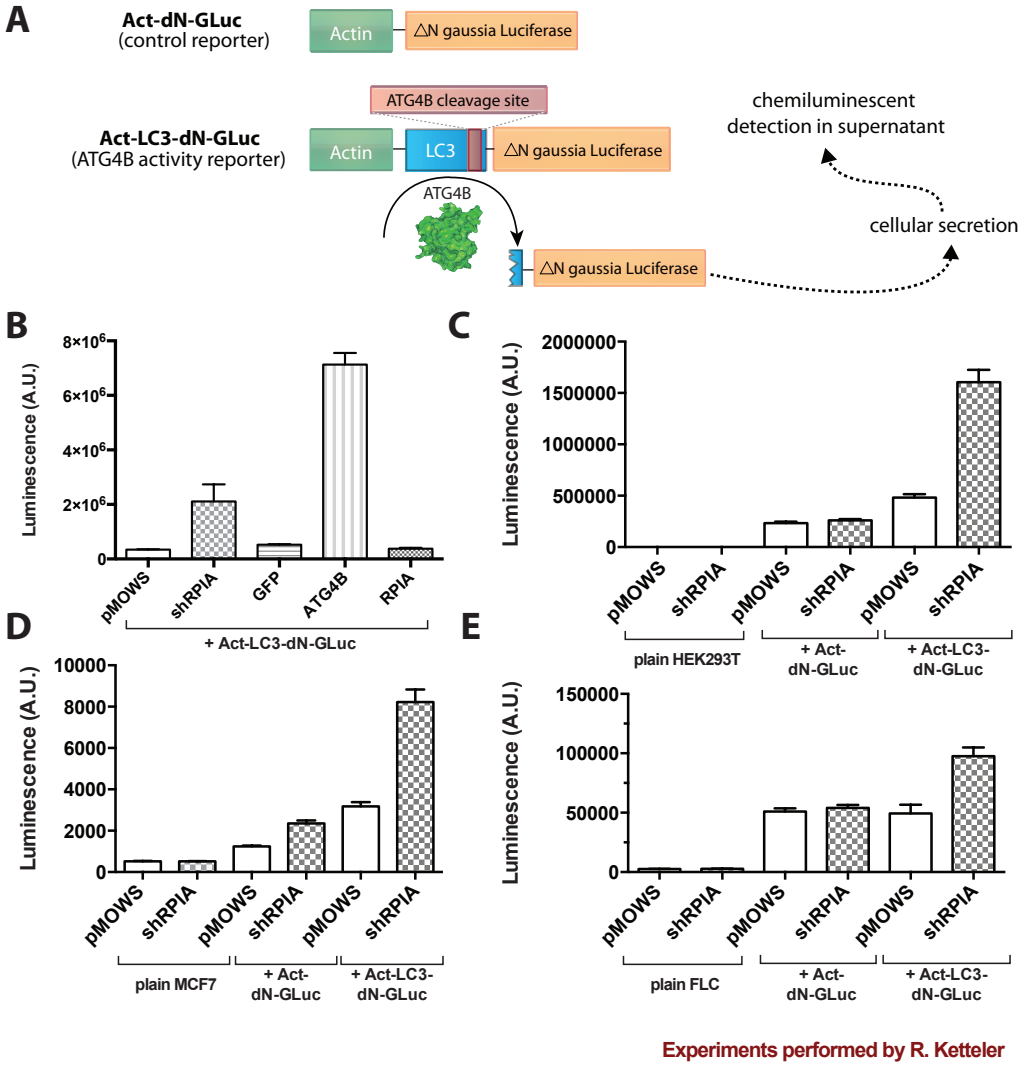

Figure A.2: Knockdown of RPIA increases ATG4B reporter activity A) Schematic overview of the ATG4B-mediated luciferase release assay. Luciferase is secreted from the cells and a chemiluminescent signal in the supernatant can be measured. B) Luciferase release assay 24 hours post-transfection with the indicated plasmids in 293ET cells transduced with the indicated reporter constructs. Data represent mean SD, n=3. C) Luciferase activity of supernatant collected 96 hours post-transduction with control (pMOWS) and shRPIA in 293ET cells as indicated. Data represent mean SD, n=3. D, E) Luciferase activity of supernatants in transduced MCF7 (E) and primary murine fetal liver cells

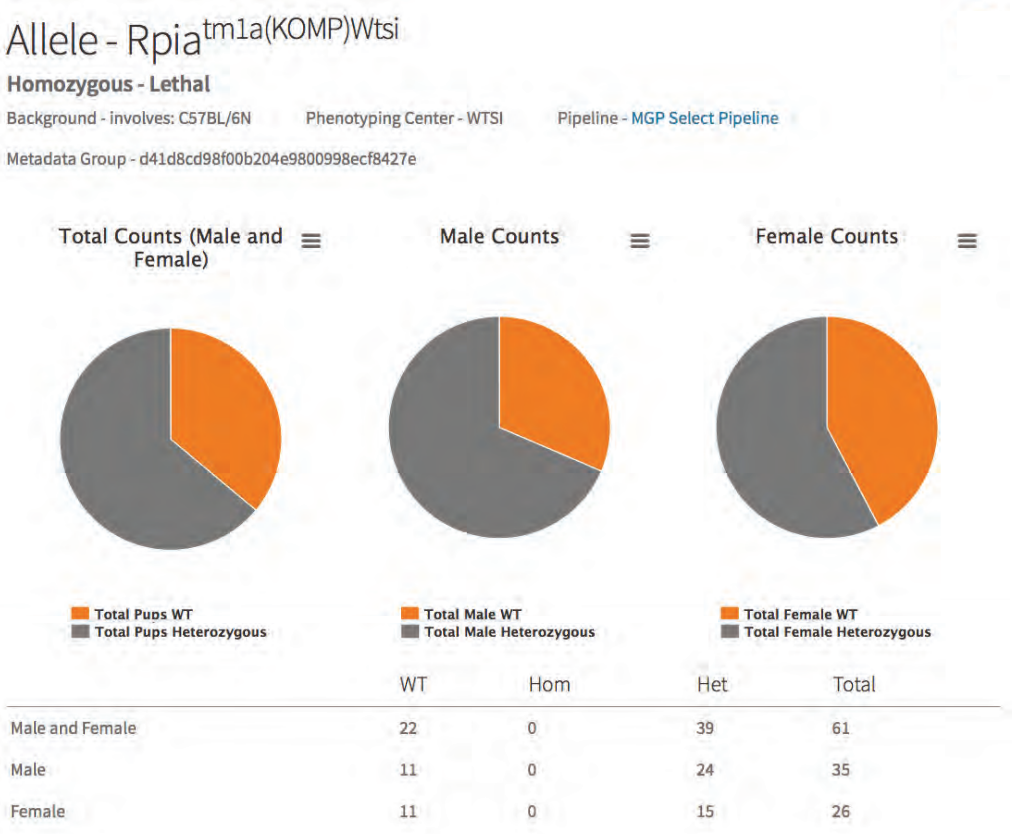

	WT	Hom	Het	Total
Male and Female	22	0	39	61
Male	11	0	24	35
Female	11	0	15	26

Home » Search » Statistics » RPIA on www.mousephenotype.org/data/
last accessed on 23rd May 2016

Figure A.3: Complete pre-weaning lethality in homozygous RPIA knock-out mice. For mice with C57BL/6N background, no homozygous RPIA knock-out mice survived before the pre-weaning stage. Data was obtained from www.mousephenotype.org/data.

Appendix B

Colophon

This document was set in the Times Roman typeface using LaTeX and BibTeX, and compiled with TexStudio 2.10. All figures were generated in Adobe Illustrator CS6. All graphs were generated using GraphPad Prism 6. All great tools that help to draft, write and compile a thesis!

Bibliography

[1] D J Klionsky and S D Emr. “Autophagy as a regulated pathway of cellular degradation.” In: *Science (New York, NY)* 290.5497 (Dec. 2000), pp. 1717–1721.

[2] Lorenzo Galluzzi et al. “Metabolic Control of Autophagy”. In: *Cell* 159.6 (Dec. 2014), pp. 1263–1276.

[3] Noboru Mizushima and Masaaki Komatsu. “Autophagy: renovation of cells and tissues.” In: *Cell* 147.4 (Nov. 2011), pp. 728–741.

[4] Claudine Kraft and Sascha Martens. “Mechanisms and regulation of autophagosome formation.” In: *Current opinion in cell biology* 24.4 (Aug. 2012), pp. 496–501.

[5] Akiko Kuma et al. “The role of autophagy during the early neonatal starvation period.” In: *Nature* 432.7020 (Dec. 2004), pp. 1032–1036.

[6] Ellen Wirawan et al. “Autophagy: for better or for worse.” In: *Cell research* 22.1 (Jan. 2012), pp. 43–61.

[7] Ryan C Russell, Hai-Xin Yuan, and Kun-Liang Guan. “Autophagy regulation by nutrient signaling.” In: *Cell research* 24.1 (Jan. 2014), pp. 42–57.

[8] Daniel J Klionsky. “Autophagy: from phenomenology to molecular understanding in less than a decade.” In: *Nature reviews Molecular cell biology* 8.11 (Nov. 2007), pp. 931–937.

[9] Noboru Mizushima, Tamotsu Yoshimori, and Beth Levine. “Methods in mammalian autophagy research.” In: *Cell* 140.3 (Feb. 2010), pp. 313–326.

[10] Danielle Glick, Sandra Barth, and Kay F Macleod. “Autophagy: cellular and molecular mechanisms.” In: *The Journal of pathology* 221.1 (May 2010), pp. 3–12.

[11] Natalya N Pavlova and Craig B Thompson. “The Emerging Hallmarks of Cancer Metabolism.” In: *Cell metabolism* 23.1 (Jan. 2016), pp. 27–47.

[12] Daniel J Klionsky et al. “Guidelines for the use and interpretation of assays for monitoring autophagy (3rd edition).” In: *Autophagy* 12.1 (Jan. 2016), pp. 1–222.

[13] Noboru Mizushima et al. “Autophagy fights disease through cellular self-digestion.” In: *Nature* 451.7182 (Feb. 2008), pp. 1069–1075.

[14] Wen-wen Li, Jian Li, and Jin-ku Bao. “Microautophagy: lesser-known self-eating.” In: *Cellular and molecular life sciences : CMLS* 69.7 (Apr. 2012), pp. 1125–1136.

[15] Dalibor Mijaljica, Mark Prescott, and Rodney J Devenish. “Microautophagy in mammalian cells: revisiting a 40-year-old conundrum.” In: *Autophagy* 7.7 (Oct. 2014), pp. 673–682.

[16] Daniel J Klionsky. “For the last time, it is GFP-Atg8, not Atg8-GFP (and the same goes for LC3).” In: *Autophagy* 7.10 (Oct. 2011), pp. 1093–1094.

[17] Zhiping Xie and Daniel J Klionsky. “Autophagosome formation: core machinery and adaptations.” In: *Nature cell biology* 9.10 (Oct. 2007), pp. 1102–1109.

[18] Lukas A Huber and David Teis. “Lysosomal signaling in control of degradation pathways.” In: *Current opinion in cell biology* 39 (Jan. 2016), pp. 8–14.

[19] Joana R Costa, Jacob Heintze, and Robin Ketteler. “LC3 – Autophagy’s achilles’ heel?” In: *Drug Target Review* 2.1 (), pp. 18–21.

[20] Muriel Mari, Sharon A Tooze, and Fulvio Reggiori. “The puzzling origin of the autophagosomal membrane.” In: *F1000 biology reports* 3 (2011), p. 25.

[21] Elizabeth L Axe et al. “Autophagosome formation from membrane compartments enriched in phosphatidylinositol 3-phosphate and dynamically connected to the endoplasmic reticulum.” In: *The Journal of cell biology* 182.4 (Aug. 2008), pp. 685–701.

[22] Päivi Ylä-Anttila et al. “3D tomography reveals connections between the phagophore and endoplasmic reticulum.” In: *Autophagy* 5.8 (Nov. 2009), pp. 1180–1185.

[23] Noboru Mizushima and Daniel J Klionsky. “Protein turnover via autophagy: implications for metabolism.” In: *Annual review of nutrition* 27 (2007), pp. 19–40.

[24] Kevin Moreau and David C Rubinsztein. “The plasma membrane as a control center for autophagy.” In: *Autophagy* 8.5 (May 2012), pp. 861–863.

[25] Luc English et al. “Autophagy enhances the presentation of endogenous viral antigens on MHC class I molecules during HSV-1 infection.” In: *Nature immunology* 10.5 (May 2009), pp. 480–487.

[26] Ian G Ganley et al. “ULK1.ATG13.FIP200 complex mediates mTOR signaling and is essential for autophagy.” In: *The Journal of biological chemistry* 284.18 (May 2009), pp. 12297–12305.

[27] Taichi Hara et al. “FIP200, a ULK-interacting protein, is required for autophagosome formation in mammalian cells.” In: *The Journal of cell biology* 181.3 (May 2008), pp. 497–510.

[28] J Yan et al. “Identification of mouse ULK1, a novel protein kinase structurally related to C. elegans UNC-51.” In: *Biochemical and biophysical research communications* 246.1 (May 1998), pp. 222–227.

[29] Chang Hwa Jung et al. “ULK-Atg13-FIP200 complexes mediate mTOR signaling to the autophagy machinery.” In: *Molecular biology of the cell* 20.7 (Apr. 2009), pp. 1992–2003.

[30] Chengyu Liang et al. “Autophagic and tumour suppressor activity of a novel Beclin1-binding protein UVRAG.” In: *Nature cell biology* 8.7 (July 2006), pp. 688–699.

[31] Kohichi Matsunaga et al. “Two Beclin 1-binding proteins, Atg14L and Rubicon, reciprocally regulate autophagy at different stages.” In: *Nature cell biology* 11.4 (Apr. 2009), pp. 385–396.

[32] Gian Maria Fimia et al. “Ambra1 regulates autophagy and development of the nervous system.” In: *Nature* 447.7148 (June 2007), pp. 1121–1125.

[33] Juliet Goldsmith, Beth Levine, and Jayanta Debnath. “Autophagy and cancer metabolism.” In: *Methods in enzymology* 542 (2014), pp. 25–57.

[34] Asad M Taherbhoy et al. “Atg8 transfer from Atg7 to Atg3: a distinctive E1-E2 architecture and mechanism in the autophagy pathway.” In: *Molecular cell* 44.3 (Nov. 2011), pp. 451–461.

[35] Zoltan Metlagel et al. “Structural insights into E2-E3 interaction for LC3 lipidation.” In: *Autophagy* 10.3 (Mar. 2014), pp. 522–523.

[36] Y Kabeya et al. “LC3, a mammalian homologue of yeast Apg8p, is localized in autophagosome membranes after processing.” In: *The EMBO journal* 19.21 (Nov. 2000), pp. 5720–5728.

[37] Kenji Sugawara et al. “Structural basis for the specificity and catalysis of human Atg4B responsible for mammalian autophagy.” In: *The Journal of biological chemistry* 280.48 (Dec. 2005), pp. 40058–40065.

[38] Wei Wang et al. “The carboxyl-terminal amino acids render pro-human LC3B migration similar to lipidated LC3B in SDS-PAGE.” In: *PloS one* 8.9 (2013), e74222.

[39] Christian Behrends et al. “Network organization of the human autophagy system”. In: *Nature* 466.7302 (Jan. 2010), pp. 68–76.

[40] Geir Bjørkøy et al. “p62/SQSTM1 forms protein aggregates degraded by autophagy and has a protective effect on huntingtin-induced cell death.” In: *The Journal of cell biology* 171.4 (Nov. 2005), pp. 603–614.

[41] Philipp Wild et al. “Phosphorylation of the autophagy receptor optineurin restricts Salmonella growth.” In: *Science (New York, NY)* 333.6039 (July 2011), pp. 228–233.

[42] Teresa L M Thurston et al. “The TBK1 adaptor and autophagy receptor NDP52 restricts the proliferation of ubiquitin-coated bacteria.” In: *Nature immunology* 10.11 (Nov. 2009), pp. 1215–1221.

[43] Vladimir Kirkin et al. “NBR1 cooperates with p62 in selective autophagy of ubiquitinated targets.” In: *Autophagy* 5.5 (July 2009), pp. 732–733.

[44] Trond Lamark et al. “NBR1 and p62 as cargo receptors for selective autophagy of ubiquitinated targets.” In: *Cell cycle (Georgetown, Tex)* 8.13 (July 2009), pp. 1986–1990.

[45] Philipp Wild, David G McEwan, and Ivan Dikic. “The LC3 interactome at a glance.” In: *Journal of cell science* 127.Pt 1 (Jan. 2014), pp. 3–9.

[46] Hilla Weidberg et al. “LC3 and GATE-16 N termini mediate membrane fusion processes required for autophagosome biogenesis.” In: *Developmental cell* 20.4 (Apr. 2011), pp. 444–454.

[47] T Noda, N Fujita, and T Yoshimori. “The late stages of autophagy: how does the end begin?” In: *Cell death and differentiation* 16.7 (July 2009), pp. 984–990.

[48] Yuchen Feng, Zhiyuan Yao, and Daniel J Klionsky. “How to control self-digestion: transcriptional, post-transcriptional, and post-translational regulation of autophagy.” In: *Trends in Cell Biology* 25.6 (June 2015), pp. 354–363.

[49] Yi Yang, Lin-Qing Feng, and Xiao-Xiang Zheng. “Microtubule and kinesin/dynein-dependent, bi-directional transport of autolysosomes in neurites of PC12 cells.” In: *The international journal of biochemistry & cell biology* 43.8 (Aug. 2011), pp. 1147–1156.

[50] Eisuke Itakura, Chieko Kishi-Itakura, and Noboru Mizushima. “The hairpin-type tail-anchored SNARE syntaxin 17 targets to autophagosomes for fusion with endosomes/lysosomes.” In: *Cell* 151.6 (Dec. 2012), pp. 1256–1269.

[51] Alexey V Berezhnov et al. “Intracellular pH modulates autophagy and mitophagy.” In: *The Journal of biological chemistry* (Feb. 2016).

[52] Nobuo N Noda and Fuyuhiko Inagaki. “Mechanisms of Autophagy.” In: *Annual review of biophysics* 44 (2015), pp. 101–122.

[53] Fred Lozy and Vassiliki Karantza. “Autophagy and cancer cell metabolism.” In: *Seminars in cell & developmental biology* 23.4 (June 2012), pp. 395–401.

[54] Emma Y Liu and Kevin M Ryan. “Autophagy and cancer–issues we need to digest.” In: *Journal of cell science* 125.Pt 10 (May 2012), pp. 2349–2358.

[55] Brinda Ravikumar and David C Rubinsztein. “Can autophagy protect against neurodegeneration caused by aggregate-prone proteins?” In: *Neuroreport* 15.16 (Nov. 2004), pp. 2443–2445.

[56] Masaaki Komatsu et al. “Loss of autophagy in the central nervous system causes neurodegeneration in mice.” In: *Nature* 441.7095 (June 2006), pp. 880–884.

[57] Taichi Hara et al. “Suppression of basal autophagy in neural cells causes neurodegenerative disease in mice.” In: *Nature* 441.7095 (June 2006), pp. 885–889.

[58] Ana Maria Cuervo. “Autophagy: in sickness and in health.” In: *Trends in Cell Biology* 14.2 (Feb. 2004), pp. 70–77.

[59] Beth Levine, Noboru Mizushima, and Herbert W Virgin. "Autophagy in immunity and inflammation." In: *Nature* 469.7330 (Jan. 2011), pp. 323–335.

[60] Saleh A Naser et al. "Role of ATG16L, NOD2 and IL23R in Crohn's disease pathogenesis." In: *World journal of gastroenterology* 18.5 (Feb. 2012), pp. 412–424.

[61] Heesun Cheong et al. "Therapeutic targets in cancer cell metabolism and autophagy." In: *Nature biotechnology* 30.7 (July 2012), pp. 671–678.

[62] J Y Guo et al. "Autophagy suppresses progression of K-ras-induced lung tumors to oncocytomas and maintains lipid homeostasis". In: *Genes & development* 27.13 (July 2013), pp. 1447–1461.

[63] Jing-Wen Yang et al. "Autophagy in SDF-1α-mediated DPSC migration and pulp regeneration." In: *Biomaterials* 44 (Mar. 2015), pp. 11–23.

[64] Jessie Yanxiang Guo et al. "Activated Ras requires autophagy to maintain oxidative metabolism and tumorigenesis." In: *Genes & development* 25.5 (Mar. 2011), pp. 460–470.

[65] Rebecca Lock et al. "Autophagy facilitates glycolysis during Ras-mediated oncogenic transformation." In: *Molecular biology of the cell* 22.2 (Jan. 2011), pp. 165–178.

[66] Min-Jung Kim et al. "Involvement of autophagy in oncogenic K-Ras-induced malignant cell transformation." In: *The Journal of biological chemistry* 286.15 (Apr. 2011), pp. 12924–12932.

[67] Huijun Wei et al. "Suppression of autophagy by FIP200 deletion inhibits mammary tumorigenesis." In: *Genes & development* 25.14 (July 2011), pp. 1510–1527.

[68] Saurabh V Laddha et al. "Mutational landscape of the essential autophagy gene BECN1 in human cancers." In: *Molecular cancer research : MCR* 12.4 (Apr. 2014), pp. 485–490.

[69] Robert D Leone and Ravi K Amaravadi. “Autophagy: a targetable linchpin of cancer cell metabolism.” In: *Trends in endocrinology and metabolism: TEM* 24.4 (Apr. 2013), pp. 209–217.

[70] Roberto Zoncu, Alejo Efeyan, and David M Sabatini. “mTOR: from growth signal integration to cancer, diabetes and ageing.” In: *Nature reviews Molecular cell biology* 12.1 (Jan. 2011), pp. 21–35.

[71] Liron Bar-Peled and David M Sabatini. “Regulation of mTORC1 by amino acids.” In: *Trends in Cell Biology* 24.7 (July 2014), pp. 400–406.

[72] Joungmok Kim and Eunjung Kim. “Rag GTPase in amino acid signaling.” In: *Amino acids* 48.4 (Apr. 2016), pp. 915–928.

[73] Ewan M Smith et al. “The tuberous sclerosis protein TSC2 is not required for the regulation of the mammalian target of rapamycin by amino acids and certain cellular stresses.” In: *The Journal of biological chemistry* 280.19 (May 2005), pp. 18717–18727.

[74] Eunjung Kim et al. “Regulation of TORC1 by Rag GTPases in nutrient response.” In: *Nature cell biology* 10.8 (Aug. 2008), pp. 935–945.

[75] Jung Min Han et al. “Leucyl-tRNA synthetase is an intracellular leucine sensor for the mTORC1-signaling pathway.” In: *Cell* 149.2 (Apr. 2012), pp. 410–424.

[76] Yasemin Sancak et al. “Ragulator-Rag complex targets mTORC1 to the lysosomal surface and is necessary for its activation by amino acids.” In: *Cell* 141.2 (Apr. 2010), pp. 290–303.

[77] Jennifer Jung, Heide Marika Genau, and Christian Behrends. “Amino Acid-Dependent mTORC1 Regulation by the Lysosomal Membrane Protein SLC38A9.” In: *Molecular and cellular biology* 35.14 (July 2015), pp. 2479–2494.

[78] Shuyu Wang et al. “Metabolism. Lysosomal amino acid transporter SLC38A9 signals arginine sufficiency to mTORC1.” In: *Science (New York, NY)* 347.6218 (Jan. 2015), pp. 188–194.

[79] Dan Egan et al. “The autophagy initiating kinase ULK1 is regulated via opposing phosphorylation by AMPK and mTOR.” In: *Autophagy* 7.6 (June 2011), pp. 643–644.

[80] Ping Xu et al. “JNK regulates FoxO-dependent autophagy in neurons.” In: *Genes & development* 25.4 (Feb. 2011), pp. 310–322.

[81] Einat Zalckvar et al. “DAP-kinase-mediated phosphorylation on the BH3 domain of beclin 1 promotes dissociation of beclin 1 from Bcl-XL and induction of autophagy.” In: *EMBO reports* 10.3 (Mar. 2009), pp. 285–292.

[82] Yasuhiro Maejima et al. “Mst1 inhibits autophagy by promoting the interaction between Beclin1 and Bcl-2.” In: *Nature medicine* 19.11 (Nov. 2013), pp. 1478–1488.

[83] Richard C Wang et al. “Akt-mediated regulation of autophagy and tumorigenesis through Beclin 1 phosphorylation.” In: *Science (New York, NY)* 338.6109 (Nov. 2012), pp. 956–959.

[84] Michael Degtyarev et al. “Akt inhibition promotes autophagy and sensitizes PTEN-null tumors to lysosomotropic agents.” In: *The Journal of cell biology* 183.1 (Oct. 2008), pp. 101–116.

[85] N Z Kara et al. “Trehalose induced antidepressant-like effects and autophagy enhancement in mice.” In: *Psychopharmacology* 229.2 (Sept. 2013), pp. 367–375.

[86] Christina H Eng and Robert T Abraham. “Glutaminolysis yields a metabolic by-product that stimulates autophagy.” In: *Autophagy* 6.7 (Oct. 2010), pp. 968–970.

[87] Andrew N Lane and Teresa W M Fan. “Regulation of mammalian nucleotide metabolism and biosynthesis.” In: *Nucleic acids research* 43.4 (Feb. 2015), pp. 2466–2485.

[88] Matthias Kappler et al. “Normoxic accumulation of HIF1α is associated with glutaminolysis.” In: *Clinical oral investigations* (Mar. 2016).

[89] S Mordier et al. “Leucine limitation induces autophagy and activation of lysosome-dependent proteolysis in C2C12 myotubes through a mammalian target of rapamycin-independent signaling pathway.” In: *The Journal of biological chemistry* 275.38 (Sept. 2000), pp. 29900–29906.

[90] Cristina Mammucari et al. “FoxO3 controls autophagy in skeletal muscle in vivo.” In: *Cell metabolism* 6.6 (Dec. 2007), pp. 458–471.

[91] Ralph J DeBerardinis et al. “The biology of cancer: metabolic reprogramming fuels cell growth and proliferation.” In: *Cell metabolism* 7.1 (Jan. 2008), pp. 11–20.

[92] Ruth Scherz-Shouval et al. “Reactive oxygen species are essential for autophagy and specifically regulate the activity of Atg4.” In: *The EMBO journal* 26.7 (Apr. 2007), pp. 1749–1760.

[93] Y Chen, M B Azad, and S B Gibson. “Superoxide is the major reactive oxygen species regulating autophagy.” In: *Cell death and differentiation* 16.7 (July 2009), pp. 1040–1052.

[94] Xin Wen et al. “Deconvoluting the role of reactive oxygen species and autophagy in human diseases.” In: *Free radical biology & medicine* 65 (Dec. 2013), pp. 402–410.

[95] Tobias Eisenberg et al. “Nucleocytosolic depletion of the energy metabolite acetyl-coenzyme a stimulates autophagy and prolongs lifespan.” In: *Cell metabolism* 19.3 (Mar. 2014), pp. 431–444.

[96] Guillermo Mariño et al. “Regulation of autophagy by cytosolic acetyl-coenzyme A.” In: *Molecular cell* 53.5 (Mar. 2014), pp. 710–725.

[97] Tao Xie et al. “Untangling knots between autophagic targets and candidate drugs, in cancer therapy.” In: *Cell proliferation* 48.2 (Apr. 2015), pp. 119–139.

[98] S Jane Henley et al. “Invasive Cancer Incidence and Survival - United States, 2012.” In: *MMWR. Morbidity and mortality weekly report* 64.49 (2015), pp. 1353–1358.

[99] Cancer Research. “http://www.cancerresearchuk.org/health-professional/cancer-statistics/incidence”. In: *Cancer Research UK* (May 2016).

[100] Alessio Giubellino, Terrence R Burke, and Donald P Bottaro. “Grb2 signaling in cell motility and cancer.” In: *Expert opinion on therapeutic targets* 12.8 (Aug. 2008), pp. 1021–1033.

[101] International Cancer Genome Consortium et al. “International network of cancer genome projects.” In: *Nature* 464.7291 (Apr. 2010), pp. 993–998.

[102] Frank Weinberg et al. “Mitochondrial metabolism and ROS generation are essential for Kras-mediated tumorigenicity.” In: *Proceedings of the National Academy of Sciences of the United States of America* 107.19 (May 2010), pp. 8788–8793.

[103] Tomoyoshi Soga. “Cancer metabolism: Key players in metabolic reprogramming.” In: *Cancer science* 104.3 (Mar. 2013), pp. 275–281.

[104] Chi V Dang. “Links between metabolism and cancer.” In: *Genes & development* 26.9 (May 2012), pp. 877–890.

[105] Patrick S Ward and Craig B Thompson. “Metabolic reprogramming: a cancer hallmark even warburg did not anticipate.” In: *Cancer cell* 21.3 (Mar. 2012), pp. 297–308.

[106] Kirstie E Keller, Irene S Tan, and Young-Sam Lee. “SAICAR stimulates pyruvate kinase isoform M2 and promotes cancer cell survival in glucose-limited conditions.” In: *Science (New York, NY)* 338.6110 (Nov. 2012), pp. 1069–1072.

[107] Beverly A Teicher, W Marston Linehan, and Lee J Helman. “Targeting cancer metabolism.” In: *Clinical cancer research : an official journal of the American Association for Cancer Research* 18.20 (Oct. 2012), pp. 5537–5545.

[108] Kirsten L Bryant et al. “KRAS: feeding pancreatic cancer proliferation.” In: *Trends in biochemical sciences* 39.2 (Feb. 2014), pp. 91–100.

[109] Alexei Vazquez et al. “Catabolic efficiency of aerobic glycolysis: the Warburg effect revisited.” In: *BMC systems biology* 4 (2010), p. 58.

[110] O Warburg, F Wind, and E Negelein. “THE METABOLISM OF TUMORS IN THE BODY.” In: *The Journal of general physiology* 8.6 (Mar. 1927), pp. 519–530.

[111] Xin Lin Zu and Michael Guppy. “Cancer metabolism: facts, fantasy, and fiction.” In: *Biochemical and biophysical research communications* 313.3 (Jan. 2004), pp. 459–465.

[112] Luke A J O’Neill and D Grahame Hardie. “Metabolism of inflammation limited by AMPK and pseudo-starvation.” In: *Nature* 493.7432 (Jan. 2013), pp. 346–355.

[113] Imoh S Okon and Ming-Hui Zou. “Mitochondrial ROS and cancer drug resistance: Implications for therapy.” In: *Pharmacological research* 100 (Oct. 2015), pp. 170–174.

[114] K Irani et al. “Mitogenic signaling mediated by oxidants in Ras-transformed fibroblasts.” In: *Science (New York, NY)* 275.5306 (Mar. 1997), pp. 1649–1652.

[115] Shuxi Qiao et al. “A REDD1/TXNIP pro-oxidant complex regulates ATG4B activity to control stress-induced autophagy and sustain exercise capacity.” In: *Nature communications* 6 (2015), p. 7014.

[116] D J Roberts and S Miyamoto. “Hexokinase II integrates energy metabolism and cellular protection: Akting on mitochondria and TORCing to autophagy.” In: *Cell death and differentiation* (Oct. 2014).

[117] R A Nakashima et al. “Hexokinase receptor complex in hepatoma mitochondria: evidence from N,N’-dicyclohexylcarbodiimide-labeling studies for the involvement of the pore-forming protein VDAC.” In: *Biochemistry* 25.5 (Mar. 1986), pp. 1015–1021.

[118] Paolo E Porporato et al. “Anticancer targets in the glycolytic metabolism of tumors: a comprehensive review.” In: *Frontiers in pharmacology* 2 (2011), p. 49.

[119] John G Pastorino, Nataly Shulga, and Jan B Hoek. “Mitochondrial binding of hexokinase II inhibits Bax-induced cytochrome c release and apoptosis.” In: *The Journal of biological chemistry* 277.9 (Mar. 2002), pp. 7610–7618.

[120] Prashanth T Bhaskar et al. “mTORC1 hyperactivity inhibits serum deprivation-induced apoptosis via increased hexokinase II and GLUT1 expression, sustained Mcl-1 expression, and glycogen synthase kinase 3beta inhibition.” In: *Molecular and cellular biology* 29.18 (Sept. 2009), pp. 5136–5147.

[121] G Weber. “Enzymology of cancer cells (second of two parts).” In: *The New England journal of medicine* 296.10 (Mar. 1977), pp. 541–551.

[122] Abdullah Yalcin et al. “Regulation of glucose metabolism by 6-phosphofructo-2-kinase/fructose-2,6-bisphosphatases in cancer.” In: *Experimental and molecular pathology* 86.3 (June 2009), pp. 174–179.

[123] Katherine R Mattaini and Matthew G Vander Heiden. “Cancer. Glycosylation to adapt to stress.” In: *Science (New York, NY)* 337.6097 (Aug. 2012), pp. 925–926.

[124] Zhen Yang et al. “Phosphofructokinase deficiency impairs ATP generation, autophagy, and redox balance in rheumatoid arthritis T cells.” In: *The Journal of experimental medicine* 210.10 (Sept. 2013), pp. 2119–2134.

[125] Zhen Yang, Jörg J Goronzy, and Cornelia M Weyand. “The glycolytic enzyme PFKFB3/phosphofructokinase regulates autophagy.” In: *Autophagy* 10.2 (Feb. 2014), pp. 382–383.

[126] Alden C Klarer et al. “Inhibition of 6-phosphofructo-2-kinase (PFKFB3) induces autophagy as a survival mechanism.” In: *Cancer & metabolism* 2.1 (2014), p. 2.

[127] A M Strohecker et al. “Identification of 6-phosphofructo-2-kinase/fructose-2,6-bisphosphatase as a novel autophagy regulator by high content shRNA screening.” In: *Oncogene* 34.45 (Nov. 2015), pp. 5662–5676.

[128] Wen Yi et al. “Phosphofructokinase 1 glycosylation regulates cell growth and metabolism.” In: *Science (New York, NY)* 337.6097 (Aug. 2012), pp. 975–980.

[129] Philippe Icard and Hubert Lincet. “A global view of the biochemical pathways involved in the regulation of the metabolism of cancer cells.” In: *Biochimica et biophysica acta* 1826.12 (Dec. 2012), pp. 423–433.

[130] Nana-Maria Grüning and Markus Ralser. “Cancer: Sacrifice for survival.” In: *Nature* 480.7376 (Dec. 2011), pp. 190–191.

[131] Heather R Christofk et al. “The M2 splice isoform of pyruvate kinase is important for cancer metabolism and tumour growth.” In: *Nature* 452.7184 (Mar. 2008), pp. 230–233.

[132] Gaochuan Zhang et al. “Unraveling the mystery of cancer metabolism in the genesis of tumor-initiating cells and development of cancer.” In: *Biochimica et biophysica acta* 1836.1 (Aug. 2013), pp. 49–59.

[133] Weibo Luo et al. “Pyruvate kinase M2 is a PHD3-stimulated coactivator for hypoxia-inducible factor 1.” In: *Cell* 145.5 (May 2011), pp. 732–744.

[134] Xueliang Gao et al. “Pyruvate kinase M2 regulates gene transcription by acting as a protein kinase.” In: *Molecular cell* 45.5 (Mar. 2012), pp. 598–609.

[135] Weiwei Yang et al. “PKM2 phosphorylates histone H3 and promotes gene transcription and tumorigenesis.” In: *Cell* 150.4 (Aug. 2012), pp. 685–696.

[136] Heather R Christofk et al. “Pyruvate kinase M2 is a phosphotyrosine-binding protein.” In: *Nature* 452.7184 (Mar. 2008), pp. 181–186.

[137] Sara Altuntas et al. “The transglutaminase type 2 and pyruvate kinase isoenzyme M2 interplay in autophagy regulation.” In: *Oncotarget* (Dec. 2015).

[138] Phatchariya Phannasil et al. “Pyruvate Carboxylase Is Up-Regulated in Breast Cancer and Essential to Support Growth and Invasion of MDA-MB-231 Cells.” In: *PloS one* 10.6 (2015), e0129848.

[139] Katherine Sellers et al. “Pyruvate carboxylase is critical for non-small-cell lung cancer proliferation.” In: *The Journal of clinical investigation* 125.2 (Feb. 2015), pp. 687–698.

[140] H EAGLE. “Nutrition needs of mammalian cells in tissue culture.” In: *Science (New York, NY)* 122.3168 (Sept. 1955), pp. 501–514.

[141] Mariia O Yuneva et al. “The metabolic profile of tumors depends on both the responsible genetic lesion and tissue type.” In: *Cell metabolism* 15.2 (Feb. 2012), pp. 157–170.

[142] Paul Nicklin et al. “Bidirectional transport of amino acids regulates mTOR and autophagy.” In: *Cell* 136.3 (Feb. 2009), pp. 521–534.

[143] O Yanagida et al. “Human L-type amino acid transporter 1 (LAT1): characterization of function and expression in tumor cell lines.” In: *Biochimica et biophysica acta* 1514.2 (Oct. 2001), pp. 291–302.

[144] Christian Meier et al. “Activation of system L heterodimeric amino acid exchangers by intracellular substrates.” In: *The EMBO journal* 21.4 (Feb. 2002), pp. 580–589.

[145] T Osada et al. “Prognostic significance of glutamine synthetase expression in unifocal advanced hepatocellular carcinoma.” In: *Journal of hepatology* 33.2 (Aug. 2000), pp. 247–253.

[146] Robert A Casero and Laurence J Marton. “Targeting polyamine metabolism and function in cancer and other hyperproliferative diseases.” In: *Nature reviews. Drug discovery* 6.5 (May 2007), pp. 373–390.

[147] Tawnya L Bowles et al. “Pancreatic cancer cell lines deficient in argininosuccinate synthetase are sensitive to arginine deprivation by arginine deiminase.” In: *International journal of cancer. Journal international du cancer* 123.8 (Oct. 2008), pp. 1950–1955.

[148] Jennifer A McAlpine et al. “Down-regulation of argininosuccinate synthetase is associated with cisplatin resistance in hepatocellular carcinoma cell lines: implications for PEGylated arginine deiminase combination therapy.” In: *BMC cancer* 14 (2014), p. 621.

[149] G C Yeh and J M Phang. “Stimulation of phosphoribosyl pyrophosphate and purine nucleotide production by pyrroline 5-carboxylate in human erythrocytes.” In: *The Journal of biological chemistry* 263.26 (Sept. 1988), pp. 13083–13089.

[150] Wei Liu and James M Phang. “Proline dehydrogenase (oxidase), a mitochondrial tumor suppressor, and autophagy under the hypoxia microenvironment.” In: *Autophagy* 8.9 (Sept. 2012), pp. 1407–1409.

[151] Roland Nilsson et al. “Metabolic enzyme expression highlights a key role for MTHFD2 and the mitochondrial folate pathway in cancer.” In: *Nature communications* 5 (2014), p. 3128.

[152] Wei Liu et al. “Proline biosynthesis augments tumor cell growth and aerobic glycolysis: involvement of pyridine nucleotides.” In: *Scientific reports* 5 (2015), p. 17206.

[153] Ilona Zareba and Jerzy Palka. “Prolidase-proline dehydrogenase/proline oxidase-collagen biosynthesis axis as a potential interface of apoptosis/autophagy.” In: *BioFactors (Oxford, England)* (Apr. 2016).

[154] S P Donald et al. “Proline oxidase, encoded by p53-induced gene-6, catalyzes the generation of proline-dependent reactive oxygen species.” In: *Cancer Research* 61.5 (Mar. 2001), pp. 1810–1815.

[155] Jason W Locasale et al. “Phosphoglycerate dehydrogenase diverts glycolytic flux and contributes to oncogenesis.” In: *Nature Genetics* 43.9 (Sept. 2011), pp. 869–874.

[156] Taro Hitosugi et al. “Phosphoglycerate mutase 1 coordinates glycolysis and biosynthesis to promote tumor growth.” In: *Cancer cell* 22.5 (Nov. 2012), pp. 585–600.

[157] Taro Hitosugi et al. “Tyr26 phosphorylation of PGAM1 provides a metabolic advantage to tumours by stabilizing the active conformation.” In: *Nature communications* 4 (2013), p. 1790.

[158] Junjie Li and Ji-Xin Cheng. “Direct visualization of de novo lipogenesis in single living cells.” In: *Scientific reports* 4 (2014), p. 6807.

[159] Evelien Rysman et al. “De novo lipogenesis protects cancer cells from free radicals and chemotherapeutics by promoting membrane lipid saturation.” In: *Cancer Research* 70.20 (Oct. 2010), pp. 8117–8126.

[160] Nousheen Zaidi, Johannes V Swinnen, and Karine Smans. “ATP-citrate lyase: a key player in cancer metabolism.” In: *Cancer Research* 72.15 (Aug. 2012), pp. 3709–3714.

[161] L Tong. “Acetyl-coenzyme A carboxylase: crucial metabolic enzyme and attractive target for drug discovery.” In: *Cellular and molecular life sciences : CMLS* 62.16 (Aug. 2005), pp. 1784–1803.

[162] Javier A Menendez and Ruth Lupu. “Fatty acid synthase and the lipogenic phenotype in cancer pathogenesis.” In: *Nature reviews. Cancer* 7.10 (Oct. 2007), pp. 763–777.

[163] R Ariel Igal. “Stearoyl-CoA desaturase-1: a novel key player in the mechanisms of cell proliferation, programmed cell death and transformation to cancer.” In: *Carcinogenesis* 31.9 (Sept. 2010), pp. 1509–1515.

[164] Daniel C Berwick et al. “The identification of ATP-citrate lyase as a protein kinase B (Akt) substrate in primary adipocytes.” In: *The Journal of biological chemistry* 277.37 (Sept. 2002), pp. 33895–33900.

[165] Katharina Tomek et al. “Blockade of fatty acid synthase induces ubiquitination and degradation of phosphoinositide-3-kinase signaling proteins in ovarian cancer.” In: *Molecular cancer research : MCR* 9.12 (Dec. 2011), pp. 1767–1779.

[166] Olga Aprelikova et al. “Regulation of HIF prolyl hydroxylases by hypoxia-inducible factors.” In: *Journal of cellular biochemistry* 92.3 (June 2004), pp. 491–501.

[167] Julian J Lum et al. “The transcription factor HIF-1alpha plays a critical role in the growth factor-dependent regulation of both aerobic and anaerobic glycolysis.” In: *Genes & development* 21.9 (May 2007), pp. 1037–1049.

[168] G L Semenza et al. “Transcriptional regulation of genes encoding glycolytic enzymes by hypoxia-inducible factor 1.” In: *The Journal of biological chemistry* 269.38 (Sept. 1994), pp. 23757–23763.

[169] Jung-whan Kim et al. “HIF-1-mediated expression of pyruvate dehydrogenase kinase: a metabolic switch required for cellular adaptation to hypoxia.” In: *Cell metabolism* 3.3 (Mar. 2006), pp. 177–185.

[170] M Tatibana et al. “Mammalian phosphoribosyl-pyrophosphate synthetase.” In: *Advances in enzyme regulation* 35 (1995), pp. 229–249.

[171] A M Robitaille et al. “Quantitative Phosphoproteomics Reveal mTORC1 Activates de Novo Pyrimidine Synthesis”. In: *Science (New York, NY)* 339.6125 (Mar. 2013), pp. 1320–1323.

[172] I Ben-Sahra et al. “Stimulation of de Novo Pyrimidine Synthesis by Growth Signaling Through mTOR and S6K1”. In: *Science (New York, NY)* 339.6125 (Mar. 2013), pp. 1323–1328.

[173] Javier R Revollo, Andrew A Grimm, and Shin-ichiro Imai. “The regulation of nicotinamide adenine dinucleotide biosynthesis by Nampt/PBEF/visfatin in mammals.” In: *Current opinion in gastroenterology* 23.2 (Mar. 2007), pp. 164–170.

[174] Robert W Sobol. “Preface. NAD metabolism and signaling: Critical pathways in bacteria, yeast and mammals influencing genome stability, cell survival and disease.” In: *DNA repair* 23 (Nov. 2014), pp. 1–3.

[175] Andreas H Guse. “Regulation of calcium signaling by the second messenger cyclic adenosine diphosphoribose (cADPR).” In: *Current molecular medicine* 4.3 (May 2004), pp. 239–248.

[176] Mareike Bütepage et al. “Intracellular Mono-ADP-Ribosylation in Signaling and Disease.” In: *Cells* 4.4 (2015), pp. 569–595.

[177] Henning Kleine et al. “Dynamic subcellular localization of the mono-ADP-ribosyltransferase ARTD10 and interaction with the ubiquitin receptor p62.” In: *Cell communication and signaling : CCS* 10.1 (2012), p. 28.

[178] Xuan Ou et al. “SIRT1 positively regulates autophagy and mitochondria function in embryonic stem cells under oxidative stress.” In: *Stem cells (Dayton, Ohio)* 32.5 (May 2014), pp. 1183–1194.

[179] Jing Wang et al. “Sirtinol, a class III HDAC inhibitor, induces apoptotic and autophagic cell death in MCF-7 human breast cancer cells.” In: *International journal of oncology* 41.3 (Sept. 2012), pp. 1101–1109.

[180] Riekelt H Houtkooper, Eija Pirinen, and Johan Auwerx. “Sirtuins as regulators of metabolism and healthspan.” In: *Nature reviews Molecular cell biology* 13.4 (Apr. 2012), pp. 225–238.

[181] Chiara Riganti et al. “The pentose phosphate pathway: an antioxidant defense and a crossroad in tumor cell fate.” In: *Free radical biology & medicine* 53.3 (Aug. 2012), pp. 421–436.

[182] Matthew G Vander Heiden, Lewis C Cantley, and Craig B Thompson. “Understanding the Warburg effect: the metabolic requirements of cell proliferation.” In: *Science (New York, NY)* 324.5930 (May 2009), pp. 1029–1033.

[183] Haoqiang Ying et al. “Oncogenic Kras maintains pancreatic tumors through regulation of anabolic glucose metabolism.” In: *Cell* 149.3 (Apr. 2012), pp. 656–670.

[184] M Krockenberger et al. “Expression of transketolase-like 1 protein (TKTL1) in human endometrial cancer.” In: *Anticancer research* 30.5 (May 2010), pp. 1653–1659.

[185] Iris Ming-Jing Xu et al. “Transketolase counteracts oxidative stress to drive cancer development.” In: *Proceedings of the National Academy of Sciences of the United States of America* 113.6 (Feb. 2016), E725–34.

[186] Hui Chen et al. “Overexpression of transketolase-like gene 1 is associated with cell proliferation in uterine cervix cancer.” In: *Journal of experimental & clinical cancer research : CR* 28 (2009), p. 43.

[187] Santiago Diaz-Moralli et al. “Transketolase-like 1 expression is modulated during colorectal cancer progression and metastasis formation.” In: *PloS one* 6.9 (2011), e25323.

[188] Alfonso Martín-Bernabé et al. “Quantitative proteomic approach to understand metabolic adaptation in non-small cell lung cancer.” In: *Journal of proteome research* 13.11 (Nov. 2014), pp. 4695–4704.

[189] E Tsouko et al. “Regulation of the pentose phosphate pathway by an androgen receptor-mTOR-mediated mechanism and its role in prostate cancer cell growth.” In: *Oncogenesis* 3 (2014), e103.

[190] R C Stanton et al. “Rapid release of bound glucose-6-phosphate dehydrogenase by growth factors. Correlation with increased enzymatic activity.” In: *The Journal of biological chemistry* 266.19 (July 1991), pp. 12442–12448.

[191] Zhaoping Qiu et al. “MicroRNA-124 Reduces the Pentose Phosphate Pathway and Proliferation by Targeting PRPS1 and RPIA mRNAs in Human Colorectal Cancer Cells.” In: *Gastroenterology* (Aug. 2015).

[192] Peng Jiang et al. “p53 regulates biosynthesis through direct inactivation of glucose-6-phosphate dehydrogenase.” In: *Nature cell biology* 13.3 (Mar. 2011), pp. 310–316.

[193] B Hove-Jensen and M Maigaard. “Escherichia coli rpiA gene encoding ribose phosphate isomerase A.” In: *Journal of bacteriology* 175.17 (Sept. 1993), pp. 5628–5635.

[194] T W Apel et al. “The ribose 5-phosphate isomerase-encoding gene is located immediately downstream from that encoding murine immunoglobulin kappa.” In: *Gene* 156.2 (Apr. 1995), pp. 191–197.

[195] Rong guang Zhang et al. “Structure of Escherichia coli ribose-5-phosphate isomerase: a ubiquitous enzyme of the pentose phosphate pathway and the Calvin cycle.” In: *Structure (London, England : 1993)* 11.1 (Jan. 2003), pp. 31–42.

[196] Preet Kamal Kaur et al. “Mutational and Structural Analysis of Conserved Residues in Ribose-5-Phosphate Isomerase B from Leishmania donovani: Role in Substrate Recognition and Conformational Stability.” In: *PloS one* 11.3 (2016), e0150764.

[197] John C Obenauer, Lewis C Cantley, and Michael B Yaffe. “Scansite 2.0: Proteome-wide prediction of cell signaling interactions using short sequence motifs.” In: *Nucleic acids research* 31.13 (July 2003), pp. 3635–3641.

[198] Ching-Tzu Wang et al. “Reduced neuronal expression of ribose-5-phosphate isomerase enhances tolerance to oxidative stress, extends lifespan, and attenuates polyglutamine toxicity in Drosophila.” In: *Aging cell* 11.1 (Feb. 2012), pp. 93–103.

[199] Jojanneke H J Huck et al. “Ribose-5-phosphate isomerase deficiency: new inborn error in the pentose phosphate pathway associated with a slowly progressive leukoencephalopathy.” In: *American journal of human genetics* 74.4 (Apr. 2004), pp. 745–751.

[200] Vassili Valayannopoulos et al. “Transaldolase deficiency: a new cause of hydrops fetalis and neonatal multi-organ disease.” In: *The Journal of pediatrics* 149.5 (Nov. 2006), pp. 713–717.

[201] M M C Wamelink, E A Struys, and C Jakobs. “The biochemistry, metabolism and inherited defects of the pentose phosphate pathway: a re-

view." In: *Journal of inherited metabolic disease* 31.6 (Dec. 2008), pp. 703–717.

[202] Shih-Ci Ciou et al. "Ribose-5-phosphate isomerase a regulates hepatocarcinogenesis via PP2A and ERK signaling." In: *International journal of cancer. Journal international du cancer* (Nov. 2014), n–a–n–a.

[203] Ralph J DeBerardinis and Craig B Thompson. "Cellular metabolism and disease: what do metabolic outliers teach us?" In: *Cell* 148.6 (Mar. 2012), pp. 1132–1144.

[204] L G Boros et al. "Oxythiamine and dehydroepiandrosterone inhibit the nonoxidative synthesis of ribose and tumor cell proliferation." In: *Cancer Research* 57.19 (Oct. 1997), pp. 4242–4248.

[205] Krushna C Patra and Nissim Hay. "The pentose phosphate pathway and cancer." In: *Trends in biochemical sciences* 39.8 (Aug. 2014), pp. 347–354.

[206] Arindam Saha et al. "Akt phosphorylation and regulation of transketolase is a nodal point for amino acid control of purine synthesis." In: *Molecular cell* 55.2 (July 2014), pp. 264–276.

[207] S Langbein et al. "Expression of transketolase TKTL1 predicts colon and urothelial cancer patient survival: Warburg effect reinterpreted." In: *British journal of cancer* 94.4 (Feb. 2006), pp. 578–585.

[208] Ludmilla E Meshalkina et al. "Is transketolase-like protein, TKTL1, transketolase?" In: *Biochimica et biophysica acta* 1832.3 (Mar. 2013), pp. 387–390.

[209] Robert Hanczko et al. "Prevention of hepatocarcinogenesis and increased susceptibility to acetaminophen-induced liver failure in transaldolase-deficient mice by N-acetylcysteine." In: *The Journal of clinical investigation* 119.6 (June 2009), pp. 1546–1557.

[210] Ana Mesquita et al. "Dissecting the function of Atg1 complex in Dictyostelium autophagy reveals a connection with the pentose phosphate pathway enzyme transketolase." In: *Open biology* 5.8 (Aug. 2015).

[211] Joseph Schlessinger. "Receptor tyrosine kinases: legacy of the first two decades." In: *Cold Spring Harbor perspectives in biology* 6.3 (Mar. 2014).

[212] Mark A Lemmon and Joseph Schlessinger. "Cell signaling by receptor tyrosine kinases." In: *Cell* 141.7 (June 2010), pp. 1117–1134.

[213] Bert Vogelstein and Kenneth W Kinzler. "Cancer genes and the pathways they control." In: *Nature medicine* 10.8 (Aug. 2004), pp. 789–799.

[214] Shai Gavi et al. "G-protein-coupled receptors and tyrosine kinases: crossroads in cell signaling and regulation." In: *Trends in endocrinology and metabolism: TEM* 17.2 (Mar. 2006), pp. 48–54.

[215] B Gay et al. "Selective GRB2 SH2 inhibitors as anti-Ras therapy." In: *International journal of cancer. Journal international du cancer* 83.2 (Oct. 1999), pp. 235–241.

[216] Helen Morrison et al. "Merlin/neurofibromatosis type 2 suppresses growth by inhibiting the activation of Ras and Rac." In: *Cancer Research* 67.2 (Jan. 2007), pp. 520–527.

[217] Ihn Kyung Jang, Jinping Zhang, and Hua Gu. "Grb2, a simple adapter with complex roles in lymphocyte development, function, and signaling." In: *Immunological reviews* 232.1 (Nov. 2009), pp. 150–159.

[218] A M Cheng et al. "Mammalian Grb2 regulates multiple steps in embryonic development and malignant transformation." In: *Cell* 95.6 (Dec. 1998), pp. 793–803.

[219] Chi-Chuan Lin et al. "Inhibition of Basal FGF Receptor Signaling by Dimeric Grb2". In: *Cell* 149.7 (June 2012), pp. 1514–1524.

[220] Artur A Belov and Moosa Mohammadi. "Grb2, a double-edged sword of receptor tyrosine kinase signaling." In: *Science signaling* 5.249 (2012), pe49.

[221] E J Lowenstein et al. "The SH2 and SH3 domain-containing protein GRB2 links receptor tyrosine kinases to ras signaling." In: *Cell* 70.3 (Aug. 1992), pp. 431–442.

[222] Xuejun Jiang et al. “Grb2 regulates internalization of EGF receptors through clathrin-coated pits.” In: *Molecular biology of the cell* 14.3 (Mar. 2003), pp. 858–870.

[223] Jochen A Ackermann et al. “Grb2 regulates B-cell maturation, B-cell memory responses and inhibits B-cell Ca2+ signalling.” In: *The EMBO journal* 30.8 (Apr. 2011), pp. 1621–1633.

[224] Caleb B McDonald et al. “Multivalent binding and facilitated diffusion account for the formation of the Grb2-Sos1 signaling complex in a cooperative manner.” In: *Biochemistry* 51.10 (Mar. 2012), pp. 2122–2135.

[225] Jon C D Houtman et al. “Oligomerization of signaling complexes by the multipoint binding of GRB2 to both LAT and SOS1.” In: *Nature structural & molecular biology* 13.9 (Sept. 2006), pp. 798–805.

[226] Yuliya Pylayeva-Gupta, Elda Grabocka, and Dafna Bar-Sagi. “RAS oncogenes: weaving a tumorigenic web.” In: *Nature reviews. Cancer* 11.11 (Nov. 2011), pp. 761–774.

[227] Norbert Berndt, Andrew D Hamilton, and Saïd M Sebti. “Targeting protein prenylation for cancer therapy.” In: *Nature reviews. Cancer* 11.11 (Nov. 2011), pp. 775–791.

[228] Jasminka Omerovic and Ian A Prior. “Compartmentalized signalling: Ras proteins and signalling nanoclusters.” In: *The FEBS journal* 276.7 (Apr. 2009), pp. 1817–1825.

[229] Vivek Asati, Debarshi Kar Mahapatra, and Sanjay Kumar Bharti. “PI3K/Akt/mTOR and Ras/Raf/MEK/ERK signaling pathways inhibitors as anticancer agents: Structural and pharmacological perspectives.” In: *European journal of medicinal chemistry* 109 (Feb. 2016), pp. 314–341.

[230] Michelle C Mendoza, E Emrah Er, and John Blenis. “The Ras-ERK and PI3K-mTOR pathways: cross-talk and compensation.” In: *Trends in biochemical sciences* 36.6 (June 2011), pp. 320–328.

[231] Inbal Wortzel and Rony Seger. “The ERK Cascade: Distinct Functions within Various Subcellular Organelles.” In: *Genes & cancer* 2.3 (Mar. 2011), pp. 195–209.

[232] Claudia Wellbrock, Maria Karasarides, and Richard Marais. “The RAF proteins take centre stage.” In: *Nature reviews Molecular cell biology* 5.11 (Nov. 2004), pp. 875–885.

[233] Huira Chong, Haris G Vikis, and Kun-Liang Guan. “Mechanisms of regulating the Raf kinase family.” In: *Cellular signalling* 15.5 (May 2003), pp. 463–469.

[234] U R Rapp et al. “Structure and biological activity of v-raf, a unique oncogene transduced by a retrovirus.” In: *Proceedings of the National Academy of Sciences of the United States of America* 80.14 (July 1983), pp. 4218–4222.

[235] J C Luckett et al. “Expression of the A-raf proto-oncogene in the normal adult and embryonic mouse.” In: *Cell growth & differentiation : the molecular biology journal of the American Association for Cancer Research* 11.3 (Mar. 2000), pp. 163–171.

[236] S Zimmermann and K Moelling. “Phosphorylation and regulation of Raf by Akt (protein kinase B).” In: *Science (New York, NY)* 286.5445 (Nov. 1999), pp. 1741–1744.

[237] M Jaumot and J F Hancock. “Protein phosphatases 1 and 2A promote Raf-1 activation by regulating 14-3-3 interactions.” In: *Oncogene* 20.30 (July 2001), pp. 3949–3958.

[238] Shujie Han and Kathryn E Meier. “Integrated modulation of phorbol ester-induced Raf activation in EL4 lymphoma cells.” In: *Cellular signalling* 21.5 (May 2009), pp. 793–800.

[239] C F Zheng and K L Guan. “Properties of MEKs, the kinases that phosphorylate and activate the extracellular signal-regulated kinases.” In: *The Journal of biological chemistry* 268.32 (Nov. 1993), pp. 23933–23939.

[240] Christophe Frémin and Sylvain Meloche. “From basic research to clinical development of MEK1/2 inhibitors for cancer therapy.” In: *Journal of hematology & oncology* 3 (2010), p. 8.

[241] Robert Roskoski. “MEK1/2 dual-specificity protein kinases: structure and regulation.” In: *Biochemical and biophysical research communications* 417.1 (Jan. 2012), pp. 5–10.

[242] A Alessandrini et al. “Mek1 phosphorylation site mutants activate Raf-1 in NIH 3T3 cells.” In: *The Journal of biological chemistry* 271.49 (Dec. 1996), pp. 31612–31618.

[243] Seunghee Yoon and Rony Seger. “The extracellular signal-regulated kinase: multiple substrates regulate diverse cellular functions.” In: *Growth factors (Chur, Switzerland)* 24.1 (Mar. 2006), pp. 21–44.

[244] Xiaoqi Liu et al. “The MAP kinase pathway is required for entry into mitosis and cell survival.” In: *Oncogene* 23.3 (Jan. 2004), pp. 763–776.

[245] Alexander Plotnikov et al. “The MAPK cascades: signaling components, nuclear roles and mechanisms of nuclear translocation.” In: *Biochimica et biophysica acta* 1813.9 (Sept. 2011), pp. 1619–1633.

[246] Robert Roskoski. “ERK1/2 MAP kinases: structure, function, and regulation.” In: *Pharmacological research* 66.2 (Aug. 2012), pp. 105–143.

[247] D J Robbins et al. “MAP kinases ERK1 and ERK2: pleiotropic enzymes in a ubiquitous signaling network.” In: *Advances in cancer research* 63 (1994), pp. 93–116.

[248] Miki Ebisuya, Kunio Kondoh, and Eisuke Nishida. “The duration, magnitude and compartmentalization of ERK MAP kinase activity: mechanisms for providing signaling specificity.” In: *Journal of cell science* 118.Pt 14 (July 2005), pp. 2997–3002.

[249] Christopher J Caunt and Craig A McArdle. “ERK phosphorylation and nuclear accumulation: insights from single-cell imaging.” In: *Biochemical Society transactions* 40.1 (Feb. 2012), pp. 224–229.

[250] Chiara Vantaggiato et al. “ERK1 and ERK2 mitogen-activated protein kinases affect Ras-dependent cell signaling differentially.” In: *Journal of biology* 5.5 (2006), p. 14.

[251] G Pagès et al. “Defective thymocyte maturation in p44 MAP kinase (Erk 1) knockout mice.” In: *Science (New York, NY)* 286.5443 (Nov. 1999), pp. 1374–1377.

[252] Dong-Jun Peng, Jun-Ying Zhou, and Gen Sheng Wu. “Post-translational regulation of mitogen-activated protein kinase phosphatase-2 (MKP-2) by ERK.” In: *Cell cycle (Georgetown, Tex)* 9.23 (Dec. 2010), pp. 4650–4655.

[253] Deborah K Morrison and Roger J Davis. “Regulation of MAP kinase signaling modules by scaffold proteins in mammals.” In: *Annual review of cell and developmental biology* 19 (2003), pp. 91–118.

[254] Alan J Whitmarsh. “Regulation of gene transcription by mitogen-activated protein kinase signaling pathways.” In: *Biochimica et biophysica acta* 1773.8 (Aug. 2007), pp. 1285–1298.

[255] Xin Li et al. “ERK-dependent threonine phosphorylation of EGF receptor modulates receptor downregulation and signaling.” In: *Cellular signalling* 20.11 (Nov. 2008), pp. 2145–2155.

[256] Yuji Kamioka et al. “Multiple decisive phosphorylation sites for the negative feedback regulation of SOS1 via ERK.” In: *The Journal of biological chemistry* 285.43 (Oct. 2010), pp. 33540–33548.

[257] Siyuan Zhang and Dihua Yu. “PI(3)king apart PTEN’s role in cancer.” In: *Clinical cancer research : an official journal of the American Association for Cancer Research* 16.17 (Sept. 2010), pp. 4325–4330.

[258] Ingrid A Mayer and Carlos L Arteaga. “The PI3K/AKT Pathway as a Target for Cancer Treatment.” In: *Annual review of medicine* 67 (Jan. 2016), pp. 11–28.

[259] Camillo Porta and Robert A Figlin. “Phosphatidylinositol-3-kinase/Akt signaling pathway and kidney cancer, and the therapeutic potential of phosphatidylinositol-3-kinase/Akt inhibitors.” In: *The Journal of urology* 182.6 (Dec. 2009), pp. 2569–2577.

[260] D A Fruman, R E Meyers, and L C Cantley. “Phosphoinositide kinases.” In: *Annual review of biochemistry* 67 (1998), pp. 481–507.

[261] Brendan D Manning and Lewis C Cantley. “AKT/PKB signaling: navigating downstream.” In: *Cell* 129.7 (June 2007), pp. 1261–1274.

[262] Ingeborg Hers, Emma E Vincent, and Jeremy M Tavaré. “Akt signalling in health and disease.” In: *Cellular signalling* 23.10 (Oct. 2011), pp. 1515–1527.

[263] Thomas F Franke et al. “PI3K/Akt and apoptosis: size matters.” In: *Oncogene* 22.56 (Dec. 2003), pp. 8983–8998.

[264] P T Hawkins et al. “Signalling through Class I PI3Ks in mammalian cells.” In: *Biochemical Society transactions* 34.Pt 5 (Nov. 2006), pp. 647–662.

[265] Reuben J Shaw and Lewis C Cantley. “Ras, PI(3)K and mTOR signalling controls tumour cell growth.” In: *Nature* 441.7092 (May 2006), pp. 424–430.

[266] Mathieu Laplante and David M Sabatini. “mTOR signaling in growth control and disease.” In: *Cell* 149.2 (Apr. 2012), pp. 274–293.

[267] R Cafferkey et al. “Dominant missense mutations in a novel yeast protein related to mammalian phosphatidylinositol 3-kinase and VPS34 abrogate rapamycin cytotoxicity.” In: *Molecular and cellular biology* 13.10 (Oct. 1993), pp. 6012–6023.

[268] Timothy R Peterson et al. “DEPTOR is an mTOR inhibitor frequently overexpressed in multiple myeloma cells and required for their survival.” In: *Cell* 137.5 (May 2009), pp. 873–886.

[269] Anya Alayev and Marina K Holz. “mTOR signaling for biological control and cancer.” In: *Journal of cellular physiology* 228.8 (Aug. 2013), pp. 1658–1664.

[270] Esther J Chen and Chris A Kaiser. “LST8 negatively regulates amino acid biosynthesis as a component of the TOR pathway.” In: *The Journal of cell biology* 161.2 (Apr. 2003), pp. 333–347.

[271] Haijuan Yang et al. “mTOR kinase structure, mechanism and regulation.” In: *Nature* 497.7448 (May 2013), pp. 217–223.

[272] D D Sarbassov et al. “Rictor, a novel binding partner of mTOR, defines a rapamycin-insensitive and raptor-independent pathway that regulates the cytoskeleton.” In: *Current biology : CB* 14.14 (July 2004), pp. 1296–1302.

[273] Kenta Hara et al. “Raptor, a binding partner of target of rapamycin (TOR), mediates TOR action.” In: *Cell* 110.2 (July 2002), pp. 177–189.

[274] Xiaoju Max Ma and John Blenis. “Molecular mechanisms of mTOR-mediated translational control.” In: *Nature reviews Molecular cell biology* 10.5 (May 2009), pp. 307–318.

[275] Do-Hyung Kim et al. “mTOR interacts with raptor to form a nutrient-sensitive complex that signals to the cell growth machinery.” In: *Cell* 110.2 (July 2002), pp. 163–175.

[276] Jonathan R Hart and Peter K Vogt. “Phosphorylation of AKT: a mutational analysis.” In: *Oncotarget* 2.6 (June 2011), pp. 467–476.

[277] Jeremiah N Winter, Leonard S Jefferson, and Scot R Kimball. “ERK and Akt signaling pathways function through parallel mechanisms to promote mTORC1 signaling.” In: *American journal of physiology. Cell physiology* 300.5 (May 2011), pp. C1172–80.

[278] Ken Inoki et al. “TSC2 is phosphorylated and inhibited by Akt and suppresses mTOR signalling.” In: *Nature cell biology* 4.9 (Sept. 2002), pp. 648–657.

[279] Ken Inoki, Tianqing Zhu, and Kun-Liang Guan. “TSC2 mediates cellular energy response to control cell growth and survival.” In: *Cell* 115.5 (Nov. 2003), pp. 577–590.

[280] James J Gibbons, Robert T Abraham, and Ker Yu. “Mammalian target of rapamycin: discovery of rapamycin reveals a signaling pathway important for normal and cancer cell growth.” In: *Seminars in oncology* 36 Suppl 3 (Dec. 2009), S3–S17.

[281] Haitao Wang et al. “Proline-rich Akt substrate of 40kDa (PRAS40): a novel downstream target of PI3k/Akt signaling pathway.” In: *Cellular signalling* 24.1 (Jan. 2012), pp. 17–24.

[282] Geetu Tuteja and Klaus H Kaestner. “Forkhead transcription factors II.” In: *Cell* 131.1 (Oct. 2007), p. 192.

[283] Xinbo Zhang et al. “Akt, FoxO and regulation of apoptosis.” In: *Biochimica et biophysica acta* 1813.11 (Nov. 2011), pp. 1978–1986.

[284] Geetu Tuteja and Klaus H Kaestner. “SnapShot: forkhead transcription factors I.” In: *Cell* 130.6 (Sept. 2007), p. 1160.

[285] Astrid Eijkelenboom and Boudewijn M T Burgering. “FOXOs: signalling integrators for homeostasis maintenance.” In: *Nature reviews Molecular cell biology* 14.2 (Feb. 2013), pp. 83–97.

[286] Jinghui Zhao et al. “FoxO3 coordinately activates protein degradation by the autophagic/lysosomal and proteasomal pathways in atrophying muscle cells.” In: *Cell metabolism* 6.6 (Dec. 2007), pp. 472–483.

[287] Arunima Sengupta, Jeffery D Molkentin, and Katherine E Yutzey. “FoxO transcription factors promote autophagy in cardiomyocytes.” In: *The Journal of biological chemistry* 284.41 (Oct. 2009), pp. 28319–28331.

[288] Arnold J Kahn. “FOXO3 and Related Transcription Factors in Development, Aging, and Exceptional Longevity.” In: *The journals of gerontology. Series A, Biological sciences and medical sciences* (Apr. 2014).

[289] Hien Tran et al. “The many forks in FOXO’s road.” In: *Science’s STKE : signal transduction knowledge environment* 2003.172 (Mar. 2003), RE5.

[290] R Ketteler et al. “Enhanced transgene expression in primitive hematopoietic progenitor cells and embryonic stem cells efficiently transduced by optimized retroviral hybrid vectors.” In: *Gene therapy* 9.8 (Apr. 2002), pp. 477–487.

[291] F Ann Ran et al. “Double nicking by RNA-guided CRISPR Cas9 for enhanced genome editing specificity.” In: *Cell* 154.6 (Sept. 2013), pp. 1380–1389.

[292] Jojanneke H J Huck et al. “Profiling of pentose phosphate pathway intermediates in blood spots by tandem mass spectrometry: application to transaldolase deficiency.” In: *Clinical chemistry* 49.8 (Aug. 2003), pp. 1375–1380.

[293] Deike J Omnus et al. “Phosphoinositide kinase signaling controls ER-PM cross-talk.” In: *Molecular biology of the cell* 27.7 (Apr. 2016), pp. 1170–1180.

[294] Carlos L Arteaga and Jeffrey A Engelman. “ERBB receptors: from oncogene discovery to basic science to mechanism-based cancer therapeutics.” In: *Cancer cell* 25.3 (Mar. 2014), pp. 282–303.

[295] Christophe Antczak et al. “Domain-based biosensor assay to screen for epidermal growth factor receptor modulators in live cells.” In: *Assay and drug development technologies* 10.1 (Feb. 2012), pp. 24–36.

[296] S Y Yoon et al. “Dynamin II associates with Grb2 SH3 domain in Ras transformed NIH3T3 cells.” In: *Biochemical and biophysical research communications* 234.3 (May 1997), pp. 539–543.

[297] Anna Stincone et al. “The return of metabolism: biochemistry and physiology of the pentose phosphate pathway.” In: *Biological reviews of the Cambridge Philosophical Society* (Sept. 2014).

[298] Veronique Hannaert et al. “Plant-like traits associated with metabolism of Trypanosoma parasites.” In: *Proceedings of the National Academy of Sciences of the United States of America* 100.3 (Feb. 2003), pp. 1067–1071.

[299] Maria G Tozzi et al. “Pentose phosphates in nucleoside interconversion and catabolism.” In: *The FEBS journal* 273.6 (Mar. 2006), pp. 1089–1101.

[300] Jennifer Bordeaux et al. “Antibody validation.” In: *BioTechniques* 48.3 (Mar. 2010), pp. 197–209.

[301] Daniel J Klionsky. “Coming soon to a journal near you — the updated guidelines for the use and interpretation of assays for monitoring autophagy.” In: *Autophagy* 10.10 (Oct. 2014), p. 1691.

[302] Annette K Roos et al. “Mycobacterium tuberculosis ribose-5-phosphate isomerase has a known fold, but a novel active site.” In: *Journal of molecular biology* 335.3 (Jan. 2004), pp. 799–809.

[303] Robin Ketteler et al. “A pathway sensor for genome-wide screens of intracellular proteolytic cleavage.” In: *Genome biology* 9.4 (2008), R64.

[304] Robin Ketteler and Brian Seed. “Quantitation of autophagy by luciferase release assay.” In: *Autophagy* 4.6 (Aug. 2008), pp. 801–806.

[305] Christin Luft et al. “Application of Gaussia luciferase in bicistronic and non-conventional secretion reporter constructs.” In: *BMC biochemistry* 15 (2014), p. 14.

[306] Patrick D Hsu et al. “DNA targeting specificity of rNA-guided Cas9 nucleases”. In: *Nature biotechnology* (June 2013), pp. 1–8.

[307] Andrew Adey et al. “The haplotype-resolved genome and epigenome of the aneuploid HeLa cancer cell line.” In: *Nature* 500.7461 (Aug. 2013), pp. 207–211.

[308] Ji-Biao Huang et al. “Transaldolase is part of a supramolecular complex containing glucose-6-phosphate dehydrogenase in human neutrophils that undergoes retrograde trafficking during pregnancy.” In: *Metabolism: clinical and experimental* 54.8 (Aug. 2005), pp. 1027–1033.

[309] Ju Hee Kim et al. “Differential methylation hybridization profiling identifies involvement of STAT1-mediated pathways in breast cancer.” In: *International journal of oncology* 39.4 (June 2011), pp. 955–963.

[310] Matthew G Vander Heiden et al. “Evidence for an alternative glycolytic pathway in rapidly proliferating cells.” In: *Science (New York, NY)* 329.5998 (Sept. 2010), pp. 1492–1499.

[311] V Stone et al. “International Journal of Developmental Neuroscience”. In: *International Journal of Developmental Neuroscience* 37 (Oct. 2014), pp. 21–25.

[312] Jacob Heintze et al. “Ribose 5-phosphate isomerase inhibits LC3 processing and basal autophagy.” In: *Cellular signalling* 28.9 (June 2016), pp. 1380–1388.

[313] In Hye Lee and Toren Finkel. “Regulation of autophagy by the p300 acetyltransferase.” In: *The Journal of biological chemistry* 284.10 (Mar. 2009), pp. 6322–6328.

[314] Jiarui Wang et al. “Inhibition of transketolase by oxythiamine altered dynamics of protein signals in pancreatic cancer cells.” In: *Experimental hematology & oncology* 2 (2013), p. 18.

[315] M Nishimura and K Uyeda. “Purification and characterization of a novel xylulose 5-phosphate-activated protein phosphatase catalyzing dephosphorylation of fructose-6-phosphate,2-kinase:fructose-2,6-bisphosphatase.” In: *The Journal of biological chemistry* 270.44 (Nov. 1995), pp. 26341–26346.

[316] Bertram O Fraser-Reid, Kuniaki Tatsuta, and Joachim Thiem. *Glycoscience: Chemistry and Chemical Biology I–III*. Springer Science & Business Media, Dec. 2012.

[317] E Vives et al. “TAT Peptide Internalization: Seeking the Mechanism of Entry”. In: *Current Protein & Peptide Science* 4.2 (Apr. 2003), pp. 125–132.

[318] D Raafat, K Von Bargen, and A Haas. “Insights into the mode of action of chitosan as an antibacterial compound”. In: *Applied and . . .* (2008).

[319] John F Ryley. *Chemotherapy of Fungal Diseases*. Springer Science & Business Media, Dec. 2012.

[320] George S Krasnov et al. “Targeting VDAC-bound hexokinase II: a promising approach for concomitant anti-cancer therapy.” In: *Expert opinion on therapeutic targets* 17.10 (Oct. 2013), pp. 1221–1233.